

TOPICAL REVIEW

Time delays and advances in classical and quantum systems

E E Kolomeitsev¹ and D N Voskresensky²¹ Department of Physics, Faculty of Natural Sciences, Matej Bel University, SK-97401 Banska Bystrica, Slovakia² Department of Theoretical Nuclear Physics, National Research Nuclear University 'MEPhI', Kashirskoe sh. 31, Moscow 115409, RussiaE-mail: Evgeni.Kolomeitsev@umb.sk and D.Voskresensky@gsi.de

Received 15 March 2013

Published 11 October 2013

Online at stacks.iop.org/JPhysG/40/113101**Abstract**

This article reviews positive and negative time delays in various processes of classical and quantum physics. In the beginning, we demonstrate how a time-shifted response of a system to an external perturbation appears in classical mechanics and classical electrodynamics. Then we quantify durations of various quantum mechanical processes. The duration of the quantum tunneling is studied, and an interpretation of the Hartmann paradox is suggested. Time delays and advances appearing in the three-dimensional scattering problem on a central potential are considered. We then discuss delays and advances appearing in quantum field theory and after that we focus on the issue of time delays and advancements in quantum kinetics. We discuss problems of the application of generalized kinetic equations in simulations of the system relaxation toward equilibrium and analyze the kinetic entropy flow. Possible measurements of time delays and advancements in experiments similar to the recent OPERA neutrino experiment are also discussed.

(Some figures may appear in colour only in the online journal)

Contents

1. Introduction	3
2. Time shifts in classical mechanics and in classical field theory	5
2.1. Time shifts in classical mechanics	5
2.2. Time shifts in classical electrodynamics	19
3. Time shifts in non-relativistic quantum mechanics: 1D-scattering	22
3.1. The stationary problem	22
3.2. Characteristics of time in the stationary scattering problem	26
3.3. The non-stationary problem: the scattering of a wave packet	30
3.4. Characteristics of time for the scattering of a wave packet with negligibly small momentum uncertainty	37

3.5. Sojourn time for the scattering of an arbitrary wave-packet	40
3.6. The Hartmann effect	41
3.7. Centroid transmission and reflection time delays and asymptotic motion of packets	43
3.8. Tunneling of the Gaussian wave packet	49
3.9. Resonance states and their time evolution	55
3.10. Causality restriction	65
4. Time shifts in non-relativistic quantum mechanics: 3D-scattering	66
4.1. Scattering of the wave packet on the potential	66
4.2. Resonance scattering	68
4.3. Scattering on hard cores	69
4.4. Semiclassical scattering	69
5. Time shifts in quantum field theory	70
5.1. Time contour formulation	70
5.2. Weakening of short-range correlations and the Dyson equation	72
5.3. Φ -derivable approximation scheme	74
5.4. The space–time structure of self-energy diagrams	74
5.5. Typical time delays and advances	77
6. Time shifts in quantum kinetics	79
6.1. Wigner transformation and gradient expansion	79
6.2. Three forms of the quantum kinetic equation	80
6.3. Memory effects	85
6.4. Positive definiteness of kinetic quantities	86
6.5. Time advances and delays	87
6.6. Test-particle method	89
6.7. The quasiparticle limit	91
6.8. Kinetic entropy and time delays	93
6.9. Examples of the solutions of kinetic equations	95
6.10. Validity of the gradient expansion	98
6.11. Hydrodynamical and thermodynamical limits	98
7. Space–time delays and measurements	99
7.1. The speed of the propagating wave packet	99
7.2. Measurements and resulting time delays and advances	100
7.3. Apparent superluminality in neutrino experiments as a time advance effect	101
8. Conclusion	102
8.1. Classical mechanics	102
8.2. Quantum mechanics	104
8.3. Quantum field theory	107
8.4. Quantum kinetics	108
Acknowledgements	109
Appendix A. Virial theorem for infinite classical motion in a central potential	110
Appendix B. Relations for wave functions obeying the Schrödinger equation	111
Appendix C. Asymptotic centroids of the wave packets	112
Appendix D. Relations for the sojourn time	114
Appendix E. Matrix notation	115
Appendix F. H theorem and the minimum of entropy production	116
References	117

1. Introduction

Many definitions of time, as a measure of the duration of a process, are possible in classical mechanics. In principle, for the measurement of a time duration any process is suitable which occurs at a constant pace. Naively thinking, the response of a system to an external perturbation should be delayed in accordance with the causality principle. However, it is not always the case. There may arise both delays and advancements (negative time delays) in system responses without contradiction with causality.

Time delays and possible time advances in quantum mechanical phenomena have been extensively discussed in the literature; see [1–12] and references therein. In spite of this many questions still remain not quite understood. Worth mentioning is the Hartmann effect [13], that the transition time of a quantum particle through a one-dimensional (1D) barrier is seemingly independent of the barrier length for broad barriers. This causes apparent superluminal phenomena in quantum mechanical tunneling. Many, at first glance, supporting experiments with single photons, classical light waves and microwaves have been performed, see [14–18] and references therein. Different definitions of time delays, such as the group transmission time delay δt_T , the group reflection time delay δt_R , the interference time delay δt_i , the dwell time t_d , the sojourn time t_{soj} and some other quantities have been introduced to treat the problem. All these time-scales suffer from the Hartmann effect and are at odds with the natural expectation that the tunneling time should be proportional to the length of the barrier. A re-interpretation consistent with special relativity suggested in [8] is that these times should be treated as the life-times of the corresponding wave packets rather than the traveling time. If so, the so-far-performed experiments measured an energy dissipation at the edges of the barrier rather than particle traveling time.

In addition to the mentioned time delays other relevant time quantities were introduced and the differences between the averaged scattering time delay δt_s and the Wigner scattering time delay δt_W were discussed in [3, 19, 20]; see also [4–6] and references therein. Based on these analyses the authors of [20] argued that kinetic simulations describing the relaxation of a system, first, toward the local equilibrium and, then, toward the global one must account for delays in scattering events consistent with mean fields acting on particles, in order to model consistently the thermodynamic properties of the system. For practical simulations, as the relevant relaxation time they suggested to use the scattering time delay δt_s , as it follows from the phase shift analysis, rather than the collision time t_{col} , as it appears in the original Boltzmann equation. A number of BUU (Boltzmann–Uehling–Uhlenbeck) simulations of heavy-ion collision reactions were performed using this argumentation; see [21] and references therein.

The appropriate frame for the description of non-equilibrium many-body processes is the real-time formalism of quantum field theory developed by Schwinger, Kadanoff, Baym and Keldysh [22–25]. A generalized kinetic description of off-mass-shell (virtual) particles has been developed based on the quasiclassical treatment of the Dyson equations for non-equilibrium systems, see [24, 26–31]. This treatment assumes the validity of the first-order gradient approximation to the Wigner-transformed Dyson equations. As it is ordinarily sought, the gradient approximation is valid if the typical time–space scales are much larger than the microscopic scales, such as $1/E_F$ and $1/p_F$ for slightly excited Fermi systems, where E_F is the Fermi energy and p_F is the Fermi momentum. As the result, a quantum kinetic equation is derived for off-mass-shell particles, for which the energy and momentum are not connected by any dispersion relation. We call this generalized kinetic equation the Kadanoff–Baym (KB) equation. Among other terms, this equation contains the Poisson-bracket term, the origin of which has not, for a long time, been quite understood. Botermans and Malfliet in [32]

suggested replacing the production rate in that Poisson-bracket term by its approximate quasi-equilibrium value. This allowed the simplification of the KB equation for near equilibrium configurations. The resulting form of the kinetic equation is called the Botermans–Malfliet (BM) form. It is argued that the BM replacement does not spoil the validity of the first-order gradient approximation. The so-called Φ -derivable self-consistent approximations in quantum field theory were introduced by Baym in [33] for quasi-equilibrium systems. His derivation was then generalized to an arbitrary Schwinger–Keldysh contour in [34]. Reference [35] developed the self-consistent treatment of quantum kinetics. References [36, 37] demonstrated that the KB kinetic equation is compatible with the exact conservation of the Noether 4-current and the Noether energy–momentum, whereas the Noether 4-current and the Noether energy–momentum related to the BM form of equation are conserved only approximately, up to zeroth gradients. Fulfilment of the conservation laws is important in practical simulations of dynamical processes. For example, in kinetic simulations of heavy-ion collisions the gradient approximation may not work, at least on an initial stage of the expansion of the fireball. In this case the KB form of the kinetic equation should be preferable compared to the BM one due to inherent exact conservation laws for the Noether quantities in the former case. However, up to now the simulation scheme, the so-called test-particle method, has been realized in application to heavy-ion collisions only for the BM form of the kinetic equation; see [21, 38, 39]. The relaxation time arising in the kinetic equation presented in the BM form is the scattering time delay, δt_s , rather than the average collision time t_{col} , as it appears in the original KB equation. Since δt_s can be naturally interpreted in terms of the virial expansion [20], this was considered as an argument in favor of the BM form of the kinetic equation.

Recent work [40] suggested a non-local form of the quantum kinetic equation, which up to second gradients coincides with the KB equation and up to first gradients, with the BM equation. Thus, the non-local form keeps the Noether 4-current and Noether energy–momentum conserved at least up to first gradients. The second advantage of the non-local form is that it allows interpretation of the mentioned difference in the Poisson-bracket terms in the KB and BM equations, as associated with space–time and energy–momentum delays and advancements. Also the non-local form of the kinetic equation permits, in principle, to develop a test-particle method, similar to that used for the BM form of the kinetic equation.

In this review we study problems related to determination of time delays and advancements in various phenomena. In section 2 we discuss how time delays and lesser time advancements arise in the description of oscillations in classical mechanics and in classical field theory of radiation. In section 3 we consider time delays and advancements in 1D quantum mechanical tunneling and in the scattering of particles above the barrier. The problem of an apparent superluminality in the tunneling (the Hartmann effect) is considered and a solution of the paradox is suggested. In section 4 we consider time delays and advancements in the three-dimensional (3D) scattering problem. Then in section 5 we introduce the non-equilibrium Green’s function formalism and show that not only space–time delays but also advancements appear in the Feynman diagrammatic description of quantum processes within quantum field theory. In section 6 we focus on the quasiclassical description of non-equilibrium many-body phenomena. We introduce a gradient expansion scheme and arrive at a set of equations for the kinetic quantities, which should be solved simultaneously. The kinetic equation for the Wigner density is presented in three different forms, the KB, the BM and the non-local form. We discuss time delays and advancements, as they appear in the non-local form of the kinetic equation (and in the KB equation equivalent to it up to the second-order gradient terms) and consider their relation to those quantities, which arise in the quantum mechanical 1D tunneling, in motion above the barrier and in 3D scattering. To demonstrate that all three forms of the kinetic equation are not fully equivalent in the region of a formal applicability

of the first-order gradient expansion we calculate the kinetic entropy flow in all three cases and explicate their differences. Then we find some solutions for all three forms of the kinetic equation, raising the question of the applicability of the gradient expansion in the description of the relaxation of a slightly non-equilibrium system toward equilibrium. Based on this discussion we pose the question of the applicability of the BM kinetic equation for simulations of violent heavy-ion collisions. A possible explanation for the appearance of instabilities for superluminal virtual particles is also discussed. In section 7 we discuss the measurements of time delays and advancements. The origin of an apparent superluminality, as might be seen in experiments similar to those performed by the OPERA and MINOS neutrino collaborations [41, 42] is discussed. In appendix A we present the formulation of the virial theorem in classical mechanics in terms of the scattering time delay. Appendix B demonstrates the derivation of some helpful relations between wave functions. Appendix E shows the relations between contour and matrix quantities. In appendix F we discuss the H theorem and demonstrate the minimum of the entropy production at the system relaxation toward the equilibrium.

Starting from section 5 we use units $\hbar = c = 1$. Where necessary we recover c and \hbar .

2. Time shifts in classical mechanics and in classical field theory

In this section we introduce a number of time characteristics of the dynamics of physical processes. We demonstrate how a time-shifted response of a system to an external perturbation appears in classical mechanics and classical electrodynamics. We show that there may arise both delays and advancements in the system response.

2.1. Time shifts in classical mechanics

Let us introduce some definitions of time, as a measure of the duration of a process in classical mechanics, which will further appear in the quantum mechanical description.

To measure a time duration, any process which occurs at a constant pace is suitable. For example, to measure the time of motion one can use a camel moving forward with a constant velocity \vec{v} , then $t = l/v$, where $l \simeq N l_0$ is the distance passed by the camel, N is the number of its steps; l_0 is the step size. Such a simple measurement of time (in camel steps) is certainly inconvenient, because the distance between initial and final camel positions can be very large for large times. To overcome the problem one may use a ‘mechanical camel’ moving around in a circle with a constant angular velocity or linear speed. Our watches are constructed in such a manner, where the clock hand takes the role of the camel. More generally, for time measurement one may use any periodic process described by an ideal oscillator (e.g. one may use the atomic clock). Then time is measured in a number of half-periods $P/2$ of the oscillator motion.

Another way of measuring time is to exploit the particle conservation law. One of the oldest time-measuring devices constructed in such a manner is a clepsydra, or a water clock. Its usage is based on the principle of the conservation of an amount of water. Water can of course be replaced by any substance, which local density $\rho(\vec{r}, t)$ obeys the continuity equation $\partial\rho/\partial t + \text{div}\vec{j} = 0$, where $\vec{j} = \rho\vec{v}$ is a 3D flux density, dependent on the local velocity $\vec{v}(\vec{r}, t)$ of an element of the substance. Now, if we take a large container of volume V with a hole of area S , the time passed can be defined as the ratio of the amount of substance inside the container to the flux draining out of the container through the hole:

$$t_d^{(\text{cl})} = \int_V \rho \, d^3r \Big/ \left| \int_S \vec{j}(\rho) \, d\vec{s} \right|. \quad (2.1)$$

We will call this quantity a *dwell time* since a similar definition of a time interval is used in quantum mechanics in stationary problems.

In the 1D case the time particles dwelling in some segment of the z -axis open at the ends z_1 and z_2 , through which particles flow outside the segment, can be found as

$$t_d^{(1,cl)} = \frac{\int_{z_1}^{z_2} \rho dz}{|j(z_1) + j(z_2)|}, \quad (2.2)$$

where $\rho(z)$ is the particle density and $j(z) = v(z)\rho(z)$ is a 1D flux density. Obviously, for a particle flux from a hole at $z = z_2$ (at $j(z_1) = 0$) with constant density ρ and constant velocity v we then have $t_d^{(cl)} = l/v$ with $l = z_2 - z_1$. If ρ depends on t , the definitions (2.1), (2.2) become inconvenient, since $t_d^{(cl)}$ is then a nonlinear function of t .

Another relevant time-quantity reflecting the temporal extent of a physical process can be defined as follows. Consider the motion of a classical particle in an arbitrary time-dependent 1D potential $U(z, t)$. The particle trajectory is described by the function $z(t) \in \mathcal{C}$, where \mathcal{C} is the space region allowed for classical motion. Let the particle move for a time τ , then a part of this time, which the particle spends within an interval $[z_1, z_2] \in \mathcal{C}$, is given by the integral

$$t_{soj}^{(cl)}(z_1, z_2, \tau) = \int_0^\tau dt \theta(z(t) - z_1) \theta(z_2 - z(t)) = \int_0^\tau dt \int_{z_1}^{z_2} ds \delta(s - z(t)). \quad (2.3)$$

Such a temporal quantity can be called *classical sojourn time*. What is notable is that this time has a well-defined exact counterpart in quantum mechanics.

Now consider particle motion in a stationary field $U(z)$. Using the equation of motion $dz/dt = v(z; E)$, where $v(z; E) = \sqrt{\frac{2}{m}(E - U(z))}$ is the particle velocity and E , the energy, for an infinite motion we can recast the sojourn time (2.3) as

$$t_{soj}^{(cl)}(z_1, z_2, \tau) = \int_{z(0)}^{z(\tau)} \frac{dz}{v(z; E)} \int_{z_1}^{z_2} ds \delta(s - z) = \int_{\max\{z_1, z(0)\}}^{\min\{z_2, z(\tau)\}} \frac{dz}{v(z; E)} \quad (2.4)$$

provided the interval $[z_1, z_2]$ overlaps with the interval $[z(0), z(\tau)]$. If the particle motion is infinite one can put $\tau \rightarrow \infty$. For finite motion the integral would diverge in this limit and τ must be kept finite. It is convenient to restrict τ by the half of period $\tau \leq P/2$, which depends on the energy of the system and is given by [43]

$$P(E) = 2 \int_{z_1(E)}^{z_2(E)} \frac{dz}{v(z; E)}, \quad (2.5)$$

where now $z_{1,2}(E)$ are the turning points, given by equation $U(z_{1,2}) = E$. For $\tau > P/2$ the sojourn time contains a trivial part, which is a multiple of the half-period, $t_{soj}^{(cl)}(z_1, z_2, \tau) = nP/2 + t_{soj}^{(cl)}(z_1, z_2, \tau - nP/2)$, where n is an integer part of the ratio $2\tau/P$.

Following (2.4), the classical sojourn time $t_{soj}^{(cl)}(z_1, z, \tau(z_1, z))$ can be rewritten through the derivative of the shortened action

$$t_{soj}^{(cl)}(z_1, z, \tau(z_1, z)) = \frac{\partial S_{sh}(z_1, z, E; U)}{\partial E},$$

$$S_{sh}(z_1, z, E; U) = \int_{z_1}^z p dz = \int_{z_1}^z \sqrt{2m(E - U(z))} dz. \quad (2.6)$$

Taking $z = z_2$ we get

$$t_{soj}^{(cl)}(z_1, z_2, P/2) = P/2, \quad (2.7)$$

provided $z_{1,2}$ are the turning points.

For an infinite motion with $E > \max U(z)$, following (2.4) we can define a classical sojourn time delay/advance for the particle traversing the region of the potential compared to

a free motion as

$$\begin{aligned} \delta t_{\text{soj}}^{\text{cl}} &= t_{\text{soj}}^{\text{cl}}(-\infty, \infty, \infty; U) - t_{\text{soj}}^{\text{cl}}(-\infty, \infty, \infty; U = 0) \\ &= \sqrt{\frac{m}{2}} \int_{-\infty}^{+\infty} \left(\frac{1}{\sqrt{E - U(z)}} - \frac{1}{\sqrt{E}} \right) dz. \end{aligned} \quad (2.8)$$

Calculating $t_{\text{soj}}^{\text{cl}}(-\infty, \infty, \infty)$ we extend the lower limit in the time integration in (2.3) to $-\infty$. The classical sojourn time delay/advance (2.8) for infinite motion can then be rewritten as

$$\delta t_{\text{soj}}^{\text{cl}} = \frac{\partial(S_{\text{sh}}(E; U) - S_{\text{sh}}(E; 0))}{\partial E}, \quad (2.9)$$

where $S_{\text{sh}}(E; U) = \int_{-\infty}^{+\infty} p \, dz$.

The definition (2.9) of the time delay is similar to the definition of the group time delay δt_{gr} appearing in consideration of waves in classical and quantum mechanics. In the latter case the Ψ -function of semiclassical stationary motion is expressed as $\Psi \propto e^{iS_{\text{sh}}(z_1, z, E; U)/\hbar}$. With the help of a classical analogue of the phase shift,

$$\hbar \delta^{(\text{cl})}(z_1, z, E; U) \equiv S_{\text{sh}}(z_1, z, E; U), \quad (2.10)$$

we now introduce the group time

$$t_{\text{gr}}^{\text{(cl,1D)}}(z_1, z, E; U) \equiv \hbar \frac{\partial \delta^{(\text{cl})}(z_1, z, E; U)}{\partial E}. \quad (2.11)$$

Thus,

$$t_{\text{gr}}^{\text{(cl,1D)}}(z_1, z_2, E; U) = \hbar \frac{\partial \delta^{(\text{cl})}(z_1, z_2, E; U)}{\partial E} = P/2, \quad (2.12)$$

provided $z_{1,2}$ are turning points.

For 1D infinite motion, introducing $\delta^{(\text{cl})} = S_{\text{sh}}(-\infty, \infty, E; U)/\hbar \equiv S_{\text{sh}}(E; U)/\hbar$ and $\delta_{\text{free}}^{(\text{cl})} = S_{\text{sh}}(E; 0)/\hbar$, we can write the group time delay and, respectively, the free motion as

$$\delta t_{\text{gr}}^{\text{(cl,1D)}} = \hbar \frac{\partial(\delta^{(\text{cl})} - \delta_{\text{free}}^{(\text{cl})})}{\partial E} = \delta t_{\text{soj}}^{\text{(cl,1D)}}. \quad (2.13)$$

Moreover, one may introduce another temporal scale—*phase time delay*,

$$\delta t_{\text{ph}}^{\text{(cl)}} = \hbar \delta^{(\text{cl})}/E. \quad (2.14)$$

Also, from equation (2.8) we immediately conclude that in one dimension the time shift is negative (advance), $\delta t_{\text{soj}}^{\text{cl}} < 0$, for an attractive potential $U < 0$ and it is positive (delay) for a repulsive potential $U > 0$.

Extensions of the definitions of the full classical sojourn time and classical sojourn time delay/advance concepts to the 3D motion are straightforward. In analogy to equation (2.3) the time a particle spends within a 3D volume Ω during the time τ can be defined as

$$t_{\text{soj}}^{\text{(cl)}}(\Omega, \tau) = \int_0^\tau dt \int_{\vec{r} \in \Omega} d\vec{r} \delta(\vec{r} - \vec{r}(t)). \quad (2.15)$$

Consider now the radial motion of a particle in a central stationary field decreasing sufficiently rapidly with the distance from the center. Using the symmetry of the motion toward the center and away from it, we can choose the moment $t = 0$, as corresponding to the position of the closest approach to the center. Then for times $t \rightarrow \pm\infty$ the particle moves freely and its speed is v_∞ . We can define a classical time delay by which the free particle motion differs from the motion in the potential as

$$\delta t_{\text{W}}^{\text{(cl)}} = 2 \lim_{t \rightarrow \infty} (t(r, U) - r(t, U = 0)/v_\infty), \quad (2.16)$$

where $r(t, U = 0)$ is the particle's radial coordinate for free motion. Factor 2 counts forward and backward motions in radial direction. We will call this time delay the *Wigner time delay*. One can see that this time is equivalent to a classical sojourn time delay, $\delta t_{\text{W}}^{(\text{cl})} = \delta t_{\text{soj}}^{(\text{cl})}$, defined similarly to equation (2.8). Using the virial theorem for classical scattering on a central potential $U(r)$ [44], one may show that (see appendix A)

$$\delta t_{\text{soj}}^{(\text{cl})} = \delta t_{\text{W}}^{(\text{cl})} = \frac{1}{E} \int_0^\infty (2U(r(t)) + r(t)U'(r(t))) dt, \quad (2.17)$$

where the integration goes along the particle trajectory $r(t)$. The result holds for potentials decreasing faster than $1/r$. We see that in the 3D-case there is no direct correspondence between the signs of the potential and the time shift $\delta t_{\text{soj}}^{(\text{cl})}$. For a power-law potential $U = a/r^\alpha$, $\alpha > 0$, we have a delay, $\delta t_{\text{W}}^{(\text{cl})} > 0$, for $a(2 - \alpha) > 0$, and we have an advance, $\delta t_{\text{W}}^{(\text{cl})} < 0$, for $a(2 - \alpha) < 0$. For $\alpha = 2$ there is no time shift compared to the free motion.

Now, using that in a central field [43]

$$t(r) = \int_{r_0}^r \frac{dr}{v_r}, \quad v_r = \sqrt{v_\infty^2 - \frac{2U(r)}{m} - \frac{M^2}{m^2 r^2}}, \quad (2.18)$$

where $r_0 = r(v_r = 0)$ is the turning point³, and M is the angular momentum, we can rewrite the limit in equation (2.16) as

$$\lim_{r \rightarrow \infty} (t(r) - r/v_\infty) = \lim_{r \rightarrow \infty} \left(\int_{r_0}^r \frac{dr}{v_r} - \frac{r}{v_\infty} \right). \quad (2.19)$$

For a central potential the shortened action is $S_{\text{sh}}(r_0, r, E, U) = \int_{r_0}^r p_r dr$, $S_{\text{sh}}(E, U) = \int_{r_0}^\infty p_r dr$, and the classical analogue of the phase shift is given by

$$\hbar \delta^{\text{cl}}(v_\infty, M) - \hbar \delta^{\text{cl}}(v_\infty, M, U = 0) = \lim_{r \rightarrow \infty} \left[\int_{r_0}^r p_r dr - \int_{r_0}^r p_r(U = 0) dr \right], \quad p_r = mv_r. \quad (2.20)$$

Then, similarly to equation (2.9) we can define the group time delay, as the energy derivative of the phase acquired during the whole period of motion (forward and backward), and from comparison with equation (2.19) we have

$$\delta t_{\text{gr}}^{(\text{cl}, 3\text{D})} \equiv 2\hbar \frac{\partial (\delta^{\text{cl}} - \delta_{\text{free}}^{\text{cl}})}{\partial E} = \delta t_{\text{W}}^{(\text{cl})}. \quad (2.21)$$

As we see, compared to the 1D case (2.13) (where integration limits in the expression for S_{sh} are from $-\infty$ to ∞), in the 3D case (2.21) for the delay in the radial motion there appears an extra factor 2. In section 3 we shall see that such a delay corresponds to divergent waves, whereas scattered waves are characterized by half the delay, as it is in 1D classical motion. Also, in the 3D case one may introduce a phase time-scale given by the same expression (2.14), as in the 1D case.

Moreover, for systems under the action of external time-dependent forces there appear extra time-scales characterizing dynamics. Above we considered undamped mechanical motion; below we study damped motion. We consider several examples of such a kind, when mechanical trajectories can be explicitly found. We introduce typical time-scales and demonstrate possibility, as time delays of the processes, as time-advancements.

³ If there is no turning point, one puts $r_0 = 0$.

2.1.1. Anharmonic damped 1D-oscillator under the action of an external force: general solution. Consider a particle with a mass m performing a 1D motion along the z -axis in a slightly anharmonic potential under the action of an external time-dependent force $F(t)$ and some non-conservative force (friction) leading to a dissipation. The equation of motion of the particle is

$$\ddot{z}(t) + E_R^2 z(t) + \Gamma \dot{z}(t) + \Lambda z^2(t) = \frac{1}{m} F(t), \quad (2.22)$$

where E_R is the oscillator frequency and $\Gamma > 0$ is the energy dissipation parameter. The anharmonicity of the oscillator is controlled by the parameter Λ . Within the Hamilton or Lagrange formalism, equation (2.22) can be derived, e.g., with the help of the introduction of an artificial doubling of the number of degrees of freedom, as in [45–47], or if one assumes that the oscillator is coupled to the environment (‘a viscous medium’), as in [48]. To establish a closer link to the formalism of the quantum field theory, which we will pursue in section 5, we introduce the dynamical variable (the ‘field’) $\phi(t) = m z(t)$ obeying the equations

$$-\hat{S}_t \phi(t) = J(t), \quad -\hat{S}_t = \frac{d^2}{dt^2} + E_R^2 + \Gamma \frac{d}{dt}, \quad J(t) = F(t) - \frac{1}{m} \Lambda \phi^2(t), \quad (2.23)$$

with the differential operator \hat{S}_t and the source term J , which depends nonlinearly on ϕ and on the external force $F(t)$.

In absence of anharmonicity, $\Lambda = 0$, solution of equation (2.22) can be written as

$$z(t; \Lambda = 0) = z_0(t) - \int_{-\infty}^{+\infty} dt' G_0(t-t') w(t'), \quad w(t') = \frac{1}{m} F(t'), \quad (2.24)$$

where the Green’s function $G_0(t-t')$ satisfies the equation

$$\hat{S}_t G_0(t-t') = \delta(t-t'). \quad (2.25)$$

The quantity $z_0(t)$ in equation (2.24) stands for the solution of the homogeneous equation $\hat{S}_t z(t) = 0$ with initial conditions of the oscillator, namely, its position $z_0(0)$ and velocity $\dot{z}_0(0)$ (both are encoded in the oscillation amplitude a_0 and the phase α_0):

$$z_0(t) = a_0 \exp\left(-\frac{1}{2}\Gamma t\right) \cos(\omega_R t + \alpha_0), \quad (2.26)$$

where $\omega_R = \sqrt{E_R^2 - \frac{1}{4}\Gamma^2}$. Two time-scales characterize this solution: the time of the amplitude quenching—the *decay time*,

$$t_{\text{dec}}^{(\text{cl})} = 2/\Gamma \quad (2.27)$$

and the period of oscillation $P = \frac{2\pi}{\omega_R}$, see equation (2.5). The value $t_{\text{dec}}^{(\text{cl})}$ describes the decay of the field ($\phi = mz$ variable). The quantity ϕ^2 is damped on the time scale which is twice shorter than $t_{\text{dec}}^{(\text{cl})}$. Note that in quantum mechanics we ordinarily consider damping of the density variable, $|\Psi|^2$. The definition of the sojourn time (2.4) provides a relation for the period $t_{\text{soj}}^{(\text{cl})}(z_0(P/2), z_0(0), \tau = P/2) = P/2$. The phase time shift $\delta t_{\text{ph}} = \alpha_0/\omega_R$ can be eliminated by the choice of the initial time moment.

In the Fourier representation equation (2.24) acquires the simple form

$$z(\omega; \Lambda = 0) = z_0(\omega) - G_0(\omega)w(\omega), \quad (2.28)$$

where $w(\omega)$ is the Fourier transform of the external acceleration $w(t)$,

$$w(\omega) = \int_{-\infty}^{+\infty} dt e^{+i\omega t} \frac{F(t)}{m}. \quad (2.29)$$

The Fourier transform of equation (2.25) yields the Green’s function

$$G_0(\omega) = \int_{-\infty}^{+\infty} dt e^{i\omega t} G_0(t) = \frac{1}{\omega^2 - E_R^2 + i\Gamma\omega}. \quad (2.30)$$

This Green's function has the retarded property having poles in the lower complex semi-plane at $\omega = \pm\omega_R - \frac{1}{2}\Gamma$. As a function of time, it equals to

$$G_0(t) = \frac{e^{-\frac{1}{2}\Gamma t}}{\omega_R} \sin(\omega_R t + \pi)\theta(t), \quad \theta(t) = \begin{cases} 0, & t < 0 \\ 1, & t \geq 0. \end{cases} \quad (2.31)$$

For $\Gamma < 2E_R$ the particle oscillates in response to the external force while for $\Gamma \geq 2E_R$ the oscillations become over-damped. Further, to be specific, we always assume that $\Gamma < 2E_R$.

Note that the Green's function $G_0(\omega)$ satisfies the exact sum-rule

$$\int_{-\infty}^{\infty} A 2\omega \frac{d\omega}{2\pi} = 1, \quad A = -2 \text{Im} G_0. \quad (2.32)$$

This sum-rule is actually a general property of the retarded Green's function for the stationary system of relativistic bosons, see [49] and our further considerations in section 6.

The solution (2.26) of the homogeneous equation can be also represented through the Green's function convoluted with the source term $w_0(t)$ expressed through the δ -function and its derivative

$$z_0(t) = - \int_0^t dt' G_0(t-t') w_0(t'), \quad w_0(t) = a_0 E_R \sin(\beta - \alpha_0) \delta(t-0) - a_0 \cos \alpha_0 \delta'(t-0), \quad (2.33)$$

$$\beta = \arctan\left(\frac{\Gamma}{2\omega_R}\right). \quad (2.34)$$

In the Fourier representation we have $z_0(\omega) = -G_0(\omega) w_0(\omega)$, where $w_0(\omega) = a_0(E_R \sin(\beta - \alpha_0) + i\omega \cos \alpha_0)$.

Now we are at the position to include effects of anharmonicity, $\Lambda \neq 0$. In the leading order with respect to a small parameter Λ the Fourier transform of the solution $z(\omega)$ of the equation of motion acquires the form

$$z(\omega, \Lambda) = -G_0(\omega) \tilde{w}(\omega) + \Lambda G_0(\omega) \int_{-\infty}^{+\infty} \frac{d\omega'}{2\pi} \frac{d\omega''}{2\pi} (2\pi) \delta(\omega - \omega' - \omega'') \times [G_0(\omega') \tilde{w}(\omega')] [G_0(\omega'') \tilde{w}(\omega'')], \quad (2.35)$$

where $\tilde{w}(\omega) = w_0(\omega) + w(\omega)$. Equation (2.35) has a straightforward diagrammatic interpretation

$$z(\omega) = \text{---} \star i\tilde{w}(\omega) + \text{---} \overset{iG_0(\omega)}{\bullet} \begin{cases} \overset{iG_0(\omega')}{\star} i\tilde{w}(\omega') \\ \underset{-i\Lambda\delta_{\omega, \omega'+\omega''}}{\star} i\tilde{w}(\omega'') \end{cases}, \quad (2.36)$$

where the thin line stands for the free Green's function $iG_0(\omega)$, the cross depicts the source $i\tilde{w}(\omega)$ and the dot represents the coupling constant $-i\Lambda$. The integration is to be performed over the source frequencies with the δ -function responsible for the proper frequency addition. The diagrammatic representation can, of course, be extended further to higher orders of Λ . The full solution $z(\omega)$ is presented by the thick line with the cross

$$z(\omega) = \text{---} \star, \quad (2.37)$$

where the thick line stands for the full Green's function $iG(\omega)$ satisfying the Dyson equation shown in figure 1.

Let us consider another aspect of the problem. For simplicity consider a linear oscillator ($\Lambda = 0$). Assume that in vacuum oscillations are determined by the equation

$$\ddot{z}(t) + E_0^2 z(t) = 0. \quad (2.38)$$

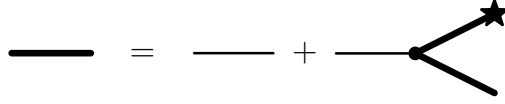


Figure 1. The Dyson equation for the full Green's function of the anharmonic oscillator described by the equation of motion (2.22).

The Fourier transform of the retarded Green's function describing these oscillations is as follows

$$G_0^0(\omega) = \frac{1}{\omega^2 - \omega_0^2 + i0\omega}. \quad (2.39)$$

Being placed in an absorbing medium the oscillator changes its frequency and acquires the width, which can be absorbed in the quantity $\text{Re}\Sigma = E_R^2 - E_0^2$, $\text{Im}\Sigma = -\Gamma\omega$, meaning a retarded self-energy. Then we rewrite (2.30) as

$$G_0(\omega) = \frac{1}{\omega^2 - \omega_0^2 - \Sigma} = \frac{1}{(G_0^0)^{-1} - \Sigma} \quad (2.40)$$

and we arrive at equation

$$G_0 = G_0^0 + G_0^0 \Sigma G_0, \quad (2.41)$$

known in quantum field theory as the Dyson equation for the retarded Green's function.

2.1.2. Anharmonic damped oscillator under the action of an external force: specific solutions.

Now we illustrate the above general formula with the help of examples. To be specific we assume that the oscillator was at rest initially and we start with the case $\Lambda = 0$.

Example 1. Consider a response of the system to a sudden change of an external constant force

$$F(t) \equiv F_1(t) = F_0\theta(-t). \quad (2.42)$$

The solution of equation (2.22) for $\Lambda = 0$ is

$$z(t) \equiv z_1(t) = - \int_{-\infty}^{+\infty} \frac{d\omega}{2\pi i} e^{-i\omega t} G_0(\omega) \frac{F_0/m}{\omega + i\epsilon} = \frac{F_0/m}{E_R \omega_R} e^{-\frac{1}{2}\Gamma t} \cos(\omega_R t - \beta)\theta(t) + \frac{F_0}{mE_R^2} \theta(-t), \quad (2.43)$$

where β is defined as in equation (2.34). The solution is purely causal, meaning that there are no oscillations for $t < 0$ and that they start exactly at the moment when the force ceases. This naturally follows from the retarded properties of the Green's function (2.31), where the θ -function cuts off any response for negative times. The latter occurs because both poles of the Green's function are located in the lower complex semi-plane and the parameter Γ is positive corresponding to the dissipation of the energy in the system.

Solution (2.43) is characterized by three time-scales. Two time-scales, the period of oscillations $P = \frac{2\pi}{\omega_R}$, cf. (2.5), and the time of the amplitude quenching, i.e. the decay time $t_{\text{dec}}^{(\text{cl})} = 2/\Gamma$, cf. (2.27), appear already in the free solution (2.26). Another time-scale appears as the phase time delay in the system response on a perturbation occurring at the time moment $t = 0$ (cf. equation (2.14)),

$$\delta t_{\text{ph}}^{(\text{cl})} = \beta/\omega_R > 0. \quad (2.44)$$

The solution (2.43) is depicted on the left panel of figure 2 for three values of Γ . Arrows demonstrate that for $\Gamma \neq 0$ the response of the oscillator on the action of the external

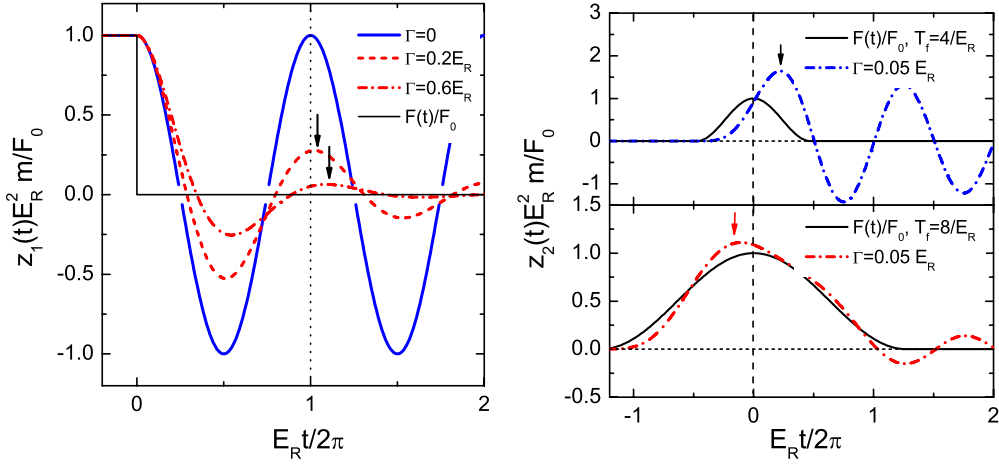


Figure 2. The response of the oscillator to the external force. Left panel—example 1: the external force is given by (2.42). Solution (2.43) is shown for different values of Γ . Right panel—example 2: the external force (2.45) is shown by the solid line. Dash-dotted lines depict solutions (2.47). Values of Γ and T_f are shown in the legends.

perturbation is purely causal. The larger Γ is, the smaller is $t_{\text{dec}}^{(\text{cl})}$ and the larger is $\delta t_{\text{ph}}^{(\text{cl})}$, i.e. the larger is the time shift of the oscillations. For $\Gamma \rightarrow 2E_R$ the oscillation period $P \rightarrow \infty$ and the phase shift $\delta t_{\text{ph}}^{(\text{cl})}$ becomes infinite, but the ratio $\delta t_{\text{ph}}^{(\text{cl})}/P$ remains finite, $\delta t_{\text{ph}}^{(\text{cl})}/P = \beta/2\pi \rightarrow 1/4$.

Example 2. Interestingly, the same oscillating system being placed in another external field can exhibit an apparently acausal reaction. To demonstrate this possibility consider the driving force acting within a finite time interval $[-T_f, +T_f]$ and having a well-defined peak occurring at $t = 0$:

$$F(t) \equiv F_2(t) = F_0 \cos^2\left(\frac{\pi t}{2T_f}\right) \theta(T_f - |t|). \quad (2.45)$$

The oscillator response to this pulse-force is given by

$$z(t) \equiv z_2(t) = -\frac{F_0}{m} \int_{-\infty}^{+\infty} \frac{d\omega}{2\pi} e^{-i\omega t} G_0(\omega) \frac{\sin(\omega T_f)}{\omega + i\epsilon} \frac{\pi^2/T_f^2}{(\omega + i\epsilon)^2 - \pi^2/T_f^2}. \quad (2.46)$$

After some manipulations the solution acquires the form

$$z_2(t) = \frac{F_0}{mE_R^2} [\zeta(t + T_f)\theta(t + T_f) - \zeta(t - T_f)\theta(t - T_f)],$$

$$\zeta(t) = \frac{1}{2} \left[1 - \frac{E_R^2}{r_+ r_-} \cos\left(\frac{\pi}{T_f} t - \beta_- + \beta_+\right) + \frac{E_R}{\omega_R} \frac{(\pi^2/T_f^2)}{r_+ r_-} e^{-\frac{1}{2}\Gamma t} \cos(\omega_R t - \beta - \beta_- - \beta_+) \right],$$

$$r_{\pm} = \sqrt{(\omega_R \pm \pi/T_f)^2 + \frac{1}{4}\Gamma^2}, \quad \beta_{\pm} = \arctan\left(\frac{1}{2}\Gamma/[\omega_R \pm \pi/T_f]\right), \quad (2.47)$$

and the phase shift β here is given by equation (2.34). The first two terms in $\zeta(t)$ are operative only for $-T_f \leq t \leq T_f$ and cancel out exactly for $t > T_f$. If the interval of the action of the force is very short, i.e. $T_f E_R \ll 1$, then for $t > T_f$ the oscillator moves after a single momentary kick similarly to that in example 1, and up to the terms $\sim O(E_R^2 T_f^2/\pi^2)$ the solution (2.47) yields $z_2(t) \approx z_1(t + T_f)$. In the opposite case, i.e. for $T_f E_R \gg 1$ and $t \in [-T_f, T_f]$, the

solution $z_2(t)$ oscillates around the profile of the driving force (2.45) with a small amplitude $\sim (F_0/mE_R^2)O(\pi^2/E_R^2)T_f^2$,

$$(mE_R^2/F_0)z_2(t) = \frac{1}{F_0}F_2(t - \Gamma/E_R^2) + \frac{\pi^2}{2T_f^2 E_R^2} \left\{ \left(1 - \frac{1}{2} \frac{\Gamma^2}{E_R^2}\right) \cos\left(\frac{\pi}{T_f} \left[t - \frac{\Gamma}{E_R^2}\right]\right) + e^{-\frac{1}{2}\Gamma(t+T_f)} \frac{E_R}{\omega_R} \cos(\omega_R(t + T_f) - 3\beta) \right\}. \quad (2.48)$$

In the given example besides P and $t_{\text{dec}}^{(\text{cl})}$ the system is characterized by the initial pulse-time

$$t_{\text{pulse}} = 2T_f \quad (2.49)$$

and by two phase time-scales

$$\delta t_{\text{ph}}^{(1)} = T_f(\beta_- - \beta_+)/\pi \quad \text{and} \quad \delta t_{\text{ph}}^{(2)} = (\beta + \beta_- + \beta_+)/\omega_R. \quad (2.50)$$

The solution (2.47) is shown in figure 2, right panel. As we see from the lower panel, for some values of T_f and Γ the maximum of the oscillator response may occur *before* the maximum of the driving force. Therefore, if for the identification of a signal we use a detector with the threshold close to the pulse peak, such a detector would register a peak of the response of the system before the input's peak. In [16] a similar mathematical model was used to simulate and analyze 'a causal loop paradox', when a signal from the 'future' switches off the input signal. A system with such a bizarre property has been realized experimentally [50].

Example 3. The temporal response of the system depends on characteristic frequencies of the driving force variation. For a monochromatic driving force

$$F(t) \equiv F_3(t) = F_0 \cos(E_p t) \quad (2.51)$$

the solution of the equation of motion for $t > 0$ is

$$z(t) = z_3(t) = \frac{F_0}{m} |G_0(E_p)| \cos(E_p t - \delta(E_p)) = \frac{(F_0/m) \cos(E_p t - \delta(E_p))}{\sqrt{(E_R^2 - E_p^2)^2 + \Gamma^2 E_p^2}}, \quad (2.52)$$

where the phase shift of the oscillations compared to the oscillations of the driving force, $\delta(E_p)$, is determined by the argument of the Green's function

$$\delta(E_p) = \pi + \arg G_0(E_p) = \frac{i}{2} (\log [(E_R^2 - E_p^2)/(E_p \Gamma) - i] - \log [(E_R^2 - E_p^2)/(E_p \Gamma) + i]). \quad (2.53)$$

The phase shift δ is determined such that $\delta(E_p = 0) = 0$. In equation (2.53) the logarithm is continued to the complex plane as $\log(\pm i) = \pm \pi$ so that the function $\delta(E_p)$ is continuous at $E_p = E_R$, see figure 3(a), and at other points

$$\tan \delta(E_p) = -E_p \Gamma / (E_p^2 - E_R^2). \quad (2.54)$$

The amplitude of the solution (2.52) has a resonance shape peaking at $E_p = E_R$ with a width determined by the parameter Γ . In contrast to examples 1 and 2, solution (2.52) does not contain the time-scale $t_{\text{dec}}^{(\text{cl})}$, since the external force does not cease with time and continuously pumps-in the energy to the system. So, two time-scales, the period $P = 2\pi/E_p$ and the phase time

$$\delta t_{\text{ph}}^{(1)} = \delta(E_p)/E_p \quad (2.55)$$

fully control the dynamics. Note that in contrast to (2.14), here E_p is the frequency rather than the particle energy.

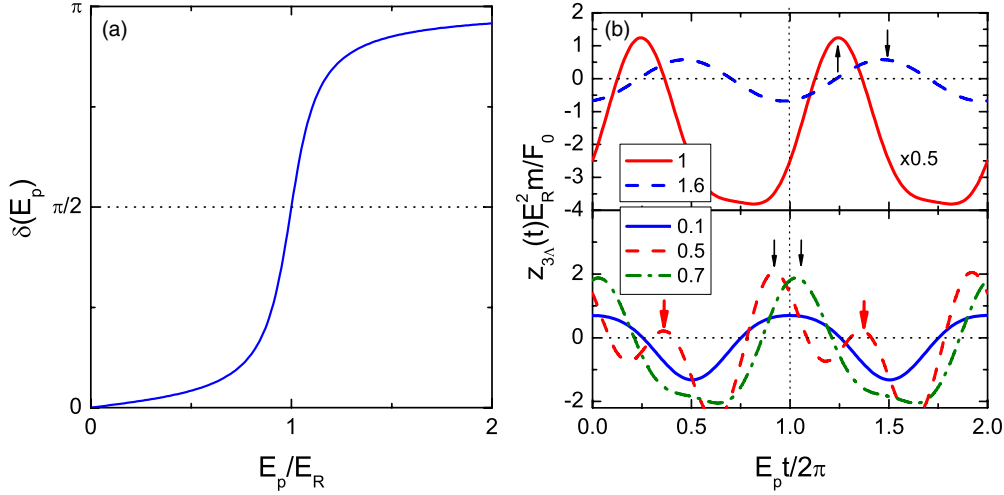


Figure 3. (a) The phase shift $\delta(E_p)$ given by equation (2.53). (b) The response of the damped anharmonic oscillator to a harmonic external force (2.51) for different values of the force frequency E_p shown by line labels in units of E_R for $\Gamma = 0.2 E_R$ and $\Lambda = 0.3 E_R^4 m/F_0$. Arrows show response maxima. The vertical dotted line shows the maximum of the driving force.

We have seen in example 2 that for some choices of the external force restricted in time the oscillating system can provide an apparently advanced response. The anharmonicity can produce a similar effect. For the case of small anharmonicity, $\Lambda \neq 0$, the solution (2.52) acquires a new term (an overtone)

$$z_{3\Lambda}(t) = z_3(t) - \frac{(F_0/m)^2 \Lambda / (2E_R^2)}{[(E_R^2 - E_p^2)^2 + \Gamma^2 E_p^2]} \left[1 + E_R^2 \frac{\cos(2[E_p t - \delta(E_p)] - \delta(2E_p))}{\sqrt{(E_R^2 - 4E_p^2)^2 + 4\Gamma^2 E_p^2}} \right], \quad (2.56)$$

which oscillates on the double frequency $2E_p$ and the phase is shifted with respect to the solution (2.52) by $\delta(2E_p)$. The Fourier transform of this solution is given by equation (2.35) provided w_0 is put to zero. Respectively, there appears an additional phase time-scale

$$\delta t_{ph}^{(2)} = (\delta(E_p) + \frac{1}{2}\delta(2E_p)) / E_p, \quad (2.57)$$

characterizing the dynamics of the overtone.

In figure 3(b) we show the solution (2.56) for several frequencies, E_p . If we watch for maxima in the system response $z(t)$ (shown by arrows) and compare how their occurrence is shifted in time with respect to the maxima of the driving force, we observe that for most values of E_p the overtone in (2.56) induces a small variation of the phase shift with time. However for $E_p \sim \frac{1}{2}E_R$ the overtone can produce an additional maximum in $z(t)$, which would appear to occur before the actual action of the force. The system would seem to ‘react’ in advance.

Example 4. In realistic cases the driving force can rarely be purely monochromatic, but is usually a superposition of modes grouped around a frequency E_p :

$$F(t) \equiv F_4(t) = F_0 \int_{-\infty}^{+\infty} dE g(E - E_p; \gamma) \cos(Et), \quad (2.58)$$

where an envelope function $g(\epsilon; \gamma)$, $\epsilon = E - E_p$, is a symmetrical function of frequency deviation picked around $\epsilon = 0$ with a width γ and normalized as $\int_{-\infty}^{+\infty} d\epsilon g(\epsilon; \gamma) = 1$. The integral (2.58) can be rewritten as

$$F_4(t) = F_0 \cos(E_p t) \int_{-\infty}^{+\infty} d\epsilon g(\epsilon; \gamma) \cos(\epsilon t) = \mathcal{A}_F(\gamma t) \cos(E_p t), \quad (2.59)$$

that allows us to identify E_p as the carrier frequency and $\mathcal{A}_F(\gamma t)$, as the amplitude modulation depending on the dimensionless variable γt .

For $\Lambda = 0$, the particle motion is described by the function

$$\begin{aligned} z_4(t) &= - \int_{-\infty}^{+\infty} \frac{d\omega}{2\pi} e^{-i\omega t} G_0(\omega) \frac{1}{m} F(\omega) \\ &= - \frac{F_0}{m} \int_{-\infty}^{+\infty} \frac{d\omega}{2\pi} e^{-i\omega t} G_0(\omega) \pi [g(\omega + E_p; \gamma) + g(\omega - E_p; \gamma)] \\ &= - \frac{F_0}{m} \operatorname{Re} \int_{-\infty}^{+\infty} d\epsilon e^{-i(E_p + \epsilon)t} G_0(E_p + \epsilon) g(\epsilon; \gamma). \end{aligned} \quad (2.60)$$

The last integral can be formally written as

$$mz_4(t) = |G_0(E_p)| \operatorname{Re} e^{-i(E_p t - \delta(E_p))} e^{-\frac{1}{2} \partial_E^2 \log G_0(E_p) \partial_t^2 + O(\partial_t^3)} \mathcal{A}_F(\gamma(t + i \partial_E \log G_0(E_p))). \quad (2.61)$$

Here $O(\partial_t^3)$ represents time derivatives of the third order and higher. We used the relation $\log G_0(E) = \log |G_0(E)| + i \delta(E) - i \pi$, where $\delta(E)$ is defined as in equation (2.53), but now as a function of E rather than E_p . The first-order derivatives generate the shift of the argument of the amplitude modulation via the relation $\exp(a \partial_t) \mathcal{A}_F(t) = \mathcal{A}_F(t + a)$. Note that the time shift of $\mathcal{A}_F(t)$ involves formally the ‘imaginary time’. As we will see later in section 3, the same concept appears also in quantum mechanics.

To proceed further with equation (2.61) one may assume that the function $\mathcal{A}_F(t)$ varies weakly with time so that the second and higher time derivatives can be neglected. In terms of the envelop function, this means that $g(\epsilon)$ is a very sharp function falling rapidly off for $\epsilon \gtrsim \gamma$ while $\gamma \ll \Gamma$. A typical time, on which the function $\mathcal{A}_F(t)$ fades away, can be estimated as

$$t_{\text{dec}}^{\gamma, (\text{cl})} = 1/\gamma. \quad (2.62)$$

If, additionally, the oscillator system has a high quality factor, i.e., $\Gamma \ll E_R$ and $|\partial_E \log |G_0(E_p)|| \ll \delta'(E_p)$, that is correct for E_p very near E_R , we arrive at the expression

$$mz_4(t) = \mathcal{A}_F(t - \delta'(E_p)) |G_0(E_p)| \cos(E_p t - \delta(E_p)). \quad (2.63)$$

We see that in this approximation there are five time-scales determining the response of the system. The oscillations are characterized by the period $P = 2\pi/E_p$ and the damping time $t_{\text{dec}}^{(\text{cl})} = 2/\Gamma$. Moreover, the envelope function is damping on the time-scale $t_{\text{dec}}^{\gamma, (\text{cl})}$. Additionally, there are two delay time-scales: *oscillations of the carrier wave are delayed by the phase time* $\delta t_{\text{ph}}^{(\text{cl})}(E_p) = \delta(E_p)/E_p$, see (2.55), whereas the amplitude modulation \mathcal{A}_F is delayed by the group time

$$t_{\text{gr}}^{(\text{cl})}(E_p) = \frac{\partial \delta(E_p)}{\partial E_p} = - \frac{E_R^2 + E_p^2}{E_p} \operatorname{Im} G_0(E_p). \quad (2.64)$$

This time shift appears because the system responds slightly differently to various frequency modes contributing to the force envelop (2.58).

The group and phase times are shown in figure 4. The group time is a much more rapidly varying function of the external frequency E_p and is strongly peaked at $E_p \sim E_R$. Close to the resonance the group time can be written as

$$t_{\text{gr}}^{(1)}(E_p) \approx \frac{\Gamma/2}{(E_p - E_R)^2 + \frac{1}{4}\Gamma^2} = \frac{1}{2} A_1(E_p) > 0. \quad (2.65)$$

For $\Lambda \neq 0$ there also appear other resonances in the system response, see equation (2.56). In the linear in Λ approximation the resonance with $E_p \simeq \frac{1}{2} E_R$ is excited. Close to this resonance the group time is

$$t_{\text{gr}}^{(2)}(E_p) \approx \frac{\Gamma/4}{(E_p - E_R/2)^2 + \frac{1}{4}(\Gamma/2)^2} = \frac{1}{2} A_2(E_p) > 0 \quad (2.66)$$

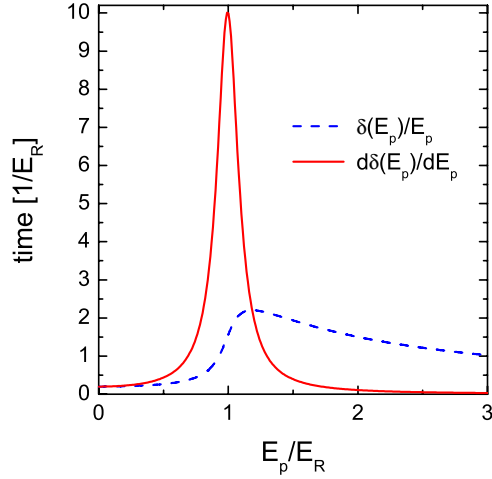


Figure 4. The phase and group time delays given by equations (2.55) and (2.64), respectively, calculated for $\Gamma = 0.2E_R$. The maximum of the group time coincides with $t_{\text{dec}}^{(cl)}$.

with a maximum at $E_p = E_R/2$. The width of the peak is $\Gamma/4$. Note that for both modes the functions $A_{1,2}(E_p)$ satisfy the sum-rule

$$\int_{-\infty}^{\infty} A_{1,2}(E) dE/(2\pi) = 1, \quad \text{or} \quad \int_{-\infty}^{\infty} t_{\text{gr}}^{(1,2)}(E) dE/\pi = 1. \quad (2.67)$$

The energy–time sum-rules demonstrate the relation of the group times to the density of states, i.e. the re-grouping of the number of degrees of freedom.

The time-difference

$$\delta t_f^\gamma = t_{\text{gr}}^{(i)} - t_{\text{dec}}^{\gamma, (cl)}, \quad (2.68)$$

(we call it forward time delay/advance) demonstrates to what extent the groups of waves are delayed on the scale of degradation of the envelop function. As is seen from figure 4 in the near-resonance region $\delta t_f^\gamma > 0$, whereas in the off-resonance region $\delta t_f^\gamma < 0$. As we shall see in section 3, an important case is when $\gamma \sim \Gamma$.

To study corrections to equation (2.63) due to the second-order derivatives in equation (2.61) we turn back to the case $\Lambda = 0$ and take the Gaussian envelope function $g_{\text{Gauss}}(\epsilon)$ and the corresponding amplitude modulation $\mathcal{A}_{F, \text{Gauss}}(\gamma t)$, such that

$$g_{\text{Gauss}}(\epsilon; \gamma) = \frac{\exp(-\epsilon^2/2\gamma^2)}{\sqrt{2\pi}\gamma^2}, \quad \mathcal{A}_{F, \text{Gauss}}(t; \gamma) = F_0 \exp(-\gamma^2 t^2/2). \quad (2.69)$$

Then, using the identity

$$e^{a\partial_t^2} e^{-\gamma^2 t^2/2} \equiv \sum_{n=0}^{\infty} \frac{a^n}{n!} \partial_t^{2n} e^{-\gamma^2 t^2/2} = \frac{e^{-\gamma^2 t^2/2(1+2a\gamma^2)}}{\sqrt{1+2a\gamma^2}}, \quad (2.70)$$

we obtain the response of the system to the Gaussian force in the form

$$z_{4\text{Gauss}}(t) = \frac{F_0}{m} |G_0(E_p)| \text{Re} \frac{e^{-i(E_p t - \delta(E_p))}}{\sqrt{1 - \gamma^2 \partial_E^2 \log G_0(E_p)}} \exp \left[-\gamma^2 \frac{(t + i\partial_E \log G_0(E_p))^2}{2(1 - \gamma^2 \partial_E^2 \log G_0(E_p))} \right]. \quad (2.71)$$

The derivatives of the Green's function can be conveniently expressed through the Green's function as

$$\begin{aligned}\partial_E \log G_0(E) &= i \delta'(E) + \partial_E \log |G_0(E)| = -(2E + i\Gamma) G_0(E), \\ \partial_E^2 \log G_0(E) &= i \delta''(E) + \partial_E^2 \log |G_0(E)| = 2 G_0(E) + (4E_R^2 - \Gamma^2) G_0^2(E).\end{aligned}\quad (2.72)$$

After some algebra we can cast this expression in the form similar to equation (2.63) with the amplitude modulation (2.69):

$$m z_{4\text{Gauss}}(t) = \mathcal{A}_{F,\text{Gauss}}(t - \tilde{t}_{\text{gr}}^{(\text{cl})}; \tilde{\gamma}) C_\gamma |G_0(E_p)| \cos(\tilde{E}_p(t) t - \tilde{\delta}(E_p)), \quad (2.73)$$

where, however, we have to redefine the parameters of both the carrier wave and the amplitude modulation function. The width of the Gaussian packet is determined from expression

$$\tilde{\gamma}^2 = \gamma^2 \frac{1 - \gamma^2 \partial_E^2 \log |G_0(E_p)|}{|1 - \gamma^2 \partial_E^2 \log G_0(E_p)|^2}, \quad (2.74)$$

and the amplitude modulation is delayed by the group time

$$\tilde{t}_{\text{gr}}^{(\text{cl})} = \delta'(E_p) + \partial_E \log |G_0(E_p)| \frac{\gamma^2 \delta''(E_p)}{1 - \gamma^2 \partial_E^2 \log |G_0(E_p)|}. \quad (2.75)$$

An interesting effect is that *the frequency of the carrier wave is changed and even becomes time dependent*,

$$\tilde{E}_p(t) = E_p + \tilde{\gamma}^2 \left[\partial_E \log |G_0(E_p)| + \left(\frac{1}{2} t - \delta'(E_p) \right) \frac{\gamma^2 \delta''(E_p)}{1 - \gamma^2 \partial_E^2 \log |G_0(E_p)|} \right], \quad (2.76)$$

and the phase shift is given by

$$\begin{aligned}\tilde{\delta} &= \delta(E_p) + \frac{1}{2} \arctan \left(\frac{\gamma^2 \delta''(E_p)}{1 - \gamma^2 \partial_E^2 \log |G_0(E_p)|} \right) + \tilde{\gamma}^2 \left[\delta'(E_p) \partial_E \log |G_0(E_p)| \right. \\ &\quad \left. + \frac{1}{2} ([\partial_E \log |G_0(E_p)|]^2 - [\delta'(E_p)]^2) \frac{\gamma^2 \delta''(E_p)}{1 - \gamma^2 \partial_E^2 \log |G_0(E_p)|} \right].\end{aligned}\quad (2.77)$$

The amplitude of the system response is modulated by the factor

$$C_\gamma = \exp \left[\frac{1}{2} \gamma^2 \frac{[\partial_E \log |G_0(E_p)|]^2}{(1 - \gamma^2 \partial_E^2 \log |G_0(E_p)|)^2} \right] / |1 - \gamma^2 \partial_E^2 \log G_0(E_p)|. \quad (2.78)$$

Keeping terms quadratic in γ we find the corrected group and phase times

$$\tilde{t}_{\text{gr}}^{(\text{cl})} \simeq \delta'(E_p) + \gamma^2 \partial_E \log |G_0(E_p)| \delta''(E_p) + O(\gamma^4), \quad (2.79)$$

$$E_p \delta \tilde{t}_{\text{ph}}^{(\text{cl})} \simeq \delta(E_p) + \gamma^2 \left(\frac{1}{2} \delta''(E_p) + \partial_E \log |G_0(E_p)| (\delta'(E_p) - \delta(E_p)/E_p) \right) + O(\gamma^4). \quad (2.80)$$

The importance of various correction terms depends on how close the carrier frequency E_p is to the resonance frequency E_R . Assuming that the oscillator has a high quality factor $\Gamma \ll E_R$, we can distinguish three different regimes: (i) very near to the resonance, $|E_p - E_R| \lesssim \Gamma^2/E_R$, (ii) an intermediate regime, $\Gamma^2/E_R \ll |E_p - E_R| \lesssim \Gamma$ and (iii) far from the resonance $\Gamma \ll |E_p - E_R|$. In the regime (i) corrections in (2.79), (2.80) are respectively of the order of $O(\gamma^2/E_R^2)$ and $O(\gamma^2/E_R \Gamma)$. In the regime (ii) correction terms are of the order of $O(\gamma^2/\Gamma^2)$. In the regime (iii) corrections are respectively of the order of $O(\gamma^2/E_R^2)$ and $O(\gamma^2 \Gamma/E_R^3)$ at most.

To illustrate the applicability range of the leading-order expression (2.63) and the size of the corrections in equation (2.73) we plot in figure 5 the quantities (2.74), (2.75), (2.76), (2.78) versus the force oscillation frequency E_p for various values of the envelop width γ and $\Gamma = 0.3 E_R$. We see that, as argued before, the corrections are small for E_p far from

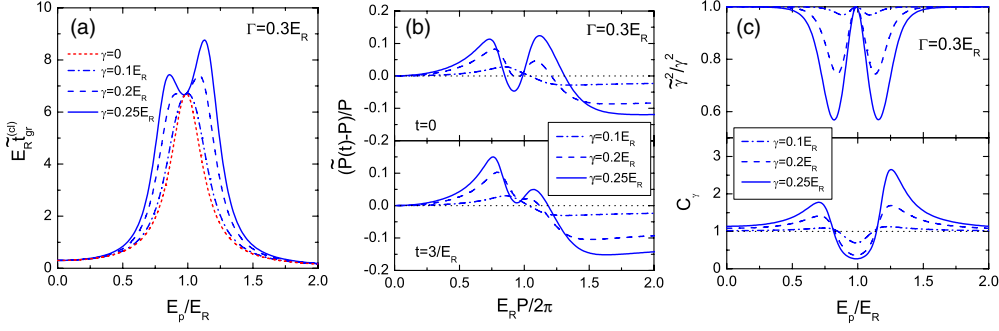


Figure 5. Parameters of the system response (2.71) to the modulated periodic external force (2.59) with the Gaussian envelop (2.69) calculated including the second-order derivatives for several values of the envelop width γ as functions of the force oscillation frequency E_p . The damping parameter of the system is $\Gamma = 0.3 E_R$. (a) The time shift of the amplitude modulation (2.75) for various values of γ . The dotted line shows the time shift (2.64) entering in the leading-order expression (2.63) involving the first-order derivatives only. (b) The relative deviation of the oscillation quasi-period $\tilde{P}(t) = 2\pi/\tilde{E}_p(t)$, see equation (2.76), from the force oscillation period $P = 2\pi/E_p$ for two moments of time $t = 0$ and $t = 3/E_R$. (c) The modification of the packet width $(\tilde{\gamma}/\gamma)^2$ given by equation (2.74) and the amplitude scaling factor C_γ given by equation (2.78).

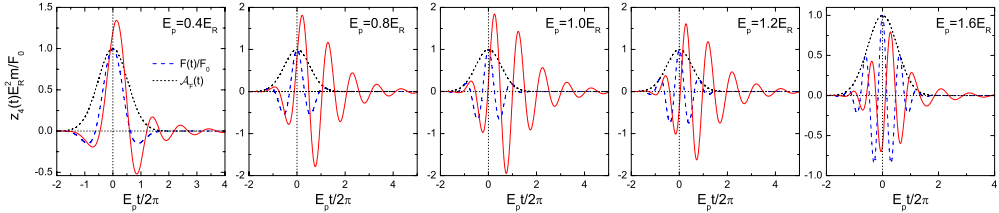


Figure 6. Solid lines: the response (2.60) of the oscillatory system to the modulated periodic external force (2.59) with the Gaussian envelop (2.69) calculated for $\gamma = \Gamma = 0.3 E_R$ and various values of the force frequency E_p . Dashed lines show the external force (2.59) and dotted lines depict the envelop function (2.69).

the resonance frequency E_R and right at the resonance. The corrections are maximal for $E_p \sim E_R \pm \Gamma$. Remarkably, at these frequencies the system response could become significantly broader (i.e. it lingers longer in time) than the driving force, $\tilde{\gamma} < \gamma$. Figure 5 shows also that equation (2.63) can be used only for $\gamma/\Gamma \ll 0.3$. The expression (2.73) is applicable for $\gamma/\Gamma \lesssim 0.5$ and $\Gamma/E_R \lesssim 0.3$ at the 30% accuracy level. For higher values of γ the corrections become too large and further terms in expansion (2.61) have to be taken into account.

In figure 6 we depict the response of the system to the force (2.59) with the ‘broad’ Gaussian envelop (2.69), $\gamma = \Gamma$, as it follows from numerical evaluation of the integral (2.60). We clearly see that when E_p approaches the interval $E_R \pm \Gamma$ not only the amplitude of the system response grows, but also the response lasts much longer than the force acts. Thus we demonstrated peculiarities of the effect of a smearing of the wave packet in classical mechanics.

2.1.3. A simple 3D-example: the scattering of particles on hard spheres. Consider a simplest case when a beam of (point-like) particles falls onto a hard sphere of a radius R , cf. [4]. The particles scatter at different angles θ , $\sin(\theta/2) = \sqrt{1 - b^2/R^2}$ depending on the impact

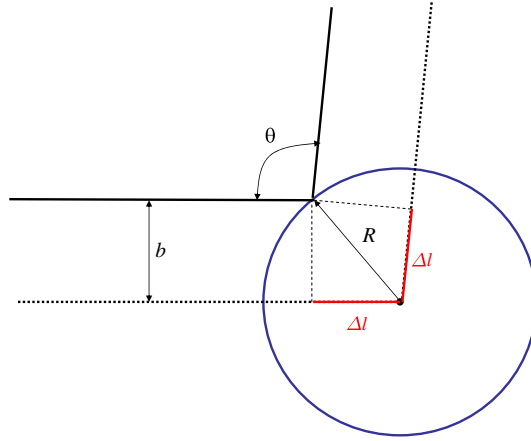


Figure 7. Particle scattering at angle θ off the hard sphere of radius R .

parameter b . The arrival time of the scattered particle to the detector decreases with an increase of the size of the sphere. The time advance for the particle scattered on the sphere's surface compared to that should it scatter on the center in the same θ direction is

$$\delta t_W^{(cl)} = -2 \frac{\Delta l}{v} = -\frac{2R}{v} \sin \frac{\theta}{2} \geq -\frac{2R}{v}; \tag{2.81}$$

see figure 7. In the given example $\delta t_{soj}^{(cl)} = \delta t_W^{(cl)}$, as they were introduced above, see equations (2.15), (2.17). As is seen from (2.17), for the repulsive potential $V = a/(r - b)^\alpha$, $r > r_0 = r(v_r = 0)$, $a > 0$, $\alpha > 0$, as in the case of the scattering on the hard sphere, there appears a time advancement, provided r_0 is very close to b . However the value of the Wigner time advancement is limited.

As we shall see below, the relevant quantity related to the advance/delay of the scattered wave, the scattering advance/delay time, is half of the Wigner advance/delay time. In the given hard sphere example thus is introduced

$$\delta t_s^{(cl)} = \frac{1}{2} \delta t_W^{(cl)}, \tag{2.82}$$

the difference between the time when the particle touches the sphere surface and the time when the particle freely reaches the center of the sphere. The advance $\delta t_s^{(cl)}$ is limited by the value $-R/v$.

Note that the averaged advance time for all scattered particles incident on the sphere at various impact parameters $0 \leq b \leq R$ is

$$\langle \delta t_W^{(cl)} \rangle = \int_0^R \delta t_W^{(cl)} \frac{2\pi b db}{\pi R^2} = -\frac{4}{v R^2} \int_0^R \sqrt{R^2 - b^2} b db = -\frac{4R}{3v}. \tag{2.83}$$

From the above analysis we are able also to conclude that the collision term in the kinetic equation describing the behavior of a non-equilibrium gas of hard spheres should incorporate the mentioned non-local time advancement effects.

2.2. Time shifts in classical electrodynamics

2.2.1. *Dipole radiation of a charged oscillator.* Let us consider the same damped oscillatory system as in the previous subsections, assuming now that the particle is charged and oscillates

in the z direction near the point $z = 0$ under the action of an incident electromagnetic wave propagating in the x direction with the electric field polarized along the z -axis:

$$\vec{\mathcal{E}}_{\text{in}}(t, \vec{r}) = \mathcal{E}_0 \vec{e}_z \cos(\vec{p}\vec{r} - E_p t), \quad \vec{\mathcal{H}}_{\text{in}}(t, \vec{r}) = [\vec{e}_x \times \vec{\mathcal{E}}_{\text{in}}], \quad \vec{p} = p \vec{e}_x. \quad (2.84)$$

Here $\vec{e}_{x(yz)}$ denotes the unit vector along the $x(yz)$ direction, $E_p = c p$ and c is the speed of light. We assume that the field weakly changes over the range of particle oscillations. Then the force acting on the charge is $\vec{F}(t) \approx \mathcal{E}_0 \vec{e}_z \cos(E_p t)$ and the oscillations are described by equation (2.52) of the previous section. The electric dipole moment induced in the system by the incident wave is given by

$$\vec{d}(t) = ez(t) = \frac{e^2 \mathcal{E}_0}{m} \frac{\cos(E_p t - \delta(E_p))}{\sqrt{(E_R^2 - E_p^2)^2 + \Gamma_{\text{tot}}^2 E_p^2}} \vec{e}_z, \quad \Gamma_{\text{tot}} = \Gamma + \Gamma_{\text{rad}}, \quad (2.85)$$

Γ_{tot} is the total width of the oscillator. The oscillating dipole emits electromagnetic waves. Therefore, there is a dissipative process due to the radiation friction force, $\Gamma_{\text{rad}} = 2e^2 E_p^2 / (3m c^3)$ for $E_p \lesssim E_R$, which we consider. The additional damping effects included in Γ are, e.g., due to atomic collisions, provided the charged particle oscillates in a medium. The formulated model is the well-known Lorentz model for vibrations of an electron in an atom. An ensemble of such oscillators resembles a dispersive medium.

Far from the dipole in the so-called wave zone $|d_{\text{max}}/e| \ll \lambda \ll r$, where $\lambda = 2\pi/p$ is the radiation wavelength and $|d_{\text{max}}/e|$ is the amplitude of the oscillations, the out-going waves of electric and magnetic fields are given by [51]

$$\begin{aligned} \vec{\mathcal{E}}_{\text{out}}(t, \vec{r}) &= \frac{1}{rc^2} [\vec{n}_r \times [\vec{n}_r \times \ddot{\vec{d}}(t - r/c)]], \\ \vec{\mathcal{H}}_{\text{out}}(t, \vec{r}) &= [\vec{n}_r \times \vec{\mathcal{E}}_{\text{out}}(t, \vec{r})] = \frac{1}{rc^2} [\ddot{\vec{d}}(t - r/c) \times \vec{n}_r] \end{aligned} \quad (2.86)$$

with $\vec{n}_r = \vec{r}/|\vec{r}|$. The time shift $t - r/c$ arises due to the finiteness of the speed of light. The scattered electric field is polarized along a meridian, $\vec{\mathcal{E}}_{\text{out}} \parallel \vec{e}_\theta$.

The differential cross-section for the scattering process can be defined as the ratio of the time-averaged intensity of the induced radiation $d\bar{I}$, passing through a sufficiently large sphere of radius R_0 , to the time-averaged energy flux of the incident wave falling on the oscillator; see section 78 in [51],

$$d\sigma = \frac{1}{\bar{S}_{\text{in}}} d\bar{I}, \quad dI = \bar{S}_{\text{out}} d\vec{s}_r. \quad \bar{S}_{\text{in(out)}} = \frac{c}{4\pi} [\vec{E}_{\text{in(out)}} \times \vec{H}_{\text{in(out)}}].$$

Here the line over a symbol means a time average over the oscillation period and $d\vec{s}_r$ is the element of the surface oriented in the direction \vec{n}_r . With the help of equations (2.84) and (2.86) we find

$$\bar{S}_{\text{in}} = \frac{c}{4\pi} \mathcal{E}_0^2 \cos^2(E_p t) \vec{e}_x, \quad dI = (\bar{S}_{\text{out}} \vec{n}_r) R_0^2 d\Omega = \frac{1}{4\pi c^3} [\ddot{\vec{d}}(t - R_0/c) \times \vec{n}_r]^2 d\Omega. \quad (2.87)$$

Using equation (2.85) and performing the averaging over time we obtain [51]

$$\frac{d\sigma}{d\Omega} = \left(\frac{e^2}{mc^2} \right)^2 \frac{E_p^4}{(E_R^2 - E_p^2)^2 + \Gamma_{\text{tot}}^2 E_p^2} [\vec{e}_z \times \vec{n}_r]^2. \quad (2.88)$$

We chose the spherical coordinate system so that the polar angle corresponds to the scattering angle θ —the angle between the propagation directions of in-coming and out-going waves, $\cos \theta = (\vec{n}_r \vec{p})/p$. Then the vector product in (2.88) can be written as $[\vec{e}_z \times \vec{n}_r]^2 = \cos^2 \theta + \sin^2 \theta \sin^2 \phi$. Thus the cross-section depends on the azimuthal angle that corresponds to a scattering of photons with different magnetic quantum numbers: $[\vec{e}_z \times \vec{n}_r]^2 = \frac{4\pi}{3} |Y_{1,0}(\theta, \phi) + (Y_{1,+1}(\theta, \phi) + Y_{1,-1}(\theta, \phi))/\sqrt{2}|^2$, where $Y_{l,m}(\theta, \phi)$ are the

spherical functions. The magnetic quantum number dependence appears because we have confined the oscillator motion to one dimension. For a spherically symmetric scattering this dependence would be averaged out.

The differential cross-section can now be written as

$$\frac{d\sigma}{d\Omega} = \frac{\pi}{p^2} \frac{3\Gamma_{\text{tot}}^2 E_p^2}{(E_{\text{R}}^2 - E_p^2)^2 + \Gamma_{\text{tot}}^2 E_p^2} B_{\text{rad}}^2 \left| Y_{10}(\theta, \phi) + \frac{1}{\sqrt{2}} (Y_{1-1}(\theta, \phi) + Y_{11}(\theta, \phi)) \right|^2, \quad (2.89)$$

where we introduced the branching ratio $B_{\text{rad}} = \Gamma_{\text{rad}}/\Gamma_{\text{tot}}$. One can introduce the scattering amplitude as

$$\frac{d\sigma}{d\Omega} = |f(\theta, \phi)|^2, \quad f(\theta, \phi) = \sum_{l=0}^{\infty} \sqrt{2l+1} \sqrt{4\pi} \sum_{m=-l}^l f_{l,m} Y_{l,m}(\theta, \phi). \quad (2.90)$$

For the spherically symmetrical scattering the amplitude would be

$$f(\theta) = \sum_{l=0}^{\infty} (2l+1) f_l P_l(\cos \theta). \quad (2.91)$$

Here $P_l(\cos \theta)$ are Legendre polynomials normalized as [52]: $\int_{-1}^1 P_l^2(x) dx = 2/(2l+1)$.

In our case the scattering amplitude has only terms with $l = 1$ and $\sqrt{2} f_{1,\pm 1} = f_{1,0} \equiv f_1$ with

$$2pf_1 = \frac{B_{\text{rad}} \Gamma_{\text{tot}} E_p}{E_{\text{R}}^2 - E_p^2 - i\Gamma_{\text{tot}} E_p} = \frac{B_{\text{rad}}}{\cot \delta(E_p) - i} = B_{\text{rad}} \sin \delta(E) e^{i\delta(E_p)}. \quad (2.92)$$

The phase of the scattered waves $\delta(E_p)$ is defined as in equations (2.53) and (2.54) but now with Γ_{tot} instead of Γ , i.e. $\tan \delta(E_p) = -\Gamma_{\text{tot}} E_p / (E_p^2 - E_{\text{R}}^2)$.

After integration over the scattering angle the total cross-section can be cast in the standard spin-averaged Breit–Wigner resonance form (see page 374 in [53])

$$\sigma = 2(2l+1)4\pi |f_l|^2 = \frac{3}{2} \frac{4\pi}{p^2} \frac{\Gamma_{\text{tot}}^2 E_p^2}{(E_{\text{R}}^2 - E_p^2)^2 + \Gamma_{\text{tot}}^2 E_p^2} B_{\text{rad}}^2. \quad (2.93)$$

Here the statistical factors correspond to the angular momentum, $l = 1$ in our case.

From the structure of equation (2.85) we see that the concepts of the phase and group time delays (2.55) and (2.64) are also applicable to electromagnetic waves, if we deal with not a monochromatic wave but a wave packet instead. If the in-coming waves were like $|\vec{\mathcal{E}}_{\text{in}}| = \mathcal{E}_0 f_{\mathcal{E}}(\vec{p}\vec{r} - E_p t) \cos(\vec{p}\vec{r} - E_p t)$ with some function $f_{\mathcal{E}}(x)$ integrable in the interval $(-\infty, +\infty)$, then the out-going wave would be $|\vec{\mathcal{E}}_{\text{out}}| \propto \mathcal{E}_0 f_{\mathcal{E}}(t - \delta t_s^{(\text{cl})} - r/c) \cos(pr - E_p [t - \delta(E_p)])$. The propagation of the scattered wave packet is delayed by the group time (2.64), see also (2.65), (2.66),

$$t_s^{(\text{cl})} = \frac{\partial \delta}{\partial E_p} \approx \frac{A}{2} = \frac{\Gamma_{\text{tot}}/2}{(E_p - E_{\text{R}})^2 + \Gamma_{\text{tot}}^2/4} > 0, \quad (2.94)$$

which here in the 3D case has the meaning of the scattering delay time, being twice as small compared to the Wigner delay time introduced above, see equation (2.21). Here we performed expansion in frequencies close to the resonance $E_p \sim E_{\text{R}}$. With $t_s^{(\text{cl})}$ from equation (2.94), the scattered wave appears with a delay compared to the condition $t - r/c \geq 0$. Thus causality requires that the scattered wave arises for $t - t_s^{(\text{cl})} - r/c \geq 0$.

2.2.2. Scattering of light on hard spheres. For the scattering of light on a hard sphere of radius R , the causality condition can be formulated as [2, 4]: if the incident wave propagating along the z direction vanishes for $t < z/c$, the scattered wave in the direction θ must vanish for $t < (r - 2R \sin(\theta/2))/c$. The quantity $2R \sin(\theta/2)$ is the difference in the paths of the light scattered at angle θ on the sphere surface and on the sphere center (2.81).

The scattering process (when the beam just touches the sphere) proceeds with half the advance time compared to R/c with which the light would pass to the center of the sphere, cf. (2.81). Correspondingly, the advancement in the scattering time, $\delta t_s^{(cl)}$, proves to be half that of the advancement in the Wigner time, $\delta t_W^{(cl)}$.

3. Time shifts in non-relativistic quantum mechanics: 1D-scattering

The problem of how to quantify a duration of quantum mechanical processes has a long and vivid history. It started with a statement of Pauli [54] that in the framework of traditional non-relativistic quantum mechanics it is impossible to introduce a Hermitian (self-adjoint) linear operator of time, which is canonically conjugate to the Hamiltonian. The reason for this is that for most of the systems of physical interest the Hamiltonian is bounded from below⁴. Later on a variety of ‘time-like’ observables were introduced tailored for each particular system. For a comprehensive review of the history of this question we address the reader to the introduction of [10]. Various inter-related definitions of time appeared, for instance, in consideration of the following questions: How long does the quantum transition (the quantum jump duration) last [56, 57]? What are interpretations of time–energy uncertainty relations [58]? How can one quantify the time-of-flight or the time of arrival of a particle to a given point [59, 60]? How long does it take for a particle to tunnel through a barrier [8, 13, 61–64]? What is the life-time of a resonance [3, 5, 20, 65, 66]? What is the duration of particle collision [1–3, 67]?

Without any pretense to address all these issues, in this section we would like to introduce the basic concepts related to the temporal characteristics of typical quantum mechanical processes, such as tunneling, scattering and decay.

3.1. The stationary problem

We begin with a 1D quantum–mechanical system, described by the Hamiltonian $\hat{H} = \hat{H}_0 + \hat{U}$ consisting of the free motion Hamiltonian $\hat{H}_0 = -\frac{\hbar^2}{2m} \frac{\partial^2}{\partial z^2}$ for a particle with mass m and of an arbitrary potential $\hat{U} = U(z) \geq 0$, which is assumed to be localized within the interval $-L/2 < z < L/2$ and vanishing elsewhere outside. This Hamiltonian has a continuous spectrum $0 < E < +\infty$ and the complete set of eigenfunctions $\psi(z; E)$ obeying the equation $\hat{H}\psi(z; E) = E\psi(z; E)$. We will consider the wave functions satisfying the asymptotic conditions for the standard scattering problem⁵

$$\psi_1(z; E) = \begin{cases} e^{ikz/\hbar} + R_1(E) e^{-ikz/\hbar}, & z < -\frac{1}{2}L, \\ \psi_{U,1}(z; E), & -\frac{1}{2}L \leq z \leq \frac{1}{2}L, \\ T_1(E) e^{+ikz/\hbar}, & \frac{1}{2}L < z, \end{cases} \quad (3.1)$$

$$\psi_2(z; E) = \begin{cases} T_2(E) e^{-ikz/\hbar}, & z < -\frac{1}{2}L, \\ \psi_{U,2}(z; E), & -\frac{1}{2}L \leq z \leq \frac{1}{2}L, \\ R_2(E) e^{+ikz/\hbar} + e^{-ikz/\hbar}, & \frac{1}{2}L < z, \end{cases} \quad (3.2)$$

⁴ Nowadays there continue attempts to introduce a formal quantum observable for time; see e.g. [55].

⁵ Instead of the basis wave functions for unilateral incidence one could use the symmetrical and anti-symmetrical wave functions $\psi_s = \psi_1 + \psi_2$ and $\psi_a = \psi_1 - \psi_2$ corresponding to bilateral incidence [68].

with $k = \sqrt{2mE} > 0$. The wave functions ψ_1 and ψ_2 describe the physical situation when a particle beam from the left or from the right, respectively, incident on the potential, becomes split into a reflected part with the amplitude $R_{1,2}$ and a transmitted part with the amplitude $T_{1,2}$. The wave functions are normalized to the unit incident amplitude. Then the quantities $|R_{1,2}|^2$ and $|T_{1,2}|^2$ mean the reflection and transmission probabilities, respectively, and $|R_{1,2}|^2 + |T_{1,2}|^2 = 1$. For any given wave function Ψ the current is calculated standardly,

$$\mathcal{J}[\Psi] = \frac{i\hbar}{2m} (\Psi \nabla_z \Psi^* - \Psi^* \nabla_z \Psi). \quad (3.3)$$

Thus, for the wave function ψ_1 we can define three currents: the incident current $j_I = \mathcal{J}[\exp(ikz/\hbar)] = \frac{k}{m}$, the transmitted current $j_T = \mathcal{J}[\psi_1(z > \frac{1}{2}L)] = |T_1(E)|^2 j_I$ and the reflected current $j_R = \mathcal{J}[\psi_1(z < -\frac{1}{2}L)] - j_I = -|R_1(E)|^2 j_I$. The current conservation is fulfilled and $j_I = j_T - j_R$. Here, it is important to notice that in the region of the potential there exists an ‘internal’ current $j_{\text{int}} = \mathcal{J}[\psi_{U,1}(z)]$. In the case of the classically allowed motion above the barrier, $j_{\text{int}} = j_T$ is determined by the sum of the currents of the forward-going wave and of the backward-going wave, whereas in the region under the barrier j_{int} is determined by the contribution of the interference of waves, since the coordinate dependence of the stationary wave function is given then by real functions. Namely the latter circumstance is the reason for the so-called Hartmann paradox of apparent superluminality of the under-the-barrier motion surviving in the case of wave packets infinitely narrow in energy space (the stationary state limit), which we will consider below.

The time-reversal invariance of the Schrödinger equation implies that $T_1(E) = T_2(E)$. In the general case of asymmetric potential $R_1 \neq R_2$. The functions $R_1(E)$, $R_2(E)$ and $T(E) = T_1(E) = T_2(E)$ form the S -matrix of the 1D-scattering problem [69]. The unitarity of the S -matrix implies the relation $T^*(E) R_2(E) = -R_1^*(E) T(E)$.

To simplify, in further consideration we will assume that the potential U is symmetric, $U(-z) = U(z)$. Then there is a symmetry between the reflected amplitudes $R_1(E) = R_2(E) = R(E)$, and the ‘internal’ parts of the wave functions $\psi_{U,1}(z; E) = \psi_{U,2}(z; E) = \psi_U(z; E)$ in equations (3.1), (3.2) can be written as superpositions of symmetric and anti-symmetric wave functions $\chi_+(z; E)$ and $\chi_-(z; E)$, respectively,

$$\psi_U(z; E) = C_+ \chi_+(z; E) + C_- \chi_-(z; E). \quad (3.4)$$

The functions are chosen such that $\chi_{\pm}(0; E) = L \chi'_{\mp}(0; E)/2 = (1 \pm 1)/2$, where the prime means the coordinate derivative. The coefficients C_{\pm} in equation (3.4) can be expressed through the scattering amplitudes as follows

$$C_{\pm} = \frac{(T \pm R) e^{ikL/2\hbar} \pm e^{-ikL/2\hbar}}{2 \chi_{\pm}(L/2; E)}. \quad (3.5)$$

The transmitted and reflected amplitudes are then expressed through the logarithmic derivatives of these functions

$$d_{\pm}(E) = \frac{L}{2} \frac{\partial}{\partial z} \ln \chi_{\pm}(z; E) \Big|_{z=L/2}, \quad (3.6)$$

which can be chosen as real. The amplitudes

$$R(E) = -\frac{1}{2} e^{-ikL/\hbar} [D_+(E) + D_-(E)], \quad T(E) = -\frac{1}{2} e^{-ikL/\hbar} [D_+(E) - D_-(E)] \quad (3.7)$$

are expressed through the functions

$$D_{\pm}(E) = \frac{d_{\pm}(E) + ikL/2\hbar}{d_{\pm}(E) - ikL/2\hbar} = e^{i2\delta_{\pm}(E)}, \quad \delta_{\pm}(E) = \arctan \left(\frac{kL}{2\hbar d_{\pm}(E)} \right), \quad (3.8)$$

which have simple poles. The reflected and transmitted amplitudes can be now written as

$$\begin{aligned} R(E) &= e^{i\phi_R} \cos(\delta_+(E) - \delta_-(E)), & \phi_R(E) &= \pi - \frac{kL}{\hbar} + \delta_s(E), \\ T(E) &= e^{i\phi_T} \sin(\delta_+(E) - \delta_-(E)), & \phi_T(E) &= \frac{3}{2}\pi - \frac{kL}{\hbar} + \delta_s(E), \end{aligned} \quad (3.9)$$

where we introduced an ordinary 1D-scattering phase shift [69]

$$\delta_s(E) = \delta_+(E) + \delta_-(E). \quad (3.10)$$

For sum and differences of the phases δ_+ and δ_- one can use the following relation

$$\tan(\delta_+(E) \pm \delta_-(E)) = \frac{kL}{2\hbar} \frac{d_- \pm d_+}{d_- d_+ \mp \frac{k^2 L^2}{4\hbar^2}}. \quad (3.11)$$

The coefficients of the internal wave function (3.4) can be expressed with the help of equations (3.7) and (3.8) through the logarithmic derivatives as follows

$$2\chi_{\pm}(L/2; E)C_{\pm} = \mp \frac{ikL}{\hbar} \frac{e^{-ikL/2\hbar}}{d_{\pm} - ikL/2\hbar}. \quad (3.12)$$

Substituting a scattering wave function ψ_1 or ψ_2 in equation (B.4) of appendix B we find the relation between the integral of the internal part of the wave function, ψ_U , and the scattering amplitudes and phase derivatives

$$\int_{-L/2}^{+L/2} dz |\psi_U(z; E)|^2 = L + \hbar \frac{k}{m} |T(E)|^2 \phi'_T(E) + \hbar \frac{k}{m} |R(E)|^2 \phi'_R(E) + \frac{\hbar}{k} \text{Im}(R(E) e^{+ikL/\hbar}), \quad (3.13)$$

here the prime stands for the derivative with respect to the energy. The last term appears due to interference of the reflected and incident waves.

Note that all derived expressions are valid for the description of the scattering on an arbitrary (symmetric) finite-range potential. Thus we are able to consider on equal footing the particle tunneling, scattering above the barrier, as well as the scattering on quasi-stationary levels, provided in the latter case the potential has a hole $U_{\min} < U < U_{\max}$ in some interval $-L/2 < -a < z < a < L/2$ and $U_{\min} < E < U_{\max}$.

The above expressions can be also applied for the situation where only a half of the coordinate space is available for the particle motion. Such a situation is discussed in section 3.9, where we describe the decay of quasi-stationary states. Then we can use the wave function ψ_1 (see equation (3.1)), with the condition $\psi_1(0) = 0$, if the particle motion is allowed in the left half-space ($z < 0$), or we can use the wave function ψ_2 (equation (3.1)) with the condition $\psi_2(0) = 0$, if particles move in the right half-space ($z > 0$). The presence of the wall at $z = 0$ requires that only the anti-symmetric wave function survives in (3.4) and the internal wave function becomes equal to

$$\psi_U(z; E) = \tilde{C}_- \chi_-(z; E), \quad \tilde{C}_- = 2C_-. \quad (3.14)$$

This is easily taken into account in the above general expressions by the replacement $d_+ \rightarrow d_-$. After this, the transmitted wave disappears, $T = 0$, and the reflected wave amplitude reduces to a pure phase multiplier, $R = e^{i\phi_s(E)}$, with

$$\phi_s(E) = \pi - \frac{kL}{\hbar} + 2\delta_-(E). \quad (3.15)$$

Note that the wave function of the radial motion in a 3D scattering problem is similarly described, where δ_- ($\delta_- = \delta_+$ for symmetric potential) plays the role of the scattering phase; see section 4 below.

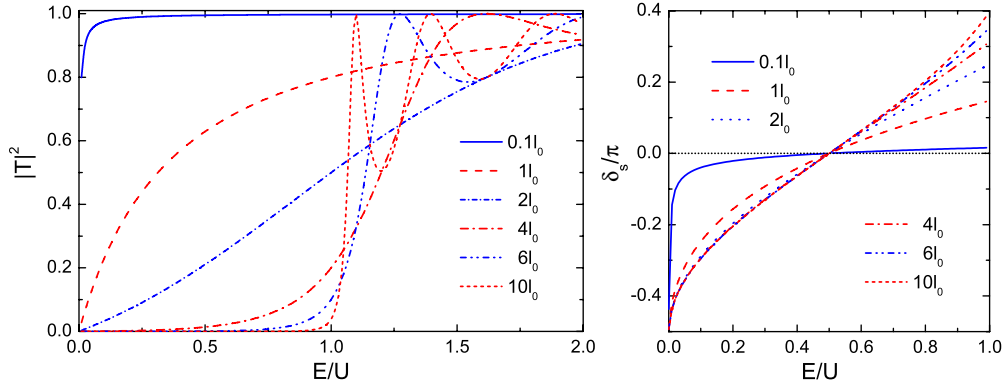


Figure 8. The amplitude and phase of the transmission wave for the rectangular barrier of height U and length L calculated according to equations (3.18) and (3.19). Various curves correspond to barriers of different lengths L , shown by labels in units of $l_0 = \hbar/\sqrt{2mU}$.

Example: scattering on a rectangular barrier

Consider a rectangular potential barrier of length L : $U(z) = U = \text{const} > 0$ for $-L/2 < z < L/2$. We assume first that $E < U$. Then we deal with a tunneling problem. The wave function ψ_U in the internal region (see equation (3.4)), is decomposed into the following even and odd functions:

$$\chi_+(z; E) = \cosh(\kappa z/\hbar), \quad \chi_-(z; E) = \sinh(\kappa z/\hbar), \quad \kappa = \sqrt{2m(U - E)} > 0. \quad (3.16)$$

The logarithmic derivatives follow then as

$$d_+ = \frac{\kappa^2 L^2}{4\hbar^2 d_-} = \frac{\kappa L}{2\hbar} \tanh(\kappa L/2\hbar). \quad (3.17)$$

The phases of transmitted and reflected amplitudes in (3.9) can now be written through the scattering phase:

$$\delta_s(E) = -\arctan\left(\frac{\kappa^2 - k^2}{2k\kappa} \tanh(\kappa L/\hbar)\right). \quad (3.18)$$

We used here the relation $\tan(\pi/2 + \arctan(1/x)) = -x$. The squared amplitudes are given by

$$|R|^2 = \frac{(\kappa^2 + k^2)^2}{(\kappa^2 - k^2)^2} \sin^2 \delta_s = \frac{(\kappa^2 + k^2)^2 \sinh^2(\kappa L/\hbar)}{(\kappa^2 + k^2)^2 \sinh^2(\kappa L/\hbar) + 4k^2 \kappa^2},$$

$$|T|^2 = 1 - |R|^2 = \frac{\cos^2 \delta_s}{\cosh^2(\kappa L/\hbar)} = \frac{4k^2 \kappa^2}{(\kappa^2 + k^2)^2 \sinh^2(\kappa L/\hbar) + 4k^2 \kappa^2}. \quad (3.19)$$

The coefficients C_{\pm} in (3.5) can be expressed now as follows

$$C_+ = \frac{-i e^{-ikL/2\hbar}}{\frac{\kappa}{k} \sinh\left(\frac{\kappa L}{2\hbar}\right) - i \cosh\left(\frac{\kappa L}{2\hbar}\right)}, \quad C_- = \frac{i e^{-ikL/2\hbar}}{\frac{\kappa}{k} \cosh\left(\frac{\kappa L}{2\hbar}\right) - i \sinh\left(\frac{\kappa L}{2\hbar}\right)}. \quad (3.20)$$

The amplitudes R and T can be written as functions of two dimensionless variables characterizing the energy of the incident particle, E/U , and the width of the potential, L/l_0 , where $l_0 = \hbar/\sqrt{2mU}$. These functions are illustrated in figure 8. For a thin barrier, $L \lesssim l_0$, the transmission probability is close to unity and the scattering phase is small except for very small energies. For $E < U$ the transmission probability decreases gradually with an increase of L until $L \simeq 2l_0$ and than falls off exponentially for larger L . The scattering phase is a monotonously growing function of the energy.

If we replace $\kappa \rightarrow i|\kappa|$, equations (3.18) and (3.19) also can be used for $E > U$ (scattering above the barrier). For $E > U$, the transmission probability is finite approaching unity for $E \gg U$ unsteadily exhibiting peaks at $E/U = 1 - \pi^2 n^2 l_0^2 / 4L^2$ with integer n . For the peaks $|T| = 1$, see figure 8.

3.2. Characteristics of time in the stationary scattering problem

Within the stationary scattering problem formulated above there is no notion of time *per se*, since the only t -dependent overall factor $e^{-iEt/\hbar}$ does not enter physical quantities. However, we have at our disposal quantities, which can be used to construct a measure with the dimensionality of time. Such a quantity describing the transmitted waves (at $z > L/2$) arises, for example, if we divide the integral of the squared wave function $\int_a^b |\psi(z; E)|^2 dz$ by a current. The flux density outside the barrier does not depend on the coordinate. So we can use an expression for the transmitted flux density $j_T = |T(E)|^2 k/m$. Then for any interval with $a, b > \frac{1}{2}L$ the quantity

$$\frac{1}{j_T} \int_a^b |\psi(z; E)|^2 dz = \frac{b-a}{v} \tag{3.21}$$

is just a passage time of the segment $[a, b]$ by a particle with the velocity $v = k/m$. An application of this quantity to the left from the barrier for $a, b < -\frac{1}{2}L$ could be meaningless, since, e.g., in the case of the full wave reflection from an infinite barrier the total flux vanishes $|j_I| - |j_R| = j_T = 0$. On the other hand, the reflected current also cannot be used since it vanishes for the free particle motion. Thus, in order to construct a relevant time-quantity for a particle moving in the segment $[a, b]$ with $a, b < -\frac{1}{2}L$ we divide the squared wave function by the incident current

$$\frac{1}{j_I} \int_a^b |\psi(z; E)|^2 dz = \frac{b-a}{v} (1 + |R|^2) + \frac{\hbar}{kv} |R| \sin(2kz/\hbar - \phi_R) \Big|_a^b. \tag{3.22}$$

The first term represents the passage time of the incident wave in the forward direction through the segment $[a, b]$ (the unity in the brackets) and the passage time of the reflected wave in the backward direction ($|R|^2$ in the brackets). For a fully opaque barrier $|R| = 1$ we obviously get $2(b-a)/v$. The second term appears due to the interference of the incident and reflected waves. It can be neglected only in the short de Broglie wavelength limit $\hbar/k \ll (b-a)$.

Another approach to the definition of time is to introduce an explicit ‘clock’—a microscopic device characterized by a simple time variation with a constant well-defined period—which is weakly coupled to a quantum system under investigation. From a change of the clock’s ‘pointer’ one can then read off a duration of the process in the quantum system measured in terms of the clock’s period. Such a procedure was proposed by Salecker and Wigner in [70] for measurements of space–time distances. Peres in [71] extended this concept to several quantum mechanical problems including a time-of-flight measurement of the velocity of a free non-relativistic particle.

Back in 1966, Baz [65] proposed the use of the Larmor precession, as a measure of a scattering time in quantum mechanics. He ascribed spin $\frac{1}{2}$ and a magnetic moment μ to the scattered particle and assumed the presence of a weak magnetic field B within the finite space region of interest, e.g. within a range of potential. The difference in the spin polarization before and after the region proportional to $-\frac{1}{2}\hbar\omega_L t_L$, where $\omega_L = \mu B/\hbar$ is the Larmor frequency, gives the time the particle takes to traverse the region. For a 1D case this approach was adopted by Rybachenko in [72]. In the framework of the time-dependent formalism the spin-clock method was analyzed in [73].

In [74] Büttiker showed that for a 1D-scattering problem the Larmor precession time introduced in [65, 72] is equivalent to the *dwell time*

$$t_d(a, b, E) = \frac{1}{j_1} \int_a^b |\psi(z; E)|^2 dz, \quad (3.23)$$

which tells us how long the incident current j_1 must be turned on to produce the necessary particle storage within the segment $[a, b]$; see (3.22). This time is a quantum-mechanical counter part of the classical 1D dwell time (2.2). Indeed, as follows from the Schrödinger equation, the probability density given by the square of the wave function satisfies the continuity equation, as for water in a clepsydra.

The value

$$\delta t_d(a, b, E) = t_d(a, b, E) - (b - a)/v \quad (3.24)$$

shows the difference between the time which a particle spends in the segment $[a, b]$ of the potential and the time if the potential in this region were switched off.

For the case $E > \max U$ the classical motion is allowed for any z and the time a particle needs to move from $-L/2$ to $+L/2$ —the *classical traversal time*—is

$$t_{\text{trav}}^{(\text{cl})}(E) = \int_{-L/2}^{+L/2} \frac{dz}{\sqrt{2(E - U(z))/m}}; \quad (3.25)$$

cf. the definition of the classical sojourn time (2.4). However, when the energy is smaller than a potential maximum, there appears an imaginary contribution to this quantity from the integration between the turning points $z_1(E)$ and $z_2(E)$, which are solutions of the equation $U(z_{1,2}) = E$. The imaginary-time pattern is used in the so-called imaginary-time formalism, being successfully applied in the problems of quantum tunneling through time-dependent barriers; see the review [75]. Nevertheless the imaginary time can hardly be used as the typical time for the passing of the barrier.

Reference [76] considered the electron–positron pair production within the imaginary-time formalism and estimated the traversal time of the barrier as its length divided by the velocity of light c (for relativistic particles). The inverse quantity $\omega_{\text{tun}} \sim |\nabla U|/mc$ separates then two regimes of particle production in rapidly varying potentials (for $\omega > \omega_{\text{tun}}$) and that in static fields (for $\omega \ll \omega_{\text{tun}}$). Similarly, Büttiker and Landauer [77] argued in favour of using the quantity

$$t_{\text{trav}}^{(\text{BL})}(E) = \int_{-L/2}^{+L/2} \frac{dz}{\sqrt{2|E - U(z)|/m}} = \int_{-L/2}^{+L/2} \frac{m dz}{\chi(z, E)} \quad (3.26)$$

for the description of the tunneling time through rapidly varying barriers at non-relativistic particle motion. Also, they conjectured using this value to estimate the traversal time of the tunneling through stationary potential barriers. Reference [78] has shown that this time arises as a standard dispersion of the tunneling time distribution. Support for the usage of (3.26) to estimate the time of particle passage through barriers comes from analysis of the radiation spectral density for charged particles traversing the barrier, which is determined by the ordinary classical formula [79]: $(\partial E_\omega / \partial \omega)_t \propto e^2 \omega^2 k^2 (t_{\text{trav}}^{\text{BL}})^2 / m^2$, where $t_{\text{trav}}^{\text{BL}}$ is entered as the time of the passing of the barrier region.

Also, one can formally construct an analogue of the phase time, as in equation (2.55) in section 2, e.g., $\delta t_{\text{ph,R}}(E) = \hbar(\phi_R(E) - \pi)/E$ and $\delta t_{\text{ph,T}}(E) = \hbar(\phi_T(E) - \pi)/E$, as time shifts between incident and reflected and transmitted waves, but these time shifts are not associated with observables.

Relevant quantities are the group times $\hbar d\phi_R(E)/dE$ and $\hbar d\phi_T(E)/dE$, cf. equation (2.11), similar to those we introduced in section 2. These quantities will be discussed in more detail below.

Another aspect of stationary problems relates to the description of bound states arising in the case of attractive stationary potentials. Inside the potential well, i.e. for $z \in [z_1, z_2]$, where z_1 and z_2 are turning points, the semiclassical wave function can be written in two ways [80]:

$$\psi^{(\text{scl})}(z; E) = \frac{C_1}{\sqrt{|\chi(z, E)|}} \cos\left(\int_{z_1}^z |\chi(z', E)| dz'/\hbar - \phi_<\right) \quad (3.27)$$

or

$$\psi^{(\text{scl})}(z; E) = \frac{C_2}{\sqrt{|\chi(z, E)|}} \cos\left(\int_z^{z_2} |\chi(z', E)| dz'/\hbar - \phi_>\right), \quad (3.28)$$

where $\phi_< = \phi_> = \pi/4$, provided the potential is a smooth function of z near the turning points. Note that in the purely quantum case the phase shifts of in-going and out-going waves for the bound states may depend on E . The condition of coincidence of these solutions yields $C_1 = C_2(-1)^n$ and we get the Bohr–Sommerfeld quantization rule

$$\int_{z_1}^{z_2} |\chi(z, E)| dz = \hbar(\pi n + \phi_< + \phi_>), \quad n = 0, \pm 1, \dots \quad (3.29)$$

From this rule for the passage time of the potential well one gets

$$t_{\text{trav}}^{(\text{scl})}(z_1, z_2, E) = \frac{1}{2}P = \hbar\pi \frac{dn}{dE} + t_{\text{gr}}^< + t_{\text{gr}}^>, \quad (3.30)$$

where P is the period of motion, $\frac{dn}{dE}$ is the number of states per unit energy, $t_{\text{gr}}^< = \hbar d\phi_</dE$, $t_{\text{gr}}^> = \hbar d\phi_>/dE$ and for the semiclassical motion $t_{\text{gr}}^< + t_{\text{gr}}^> = 0$. Replacing (3.28) with appropriate normalization in (3.23) we get $t_{\text{trav}}^{(\text{scl})}(z_1, z_2, E) \simeq t_{\text{d}}(z_1, z_2, E)$.

Example: dwell time for a rectangular barrier

We apply the dwell time definition (3.23) to the wave function (3.4), (3.16) and calculate the dwell time of the particle under the barrier. The incident current is $j_{\text{i}} = k/m$ and

$$\begin{aligned} t_{\text{d}}(-L/2, L/2, E) &= \frac{m}{k} \int_{-L/2}^{+L/2} \{|C_+|^2 \cosh^2(\chi z/\hbar) + |C_-|^2 \sinh^2(\chi z/\hbar)\} dz \\ &= \frac{mL}{2k} (|C_+|^2 - |C_-|^2) + \frac{m}{2k} \frac{\hbar}{\chi} \sinh(\chi L/\hbar) (|C_+|^2 + |C_-|^2). \end{aligned} \quad (3.31)$$

We see that the dwell time contains two time-scales: one is the free traversal time mL/k and the other is a purely quantum scale $m\hbar/k|\chi|$. Namely, the former quantity determines the traveling time for classically allowed motion with $E \gg U$. The internal wave function given by equations (3.4) and (3.16), ψ_U , is expressed in terms of evanescent and growing functions $\psi_U^{(\text{evan})} = \frac{1}{2}(C_+ - C_-) e^{-\chi z/\hbar}$ and $\psi_U^{(\text{grow})} = \frac{1}{2}(C_+ + C_-) e^{+\chi z/\hbar}$. Using equations (3.18) and (3.20), after some algebra we split equation (3.31) into the terms:

$$\begin{aligned} t_{\text{d}}^{(\text{evan})} &= \frac{m}{k} \int_{-L/2}^{+L/2} \frac{1}{4} |C_+ - C_-|^2 e^{-2\chi z/\hbar} dz = \frac{m\hbar}{k\chi} \cos^2 \delta_s \frac{k^2 + \chi^2}{2\chi^2} \tanh(\chi L/\hbar) \frac{e^{\chi L/\hbar}}{2 \cosh(\chi L/\hbar)}, \\ t_{\text{d}}^{(\text{grow})} &= \frac{m}{k} \int_{-L/2}^{+L/2} \frac{1}{4} |C_+ + C_-|^2 e^{2\chi z/\hbar} dz = \frac{m\hbar}{k\chi} \cos^2 \delta_s \frac{k^2 + \chi^2}{2\chi^2} \tanh(\chi L/\hbar) \frac{e^{-\chi L/\hbar}}{2 \cosh(\chi L/\hbar)}, \\ t_{\text{d}}^{(\text{evan})} + t_{\text{d}}^{(\text{grow})} &= \frac{m\hbar}{k\chi} \cos^2 \delta_s \frac{k^2 + \chi^2}{2\chi^2} \tanh(\chi L/\hbar), \end{aligned} \quad (3.32)$$

and the correlation term

$$t_{\text{d}}^{(\text{cor})} = \frac{1}{2} \text{Re} \{(C_+ - C_-)(C_+ + C_-)^*\} L = \frac{mL}{k} \cos^2 \delta_s \frac{(\chi^2 - k^2)}{2\chi^2 \cosh^2(\chi L/\hbar)}. \quad (3.33)$$

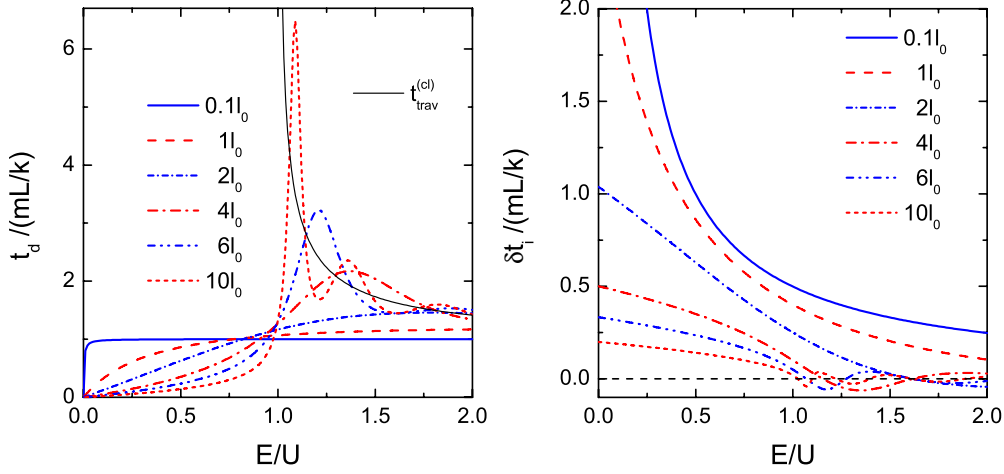


Figure 9. The dwell time (3.34) (left panel) and the interference time (3.88) (right panel) for the rectangular barrier depicted as a function of the energy for various barrier lengths measured in units $l_0 = \hbar/\sqrt{2mU}$. The thin solid curve on the left panel shows the classical traversal time (3.25) for the rectangular barrier.

Interestingly, the traversal time-scale $\propto L$ appears in an interference term $t_d^{(\text{cor})} \propto U$ between evanescent and growing waves, whereas the quantum term appears in a sum of the dwell times constructed from the pure evanescent and growing waves, $t_d^{(\text{evan})}$ and $t_d^{(\text{grow})}$.

For tunneling, $E < U$, through a thick barrier, $\kappa L/\hbar \gg 1$, we have

$$t_d \simeq t_d^{(\text{evan})},$$

since $t_d^{(\text{cor})}/t_d^{(\text{evan})} \sim t_d^{(\text{grow})}/t_d^{(\text{evan})} \sim e^{-2\kappa L/\hbar} \ll 1$. The integral in $t_d^{(\text{evan})}$ is determined by the region near $z = -L/2$ (provided particles flow on the barrier from the left). Thus in this case the dwell time of particles under the barrier is determined by the inflow near the left edge of the barrier and does not describe particle transmission. This observation partially corrects the statement in [8, p 7], that the dwell time of particles under the barrier ‘...does not distinguish transmitted particles from reflected particles’ and ‘tells us the dwell or sojourn time in the barrier regardless of whether the particle is transmitted or reflected at the end of its stay’.

Combining equations (3.32) and (3.33) we obtain

$$t_d(-L/2, L/2, E) = \frac{mL \cos^2 \delta_s}{2k} \left[\frac{k^2 + \kappa^2 \tanh(\kappa L/\hbar)}{\kappa^2} \frac{1}{\kappa L/\hbar} - \frac{k^2 - \kappa^2}{\kappa^2} \frac{1}{\cosh^2(\kappa L/\hbar)} \right]. \quad (3.34)$$

The behavior of this value is illustrated in figure 9, left. We see that for $E > U$ expression (3.34) exhibits peaks, when the system gets stuck above the barrier in resonance states, for which the barrier becomes effectively absolutely transparent (maxima of $|T|^2$ in figure 8). The resonance energy is determined by the condition $|\kappa|L/\hbar = \pi n$ for an integer $n > 0$. The peak heights increase with the barrier thickness as $(mL/k)[1 + 2L^2/(l_0^2 n^2 \pi^2)]$. The time (3.25) of the traversal of the distance L at resonance energies can be related to the density of the resonance states:

$$t_{\text{trav}}^{(\text{scl})} = \frac{Lm}{|\kappa|} = \pi \hbar \frac{dn}{dE}. \quad (3.35)$$

For $E \gg U$ we get

$$t_d(-L/2, L/2, E) = \frac{mL}{k} \left[1 + \frac{U}{2E} - \sin(2\kappa L/\hbar) \frac{l_0^2}{4L^2} \left(\frac{U}{E} \right)^{3/2} + O\left(\frac{U^2}{E^2} \right) \right]. \quad (3.36)$$

As we see from figure 9, for $E > U$ the dwell time oscillates around the classical traversal time and approaches it for $E \gg U$ as

$$|t_{\text{trav}}^{(\text{cl})}(-L/2, L/2, E) - t_{\text{d}}(-L/2, L/2, E)| < \frac{mL}{k} \left[\frac{l_0^2}{4L^2} \left(\frac{U}{E} \right)^{3/2} + O\left(\frac{U^2}{E^2} \right) \right]. \quad (3.37)$$

For a broad barrier in the limit $|\kappa|L/\hbar \gg 1$ and for $E \geq U$ we have for the dwell time

$$t_{\text{d}}(-L/2, L/2, E_p) \simeq t_{\text{d}}^{(\text{cor})} \simeq \frac{mL}{k} \frac{2k^2(k^2 + |\kappa|^2)}{[(|\kappa|^2 - k^2)^2 \sin^2(|\kappa|L/\hbar) + 4|\kappa|^2 k^2]}. \quad (3.38)$$

As follows from this expression the dwell time exceeds the classical free traversal time $t_{\text{trav}}^{\text{free}} = mL/k$.

For $E = U$ and arbitrary L the dwell time is

$$t_{\text{d}}(-L/2, L/2, E = U) = \frac{4}{3} \frac{mL}{k} \frac{1 + 3l_0^2/L^2}{1 + 4l_0^2/L^2}. \quad (3.39)$$

In the tunneling regime $E < U$ the dwell time starts from zero at $E = 0$, increases with the increase of E and reaches the free traversal time mL/k at

$$E_1 = U \frac{1 + 3bl_0^2/L^2}{1 + 4bl_0^2/L^2}, \quad b \approx 2.5484. \quad (3.40)$$

It is interesting to note that the dwell time is *always* smaller than the classical traversal time for energies of the scattered particle $E < U$ for a thick barrier and $E < \frac{3}{4}U$ for a thin barrier.

Since in the tunneling regime the dwell time decreases with an increase of the barrier depth, and $t_{\text{d}}(E \rightarrow 0) \rightarrow 0$, the dwell time cannot be an appropriate measure of the time passage through the barrier.

3.3. The non-stationary problem: the scattering of a wave packet

The evolution of a quantum-mechanical system from the time moment t_0 until the time moment t is determined by the Hamilton operator: $\Psi(z, t) = \exp(-i\hat{H}(t - t_0))\Psi(z, t_0)$. A non-stationary quantum state, i.e. a state for which physical observables change with time, thus, cannot be an eigenstate of the Hamiltonian. Otherwise the time variations reduce to a phase factor $\exp(-iE(t - t_0))$, which does not enter observables. Hence, in order to describe the passage time of some spatial interval by a quantum particle we need to deal with a *wave packet* describing by a superposition of stationary states with various energies E , $\psi(z; E)$,

$$\Psi(z, t) = \int_0^\infty \frac{dE}{2\pi\hbar} \Phi(E) \psi(z; E) e^{-iEt/\hbar}, \quad (3.41)$$

with some $\Phi(E)$ as the energy envelop function. Such a packet would necessarily have some spatial extension, which is larger the smaller the energy spread of the states collected in the packet is. As we discuss in this section, the mentioned delocalization makes determination of the passage time of a spatial interval by a quantum particle a delicate problem.

As the stationary wave function $\psi(z; E)$ we can take the wave function (3.1), $\psi(z; E) = C\psi_1(z, E)$. The normalization constant C can be determined from the relation

$$\int_{-\infty}^\infty dz \psi^*(z; E) \psi(z; E') = 2\pi\hbar \sqrt{\frac{2E}{m}} \delta(E - E') = 2\pi\hbar \delta(k - k'), \quad (3.42)$$

where $k = \sqrt{2mE}$ and $k' = \sqrt{2mE'}$. The wave function of the wave packet (3.41) can be normalized as

$$\int_{-\infty}^\infty dz |\Psi(z, t)|^2 = \int_0^\infty \frac{dE}{2\pi\hbar} \sqrt{\frac{2E}{m}} |\Phi(E)|^2 = 1. \quad (3.43)$$

Then the quantity

$$dW_E = \sqrt{\frac{2E}{m}} |\Phi(E)|^2 \frac{dE}{2\pi\hbar} \quad (3.44)$$

is interpreted as the probability for the particle described by the wave packet to have the energy within the segment $[E, E + dE]$. The average energy of the state, \bar{E} , is given by

$$\bar{E} = \int_{-\infty}^{\infty} dx \Psi^*(x, t) \hat{H} \Psi(x, t) = \int_0^{\infty} \frac{dE}{2\pi\hbar} E \sqrt{\frac{2E}{m}} |\Phi(E)|^2. \quad (3.45)$$

Similarly, the energy dispersion of the wave packet is given by

$$\gamma^2 = \int_{-\infty}^{\infty} dx \Psi^*(x, t) (\hat{H}^2 - \bar{E}^2) \Psi(x, t) = \int_0^{\infty} \frac{dE}{2\pi\hbar} (E^2 - \bar{E}^2) \sqrt{\frac{2E}{m}} |\Phi(E)|^2. \quad (3.46)$$

Formally, we can change an integration variable from E to $k = \sqrt{2mE}$ and rewrite the distribution (3.44) as

$$dW_E = |\varphi(k)|^2 \frac{dk}{2\pi\hbar}, \quad \varphi(k) = \frac{k}{m} \Phi(k^2/2m), \quad (3.47)$$

and the wave packet (3.41), as

$$\Psi(z, t) = \int_0^{\infty} \frac{dk}{2\pi\hbar} \varphi(k) \psi(z; k^2/2m) e^{-ik^2t/2m\hbar}. \quad (3.48)$$

We emphasize that the quantity $|\varphi(k)|^2$ cannot be identified with a momentum distribution of the state, since in general the wave function $\psi(z; E = k^2/2m)$ is not an eigenfunction of the momentum operator. However, in the remote past, i.e. for large and negative t , when the peak of the packet is at large and negative $z \ll -L$, we deal with a free wave packet. Then only one term of the wave function (3.1) contributes to the integral (3.48). Indeed, only in the term proportional to e^{ikz} for $z \ll -L$ the exponents under the integral in equation (3.48) can cancel each other for $z \sim tk/m$. Thus, in the past the maximum of the packet located far to the left of the barrier⁶—an incident wave packet

$$\Psi(z, t) \approx \Psi_I(z, t) = \int_0^{\infty} \frac{dk}{2\pi\hbar} \varphi(k) e^{ikz/\hbar} e^{-ik^2t/2m\hbar}, \quad (3.49)$$

moves to the right. In this limit the quantity $|\varphi(k)|^2$ defines the asymptotic momentum distribution in the packet. Note that there is always a small but finite probability for the particle to be at any point of the z -axis.

The momentum average and variance are then given by

$$p = \langle k \rangle_k, \quad \gamma_p^2 = \langle (k^2 - p^2) \rangle_k. \quad (3.50)$$

Here we use the notation

$$\langle \dots \rangle_k = \int_0^{\infty} \frac{dk}{2\pi\hbar} (\dots) |\varphi(k)|^2 \quad (3.51)$$

for the average over the momentum distribution. The average energy and momentum are related as $\bar{E} = (p^2 + \gamma_p^2)/2m$. For evaluation of the k -averages (3.51) of a function f dependent on k we can use the relation

$$\langle f(k) \rangle_k \approx f(p) + \frac{1}{2} \gamma_p^2 \frac{d^2 f(p)}{dp^2} = f(E_p) + \frac{\gamma_p^2}{2m} \frac{df(E_p)}{dE_p} + \frac{\gamma_p^2 p^2}{2m^2} \frac{d^2 f(E_p)}{dE_p^2}, \quad (3.52)$$

provided γ_p is small. We used equation (3.50) and in the second equality we changed variables from p to $E_p = p^2/2m$.

⁶ Had we taken the wave function (3.2) in equation (3.48) we would get that for large negative t the maximum of the packet is located far to the right of the barrier and the packet proceeds to the left.

The momentum profile function $\varphi(k)$ is complex, $\varphi(k) = |\varphi(k)| e^{i\xi(k)}$. The derivative of its phase with respect to momentum, $\xi'(k)$, determines the average coordinate of the incident packet [81]

$$\begin{aligned} \bar{z}_1(t) &= \int_{-\infty}^{-L/2} dz z |\Psi_1(z, t)|^2 / \int_{-\infty}^{-L/2} dz |\Psi_1(z, t)|^2 \approx \bar{z}_1^{(\text{as})}(t) = \int_{-\infty}^{+\infty} dz z |\Psi_1(z, t)|^2 \\ &= \left\langle -\hbar\xi'(k) + \frac{k}{m} t \right\rangle_k = \langle -\hbar\xi'(k) \rangle_k + v_1 t, \quad v_1 = \frac{p}{m}. \end{aligned} \quad (3.53)$$

Note that the second approximate equality in the first line is valid, if at time t the packet is located almost entirely to the left of the barrier. It is valid for $\gamma_p(-z_0 + L) \gg \hbar$ for large negative t . The derivation of this relation is given in appendix C. Let us fix the phase $\xi(k)$ so that in the remote past at t_0 the packet center was at $z_0 = v_1 t_0$, then $-\hbar\xi'(k) = z_0 - k t_0/m$ and therefore $\langle -\hbar\xi'(k) \rangle_k = 0$.

The evolution of the packet width in the coordinate space is determined by the function $\varphi(k)$ as

$$\begin{aligned} \overline{z}_1^2(t) - \bar{z}_1^2(t) &\approx \frac{\hbar}{4\pi} |\varphi(0)'| |\varphi(0)| + \hbar^2 \left\langle \left(\frac{|\varphi(k)'|}{|\varphi(k)|} \right)^2 \right\rangle_k \\ &+ \left\langle \left(\hbar\xi'(k) - \frac{k}{m} t \right)^2 \right\rangle_k - \left\langle \left(\hbar\xi'(k) - \frac{k}{m} t \right) \right\rangle_k^2. \end{aligned} \quad (3.54)$$

For the description of a remote solitary incident packet moving to the right with an initial average energy $\simeq \bar{E}$ the envelop function $\Phi(E)$ must be sharply peaked at $E = \bar{E}$, or equivalently for the description of the packet moving with the average momentum p the function $\varphi(k)$ must be sharply peaked at $k = p$. If the widths of the peaks of the functions $\Phi(E)$ and $\varphi(k)$ are sufficiently small, i.e. $\gamma_p \ll p$ and $\gamma \ll \bar{E}$, the lower limit in all momentum and energy integrations can be extended to $-\infty$. Often, the normalized momentum profile function is chosen in the Gaussian form

$$\varphi(k) = \left(\frac{2\pi \hbar^2}{\gamma_p^2} \right)^{1/4} \exp \left(-\frac{(k-p)^2}{4\gamma_p^2} + i\xi(k) \right). \quad (3.55)$$

Then, using $-\hbar\xi'(k) = z_0 - k t_0/m$ we find from equation (3.54)

$$\overline{z}_1^2(t) - \bar{z}_1^2(t) = \frac{\hbar^2}{4\gamma_p^2} + \frac{\gamma_p^2}{m^2} (t - t_0)^2, \quad (3.56)$$

where we used that for a narrow packet $|\varphi(0)| \rightarrow 0$. We recover the well-known result that the width of a free packet increases with time. For the typical time of the smearing of the packet we immediately get $t - t_0 \sim t_{\text{sm}}$, where

$$t_{\text{sm}} = \hbar m / \gamma_p^2. \quad (3.57)$$

The wave packet (3.49) contains only modes with positive momenta and describes a system which propagates freely from left to right with the center moving with the velocity v_1 , see equation (3.53). If we define the probability of finding the particle to the left from some finite coordinate z' , i.e. for any $z < z'$,

$$P_{z'}(t) = \int_{-\infty}^{z'} dz |\Psi_1(z, t)|^2,$$

it must vanish for very large t : $P_{z'}(t \rightarrow \infty) = 0$. One would also expect this probability to be a monotonically decreasing function of time, which according to the continuity equation

$$\frac{dP_{z'}(t)}{dt} = -j(z', t)$$

implies that the current flowing through the point z' is positive at any moment of time. It was noted already by Allcock in [60] that this is not always the case. However, the detailed analysis of such a possibility was conducted by Bracken and Melloy much later in [82].

Following [82], consider a freely moving wave packet (3.49) with the momentum profile function

$$\varphi_p(k) = \left(\frac{27\pi\hbar}{p} \right)^{1/2} \frac{k}{p} e^{-\frac{3k}{2p}}, \quad p > 0. \quad (3.58)$$

This function is normalized as $\langle 1 \rangle_k = 1$ and corresponds to the average momentum $\langle k \rangle_k = p$ with the variance $\langle (k^2 - p^2) \rangle_k = p^2/3$. The wave function at $t = 0$ can be easily calculated by

$$\Psi_{I;p}(z, 0) = \frac{\sqrt{4p/(3\pi\hbar)}}{\left(1 - i\frac{2pz}{3\hbar}\right)^2} \quad (3.59)$$

and describes the symmetrical distribution centered at $z = 0$ with the width $\overline{\Delta z^2} = 9\hbar^2/(4p^2) \equiv \Delta_z^2$. We note that the larger p is the smaller is the spatial width of the packet. The current corresponding to the wave function (3.59) is equal to

$$j_{I;p}(z, 0) = \mathcal{J}[\Psi_{I;p}(z, 0)] = \frac{4}{\pi m\hbar} \frac{4p^2/(9\hbar^2)}{\left(1 + \frac{4p^2 z^2}{9\hbar^2}\right)^3} = \frac{j_{I;p}(0, 0)}{\left(1 + \frac{z^2}{\Delta_z^2}\right)^3}, \quad j_{I;p}(0, 0) = \frac{4}{\pi m\hbar \Delta_z^2} \quad (3.60)$$

and is always positive.

Consider now the normalized packet which is a superposition of two packets (3.58) with momenta p and αp , $\alpha > 1$,

$$\varphi(k) = \frac{\varphi_p(k) + A\varphi_{\alpha p}(k)}{\sqrt{1 + A^2 + 2A\chi^3}}, \quad \chi = \frac{2\alpha^{1/2}}{1 + \alpha}, \quad (3.61)$$

where A is a real number. The mean momentum for this packet is equal to

$$\langle k \rangle_k = \frac{1 + \alpha A^2 + 2A\alpha^{1/2}\chi^4}{1 + A^2 + 2A\chi^3} p.$$

Using the superposition of the wave functions (3.59)

$$\Psi_I(z, 0) = \frac{\Psi_{I;p}(z, 0) + A\Psi_{I;\alpha p}(z, 0)}{\sqrt{1 + A^2 + 2A\chi^3}}, \quad (3.62)$$

we obtain the expression for the current

$$j_I(z, 0) = j_{I;p}(z, 0) + A^2 j_{I;\alpha p}(z, 0) + 2\frac{A}{\alpha\chi} \frac{j_{I;1}(z, 0)}{j_{I;1}(0, 0)} j_{I;\alpha p}(z, 0) \left(1 + \alpha\frac{z^2}{\Delta_z^2}\right) \left(\left[1 + \alpha\frac{z^2}{\Delta_z^2}\right]^2 - 3(\alpha - 1)^2 \frac{z^2}{\Delta_z^2}\right), \quad (3.63)$$

which is not necessarily positive if $A < 0$. Indeed, for $z = 0$ the expression for the current reduces to

$$j_I(0, 0) = j_{I;1}(0, 0) (1 + A\alpha^{1/2}) (1 + A\alpha^{3/2}), \quad (3.64)$$

and, as we see, it is negative for $-\alpha^{-1/2} < A < -\alpha^{-3/2}$. The current remains negative within a narrow interval of z

$$\frac{z^2}{\Delta_z^2} \lesssim \frac{(1 + A\alpha^{1/2})(1 + A\alpha^{3/2})}{3(1 + A^2\alpha^4 + A\alpha^{1/2}(\alpha + 1)(2(\alpha - 1)^2 + \alpha))} < \frac{\chi^2/(3\alpha)}{16 - (\chi - \sqrt{8})^2} \ll 1. \quad (3.65)$$

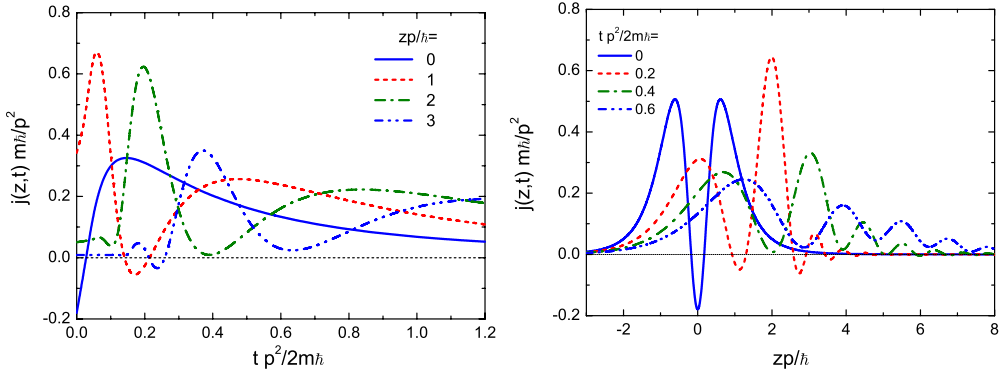


Figure 10. The current (3.3) constructed from the wave function (3.49) with the momentum profile function (3.61) for $\alpha = 2$ and $A = -\frac{3}{4\sqrt{2}}$ as a function of time for various values of z (left panel) and as a function of coordinate for various moments of time (right panel).

This phenomenon is called in the literature *the quantum back-flow effect* [83]. It has a purely quantal nature owing to the wave interference, the third term in equation (3.63). The occurrence of the negative current depends on a fine tuning of parameters of the packet superposition (3.61). As we see from equation (3.64), the larger is the difference between the averaged momenta of two wave packets contributing to (3.61), i.e. the larger is α , the narrower is the interval of the values of A , for which the effect exists.

The current (3.3) constructed with the time-dependent wave functions (3.49) with $\varphi(k)$ given by equation (3.61) for $\alpha = 2$, and $A = -\frac{3}{4\sqrt{2}}$ is shown in figure 10 as a function of time for several coordinates (left panel) and as a function of coordinate for several moments of time (right panel). We see (left panel) that the negative current exists for a very short time interval for a fixed coordinate z . There are special values of z for which the current is positive for all t , in our case it is $z \sim 2$. The intervals of z , where $j(z, t) < 0$, move to higher z with an increase of time and the negative current amplitude becomes smaller and smaller, see the right panel of figure 10.

It was pointed out in [82] that the total probability flux over the period of negative current, e.g. $[t_1, t_2]$, is limited from below

$$\int_{t_1}^{t_2} j(z, t) dt \geq -c_{bm}. \tag{3.66}$$

Interestingly, although the back-flow effect is of purely quantum origin, the parameter c_{bm} does not depend on \hbar and is universal being independent of the particle mass and the time duration of the effect. The numerical calculations [84] give the value $c_{bm} \approx 0.038452$. In [85] it was proposed how the back-flow effect can be experimentally observed with the help of Bose–Einstein condensates.

The quantum back-flow effect can also be viewed with the help of the Wigner density function

$$W(z, v, t) = \frac{m}{2\pi\hbar} \int_{-\infty}^{\infty} \Psi^* \left(z - \frac{1}{2}y, t \right) \Psi \left(z + \frac{1}{2}y, t \right) e^{-imvy/\hbar} dy, \tag{3.67}$$

for the free particle $W(z, v, t) = W(z - vt, v, 0)$.

For wave functions of the form (3.48), which lead to W vanishing for negative values of v , the current density (3.3) can be expressed as

$$j(z, t) = \int_0^{\infty} W(z - vt, v, 0) v dv. \tag{3.68}$$

The appearance of negative values of j , despite of the restriction of the integral to the positive values of v , is the direct consequence of the Wigner function taking negative values. We return to the question of the sign of the Wigner density in section 6.4.

So far we have considered the wave packets which occupy the whole space at any moment of time. Special attention should be paid to problems when the wave function is initially confined to a particular space region—the so-called *cut-off wave initial conditions* [86]. The simplest of such problems was considered by Moshinsky in his seminal paper [87]. He considered a monochromatic beam of free particles moving parallel to the z -axis from left to right and stopped by a perfectly absorbing shutter at $z = 0$. The shutter promptly opens at $t = 0$ and the particle beam proceeds freely to the right. One may ask the question: How fast are the particles at a certain (registration) point $z > 0$? The initial wave function is

$$\Psi(z, 0) = \begin{cases} e^{ipz/\hbar}, & z < 0 \\ 0, & z \geq 0. \end{cases} \quad (3.69)$$

The solution of the free time-dependent Schrödinger equation with the initial condition (3.69) is given by

$$\Psi(z, t) = \int_{-\infty}^{+\infty} \frac{dk}{2\pi\hbar} \tilde{\varphi}(k) e^{ikz/\hbar - ik^2 t/2m\hbar} \quad (3.70)$$

where the momentum envelop function is

$$\tilde{\varphi}(k) = \int_{-\infty}^{+\infty} dz \Psi(z, 0) e^{-ikz/\hbar} = \frac{i\hbar}{k - p}. \quad (3.71)$$

The k -integration in equation (3.70) can be performed analytically [87] with the result expressed through the complementary error function

$$\Psi(z, t) = \frac{1}{2} \exp\left[i\frac{pz}{\hbar} - i\frac{p^2 t}{2m\hbar}\right] \operatorname{erfc}\left[\sqrt{\frac{m}{2\hbar t i}}(z - pt/m)\right]. \quad (3.72)$$

Here $\sqrt{i} = \exp(i\pi/4)$. The relative probability density to register the particles at the point z at the moment of time t is given by

$$P(z, t) = |\Psi(z, t)|^2 = \frac{1}{2} \left(\left[\frac{1}{2} + C(u) \right]^2 + \left[\frac{1}{2} + S(u) \right]^2 \right), \quad u = \sqrt{\frac{pz}{\pi\hbar}} \sqrt{\frac{T}{t}} \left(\frac{t}{T} - 1 \right). \quad (3.73)$$

Here $T = mz/p$ is the classical time needed for a particle with the velocity p/m to reach the point z ($z > 0$), if at $t = 0$ the particle was at the point $z = 0$. The functions $C(u)$ and $S(u)$ are the standard Fresnel integrals

$$C(u) = \int_0^u \cos(\pi\xi^2/2) d\xi, \quad S(u) = \int_0^u \sin(\pi\xi^2/2) d\xi. \quad (3.74)$$

In the classical limit $\hbar \rightarrow 0$ or for very large distances from the shutter, $zp/\hbar \gg 1$, the probability P tends to the classical result $P \rightarrow P^{(cl)} = \theta(t - T)$. However, for any finite value of zp/\hbar the probability that the particle is registered in the point z at the time $t = T$ is smaller than the classical value, $P(z, t = T) = 1/4$. In figure 11 we show the probability (3.73) as a function of time for various coordinates. We see that P reaches its classically expected value of one for the first time at $t_1 > T$ and oscillates for $t > t_1$ around unity with a decreasing amplitude and a frequency increasing as $\sim (t/T - 1)^2 zp/2T\hbar$. This pattern resembles the Fresnel diffraction of light from the edge of a semi-infinite plane, therefore in [87] it was coined as *the diffraction in time*. The important difference of the quantum mechanical result (3.73) from the classical limit is that even for $t < T$ there exists a finite probability to register the particles. For example, for $zp/\hbar \sim 1$, $P \gtrsim 17\%$ for $0.5 \lesssim t/T \lesssim 1$. For vanishing t , $P(z, t)$

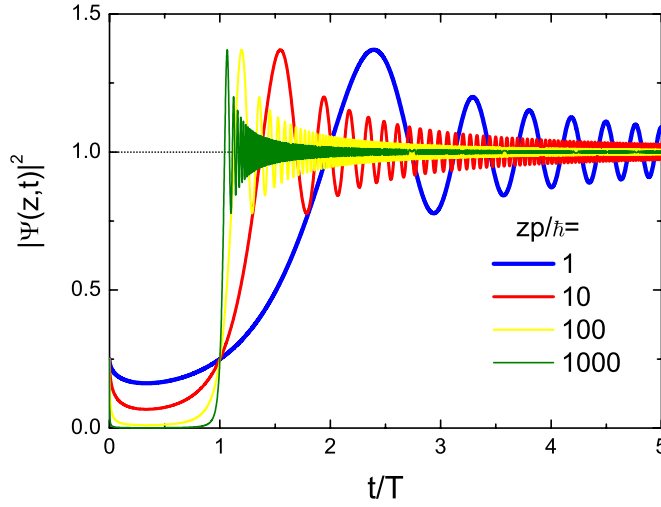


Figure 11. The relative probability density of observing particles with momentum $p > 0$ initially confined to the negative z and released at $t = 0$, see equation (3.69), at a given point $z > 0$ as a function of time after the release. The time is measured in units of $T = zm/p$. The probability is calculated according to equation (3.73) for several values of zp/\hbar .

increases again and reaches $1/4$. Here, we should bear in mind that in our non-relativistic framework $c \rightarrow \infty$, whereas in a relativistic approach we would certainly get the restriction $t > z/c$.

Let τ be a time of shutter opening. The appearance of the quantum precursor is related to the fact that after the prompt opening of the shutter the particle beam ceases to be monochromatic. The prompt perturbation of the system (a change of boundary conditions can be also considered as a perturbation) induces transitions among the initial state with the momentum p and the states with momenta k , such that $\tau |k^2 - p^2|/(2m\hbar) \lesssim 1$, see section 41 in [52]. The relative transition probability is proportional to $|\tilde{\varphi}(k)|^2 = \hbar^2/(k-p)^2$. Obviously, the modes with $k > p$ reach the point z during the times smaller than T .

The free case problem considered by Moshinsky [87] was generalized in [88] for the solution of the time-dependent Schrödinger equation for tunneling through an arbitrary potential localized within some spatial interval. To investigate the time evolution of the transmission probability density for the tunneling, the authors of [89] considered analytic solutions to the time-dependent Schrödinger equation for the cut-off wave initial conditions, e.g., selected as,

$$\Psi(z, t = 0) = \begin{cases} e^{ip(z+L/2)/\hbar} - e^{-ip(z+L/2)/\hbar}, & z \leq -L/2 \\ 0, & z > -L/2. \end{cases} \quad (3.75)$$

They demonstrated that in this particular case for a rather opaque barrier (for a barrier opacity parameter $\alpha = L\sqrt{2mU_{\max}}/\hbar > \alpha_c$) the probability density exhibits two evolving structures. One refers to the propagation of a forerunner, while the other consists of a semiclassical propagating wavefront. Forerunners disappear for $\alpha < \alpha_c$. Moreover, forerunners vanish at asymptotically long times and distances from the interaction zone ($-L/2 < z < L/2$), whereas the propagating wavefront tends to the stationary solution. It proves to be the case that forerunners exist for $t_d(-\frac{L}{2}, \frac{L}{2}, E) < t_{\text{trav}}^{\text{free}} = Lm/p$.

3.4. Characteristics of time for the scattering of a wave packet with negligibly small momentum uncertainty

Consider a wave packet (3.48) prepared far away from the potential region, so that the packet could be made sufficiently broad to assure a small momentum uncertainty and at the same time it would take a long time for the packet to reach the potential barrier. Thereby, for the long time periods considered here we are able to neglect forerunners and the negative current term mentioned above. For the single Gaussian wave packet (3.55) the current density (3.3) is always positively definite for any time. After the wave packet has reached the barrier it is split into the reflected wave packet and two forward-going (evanescent and growing) waves propagating under the barrier, which outside of the barrier transform to a transmitted wave packet.

The transmitted packet is determined by [90]

$$\Psi_{\text{T}}(z, t) = \int_0^{\infty} \frac{dk}{2\pi\hbar} \varphi(k) |T(E)| e^{i\phi_{\text{T}}(E)} e^{ikz/\hbar - iEt/\hbar}. \quad (3.76)$$

The reflected packet moving backwards is

$$\Psi_{\text{R}}(z, t) = \int_0^{\infty} \frac{dk}{2\pi\hbar} \varphi(k) |R(E)| e^{i\phi_{\text{R}}(E)} e^{-ikz/\hbar - iEt/\hbar}, \quad (3.77)$$

where, as before, $E = k^2/2m$.

Also, one can introduce two measures of time that could characterize the wave propagation within the potential region. Consider the difference of the time, when the maximum of the incident packet (3.49) is at the coordinate $z = -L/2$, and the time, when the maximum of the transmitted packet (3.76) is at $z = +L/2$, and the difference of the time, when the maximum of the incident packet and the maximum of the reflected packet (3.77) are at the same spatial point $z = -L/2$. We call these time intervals *the transmission and reflection group times*, t_{T} and t_{R} . The construction of the delay times goes back to pioneering works by Eisenbud [91], Wigner [1] and Bohm [90]. According to the method of the stationary phase, the position of the maximum of an oscillatory integral, as those in equations (3.49), (3.76) and (3.77), is determined by the stationarity of the complex phase of the integrand. For a sufficiently narrow initial momentum distribution, $\gamma_p \ll p$, we can write

$$t_{\text{T}}(E_p) = \left(\hbar\xi'(p) + \frac{L}{2v_{\text{I}}} + \frac{\hbar}{v_{\text{I}}} \frac{d}{dp} \phi_{\text{T}}(E_p) \right) - \left(\hbar\xi'(p) - \frac{L}{2v_{\text{I}}} \right) = \frac{L}{v_{\text{I}}} + \hbar \frac{d\phi_{\text{T}}(E_p)}{dE_p} \quad (3.78)$$

and

$$t_{\text{R}}(E_p) = \left(\hbar\xi'(p) + \frac{L}{2v_{\text{I}}} + \frac{\hbar}{v_{\text{I}}} \frac{d}{dp} \phi_{\text{R}}(E_p) \right) - \left(\hbar\xi'(p) - \frac{L}{2v_{\text{I}}} \right) = \frac{L}{v_{\text{I}}} + \hbar \frac{d\phi_{\text{R}}(E_p)}{dE_p}, \quad (3.79)$$

here and below $E_p = p^2/2m$. For $E_p \gg U$, $\frac{d\phi_{\text{T,R}}(E_p)}{dE_p} \rightarrow 0$ and $t_{\text{T}}(E_p) \simeq t_{\text{R}}(E_p) \simeq \frac{L}{v_{\text{I}}}$ reduce to the passage time of the distance L . However, interpretation of these times for $E < U$ needs special care. Recall that in the case of the tunneling the transmission and reflection group times $t_{\text{T}}(E_p)$ and $t_{\text{R}}(E_p)$ are asymptotic quantities since they count time steps for events that occur at $z = -L/2$ and $z = L/2$ rather than at the turning points. Moreover, as we shall see, for tunneling through thick barriers the dependence of these times on L ceases.

One can introduce conditional transmission and reflection group times by multiplying the times t_{T} and t_{R} with the transmission and reflection probabilities, respectively. Summing them up we define a *bidirectional scattering time*, as the sum of the weighted average of transmitted and reflected group delays [8]

$$t_{\text{bs}}(E_p) = |T(E_p)|^2 t_{\text{T}}(E_p) + |R(E_p)|^2 t_{\text{R}}(E_p). \quad (3.80)$$

This time can be also expressed through the induced, transmitted and reflected currents defined for the stationary problem (see equation (3.3)),

$$t_{\text{bs}} = \frac{j_{\text{T}}}{j_{\text{I}}} t_{\text{T}} + \frac{|j_{\text{R}}|}{j_{\text{I}}} t_{\text{R}}. \quad (3.81)$$

For a symmetrical barrier, with the help of equations (3.9) and (3.10), we get

$$t_{\text{bs}}(E_p) = t_{\text{T}}(E_p) = t_{\text{R}}(E_p) = \hbar \frac{d\delta_s(E_p)}{dE_p}. \quad (3.82)$$

We should emphasize a direct correspondence of the transmission and reflection group times defined here to the classical group times defined in equations (2.21) and (2.64). For $E_p \gg U$, $\hbar \frac{d\delta_s(E_p)}{dE_p} \rightarrow L/v_1$.

There is a relation [92, 93] between the bidirectional scattering time t_{bs} , equation (3.80), and the dwell time t_{d} , equation (3.23), which follows from the general relation for the stationary wave function (3.13) and definitions (3.78), (3.79):

$$t_{\text{d}}(-L/2, L/2, E_p) = t_{\text{bs}}(E_p) - \delta t_{\text{i}}(E_p). \quad (3.83)$$

The last term here is the interference time delay. It arises due to the interference of the incident part of the wave function (the incident packet) with its reflected part. This term is of the same origin as the last term on the left-hand side of equation (3.22),

$$\delta t_{\text{i}}(E_p) = -\frac{\hbar}{pv_1} \text{Im}(R(E_p) e^{+ipL/\hbar}) = -\frac{\hbar}{pv_1} |R(E_p)| \sin(\phi_{\text{R}}(E_p) + pL/\hbar). \quad (3.84)$$

The interference time can be as positive as negative, so it represents a delay or advance of the incident packet. This term δt_{i} is especially important for low energies (small momenta), when the packet approaches the barrier very slowly. Taking into account that $|T|^2 + |R|^2 = 1$ we can rewrite equation (3.83) in the form

$$t_{\text{d}} = |T|^2 (t_{\text{T}} - \delta t_{\text{i}}) + |R|^2 (t_{\text{R}} - \delta t_{\text{i}}). \quad (3.85)$$

The times $(t_{\text{T}} - \delta t_{\text{i}})$ and $(t_{\text{R}} - \delta t_{\text{i}})$ coincide with the Larmor times introduced by Baz' and Rybachenko [65, 72] in the general case of asymmetric potentials. Naively [62], one interprets result (3.85) as the time spent by the particle under the barrier (t_{d}) is the sum of the tunneling traversal time in transmission $t_{\text{T}} - \delta t_{\text{i}}$ times the probability of transmission and the tunneling traversal time in the reflection $t_{\text{R}} - \delta t_{\text{i}}$ times the probability of reflection. Such an interpretation is actually false, since in quantum mechanics one should sum amplitudes rather than probabilities [8]. Moreover, as we mentioned, for thick barriers t_{d} is almost entirely determined by the behavior of the wave function on the left edge of the barrier and thereby does not relate to the transmission process. Else, t_{T} and t_{R} are determined when the peaks of packets are at $z = \pm L/2$ rather than at the turning points and thereby they cannot control only the tunneling.

Some authors, see [94–96], introduce tunneling transit times by dividing the probability stored within the potential region by the local transmitted flux and the reflected flux

$$\tilde{t}_{\text{T}} = \frac{1}{j_{\text{T}}} \int_{-L/2}^{L/2} dz |\psi(z, E_p)|^2 = \frac{t_{\text{d}}}{|T|^2}, \quad \tilde{t}_{\text{R}} = \frac{1}{|j_{\text{R}}|} \int_{-L/2}^{L/2} dz |\psi(z, E_p)|^2 = \frac{t_{\text{d}}}{|R|^2}, \quad (3.86)$$

from where we get $t_{\text{d}}^{-1} = \tilde{t}_{\text{T}}^{-1} + \tilde{t}_{\text{R}}^{-1}$. It follows from analogy with fluid mechanics: the local velocity $v(z)$ is related to the local density $\rho = |\psi(z)|^2$ through $j = \rho v$, see (2.2). Since $|T|^2$ is exponentially small for a broad barrier, \tilde{t}_{T} is exponentially large in this case. It is perfectly luminal and does not saturate with barrier length [93]. Reference [8] argues that the quantities (3.86) characterize net-delays of transmitted and reflected fluxes rather than tunneling times. Indeed the time \tilde{t}_{T} is a property of the entire wave function made up of

forward and backward-going components and thereby cannot be considered as the traversal time of transmitted particles only [8]. Performing minimization of \tilde{t}_T , [97] finds a variationally determined tunneling time $\tilde{t}_T^{\min} \propto 1/|T|$. Both \tilde{t}_T and $\tilde{t}_T^{\min} \rightarrow \infty$ for $|T| \rightarrow 0$. Note that the typical time, after which the particle can be observed with the probability of the order of one to the right from the barrier, if it initially was to the left from the barrier, is indeed proportional to $1/|T|^2$. But the time $\propto 1/|T|^2$ does not correspond to our expectations for the quantity characterizing traversal time of the given particle from a to b . It is associated with the life-time of metastable states, being in this case the tunneling particles treated as quasiparticles decaying from a state on one side of the barrier into another state on the other side of the barrier [64]. This time represents a mean time, in which a certain likelihood of a tunneling event may take place. After passage of this time it becomes probable that approximately a half of the original particle density has managed to tunnel away. This does not reflect the actual time of the tunneling.

Example 1. Group times for a rectangular barrier

The scattering phase for a rectangular barrier is given in equation (3.18). Substituting this expression in equation (3.82) we find

$$t_{\text{bs}} = t_T = t_R = \frac{L \cos^2 \delta_s}{2 v_I} \left[\frac{(p^2 + \kappa^2)^2 \tanh(\kappa L/\hbar)}{p^2 \kappa^2} \frac{1}{\kappa L/\hbar} - \frac{p^2 - \kappa^2}{\kappa^2} \frac{1}{\cosh^2(\kappa L/\hbar)} \right]. \quad (3.87)$$

The interference time (3.84) can be written as

$$\delta t_i = \frac{L}{v_I} \cos^2 \delta_s \frac{p^2 + \kappa^2 \tanh(\kappa L/\hbar)}{2 p^2 \kappa L/\hbar}. \quad (3.88)$$

For $E_p \ll U$, performing expansion in E_p/U we have

$$\delta t_i \approx 2 \frac{l_0}{v_I} \coth(L/l_0) - \frac{l_0}{v_I} (\coth(L/l_0) + (8 \coth(L/l_0) - L/l_0) / \sinh^2(L/l_0)) \frac{E_p}{U}. \quad (3.89)$$

The interference time is shown in figure 9, right, as a function of E_p/U for various barrier lengths. As we see, the interference time is especially significant for small energies when the incident packet approaches the barrier slowly. For $E_p < U$, $\delta t_i > 0$, for $E_p > U$, at some energies δt_i becomes negative. For $E_p \gg U$, $\delta t_i \rightarrow 0$ and $t_{\text{bs}} \simeq t_d \simeq L/v_I$.

Example 2. Group times in the semiclassical approximation

The wave function of the stationary scattering problem, which enters the wave packet (3.41), can be written in the semiclassical approximation as follows [52]

$$\psi^{(\text{scl})}(z; E_p) = \begin{cases} \sqrt{\frac{m}{|\kappa(z, E_p)|}} \left[e^{\frac{i}{\hbar} \int_{z_1}^z |\kappa(z', E_p)| dz' + i\phi_0} + e^{-\frac{i}{\hbar} \int_{z_1}^z |\kappa(z', E_p)| dz' - i\phi_0} \right], & z < z_1, \\ \sqrt{\frac{Dm}{\kappa(z, E_p)}} e^{\int_{z_1}^z \kappa(z', E_p) dz'/\hbar}, & z_1 \leq z \leq z_2, \\ \sqrt{\frac{Dm}{|\kappa(z, E_p)|}} e^{\frac{i}{\hbar} \int_{z_2}^z |\kappa(z', E_p)| dz' + i\phi_0}, & z_2 \leq z, \end{cases} \quad (3.90)$$

$$D = \exp\left(-\frac{2}{\hbar} \int_{z_1}^{z_2} \kappa(z', E_p) dz'\right),$$

where z_1 and z_2 are the left and right turning points ($z_1 < z_2$) and the phase $\phi_0 = \pi/4$ for a smooth scattering potential, cf. equation (3.28). Note that in the framework of the semiclassical approximation [52] it is legitimate to take into account only the evanescent wave inside the barrier. Being derived with the same accuracy, the reflection coefficient equals unity. Respectively, the incident current is then totally compensated by the reflected one and the current inside the barrier is absent, whereas it is present outside the barrier for $z > z_2$. This

current non-conservation is inconvenient when we study particle propagation inside the barrier. To recover the current conservation one should include the contribution of the growing wave inside the barrier, despite this procedure being beyond the scope of the formal applicability of the semiclassical approximation, see [7]. Similarly, in the non-equilibrium quantum field description one introduces so-called self-consistent approximations to keep the conservation laws on an exact level, see [33–37] and the discussion in section 6.

Repeating the procedure that leads to equations (3.78) and (3.79) from (3.90) we obtain

$$\begin{aligned}
 t_{\text{T}}^{(\text{scl})} &= \left(\hbar \xi'(p) + \frac{1}{v_1} \frac{d}{dp} \int_{z_2}^z |\chi(z', E_p)| dz' \right) \Big|_{z=z_2} \\
 &\quad - \left(\hbar \xi'(p) + \frac{1}{v_1} \frac{d}{dp} \int_{z_1}^z |\chi(z', E_p)| dz' \right) \Big|_{z=z_1} = 0, \\
 t_{\text{R}}^{(\text{scl})} &= \left(\hbar \xi'(p) + \frac{1}{v_1} \frac{d}{dp} \int_{z_1}^z |\chi(z', E_p)| dz' \right) \Big|_{z=z_1} \\
 &\quad - \left(\hbar \xi'(p) - \frac{1}{v_1} \frac{d}{dp} \int_{z_1}^z |\chi(z', E_p)| dz' \right) \Big|_{z=z_1} = 0.
 \end{aligned} \tag{3.91}$$

We see that within semiclassical approximation $t_{\text{T}}^{(\text{scl})} = t_{\text{R}}^{(\text{scl})} = t_{\text{bs}}^{(\text{scl})} = 0$, if we compare the moments of time, when the maxima of the packets are at the turning points. This was first announced in [98] but basing on this fact concluded that the tunneling time in the semiclassical approximation is zero. In our opinion, being zero, the quantity $t_{\text{T}}^{(\text{scl})}$, as well as t_{T} , can hardly be considered as an appropriate characteristic of the time passage of the barrier. The values $t_{\text{T}}^{(\text{scl})} = t_{\text{R}}^{(\text{scl})} = 0$ just show that the delay of wave packets within the region of finite potential appears due to purely quantum effects, to vanish in the semiclassical approximation. It also demonstrates that in the case of the tunneling the group delays are accumulated in the region near the turning points where the semiclassical approximation is not applicable.

Finally, we repeat that in general case the reflection group time shows nothing else than a time delay between the formation of the peak of the reflected wave at $z = -L/2$ compared to the moment, when the incident wave peak reaches $z = -L/2$. The transmission group time demonstrates the difference in time, when the peak of the transmission wave starts its propagation at $z = L/2$ and the incident wave peak reaches $z = -L/2$. In the semiclassical approximation these time delays are absent.

3.5. Sojourn time for the scattering of an arbitrary wave-packet

So far we have considered the time-like quantities, which are precise only to the extent that the packet has a small momentum uncertainty, as the group times (equations (3.78), (3.79) and (3.82)) [62] and the dwell time (equation (3.23)), originated within the stationary problem. Nevertheless it is possible to introduce another time-like quantity which measures how long the system stays within a certain coordinate region. In classical mechanics the time, which a system committing 1D motion spends within the segment $[a, b]$, is determined by the integral (2.3). In quantum mechanics the δ -function over the classical trajectory is to be replaced with the quantum probability density $|\Psi(z, t)|^2$; see [99]. Now, if we consider a wave packet starting from the left at large negative z for large negative t and proceeding to $z = +\infty$, then the time it spends within the segment $[a, b]$ is given by *the quantum mechanical sojourn time* defined as

$$t_{\text{soj}}(a, b) = \int_{-\infty}^{+\infty} dt \int_a^b dz |\Psi(z, t)|^2. \tag{3.92}$$

The packet wave function is normalized as (3.43). Between the dwell time and the sojourn time there is a relation [100], see the derivation in appendix D,⁷

$$t_{\text{soj}}(a, b) = \int_{-\infty}^{+\infty} \frac{dk}{2\pi\hbar} |\varphi(k)|^2 t_{\text{d}}(a, b, k^2/2m) = \langle t_{\text{d}}(a, b, k^2/2m) \rangle_k. \quad (3.93)$$

Using the wave function that obeys the Schrödinger equation and satisfies the continuity equation

$$\frac{d}{dt} |\Psi(z, t)|^2 = -\frac{d}{dz} j(z, t), \quad (3.94)$$

where $j(z, t) = \mathcal{J}[\Psi(z, t)]$ with the current \mathcal{J} defined in (3.3), we can rewrite the sojourn time through the currents on the borders of the interval

$$t_{\text{soj}}(a, b) = -\int_{-\infty}^{+\infty} dt \int_{-\infty}^t dt' [j(b, t') - j(a, t')]. \quad (3.95)$$

From these relations we see that the sojourn time has the same deficiencies as the dwell time. Namely, for a broad barrier both quantities demonstrate how long it takes for the particles to enter the barrier from the left end, but they do not describe particle transmission to the right end.

We now apply the relation (3.95) and the sojourn time definition to the wave function (3.1). The total time, which the packet spends in the barrier region, $-L/2 \leq z \leq L/2$, is $t_{\text{soj}}(-L/2, L/2) = \langle t_{\text{d}}(-L/2, L/2, k^2/2m) \rangle_k$. As we show in appendix D the integration of currents in equation (3.95) gives [81]

$$\begin{aligned} \int_{-\infty}^{+\infty} dt \int_{-\infty}^t dt' (j(L/2, t') - j(-L/2, t')) &= -\langle |T(E)|^2 t_{\text{T}}(E) \rangle_k \\ &\quad - \langle |R(E)|^2 t_{\text{R}}(E) \rangle_k + \langle \delta t_{\text{i}}(E) \rangle_k. \end{aligned} \quad (3.96)$$

Thus, in the case of an arbitrary momentum distribution we obtain a generalization of equations (3.83) and (3.84):

$$t_{\text{soj}}(-L/2, L/2) = \langle t_{\text{d}}(-L/2, L/2, E_k) \rangle_k = \langle |T(E)|^2 t_{\text{T}}(E) \rangle_k + \langle |R(E)|^2 t_{\text{R}}(E) \rangle_k - \langle \delta t_{\text{i}}(E) \rangle_k. \quad (3.97)$$

Thereby, from the definition of the sojourn time we extract the same information as from the definition of the dwell time but averaged over energies of the packet. We stress that both quantities do not describe the time of the particle passage of the barrier.

3.6. The Hartmann effect

For energies above the barrier the proper time for the particle to pass the region of the potential is the traversal time $t_{\text{trav}}^{(\text{cl})}$. Other times $t_{\text{d}}(-L/2, L, E_p)$, $t_{\text{soj}}(-L/2, L, E_p)$, $t_{\text{bs}}(E_p)$ introduced above also appropriately characterize the particle motion. For energies well above the barrier, $E \gg U$, we find $t_{\text{trav}}^{(\text{cl})} \simeq t_{\text{bs}}(E_p) \simeq t_{\text{d}}(-L/2, L, E_p) \simeq L/v_{\text{T}}$. However there appear problems with the interpretation of all these times, as is characteristic of a particle's passage under the barrier (for $E < U$).

In numerous works the dwell time was interpreted as the mean time the particle spends under the barrier regardless of whether it is ultimately transmitted or reflected, see the discussion in [8]. The link (3.85) between the dwell time and the group time suggested a naive interpretation of the times $t_{\text{T}} - \delta t_{\text{i}}$ and $t_{\text{R}} - \delta t_{\text{i}}$ as the mean times the transmitted

⁷ Here it is worth to mention that it is possible to introduce time operators associated with the dwell time and sojourn time, canonically conjugated to the system Hamiltonian, see [11, 83] and references therein.

and reflected particles spend under the barrier. As we mentioned, such an interpretation is based on a classical counting of possible outcomes of a scattering process in 1D, when an incident particle can be either reflected or transmitted, cf. section IIIB in [62]. In accepting such an interpretation of the group and dwell times one encounters a paradox. In order to understand it more clearly consider tunneling ($E < U$) through a thick rectangular barrier $\kappa L/\hbar = \sqrt{1 - E_p/UL}/l_0 \gg 1$. From equations (3.18), (3.82) and (3.85) we find

$$t_d(-L/2, L/2, E_p) = t_T(E_p) - \delta t_i(E_p) = t_R(E_p) - \delta t_i(E_p) = \frac{p^2}{p^2 + \kappa^2} \hbar \frac{d\delta_s(E_p)}{dE_p},$$

$$t_{bs}(E_p) = t_T(E_p) = t_R(E_p) \simeq \hbar \frac{d\delta_s(E_p)}{dE_p} = 2 \frac{\hbar}{v_1 \kappa}. \quad (3.98)$$

The characteristic length entering these expressions is the quantum depth of particle penetration inside the barrier region $\sim \hbar/\kappa$ rather than the length of the barrier L . Therefore all these characteristic times are reduced to the quantum time $t_{\text{quant}} \sim \hbar/v_1 \kappa$ not proportional to the barrier length L , as one could expect for a proper passage time of the distance L with a constant velocity. This would mean that, being evaluated with the help of these times, the average velocity of the particle passage of the barrier would exceed the speed of light for sufficiently large L . Such a phenomenon first described in [13] was then called the Hartmann effect. The effect survives independently of the specific form of the potential. The same effect arises, if one uses the relativistic Dirac and Klein–Gordon equations instead of the Schrödinger equation [101]. As Winful writes [8]: ‘Because of this apparent superluminality, there are some who dismiss it as a relevant time-scale for the tunneling process. This is part of the motivation for the ongoing search of other tunneling times.’

The Hartmann effect has not yet been observed for matter waves. However, one has used the identity of the form of the Helmholtz equation for wave propagation in a bulk inhomogeneous medium and the time-dependent Schrödinger equation, and studied the tunneling of electromagnetic waves through a barrier. Reference [102] reported that a superluminal tunneling of light was observed, which caused a vivid discussion in the literature, see for example reviews [10, 11]. The group velocity may become superluminal and even negative without any contradiction with causality [6, 63, 103]. General arguments [104] based on unitarity and causality show that the peak of the transmitted pulse is constructed mainly from the leading edge of the incident one. Namely, a pulse reshaping leading to apparent acausality was found in absorbing or amplifying media whose relaxation times are long compared with pulse duration. For a thorough analysis of the Hartmann effect and re-interpretations of the experiments free of the problems of causality we refer the reader to the review of Winful [8]. The saturation of the group delay with the barrier length is explained by the saturation of the stored energy. Winful’s argument to avoid the Hartmann effect is that ‘the transmitted pulse is not the same entity as the incident pulse’. However such an interpretation does not answer the question whether it is possible to get an appropriate time for the passage of the barrier, which is proportional to its length. This problem has not yet been solved.

Let us first formulate arguments why the group times and the dwell time are not appropriate quantities to measure the tunneling time. First of all the group times t_T , t_R and t_{bs} ought to be understood as asymptotic quantities (cf., [62, 63, 100]), which apply to events with distinct wave packets measured, in reality, far from the barrier. Approaching the barrier, the incident wave packet interferes with the reflected part of itself. One can extrapolate the time so that the freely propagating incident wave packet would need to arrive at the left border of the potential region ($z = -L/2$) in absence of the reflection. Similarly, the transmitted wave packet can be extrapolated to the right border of the potential ($z = L/2$). One can of course extrapolate further into the potential regions up to the turning points z_1 and z_2 , which are determined

by the equation $U(z_{1,2}) = E_p$. All that one can deduce from such extrapolations is that if the incident wave packet, being extrapolated from the past, reaches the point $z = -L/2$ at $t = t_-$, then the peak of the remote transmitted wave packet, being extrapolated backwards from the future, occurs at the coordinate $z = L/2$ at the time $t = t_- + t_T$. One cannot say, where the transmitted wave packet peak was at $t < t_- + t_T$ and, thus, the group times do not measure the traveling time from input to output. Reference [8] goes even further considering the incident and transmitted wave packets as different entities arguing that there is no obvious causal relation between the measurement of the incident packet somewhere to the left of the barrier and the measurement of the transmitted packet to the right of the barrier. The problem is even more subtle, if considering transmission one uses centroids $\bar{z}_T(t)$ and $\bar{z}_R(t)$ related to the transmitted, incident and reflected wave packets, see below in section 3.7.

Another argument is against the use of equation (3.85) for the interpretation of the group times t_T and t_R , as the transmission and reflection times [8]. The counting of possible outcomes for the scattering of the packet on the barrier, as being either transmitted or reflected, is not valid for a quantum system: a wave packet can be both transmitted and reflected. In quantum mechanics one sums complex amplitudes rather than probabilities [63]. As we argued in the example of the thick barrier, values t_{bs} and t_d show time delays of the wave packet on the barrier edge $z = -L/2$, not a life-time of a stored energy within the whole barrier region escaping from both sides of the barrier. For example, as follows from equations (3.31)–(3.33) the dwell time can be written as a superposition of the dwell times constructed separately from the evanescent wave and the growing wave, $t_d^{(evan)}$ and $t_d^{(grow)}$, and their interference, $t_d^{(cor)}$. For tunneling through a thick barrier, $E < U$ and $\kappa L/\hbar \gg 1$, we have $t_d^{(grow)}/t_d^{(evan)} \ll 1$ and $t_d^{(cor)}/t_d^{(evan)} \ll 1$, therefore $t_d \simeq t_d^{(evan)}$. Thus, in this particular limit, knowing the value t_d , one may only make conclusions on the delay of reflection but not on the delay of transmission. These comments also concern the quantities (3.86), which, as argued in [8, 93, 97], could characterize net-delays of transmitted and reflected fluxes.

Concluding, as Winful [8] writes: ‘The Hartmann effect is at the heart of the tunneling time conundrum. Its origin has been a mystery for decades [7, 10, 105]. Its resolution would be of fundamental importance as it would lead to conclusive answers regarding superluminality and the nature of barrier tunneling.’ Our contribution to the resolution of the Hartmann paradox is presented below. Since the origin of the problem is that the semiclassical local current is absent for the under barrier motion (there is no propagating packet peak in under-the-barrier motion), the solution is based on the particle transit time through the barrier being associated with the time variation of the amplitude of the waves under the barrier, rather than with a particle flux there, information on which one tries to extract considering the motion of the peaks of the transmitted and incident wave packets.

3.7. Centroid transmission and reflection time delays and asymptotic motion of packets

The quantities t_T and t_R , equations (3.78) and (3.79), were found with the help of the stationary phase approach. These times characterize the time delays within the segment $[-L/2, L/2]$ in transmission and reflection processes. Defining them we used the assumption that the position of a particle can be identified with the position of the maximum of the wave packet. However, it is not so easy to experimentally distinguish the peak position of a spatially broad packet. Moreover information not only about the spatial distribution in the packet but also about its average width is lost.

As a simple alternative, Hauge *et al* proposed in [81] to operate with the average coordinates of the packets to specify the position of the particle and to study the motion of the centroids of the incident, transmitted and reflected wave packets. The result depends

on the packet width but only through average quantities $\bar{z}_{T,R,I}(t)$. A price for simplicity is a loss of information about specific energy distribution within the packet that results in a loss of information about specific spatial distribution on a spatial scale \hbar/γ_p . This is the minimum length characterizing the centroid.

The average coordinate of the incident wave packet (equation (3.49)), i.e. *the incident centroid*, $\bar{z}_I(t)$, is given by equation (3.53). After the collision we deal with reflected and transmitted packets (3.76) and (3.77) to the right ($z > L/2$) and to the left ($z < -L/2$) from the potential region, respectively. The average coordinates of these packets—*the transmitted and reflected centroids*—are defined as

$$\bar{z}_T(t) = \frac{\int_{L/2}^{+\infty} dz z |\Psi_T(z, t)|^2}{\int_{L/2}^{+\infty} dz |\Psi_T(z, t)|^2}, \quad \bar{z}_R(t) = \frac{\int_{-\infty}^{-L/2} dz z |\Psi_R(z, t)|^2}{\int_{-\infty}^{-L/2} dz |\Psi_R(z, t)|^2}. \quad (3.99)$$

Note that in relations (3.53) and (3.99) the centroid motions invoke the same time parameter t . The moments when the particle enters the segment $[-L/2, L/2]$ or leaves it, being reflected or transmitted, can be specified by the requirement that the centroids are at some chosen positions nearby or at the borders of the potential region. Comparing these moments of time one can determine the delay times of the particle within the segment $[-L/2, L/2]$ during the reflection and transmission processes. In this way it is possible to study the corrections to the group times (3.78) and (3.79) induced by the packet finite width and the change of the packet shape in the process of tunneling and reflection.

The integral in equation (3.99) is difficult to calculate in general, as it requires a solution of the time-dependent Schrödinger equation. Nevertheless one can derive some rigorous results for the asymptotic time dependencies of the centroids [81]. If we consider sufficiently large times, for which $\bar{z}_T(t) \gg L/2$ and $\bar{z}_I(t), \bar{z}_R(t) \ll -L/2$, then the transmitted packet is located almost entirely to the right of the region of non-zero potential and the reflected packet is to the left of it. In this case we can extend the integration limits in (3.99) to $\pm\infty$ and define the asymptotic centroids of transmitted and reflected packets

$$\bar{z}_T^{(as)}(t) = \frac{\int_{-\infty}^{+\infty} dz z |\Psi_T(z, t)|^2}{\int_{-\infty}^{+\infty} dz |\Psi_T(z, t)|^2}, \quad \bar{z}_R^{(as)}(t) = \frac{\int_{-\infty}^{+\infty} dz z |\Psi_R(z, t)|^2}{\int_{-\infty}^{+\infty} dz |\Psi_R(z, t)|^2} \quad (3.100)$$

in analogy to the asymptotic centroid of the incident packet (3.53). From the definition (3.99) follows that the centroid of the transmitted packet \bar{z}_T is an increasing function of the lower integration limit $L/2$, indeed

$$\frac{\partial}{\partial L} \bar{z}_T(t; L) = \frac{1}{2} \frac{|\Psi(L/2, t)|^2 \int_{L/2}^{+\infty} dz (z - L/2) |\Psi(z, t)|^2}{\left(\int_{L/2}^{+\infty} dz |\Psi(z, t)|^2 \right)^2} > 0, \quad (3.101)$$

as an integral of two positive non-zero functions cannot be equal zero. Similarly, we obtain that the centroids of the incident and reflected packets are decreasing functions of the upper integration limits, $-L/2$ in this case. From these inequalities immediately follows that

$$\bar{z}_T^{(as)}(t) \equiv \bar{z}_T(t; L = -\infty) < \bar{z}_T(t; L/2), \quad \bar{z}_R^{(as)}(t) \equiv \bar{z}_R(t; L = -\infty) > \bar{z}_R(t; L/2). \quad (3.102)$$

The difference between equations (3.99) and (3.100) increases, when $\bar{z}_T^{(as)}(t)$ approaches $L/2$ and when $\bar{z}_R^{(as)}(t)$ approaches $-L/2$, and it becomes of the order of the spatial packet width, i.e. $\sim \hbar/\gamma_p$, for the incident packet and $\sim \hbar/\gamma_{p,R(T)}$ for the packets after scattering: the widths of the transmitted and reflected packets can deviate from the width of the incident packet after interaction, as we shall see in section 3.8. The width of the momentum distribution for

transmitted and reflected packets can be calculated as the inverse spatial width of the packet (in analogy to equation (3.54))

$$\frac{\hbar^2}{4\gamma_{p,T}^2} = \overline{[z_T^{(as)}(t)]^2} - [z_T^{(as)}(t)]^2, \quad \frac{\hbar^2}{4\gamma_{p,R}^2} = \overline{[z_R^{(as)}(t)]^2} - [z_R^{(as)}(t)]^2. \quad (3.103)$$

Taking the packet widths into account, we can parameterize the centroid motion as

$$\begin{aligned} \bar{z}_T(t) &= \bar{z}_T^{(as)}(t) + \varsigma_T \frac{\hbar}{\gamma_{p,T}} f_c(\gamma_{p,T} |L/2 - \bar{z}_T^{(as)}(t)|/\hbar), \quad t > 0, \quad \bar{z}_T(t) > L/2, \\ \bar{z}_R(t) &= \bar{z}_R^{(as)}(t) - \varsigma_R \frac{\hbar}{\gamma_{p,R}} f_c(\gamma_{p,R} |L/2 + \bar{z}_R^{(as)}(t)|/\hbar), \quad t > 0, \quad \bar{z}_R(t) < -L/2, \\ \bar{z}_I(t) &= \bar{z}_I^{(as)}(t) - \varsigma_I \frac{\hbar}{\gamma_p} f_c(\gamma_p |L/2 + \bar{z}_I^{(as)}(t)|/\hbar), \quad t < 0, \quad \bar{z}_I(t) < -L/2, \end{aligned} \quad (3.104)$$

where $\varsigma_{I(R,T)}$ are some positive constants of the order of unity and the transition to the asymptotic motion is controlled by the function $f_c(\zeta)$: $f_c(\zeta \lesssim 1) \sim 1$ for $0 \leq \zeta \lesssim 1$ and f_c vanishes for $\zeta \gg 1$. For the Gaussian momentum distribution (3.55), which leads to the Gaussian spatial form of the wave packets, we find $\varsigma_I = \varsigma_T = \varsigma_R = 1/\sqrt{2\pi}$ and $f_c(\zeta) = \exp(-2\zeta^2)/\text{erfc}(-\sqrt{2}\zeta)$, where erfc stands for the complementary error function.

We can proceed further with the evaluation of the integrals (3.100) (see appendix C), and obtain the results for arbitrary momentum distribution $\varphi(k)$ [81]:

$$\bar{z}_T^{(as)}(t) = \langle (-\hbar\xi'(k) - \hbar\phi'_T(k) + tk/m) \rangle_{k,T}, \quad \bar{z}_R^{(as)}(t) = \langle (\hbar\xi'(k) + \hbar\phi'_R(k) - tk/m) \rangle_{k,R}. \quad (3.105)$$

Here we introduce the averaging over the momentum weighted with the transmission or reflection probability

$$\langle (\dots) \rangle_{k,T} = \frac{\langle |T(E)|^2 (\dots) \rangle_k}{\langle |T(E)|^2 \rangle_k}, \quad \langle (\dots) \rangle_{k,R} = \frac{\langle |R(E)|^2 (\dots) \rangle_k}{\langle |R(E)|^2 \rangle_k}. \quad (3.106)$$

Recall that the momentum averaging $\langle \dots \rangle_k$ is defined in equation (3.51). The evaluation of the T -weighted k -averages (3.106) for small γ_p can be done with the help of the relations

$$\langle f(k) \rangle_{k,T} \approx f(p) + \frac{1}{2}\gamma_p^2 \frac{d^2 f(p)}{dp^2} + \gamma_p^2 \frac{df(p)}{dp} \frac{d}{dp} \log |T(p)|^2. \quad (3.107)$$

Here the primes mean derivatives with respect to the momentum. The analogous relation can be written for the R -weighted k -average. We can also use the relation, which holds up to the order γ_p^2 :

$$\langle f(k)g(k) \rangle_{k,T(R)} \approx \langle f(k) \rangle_{k,T(R)} \langle g(k) \rangle_{k,T(R)} + \gamma_p^2 f'(p)g'(p), \quad (3.108)$$

where $f(k), g(k)$ are arbitrary functions. For the packet widths defined in equation (3.103) we obtain now, using equations (C.12) and (C.13) of appendix C,

$$\begin{aligned} \frac{\hbar^2}{\gamma_{p,T}^2} &= \left\langle \hbar^2 \left[\frac{d}{dk} \log(|\varphi(k)||T(k)|) \right]^2 \right\rangle_{k,T} + \left\langle \left(\hbar\xi'(k) + \hbar\phi'_T(k) - \frac{k}{m}t \right)^2 \right\rangle_{k,T} \\ &\quad - \left\langle \hbar\xi'(k) + \hbar\phi'_T(k) - \frac{k}{m}t \right\rangle_{k,T}^2, \\ \frac{\hbar^2}{\gamma_{p,R}^2} &= \left\langle \hbar^2 \left[\frac{d}{dk} \log(|\varphi(k)||R(k)|) \right]^2 \right\rangle_{k,R} + \left\langle \left(\hbar\xi'(k) + \hbar\phi'_R(k) - \frac{k}{m}t \right)^2 \right\rangle_{k,R} \\ &\quad - \left\langle \hbar\xi'(k) + \hbar\phi'_R(k) - \frac{k}{m}t \right\rangle_{k,R}^2. \end{aligned} \quad (3.109)$$

First of all, from these expressions we see that asymptotically reflected and transmitted centroids move with velocities which differ from the velocity of the incident packet. From (3.105) we get

$$v_R = \frac{d\bar{z}_R^{(as)}(t)}{dt} = -\left\langle \frac{k}{m} \right\rangle_{k,R} = \frac{p_R}{m}, \quad v_T = \frac{d\bar{z}_T^{(as)}(t)}{dt} = \left\langle \frac{k}{m} \right\rangle_{k,T} = \frac{p_T}{m}. \quad (3.110)$$

For a sufficiently narrow initial momentum distribution $\varphi(k)$ peaked around p with the dispersion γ_p , see equations (3.50), (3.52), with the help of equation (3.52) we find

$$v_R \approx -v_I \left(1 + 2 \frac{\gamma_p^2}{m} \frac{d}{dE_p} \log |R(E_p)| \right), \quad v_T \approx v_I \left(1 + 2 \frac{\gamma_p^2}{m} \frac{d}{dE_p} \log |T(E_p)| \right). \quad (3.111)$$

In the case of the tunneling through a thick barrier the expansion (3.111) holds for $\gamma_p \ll \sqrt{\hbar|\kappa|/L}$.

From figure 8 we see that for $E_p < U$ (tunneling regime)⁸ the transmission amplitude $|T|$ is an increasing function of energy, therefore the reflection amplitude $|R|$ decreases with an energy increase. Hence in the tunneling for the transmitted packet $v_T > v_I$, while for the reflected packet $|v_R| < v_I$. The reason for this phenomenon is obvious, the barrier acts as a filter allowing higher probability penetration for the modes with higher energies. This serves as an argument against a direct comparison of characteristics of the transmitted and incident packets without a normalization to the characteristics of the corresponding stationary problem.

Using equations (3.107) and (3.108) we can rewrite expressions for the asymptotic centroid of the transmitted packet (3.105) as follows:

$$\bar{z}_T^{(as)}(t) \approx \langle (-\hbar\xi'(k)) \rangle_{k,T} + \frac{v_T}{|v_T|} L + v_T (t - \bar{t}_T) + v_I \hbar \frac{\gamma_p^2}{m} \frac{d^2 \delta(E_p)}{dE_p^2}, \quad \bar{t}_T = \left\langle \hbar \frac{d\delta_s(E)}{dE} \right\rangle_{k,T}. \quad (3.112)$$

We see that the centroid motion is delayed by the time \bar{t}_T , which is the averaged group time (3.82). From equation (3.109) the momentum width of the transmitted packet including γ_p^2 corrections is given by

$$\frac{1}{\gamma_{p,T}^2} \simeq \frac{1}{\gamma_p^2} - 2 \frac{d^2}{dp^2} \log |T(k)|. \quad (3.113)$$

The corresponding expressions for the reflected centroid differ only in the subindex ‘R’. Note that the second term in equation (3.112) will change sign if we replace v_T with v_R .

The centroid transmission and reflection time delays can be defined as

$$t_R^{(cen)} = \tau_-^{(R)} - \tau_-^{(I)}, \quad t_T^{(cen)} = \tau_+^{(T)} - \tau_-^{(I)}, \quad (3.114)$$

where $\tau_+^{(T)}$ is the time when the transmitted packet emerges to the right from the potential region, $\tau_-^{(I)}$ is the time when the incident packet enters the potential region and $\tau_-^{(R)}$ is the time when the reflected packet emerges to the left from the potential region. Quantification of the emergence moments requires some care. In [81, 100] the authors used the asymptotic expressions (3.105) and (3.53) and extrapolated them right up to the borders of the region of non-zero potential $z = \pm L/2$, going thereby beyond their application domain, since the correction terms in equations (3.104) cannot be neglected for those z . Moreover, from the very definitions of the centroids (equation (3.99)) one can easily see that $\bar{z}_T(t)$ can never reach the point $z = +L/2$ and $\bar{z}_R(t)$, the point $z = -L/2$. To avoid this problem we are forced to step

⁸ For $U - E_p \lesssim \gamma$ one cannot distinguish between a tunneling regime and particle motion above the barrier. To deal with pure tunneling one should assume that $U - E_p \gg \gamma$.

away from the borders of the region of non-zero potential by a quantity $\sim \hbar/\gamma_p$ and define $\tau_-^{(I)}$, $\tau_-^{(R)}$ and $\tau_+^{(T)}$ from relations

$$\bar{z}_1^{(as)}(\tau_-^{(I)}) = -\frac{L}{2} - \tilde{\zeta}_I \frac{\hbar}{\gamma_p}, \quad \bar{z}_R^{(as)}(\tau_-^{(R)}) = -\frac{L}{2} - \tilde{\zeta}_R \frac{\hbar}{\gamma_{p,R}}, \quad \bar{z}_T^{(as)}(\tau_+^{(T)}) = +\frac{L}{2} + \tilde{\zeta}_T \frac{\hbar}{\gamma_{p,T}}. \quad (3.115)$$

The constants $\tilde{\zeta}_{I,R,T}$ are positive and $\tilde{\zeta}_{I,R,T} \sim \zeta_{I,R,T} \sim 1$. Note that for the Gaussian packets at the time moments defined by these conditions with $\tilde{\zeta}_{I,R,T} = \zeta_{I,R,T}$, the maxima of the packets are located exactly at the barrier borders $z = \pm L/2$.

Let us use such initial wave packet distributions that correspond to $\hbar\xi'(k) = z_0 - kt_0/m$, see equations (3.53). Then the solutions of equations (3.115) are

$$\begin{aligned} \tau_-^{(I)} &= -\frac{1}{v_I} \left(\frac{L}{2} + \frac{\tilde{\zeta}_I \hbar}{\gamma_p} \right), \\ \tau_-^{(R)} &= -\frac{1}{v_R} \left(\frac{L}{2} + \frac{\tilde{\zeta}_R \hbar}{\gamma_{p,R}} \right) - \frac{1}{v_R} \left\langle \frac{k}{m} \hbar \frac{d}{dE} \phi_R(E) \right\rangle_{k,R}, \\ \tau_+^{(T)} &= \frac{1}{v_T} \left(\frac{L}{2} + \frac{\tilde{\zeta}_T \hbar}{\gamma_{p,T}} \right) + \frac{1}{v_T} \left\langle \frac{k}{m} \hbar \frac{d}{dE} \phi_T(E) \right\rangle_{k,T}. \end{aligned} \quad (3.116)$$

Substituting equation (3.9) into equations (3.116) for the centroid reflection and transmission time delays (3.114) we find

$$\begin{aligned} t_R^{(cen)} &= t_{form,R} + \frac{L}{2} \frac{v_I - |v_R|}{v_I |v_R|} + \frac{1}{|v_R|} \left\langle \frac{k}{m} \hbar \frac{d\delta_s(E)}{dE} \right\rangle_{k,R}, \\ t_T^{(cen)} &= t_{form,T} + \frac{L}{2} \frac{v_T - v_I}{v_I v_T} + \frac{1}{v_T} \left\langle \frac{k}{m} \hbar \frac{d\delta_s(E)}{dE} \right\rangle_{k,T}, \end{aligned} \quad (3.117)$$

where we introduced new quantities

$$t_{form,R} = t_{form,I} + \frac{\tilde{\zeta}_R \hbar}{\gamma_{p,R} |v_R|}, \quad t_{form,T} = t_{form,I} + \frac{\tilde{\zeta}_T \hbar}{\gamma_{p,T} v_T}, \quad t_{form,I} = \frac{\tilde{\zeta}_I \hbar}{\gamma_p v_I}, \quad (3.118)$$

which can be called the wave packet formation times. These quantities characterize the time needed to the packets to ‘complete the scattering event’, i.e., enter the potential zone and emerge from it. We note that $t_R^{(cen)} \neq t_T^{(cen)}$ even for a symmetrical barrier in contrast to the group times (3.82). These times show averaged passage times by particles of the typical spatial packet length \hbar/γ_p .

Due to performed averaging, in dealing with centroids one loses information about specific forms of spatial distribution in the packet on a scale $\lesssim \hbar/\gamma_p$, which could be extracted, if one worked with non-averaged spatial distributions. The mentioned uncertainty is small provided the formation times are shorter than other quantities in (3.118), for $\gamma_p \gg |\varkappa|$, i.e. when the incident wave packet is very narrow in space and broad in momentum. Then $t_{form,R(T)} \ll t_{quant} \sim \hbar/v_I |\varkappa|$ and the formation times in equation (3.117) can be neglected. In this case the wave packet is well localized spatially and the centroids can serve as appropriate characteristics of the particle position. However, unfortunately, for the case of large γ_p we cannot speak further about tunneling, since the large part of the wave packet propagates above the barrier.

In contrast, for a very narrow momentum distribution ($\gamma_p \ll |\varkappa|$) we would expect to recover previously obtained results for the group times (3.82) and (3.80). The latter quantities determined with the help of the packet peaks (by method of the stationary phase) do not depend on the widths of the packets. Therefore, to make both approaches compatible we have to subtract from $\tau_{R,T}$ formation times being divergent for $\gamma_p \rightarrow 0$. This reflects the fact that

the spatially broad packet needs a very long time to complete the scattering, in line with the uncertainty relation. In the limit $\gamma_p \rightarrow 0$ from equation (3.117) we obtain

$$v_T \approx |v_R| \approx v_I, \quad t_T^{(\text{cen})} - t_{\text{form},T} \approx t_R^{(\text{cen})} - t_{\text{form},T} \approx t_{\text{bs}} = \hbar \frac{d\delta_s(E_p)}{dE_p}. \quad (3.119)$$

Now, let us apply results (3.111) and (3.117) to the case of a narrow momentum distribution (small γ_p) and a very thick rectangular barrier $\kappa L/\hbar \gg 1$. The transmission and reflection amplitudes (3.19) and their log-derivatives can be approximated as

$$|T(E_p)| \approx \frac{4\kappa p}{\kappa^2 + p^2} e^{-\kappa L/\hbar}, \quad |R| \approx 1, \\ \frac{d}{dE_p} \log |T(E_p)| = \frac{mL}{\hbar \kappa} + \frac{m}{p^2} - \frac{m}{\kappa^2}, \quad \frac{d}{dE} \log |R(E_p)| = 0 \quad (3.120)$$

and

$$v_T \simeq v_I \left[1 + 2\gamma_p^2 \left(\frac{L}{\hbar \kappa} + \frac{1}{p^2} - \frac{1}{\kappa^2} \right) \right], \quad v_R \simeq v_I. \quad (3.121)$$

Recall that $p = \sqrt{2mE_p}$ and $\kappa = \sqrt{2m(U - E_p)}$. Since in the case of a thick barrier the reflection probability is close to unity, we have $v_R \approx -v_I$. Using equation (3.52), for the centroid reflection time delay we find

$$t_R^{(\text{cen})} - t_{\text{form},R} \approx \frac{1}{v_I} \left\langle \frac{k}{m} \hbar \frac{d\delta_s(E)}{dE} \right\rangle_k \approx \hbar \frac{d\delta_s(E_p)}{dE_p} + \frac{3\gamma_p^2}{2m} \hbar \frac{d^2\delta_s(E_p)}{dE_p^2} + \frac{\gamma_p^2 p^2}{2m^2} \hbar \frac{d^3\delta_s(E_p)}{dE_p^3} \\ = 2 \frac{\hbar}{v_I \kappa} \left(1 + \gamma_p^2 \frac{\kappa^2 + 3p^2}{2\kappa^4} \right). \quad (3.122)$$

For the Gaussian wave packet the reflection packet formation time coincides with the incident packet formation time $t_{\text{form},I} \simeq t_{\text{form},R} \simeq (\hbar\sqrt{2/\pi})/(\gamma_p v_I)$.

An expression for the centroid transmission time delay is more cumbersome. Using approximate relations (3.111) and the expansion

$$\frac{1}{v_T} \left\langle \frac{k}{m} \hbar \frac{d\delta_s(E)}{dE} \right\rangle_{k,T} = \frac{d\delta_s(E_p)}{dE_p} \left[1 + 2\gamma_p^2 \left(\frac{\delta_s''(p)}{\delta_s'(p)} - \frac{1}{p} \right) \frac{d}{dp} \log |T(p)| + \gamma_p^2 \frac{\delta_s'''(p)}{2\delta_s'(p)} \right], \quad (3.123)$$

we finally find

$$t_T^{(\text{cen})} - t_{\text{form},T} \simeq \frac{2\hbar}{v_I \kappa} \left[1 + \gamma_p^2 \left(\frac{L}{\hbar} \left(\frac{L}{\hbar} + \frac{\kappa^2 - p^2}{\kappa p^2} \right) + \frac{2L(p^2 - \kappa^2)}{\hbar \kappa^3} \right. \right. \\ \left. \left. + \frac{9\kappa^2 p^2 - 4\kappa^4 - p^4}{\kappa^4 p^2} \right) \right]. \quad (3.124)$$

For the Gaussian wave packet the transmission quantum formation time becomes

$$t_{\text{form},T} \simeq \frac{\hbar\sqrt{2}}{\sqrt{\pi}\gamma_p v_I} \left[1 - \frac{\gamma_p^2}{2} \left(\frac{L}{\hbar \kappa} \left(1 - \frac{p^2}{\kappa^2} \right) + \frac{3\kappa^4 - \kappa^2 p^2 + 2p^4}{\kappa^4 p^2} \right) \right]. \quad (3.125)$$

Expansions in (3.124), (3.125) hold provided $\frac{\hbar}{|z_0|} \ll \gamma_p \ll \hbar/L$. From these expressions we may conclude that the centroid transmission and reflection time delays contain the formation times $t_{\text{form},R(T)}$, as the largest times in the limit of small γ_p , which arise because of the averaging over the spatial packet distribution. The next-to-leading term (on the right-hand side in equation (3.124)) not depending on γ_p coincides with t_T given by equation (3.98). The Hartmann effect discussed above is described by this quantum term. Corrections to the group times (3.78), (3.79) that appeared due to the finite packet width, invoke dependence on the length L of the region of non-zero potential. Dependence on L may indicate that the passage

time of the barrier is proportional to its length. The concepts of the group times introduced in the previous section can be reliably used if $\gamma_p \ll \hbar/L$. Also, if these inequalities are fulfilled and $\frac{\hbar}{|z_0|} \ll \gamma_p$, we can exploit asymptotic centroids. The quantity

$$\delta t_f^\gamma = t_T^{(\text{cen})} - t_{\text{form},1} \simeq \frac{2\hbar}{v_1 \kappa} - \frac{\gamma_p}{\sqrt{2\pi} v_1} \frac{L}{\hbar \kappa} \left(1 - \frac{p^2}{\kappa^2}\right) \quad (3.126)$$

has a meaning of the forward delay time, compare with equation (2.68). The second (correction) term in the second equality is positive for $E > U/2$ and negative for $E < U/2$.

More complete information about the temporal behavior of the packets can be extracted from explicit forms of spatial distributions. To elucidate these aspects further, in the next section we consider a specific example of the propagation of the Gaussian momentum packet.

3.8. Tunneling of the Gaussian wave packet

We now consider in detail the tunneling of the packet with the Gaussian envelop in the momentum space, see equation (3.55). To be sure that we really operate in the tunneling regime we have to keep $\gamma_p \ll \kappa$, $\kappa > 0$. Moreover we assume that $\gamma_p \ll p$. Thus, the integration over k in equations (3.49), (3.76) and (3.77) can be extended to $-\infty$. As in the previous section we assume that $\hbar \xi'(k) = z_0 - k t_0/m$ and we choose the initial position of the packet z_0 and time t_0 such that $\langle \hbar \xi'(k) \rangle_k = 0$.

The probability densities to find a particle in the point z at the moment of time t is given by $|\Psi_{>}(z, t)|^2 = |\Psi_T(z, t)|^2$ for $z \geq L/2$ and by $|\Psi_{<}(z, t)|^2 = |\Psi_I(z, t)|^2 + |\Psi_R(z, t)|^2 + 2\text{Re}(\Psi_I^*(z, t)\Psi_R(z, t))$ for $z \leq -L/2$, where the wave functions are given by equations (3.49), (3.76) and (3.77). The interference term in $\text{Re}(\Psi_I^*(z, t)\Psi_R(z, t))$ is small, if z is sufficiently far from the left border of the potential, $|z + L/2| \gg \hbar/\gamma_p$. Then the first term in $|\Psi_{<}(z, t)|^2$ describes the free motion of a wave packet with a Gaussian envelop and equals to

$$|\Psi_I(z, t)|^2 = \sqrt{\frac{2\gamma_{p,1}^2(t)}{\pi \hbar^2}} \exp(-2\gamma_{p,1}^2(t) (z - \tilde{z}_1(t))^2/\hbar^2), \quad (3.127)$$

where the time evolution of the packet centrum and the width are determined by

$$\tilde{z}_1(t) = v_1 t, \quad \gamma_{p,1}^2(t) = \gamma_p^2 / \left(1 + 4\gamma_p^4 \frac{(t - t_0)^2}{m^2 \hbar^2}\right). \quad (3.128)$$

The packet becomes smeared on the time-scale $t - t_0 \gtrsim t_{\text{sm}} = \hbar m/\gamma_p^2$. This corresponds to $z - z_0 \gtrsim v_1 t_{\text{sm}}$. Further, to simplify expressions we will restrict ourselves to the times $t - t_0 \ll t_{\text{sm}}$, and to the distances $z - z_0 \ll v_1 t_{\text{sm}}$. For a particle moving not too far from the barrier, the typical values of time and space coordinates are $t - t_0 \sim |t_0|$ and $z - z_0 \sim |z_0|$. Then assuming $|z_0| \ll \hbar p/\gamma_p^2$ we can neglect the smearing of the wave packet and put further $\gamma_{p,1} \simeq \gamma_p$.

It is important to realize that for the packet described by equation (3.127), freely moving through the spatial segment $[-L/2, L/2]$, even for large L there is a small but finite probability $|\Psi_I(L/2, -L/(2v_1))|^2 = \exp(-2\gamma_p^2 L^2/\hbar^2)$ to find the particle at $z = L/2$, while the center of the packet is still at the point $z = -L/2$ and reaches the point $z = L/2$ only after the time L/v_1 .

For the transmitted wave keeping the second derivatives of the transmission amplitude we find

$$|\Psi_T(z, t)|^2 = |T(p)|^2 \frac{\gamma_{p,T}}{\gamma_p} \sqrt{\frac{2\gamma_{p,T}^2(t)}{\pi \hbar^2}} \exp\left(-2\gamma_{p,T}^2(t) \left[(z - \tilde{z}_T(t))^2 - \frac{\gamma_{p,T}^2(t)}{\gamma_{p,T}^2(t)} t_T^2 \right] / \hbar^2\right), \quad (3.129)$$

where the motion of the packet's centum is described by equation

$$\tilde{z}_T(t) = L + v_T [t - (v_I/v_T) t_T]. \quad (3.130)$$

The speed of the transmitted packet v_T given here by equation (3.111) is larger than the speed of the incident packet.

The length l_T in equation (3.129) is

$$l_T = \hbar \frac{d}{dp} \log |T(p)|. \quad (3.131)$$

The width is time dependent at the order γ_p^4 ,

$$\frac{1}{\gamma_{p,T}^2(t)} = \frac{1}{\gamma_{p,T}^2} + 4 \gamma_{p,T}^2 \frac{(t - t_0 - t_{\gamma,T})^2}{m^2 \hbar^2}. \quad (3.132)$$

Here $\gamma_{p,T}$ is given by the equation (3.113) and the time is delayed by the quantity

$$t_{\gamma,T} = m \hbar \frac{d^2}{dp^2} \phi_T(p) = m \hbar \frac{d^2}{dp^2} \delta_s(p). \quad (3.133)$$

The time-dependent term follows directly from the last two terms in the first equation in (3.109), if we apply equation (3.108).

At the points $z \simeq \tilde{z}_T(t) \pm l_T$ the exponent in equation (3.129) equals unity. For a broad barrier the tunneling amplitude $|T|$ can be presented as

$$T(p) = t(p) \exp\left(-\int_{z_1}^{z_2} \kappa(z, E) dz/\hbar\right),$$

cf. the semiclassical expression equation (3.90), $z_{1,2}$ are the classical turning points and $t(p)$ is a prefactor, which depends on p rather slowly. The value l_T contains two terms

$$l_T = v_I t_{\text{trav}}^{(\text{tun})} + \delta l_T, \quad t_{\text{trav}}^{(\text{tun})} = \int_{z_1}^{z_2} \frac{m dz}{\kappa(z, E)}, \quad \delta l_T = \hbar t'(p)/t(p). \quad (3.134)$$

The quantity $t_{\text{trav}}^{(\text{tun})}$ has the meaning of a traversal time between the turning points provided $\kappa > 0$, cf. equation (3.26). This is exactly the scale which is missing in the Hartmann effect. The second term, δl_T , in (3.134) is of the order of a quantum length scale, being much shorter for the thick barrier than the first term.

For the rectangular barrier in the limit $\kappa L/\hbar \gg 1$ (see, equation (3.120)) we have explicitly

$$l_T = v_I t_{\text{trav}}^{(\text{tun})} + \frac{\hbar}{p} \frac{\kappa^2 - p^2}{\kappa^2}. \quad (3.135)$$

Here $t_{\text{trav}}^{(\text{tun})} = mL/\kappa$. Using equations (3.113), (3.131) and (3.135) we find how the packet width changes after tunneling through the broad rectangular barrier

$$\frac{1}{\gamma_{p,T}^2} \approx \frac{1}{\gamma_p^2} + \frac{2}{\hbar} \frac{dl_T}{dp} \approx \frac{1}{\gamma_p^2} + 2 \left(\frac{L}{\hbar \kappa} + \frac{1}{p^2} \right) \left(1 + \frac{p^2}{\kappa^2} \right). \quad (3.136)$$

Thus, the longer is the barrier, the broader becomes the transmitted wave packet forming for $z \geq L/2$. Further we continue to assume that $|z_0| \ll \hbar p/\gamma_p^2$ and we assume that $L \ll \hbar \kappa/\gamma_p^2$.

For the reflected wave packet equations (3.129)–(3.132) can be applied after the formal replacement of indices ‘T’ → ‘R’ and the scattering amplitude $T(p) \rightarrow R(p)$; the reflected-packet centum moves according to $\tilde{z}_R(t) = -L - |v_R| [t - (v_I/|v_R|) t_R]$, where we take into account that $v_R < 0$. For the broad barrier we can put $|v_R| \simeq v_I$ and $|R| \simeq 1$, so that $\gamma_{p,R} = \gamma_p$ and $l_R = 0$, and we write

$$|\Psi_R(z, t)|^2 = \sqrt{\frac{2\gamma_p^2}{\pi \hbar^2}} \exp(-2\gamma_p^2(z - \tilde{z}_R(t))^2/\hbar^2), \quad \tilde{z}_R(t) = -L - v_I(t - t_R). \quad (3.137)$$

The peak of the reflected wave packet is formed at $z = -L/2$ at the time moment $t(-L/2) = -L/2v_I + t_R$, $t_R = t_T$, i.e. with a delay t_T compared to the time moment when the incident packet reached $z = -L/2$. For the thick rectangular barrier $t(-L/2) = -L/2v_I + 2\hbar/\kappa v_T$.

Comparing equations (3.127) and (3.129) we observe that the tail of the transmitted wave packet begins to be formed for $z \geq L/2$, already at a time when the maximum of the incident wave packet has not yet reached the point $z = -L/2$. For example, if the incident packet is at some coordinate $z' < -L/2$ at the time z'/v_I , the relative probability of the transmitted packet to be at $z = +L/2$ is equal to

$$\frac{|\Psi_T(L/2, z'/v_I)|^2}{|\Psi_I(z', z'/v_I)|^2} \approx |T(p)|^2 \frac{\gamma_{p,T}^2}{\gamma_p^2} \exp(2\gamma_{p,T}^2 L^2/\hbar^2) \exp\left(-2\frac{\gamma_{p,T}^2}{\hbar^2} \left[\frac{1}{2}L + \frac{v_T}{v_I} z' - v_I t_T\right]^2\right). \quad (3.138)$$

However, the maximum of the transmitted packet does not emerge from under the barrier even at the moment when the incident packet's maximum is at the left border of the potential. Indeed, from equation (3.130) we see that it happens when $t(L/2) = -(L/2 - v_I t_T)/v_T$. At free propagation at this moment the incident packet would be at $z = -(L/2 - v_I t_T) v_I/v_T > -L/2$ since $v_I < v_T$. For the thick rectangular barrier $t(L/2) = -L/2v_T + 2\hbar/\kappa v_T$. For $L\gamma_p \ll \hbar$ the formation of the transmitted wave packet peak at $z = L/2$ is delayed compared to the moment when the incident one arrives at $z = -L/2$, by the quantum time $\Delta t \simeq 2\hbar/\kappa v_I$ and the transmitted peak at $z = L/2$ is formed approximately at the same time (at negligible γ_p) as the reflected wave packet peak at $z = -L/2$ (the Hartmann effect). However for $L\gamma_p \gg \hbar$ the same difference of times is approximately $\Delta t \simeq L^2\gamma_p^2/\hbar\kappa v_I$, i.e. it depends on L .

The finite width of a packet describing a moving particle alters the notion of the particle being at some spatial point. The probability to find a particle at a given point becomes essentially non-zero already before the center of the packet has reached it, with an advancement

$$t_{\text{dec}}^\gamma = \frac{\hbar}{v_I \gamma_p} = \frac{\hbar}{\gamma}, \quad (3.139)$$

where γ_p and γ are the momentum and energy dispersions in the Gaussian packet given by equations (3.50) and (3.46), respectively. This is in accord with the uncertainty principle derived by Mandelstam and Tamm in [58],

$$\Delta E \Delta T \geq \frac{\hbar}{2} |\overline{\dot{T}}|, \quad \Delta E = (\overline{(E - \bar{E})^2})^{1/2}, \quad \Delta T = (\overline{(\mathcal{T} - \bar{\mathcal{T}})^2})^{1/2}, \quad (3.140)$$

where \mathcal{T} is a physical quantity not dependent on time explicitly; the bar means quantum-mechanical averaging. The value $\delta t_{\text{var}} = |\Delta \mathcal{T}/\overline{\dot{\mathcal{T}}}|$ is the *variation time* during which the observable \mathcal{T} changes its value more than its dispersion. Taking the coordinate as the observable \mathcal{T} and $\Delta \mathcal{T}$ as the average spatial width, we can interpret δt_{var} as the minimal time the packet needs to pass a certain space point. Since $\Delta E \sim \gamma$ is the energy width for the Gaussian wave packet under consideration, the minimal duration of the emergence of the transmitted wave packet on the right side of the barrier is $\delta t_{\text{var}} \sim \hbar/\gamma = t_{\text{dec}}^\gamma$. At the same time the incident packet needs to enter the barrier on the left side. Since the information may reach the given point with an advancement $\sim \delta t_{\text{var}}$ the real (forward) delay/advance time for the particles of the transmitted packet is not $t_T = t_{\text{bs}}$ but should be counted from $2t_{\text{dec}}^\gamma$:

$$\delta t_f^{(\text{tum})} \equiv t_{\text{bs}} - 2t_{\text{dec}}^\gamma. \quad (3.141)$$

Now consider propagation of the wave packet inside a rectangular barrier. The internal wave function (3.4) with the coefficients (3.20) contains the growing and evanescent parts

$$\begin{aligned}
\psi_U(z, E) &= \psi_{\text{grow}} + \psi_{\text{evan}} = D_+(k) e^{\kappa z/\hbar} + D_-(k) e^{-\kappa z/\hbar}, \\
D_{\pm}(k) &= \frac{1}{2}(C_+ \pm C_-) = \frac{1}{2}(1 \pm ik/\kappa) T(k) e^{(ik \mp \kappa)L/2\hbar} \\
&= \frac{1}{2} \sqrt{1 + \frac{k^2}{\kappa^2}} T(k) e^{\pm i\beta_{\kappa}(k) + (ik \mp \kappa)L/2\hbar}, \quad \beta_{\kappa}(k) = \arctan(k/\kappa).
\end{aligned} \tag{3.142}$$

Hence the internal wave packet

$$\Psi_U(z, t) = \int_0^{\infty} \frac{dk}{2\pi\hbar} \varphi(k) \psi_U(z, E) e^{-iEt/\hbar} \tag{3.143}$$

can be written as the sum of growing and evanescent parts and their interference

$$|\Psi_U(z, t)|^2 = |\Psi_{\text{grow}}(z, t)|^2 + |\Psi_{\text{evan}}(z, t)|^2 + 2 \operatorname{Re}\{\Psi_{\text{grow}}(z, t)\Psi_{\text{evan}}^*(z, t)\}. \tag{3.144}$$

The first two terms do not contribute to the current density. The current conservation for the particle motion under the barrier is due to the presence of the interference term.

Introducing the phase of the amplitudes for the growing and evanescent parts of the wave function

$$\phi_{D_{\pm}}(k) = \arg D_{\pm}(k) = \phi_T(k) + \frac{kL}{2\hbar} \pm \beta_{\kappa}(k) \tag{3.145}$$

we can cast the growing part, $|\Psi_{\text{grow}}(z, t)|^2 \equiv |\Psi_+(z, t)|^2$, and the evanescent part, $|\Psi_{\text{evan}}(z, t)|^2 \equiv |\Psi_-(z, t)|^2$, in the form

$$\begin{aligned}
|\Psi_{\pm}(z, t)|^2 &= \frac{1}{4} \left(1 + \frac{p^2}{\kappa^2}\right) |T(p)|^2 e^{\pm 2\kappa(z-L/2)/\hbar} \frac{\gamma_{p,D}^{(\pm)}}{\gamma_p} \sqrt{\frac{2\gamma_{p,D}^{(\pm)2}(t)}{\pi\hbar^2}} \\
&\times \exp \left[2 \frac{\gamma_{p,D}^{(\pm)2}}{\hbar^2} \left(l_D^{(\pm)} \mp z \frac{p}{\kappa} \right)^2 \right] \exp \left[-2 \frac{\gamma_{p,D}^{(\pm)2}(t)}{\hbar^2} \left(v_1(t - t_D^{(\pm)}) \right. \right. \\
&\left. \left. + 2\gamma_{p,D}^{(\pm)2} \frac{t - t_{\gamma,D}^{(\pm)}}{m\hbar} \left(l_D^{(\pm)} \mp z \frac{p}{\kappa} \right) \right)^2 \right].
\end{aligned} \tag{3.146}$$

The spatial widths of the internal packets are given by

$$\begin{aligned}
\frac{1}{\gamma_{p,D}^{(\pm)2}} &= \frac{1}{\gamma_p^2} - 2 \left[\frac{d^2}{dp^2} \log |D_{\pm}(p)| - \frac{z}{\kappa\hbar} \left(1 + \frac{p^2}{\kappa^2}\right) \right] \\
&= \frac{1}{\gamma_{p,T}^2} - \frac{2}{\kappa^2} \left(1 + 2\frac{p^2}{\kappa^2}\right) - 2 \frac{z \pm L/2}{\kappa\hbar} \left(1 + \frac{p^2}{\kappa^2}\right),
\end{aligned} \tag{3.147}$$

thus acquiring a weak time dependence

$$\begin{aligned}
\frac{1}{\gamma_{p,D}^{(\pm)2}(t)} &= \frac{1}{\gamma_{p,D}^{(\pm)2}} + 4\gamma_{p,D}^{(\pm)2} \frac{(t - t_0 - t_{\gamma,D}^{(\pm)})^2}{m^2 \hbar^2}, \quad t_{\gamma,D}^{(\pm)} = m\hbar \frac{d^2 \phi_{D_{\pm}}(p)}{dp^2} \\
&= m\hbar \frac{d^2 \delta_s(p)}{dp^2} \pm \frac{m\hbar p}{\kappa^3},
\end{aligned} \tag{3.148}$$

operating on the large time-scales for $t - t_0 \gg t_{\text{sm}}$, where the smearing time t_{sm} is given by equation (3.57). On the shorter time-scales and for $\gamma_p^2 L/\kappa\hbar \ll 1$ we can approximate $\gamma_{p,D}^{(\pm)}(t) \approx \gamma_{p,T}$. Then equation (3.146) simplifies as follows

$$\begin{aligned}
|\Psi_{\pm}(z, t)|^2 &\approx \frac{1}{4} \left(1 + \frac{p^2}{\kappa^2}\right) |T(p)|^2 e^{\pm 2\kappa(z-L/2)/\hbar} \sqrt{\frac{2\gamma_{p,T}^4}{\pi\hbar^2 \gamma_p^2}} \\
&\times \exp \left(2 \frac{\gamma_{p,T}^2}{\hbar^2} \left[\left(l_D^{(\pm)} \mp z \frac{p}{\kappa} \right)^2 - v_1^2 (t - t_D^{(\pm)})^2 \right] \right).
\end{aligned} \tag{3.149}$$

We see that in this approximation the time dependence decouples completely from the spatial dependence. As time elapses starting from negative values the profile of the probability density increases as a whole, reaches the maximum at $t = t_D^{(\pm)}$ and then decreases for $t > t_D^{(\pm)}$ on the time-scale t_{dec}^γ , see equation (3.139). Hence the probability to find a particle inside the barrier decreases with the passage of time on a typical time-scale t_{dec}^γ . The increase follows the approach of the incident packet with the time delay $t_D^{(\pm)} = \hbar \frac{d\phi_{D,\pm}(E_p)}{dE_p}$. Using the definitions of the phases $\phi_{D,\pm}$ and ϕ_T from equations (3.145) and (3.9) and β_κ from equation (3.142) we can write the time delay through the transmitted group time (3.82) as

$$t_D^{(\pm)} = \hbar \frac{d\phi_T(E_p)}{dE_p} + \frac{L}{2v_1} \pm \frac{\hbar}{v_1\kappa} = t_T - \frac{L}{2v_1} \pm \frac{\hbar}{v_1\kappa}. \quad (3.150)$$

We see that for the thick barriers, $\kappa L/\hbar \gg 1$, we deal with the time advance $t_D^{(\pm)} \simeq -L/2v_1$. For the thick rectangular barrier $t_D^{(+)} \simeq -L/2v_1 + 3\hbar/v_1\kappa$, $t_D^{(-)} \simeq -L/2v_1 + \hbar/v_1\kappa$. Thus the probability maxima of the evanescent and growing waves are delayed with respect to the moment when the peak of the incident wave has reached the point $z = -L/2$ by the time steps $\hbar/v_1\kappa$ and $3\hbar/v_1\kappa$, respectively.

As follows from equation (3.149), because of the finite width of the momentum distribution, the probability density is modulated by the factor $\exp(2\gamma_p^2(l_D^{(\pm)} \mp z p/\kappa)^2/\hbar^2)$ with the characteristic length

$$l_D^{(\pm)} = \hbar \frac{d}{dp} \log |D_\pm(p)| = l_T + \frac{p}{\kappa} \left(\frac{\hbar}{\kappa} \mp \frac{L}{2} \right). \quad (3.151)$$

For the growing wave this factor is maximal at $z = -L/2$, and for the evanescent wave, at $z = +L/2$. For the broad barrier the characteristic length is equal to

$$l_D^{(\pm)} = (1 \mp \frac{1}{2}) v_1 t_{\text{trav}}^{\text{(tun)}} + \frac{\hbar}{p}. \quad (3.152)$$

Thus, the length of the barrier enters the internal wave through the time delay $t_{D,\pm}$ and the length $l_D^{(\pm)}$.

For completeness we give also the expression for the last interference term in equation (3.144) in the limit $\gamma_p^2 L/\kappa \hbar \ll 1$:

$$\begin{aligned} \text{Re}\{\Psi_{\text{grow}}(z, t)\Psi_{\text{evan}}^*(z, t)\} &\approx \text{Re}\{D_+(p)D_-^*(p)\} \sqrt{\frac{2\gamma_p^2}{\pi\hbar^2}} \exp\left(2\frac{\gamma_p^2}{\hbar^2} \left[\frac{1}{4}(l_D^{(+)} + l_D^{(-)})^2\right.\right. \\ &\quad \left.\left. - v_1^2 \left(t - \frac{1}{2}(t_D^{(+)} + t_D^{(-)})\right)^2 + \frac{p^2}{\kappa^2} (z + L/2)^2 - \frac{\hbar^2}{4\kappa^2}\right]\right). \end{aligned} \quad (3.153)$$

From equations (3.129) and (3.149) we see that the probabilities of finding a particle inside the barrier ($-L/2 \leq z \leq L/2$) and being tunneled through it (at $L/2 < z$) are enhanced compared to the case of the monochromatic wave with $E = E_p$. To quantify these enhancements we introduce the following factors for the transmitted, growing and evanescent wave packets

$$C_T(z, t) = \frac{|\Psi_T(z, t)|^2}{|T(p)|^2 |\Psi_I(\tilde{z}_1(t), t)|^2} = \frac{\gamma_{p,T}^2}{\gamma_p^2} \exp\left(2\frac{\gamma_{p,T}^2}{\hbar^2} [l_T^2 - (z - \tilde{z}_T(t))^2]\right), \quad (3.154)$$

$$\begin{aligned} C_{\text{grow}}(z, t) &= \frac{e^{-2\kappa z/\hbar} |\Psi_+(z, t)|^2}{|D_+(p)|^2 |\Psi_I(\tilde{z}_1(t), t)|^2} \\ &= \frac{\gamma_{p,T}^2}{\gamma_p^2} \exp\left(2\frac{\gamma_{p,T}^2}{\hbar^2} \left[\left(l_D^{(+)} - z\frac{p}{\kappa}\right)^2 - v_1^2 (t - t_D^{(+)})^2\right]\right), \end{aligned} \quad (3.155)$$

$$\begin{aligned}
 C_{\text{evan}}(z, t) &= \frac{e^{+2xz/\hbar} |\Psi_-(z, t)|^2}{|D_-(p)|^2 |\Psi_1(\tilde{z}_1(t), t)|^2} \\
 &= \frac{\gamma_{p,T}^2}{\gamma_p^2} \exp\left(2 \frac{\gamma_{p,T}^2}{\hbar^2} \left[\left(l_D^{(-)} + z \frac{p}{x} \right)^2 - v_1^2 (t - t_D^{(-)})^2 \right]\right). \tag{3.156}
 \end{aligned}$$

These enhancements occur owing to the fact that for the waves with $E > E_p$ entering the packet the probability of penetration of the barrier is larger than for the single wave with $E = E_p$. Thus, analyzing the temporal aspects of the tunneling problem, we have to make a benchmark on the tunneling probability for the monochromatic wave. As follows from (3.154), the probability to meet the particle at $z = L/2$ becomes the same, as it were in case of the monochromatic wave with $E = E_p$, for the first time on the right wing of the Gaussian at the time moment

$$t_{\text{mon}}^{(r.w.)} = -\frac{l_T}{v_T} - \frac{L}{2v_T} + \frac{v_1}{v_T} t_T, \tag{3.157}$$

when the maximum of the incident wave packet is yet at $z = \tilde{z}_1(t_{\text{mon}}^{(r.w.)}) = v_1 t_{\text{mon}}^{(r.w.)} < -L/2$ and the maximum of the transmitted wave packet did not yet appear at $z = L/2$. Recall, the traversal time $t_{\text{trav}}^{(\text{tun})} = mL/x$ is determined, as in (3.134). At the later time, the probability again becomes the same on the left wing of the Gaussian at the time

$$t_{\text{mon}}^{(l.w.)} = +\frac{l_T}{v_T} - \frac{L}{2v_T} + \frac{v_1}{v_T} t_T, \tag{3.158}$$

when the maximum of the transmitted wave packet achieves the point $z = \tilde{z}_T(t_{\text{mon}}^{(l.w.)}) = L/2 + l_T$. Thus $\frac{1}{2}(t_{\text{mon}}^{(l.w.)} - t_{\text{mon}}^{(r.w.)}) = \frac{l_T}{v_T}$.

For the thick barrier:

$$\begin{aligned}
 t_{\text{mon}}^{(r.w.)} &= \frac{v_1}{v_T} \left[-t_{\text{trav}}^{(\text{tun})} - \frac{L}{2v_1} - \frac{m\hbar}{p^2} + \frac{m\hbar}{x^2} + \frac{2m\hbar}{px} \right], \\
 t_{\text{mon}}^{(l.w.)} &= \frac{v_1}{v_T} \left[t_{\text{trav}}^{(\text{tun})} - \frac{L}{2v_1} + \frac{m\hbar}{p^2} - \frac{m\hbar}{x^2} + \frac{2m\hbar}{px} \right], \tag{3.159}
 \end{aligned}$$

$$z = \tilde{z}_T(t_{\text{mon}}^{(l.w.)}) = L/2 + v_1 t_{\text{trav}}^{(\text{tun})} + \hbar(x^2 - p^2)/(px^2).$$

Note that working within the assumptions $|z_0| \ll \hbar p/\gamma_p^2$ and $L \ll \hbar x/\gamma_p^2$ we can use $\gamma_{p,T}(t) \simeq \gamma_{p,D}(t) \simeq \gamma_p$ and $v_T \simeq v_1$ up to $1 + O(\gamma_p^2)$ corrections. Finally for a thick barrier

$$\frac{1}{2}(t_{\text{mon}}^{(r.w.)} - t_{\text{mon}}^{(l.w.)}) \simeq t_{\text{trav}}^{(\text{tun})} \simeq t_{\text{mon}}^{(l.w.)} - t\left(\tilde{z}_1 = -\frac{L}{2}\right) \simeq t_{\text{mon}}^{(l.w.)} - t\left(\tilde{z}_T = \frac{L}{2}\right). \tag{3.160}$$

Up to small correction terms, this is the difference in the time, when the wave with $E \simeq E_p$ has passed the barrier and the time, when the incident packet peak has reached it. On the other hand it can be treated as the difference in the time, when the wave with $E \simeq E_p$ has passed the barrier and the time, when the transmitted packet peak has been formed at the same point (on its right border).

The above analysis allows us to reconsider the definition of the transmission time through the broad barrier. If we are interested in the time the waves with $E \simeq E_p$ travel through the barrier, we have to wait until at least the time $\sim t_{\text{mon}}^{(l.w.)}$ after the maximum of the transmitted packet appears to the right of the barrier. Before this, mainly the modes with energies $E > E_p$ pass through the barrier. Thus we are able to associate the time $t_{\text{trav}}^{(\text{tun})}$ with the time of penetration of the thick barrier by the peak of the wave packet. The time $t_{\text{trav}}^{(\text{tun})} \propto L$ naturally appears as the time of propagation of approximately monochromatic waves through a thick barrier. This can be considered as a resolution of the Hartmann paradox.

Summarizing, the physical picture of the tunneling of the wave packet sharply peaked in the momentum space at $E = E_p < \max U$ incident on the very thick barrier (from large

distances to the left of the barrier) is as follows. The probability to observe the particles which have passed the barrier reaches the same value as it is in the stationary problem for $E = E_p$ at the moment when the peak of the incident wave packet has not yet reached the barrier. The peak of the transmitted wave packet is formed at the right border of the barrier, after a quantum time delay (not dependent on the barrier depth) from the moment, when the peak of the incident wave packet reaches the left border of the barrier (the Hartmann effect). Then the peak of the transmitted wave packet propagates to the right away from the barrier. The peak of the reflected wave packet is formed at the left border of the barrier with approximately the same time delay. Then it propagates back to the left of the barrier. The evanescent and growing waves inside the barrier have no peaks. They increase with time until the moment when the incident wave packet reaches the left edge of the barrier with two different delays both of the quantum time order and then decrease. The modes with higher energies pass through the barrier more rapidly than the less energetic modes. The modes with $E \simeq E_p$ pass the barrier during the time $t_{\text{trav}}^{(\text{tun})} \propto L$, which resolves the Hartmann paradox.

3.9. Resonance states and their time evolution

We turn now to the question of the temporal evolution of a quantum system, which exhibits a resonance behavior. Consider an example of the particle motion restricted to a right half-space ($z > 0$) with a rectangular barrier of the height U between $z = l_R$ and $z = l$.

$$U(z) = \begin{cases} \infty, & z \leq 0 \\ 0, & 0 < z < l_R \\ U, & l_R \leq z \leq l \\ 0, & l < z. \end{cases} \quad (3.161)$$

We start this section assuming that $E < U$, so that classical motion is possible for $0 < z < l_R$ and $z > l$, and for $l_R < z < l$ we deal with the tunneling. Applying the results of section 3.1 we may use the wave function (3.2) for $z \geq 0$ and identify $l = L/2$. The internal wave function (equation (3.14)) contains only the anti-symmetric part

$$\begin{aligned} \psi_U(z, E) &= \tilde{C}_-(E) \chi_-(z, E), \\ \chi_-(z, E) &= \begin{cases} \sin(kz/\hbar), & 0 \leq z < l_R \\ \sin(kl_R/\hbar) \cosh(\kappa(z - l_R)/\hbar) + \frac{k}{\kappa} \cos(kl_R/\hbar) \sinh(\kappa(z - l_R)/\hbar), & l_R \leq z \leq l, \end{cases} \end{aligned} \quad (3.162)$$

where, as before, $k = \sqrt{2mE}$ and $\kappa = \sqrt{2m(U - E)}$. The logarithmic derivative is equal to

$$\begin{aligned} d_-(E) &= l \frac{d}{dz} \log \chi_-(z, E) \Big|_{z=l} = \frac{l\kappa k + \kappa \tan(kl_R/\hbar) \tanh(\kappa(l - l_R)/\hbar)}{\hbar k \tanh(\kappa(l - l_R)/\hbar) + \kappa \tan(kl_R/\hbar)} \\ &= \frac{l\kappa \zeta(E, l_R) + \mathfrak{p}(E)}{\hbar \zeta(E, l_R) - \mathfrak{p}(E)}, \end{aligned} \quad (3.163)$$

where we denoted

$$\zeta(E, l_R) = \frac{k \cot(kl_R/\hbar) + \kappa}{k \cot(kl_R/\hbar) - \kappa}, \quad \mathfrak{p}(E) = e^{-2\kappa(l - l_R)/\hbar}. \quad (3.164)$$

Note that for $l_R = 0$ we recover from equation (3.163) the result of equation (3.17) for d_- . Working within a half-space we have to put $d_+ \equiv d_-$, then from equations (3.7) and (3.8) we find the reflection amplitude

$$R(E) = e^{i\pi - i2kl/\hbar} \frac{d_-(E) + ikl/\hbar}{d_-(E) - ikl/\hbar} = e^{i\phi_R(E)}, \quad \phi_R(E) = \pi - 2kl/\hbar + \delta_s(E), \quad (3.165)$$

with the scattering phase δ_s given by the relation

$$e^{i\delta_s(E)} = \frac{\kappa + ik}{\kappa - ik} \frac{\zeta(E, l_R) + \frac{\kappa - ik}{\kappa + ik} \mathfrak{p}(E)}{\zeta(E, l_R) + \frac{\kappa + ik}{\kappa - ik} \mathfrak{p}(E)}. \quad (3.166)$$

The coefficient $\tilde{C}_-(E)$ of the internal wave function defined in equations (3.12) and (3.14) can be expressed with the help of equation (3.163) and the relation

$$\chi_-(l, E) = \frac{\sin(kl_R/\hbar) \zeta(E, l_R) - \mathfrak{p}(E)}{\sqrt{\mathfrak{p}(E)} \zeta(E, l_R) - 1}$$

following from equation (3.162) as

$$\begin{aligned} \tilde{C}_-(E) &= \frac{2i\sqrt{\mathfrak{p}(E)} k e^{-ikl/\hbar}}{\sin(kl_R/\hbar) \kappa - ik} \frac{1 - \zeta(E, l_R)}{\zeta(E, l_R) + \frac{\kappa + ik}{\kappa - ik} \mathfrak{p}(E)} \\ &= 2i\sqrt{\mathfrak{p}} \frac{k^2 (\zeta - 1)^2 + \kappa^2 (\zeta + 1)^2}{k^2 (\zeta - \mathfrak{p})^2 + \kappa^2 (\zeta + \mathfrak{p})^2} e^{i\pi - ikl/\hbar + i\delta_s(E)/2}. \end{aligned} \quad (3.167)$$

In the last equation we used explicitly that $E < U$ and κ is real, and we suppressed the arguments of functions ζ and \mathfrak{p} for shortness. We also used that $1/\sin^2(kl_R) = 1 + (\kappa^2/k^2)(\zeta + 1)^2/(\zeta - 1)^2$.

If $U > U^{(n)} = \pi \hbar^2 (2n + 1)/(4m l_R^2)$, equation $\zeta(E, l_R) = 0$ has n solutions, $\{\varepsilon_i\}$, $i = 1, \dots, n$, which constitute the spectrum of bound states for the rectangular potential well (3.161), provided we put $l \rightarrow \infty$. For energies close to ε_i we can expand $\zeta(E, l_R) \approx r_{\zeta,i}(E - \varepsilon_i)/4\varepsilon_i$, where $r_{\zeta,i} = (l_R \kappa_i/\hbar + 1)(k_i^2/\kappa_i^2 + 1)$, $k_i = \sqrt{2m\varepsilon_i}$ and $\kappa_i = \sqrt{2m(U - \varepsilon_i)}$. Hence, the amplitude $R(E)$ possesses simple poles at energies E_i .

Consider the case of a broad barrier. Then $\mathfrak{p}(\varepsilon_i) \ll 1$ and the poles are close to ε_i ,

$$E_i = \varepsilon_i - \frac{4\varepsilon_i \kappa_i + ik_i}{r_{\zeta,i} \kappa_i - ik_i} \mathfrak{p}(\varepsilon_i) = E_{R,i} - \frac{i}{2} \Gamma_i, \quad (3.168)$$

with the real, $E_{R,i}$ and imaginary, $-\Gamma_i/2$, parts, given by

$$E_{R,i} = \varepsilon_i - \frac{4\varepsilon_i \kappa_i^2 - k_i^2}{r_{\zeta,i} \kappa_i^2 + k_i^2} \mathfrak{p}(\varepsilon_i), \quad \Gamma_i = \frac{16 \kappa_i^2 k_i^2}{(\kappa_i^2 + k_i^2)^2} \mathfrak{p}(\varepsilon_i) \frac{\kappa_i k_i}{2m(l_R \kappa_i/\hbar + 1)}. \quad (3.169)$$

The expression for the width Γ_i has a simple semiclassical interpretation: $\Gamma_i = \hbar |T(E_{R,i})|^2/P(E_{R,i})$, where in the limit $\kappa(l - l_R)/\hbar \gg 1$, which we now consider, $|T|^2$ is the transmission coefficient of the barrier (cf. equation (3.19)), and $P = 2(m/k)(l_R + \hbar/\kappa)$ is the period of the particle motion within the potential well ($0 < z < l_R$). The latter expression takes into account that the particle can enter a depth \hbar/κ under the barrier. In other words the width is given by the product of the number of hits of the particle off the barrier per unit of time and the probability of barrier penetration after each collision. This result survives for an arbitrary barrier within applicability of the semiclassical approximation [7]. Close to the resonance, $E \sim E_{R,i}$, the amplitude can be written as

$$R(E) \approx e^{i\pi - 2ik_i l/\hbar + 2i\beta_x(\varepsilon_i)} \frac{E - E_{R,i} - \frac{i}{2} \Gamma_i}{E - E_{R,i} + \frac{i}{2} \Gamma_i} \approx e^{i\pi - 2ik_i l/\hbar + 2i\beta_x(E) + 2i\delta_i(E)}. \quad (3.170)$$

We see that the phase shift can be approximately presented as $\delta_s(E) \approx 2\beta_x(E) + 2\delta_i(E)$, where the *resonance scattering phase* is given by

$$\delta_i(E) = \arctan\left(\frac{\Gamma_i/2}{E_{R,i} - E}\right), \quad (3.171)$$

and the non-resonant (potential) phase β_x is defined by equation (3.142). Note that the values $E_{R,i}/\hbar$ and Γ_i/\hbar here have the same meaning as the values ω_R and Γ , which we used in section 2; cf. poles of the Green's functions (2.30) and equation (3.168).

For the case $\Gamma_i \ll |E_{R,i+1} - E_{R,i}|$, which we will further consider, we can write

$$R(E) \approx \sum_{i=1}^n e^{-2ik_i l / \hbar + i\beta_\chi(E)} \frac{i\Gamma_i}{E - E_{R,i} + \frac{i}{2}\Gamma_i}. \quad (3.172)$$

Consider now the temporal aspects of this scattering problem. Defining the dwell time in the same way as in section 3.2, after some manipulations we obtain, with the help of equations (3.162) and (3.167),

$$t_d(0, l, E) = \frac{1}{v} \int_0^l |\psi_U(z, E)|^2 dz = \frac{m}{k} \mathfrak{p} \frac{k^2 + \chi^2}{k^2 [\zeta - \mathfrak{p}]^2 + \chi^2 [\zeta + \mathfrak{p}]^2} \left(2l_R (\zeta + 1)^2 - \frac{8l_R \zeta k^2}{k^2 + \chi^2} + \frac{2\hbar}{\chi} \left[(1 - \zeta^2) + \frac{k^2}{k^2 + \chi^2} (2\zeta \log \mathfrak{p} + \zeta^2 / \mathfrak{p} - \mathfrak{p}) \right] \right). \quad (3.173)$$

The value $t_d(0, l, E)$ is the time needed by the incident current $j_1 = v = k/m$ to fill the internal region $[0, l]$ with the probability density $|\psi_U(z, E)|^2$. The quantity (3.173) is plotted in figure 13 as a function of the energy for different barrier penetrabilities parameterized through the value $\mathfrak{p}(E) = \exp(\sqrt{1 - E/U} \log \mathfrak{p}(0))$ at the zero energy. For a tiny barrier penetrability the internal wave function has a small amplitude for most energies $\propto |\tilde{C}_-| \propto \mathfrak{p} \ll 1$ and therefore the dwell time is very short. Only for the energies close to the resonance $\zeta \sim \mathfrak{p}$ the internal wave function can acquire a large amplitude $|\tilde{C}_-| \propto 1/\mathfrak{p}$ and the dwell time becomes very large. Exactly at the resonance energy, $E = E_{R,i}$, we find that

$$t_d(0, l, E_{R,i}) \approx \frac{4\hbar}{\Gamma_i}, \quad (3.174)$$

where we used that $\zeta(E_{R,i}) = -\mathfrak{p}(\chi_i^2 - k_i^2)/(\chi_i^2 + k_i^2)$ as follows from equation (3.169). By varying the length of the resonator l_R one can change the number of resonances in the potential, see the different panels in figure 13 plotted for different values of l_R .

Describing the scattering problem in terms of the wave packet (3.41) just collected with the wave function (3.2) with $T = 0$, R given by equation (3.165) and the internal function (3.162), we can define the reflection group time in the same way as in section 3.4: this is the time interval between the moment when the maximum of the incident wave packet moving toward the origin is at the position $z = l$, and the moment when the maximum of the reflected packet moving away from the potential region is at the same position $z = l$. Applying this definition to a wave-packet with the energy distribution $\Phi(E)$ sharply peaked at the averaged energy \bar{E} with a small energy spread γ , $\gamma \ll \Gamma_i$, we find

$$t_R(\bar{E}) = 2\frac{l}{\tilde{v}} + \hbar \frac{d\phi_R(\bar{E})}{d\bar{E}} = \hbar \frac{d\delta_s(\bar{E})}{d\bar{E}}, \quad (3.175)$$

where $\bar{E} \equiv m\tilde{v}^2/2$. The physical meaning of the quantity t_R is the following: if we send a wave packet with the well-defined energy \bar{E} and observe the reflected packet at a fixed distance z from the scattering center, $z \gg l$, then $t_R(\bar{E})$ is the time delay in the arrival of the emitted wave packet with respect to the case without a barrier. For energies close to the resonant ones $\bar{E} \sim E_{R,i}$ and $\Gamma_i \ll |E_{R,i+1} - E_{R,i}|$ the reflection group time can be written as

$$t_R(\bar{E}) \approx -2\frac{l_R}{\tilde{v}} + \sum_i 2\hbar \frac{d\delta_i(\bar{E})}{d\bar{E}} = -2\frac{l_R}{\tilde{v}} + \sum_i \frac{\hbar\Gamma_i}{(\bar{E} - E_{R,i})^2 + \frac{1}{4}\Gamma_i^2}. \quad (3.176)$$

We use that for \bar{E} close to $E_{R,i} \simeq \varepsilon_i$ we have $\beta_\chi(\bar{E}) \simeq \arctan(k_i/\chi_i) = -k_i l_R / \hbar \simeq -\tilde{k} l_R / \hbar$ with $\tilde{k} = \sqrt{2m\bar{E}}$. We see that, if $\bar{E} = E_{R,i}$, then the resonance time delay is as large as

$$t_R(E_{R,i}) \approx \frac{4\hbar}{\Gamma_i}. \quad (3.177)$$

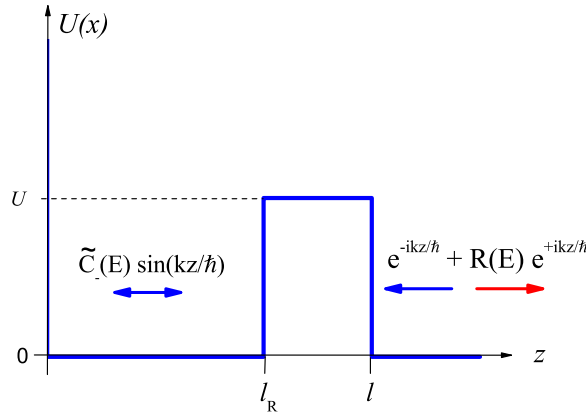


Figure 12. Sketch for the problem of the 1D-scattering on a potential given by equation (3.161) with the incident wave coming from the right. The internal wave function is given by equation (3.162).

Hence, the incident wave packet lingers in the interaction region much longer than if it crossed this distance with the mean velocity. If the particle energy is de-tuned from any resonance $|\bar{E} - E_{R,i}| \gg \Gamma_i$, then t_R changes the sign and we deal with the time advancement

$$t_R \approx -2 \frac{l_R}{v}, \tag{3.178}$$

as for classical scattering on a hard sphere, cf. equation (2.81). As we see, the internal part of the potential $0 < z < l_R$ is effectively excluded from the particle motion. Interestingly, in equation (3.178) there is no contribution from the under-barrier region $[l_R, l]$. It seems like the packet instantly passes under the barrier but does not enter the resonator $[0, l_R]$. This is a manifestation of the Hartmann phenomenon discussed in section 3.6. In this connection we have to emphasize that the group time t_R is not a proper measure of the time the tunneling particle spends under the barrier.

The dwell time (3.173) and the reflection group time (3.175) are connected by the relation similar to equation (3.83) following from equation (B.4):

$$t_d(0, l, \bar{E}) = t_R(\bar{E}) - \delta t_i(\bar{E}), \tag{3.179}$$

where the interference time delay is given by

$$\delta t_i(\bar{E}) = -\frac{\hbar}{k\tilde{v}} \sin(2kl + \phi_R(\bar{E})) = \frac{\hbar}{2\bar{E}} \sin \delta_s(\bar{E}). \tag{3.180}$$

Close to the resonance energy the interference time is not singular, vanishing at $\bar{E} = E_{R,i}$, and is much smaller than the reflection group time t_R and the dwell time t_d .

Since, as depicted in figure 12, there is obvious symmetry in the motion of a particle toward the origin and away from it, it is convenient to define a measure of time for a reflected wave only. Then we define the scattering group time,

$$t_s(\bar{E}) = \frac{1}{2} t_R(\bar{E}), \tag{3.181}$$

as a half of the bidirectional scattering time defined in equation (3.80), $t_s = t_{bs}/2$. The time t_s corresponds to the group time defined for the classical motion in equation (2.11). The similar time-quantity is introduced in equation (2.82) for classical particles undergoing the scattering on a hard sphere. In view of the relation (3.179) it is convenient to also introduce the single-way dwell time

$$t_d^{s.w.}(0, l, \bar{E}) = \frac{1}{2} t_d(0, l, \bar{E}), \tag{3.182}$$

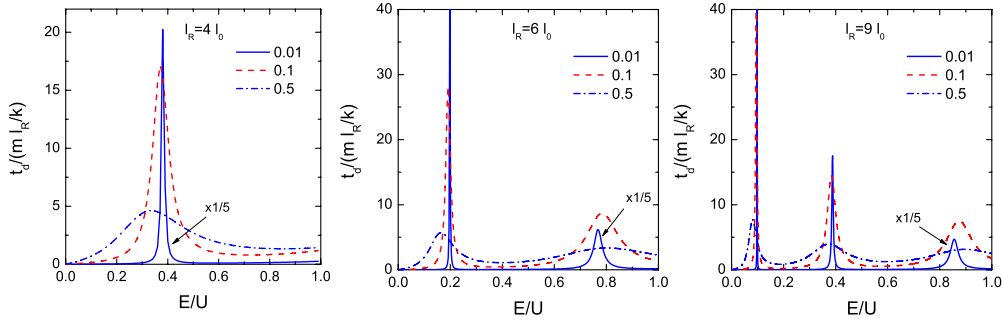


Figure 13. The dwell time (3.173) for the potential (3.161) as a function of the energy for various values of the coefficient $p(0)$, see equation (3.164), shown by the line labels. Three panels demonstrate results for various values of l_R measured in units $l_0 = \hbar/\sqrt{2mU}$. The solid lines in all panels are multiplied by a factor 1/5.

so that close to the resonance energy for a narrow resonance we have

$$t_s(\bar{E}) \approx t_d^{s.w.}(0, l, \bar{E}) \approx \sum_{i=1}^n \hbar \frac{d\delta_i(\bar{E})}{d\bar{E}} = \sum_{i=1}^n \frac{\hbar\Gamma_i/2}{(\bar{E} - E_{R,i})^2 + \frac{1}{4}\Gamma_i^2} \equiv \sum_{i=1}^n \frac{\hbar}{2} A_i(\bar{E}). \quad (3.183)$$

Each of the functions $A_i(\bar{E})$ satisfies the sum-rule

$$\int_{-\infty}^{\infty} A_i(E) \frac{dE}{2\pi} = 1, \quad (3.184)$$

cf. equations (2.65)–(2.67) in classical mechanics. Here the integral sits near each i th pole and thereby we are able to perform integration from $-\infty$ to ∞ or from 0 to ∞ . Correspondingly, the integral over the energy of the scattering group time or the single-way dwell time yield the number of resonances in the system

$$\int_0^{\infty} t_s(E) \frac{dE}{\pi\hbar} \approx \int_0^{\infty} t_d^{s.w.}(0, l, E) \frac{dE}{\pi\hbar} \approx n. \quad (3.185)$$

Thus the dwell time defined in equation (3.173) can be related to the number of states per unit energy

$$t_d(0, l, E) = 2t_d^{s.w.}(0, l, E) \approx 2\pi\hbar \frac{dn}{dE}; \quad (3.186)$$

cf. the semiclassical relation (3.30).

We now turn to a more detailed study of the wave function of the scattering problem with the potential (3.161). For the sake of further applications let us now re-organize the wave functions of the stationary problem shown in figure 12 to deal with the incident and reflected currents equal to unity outside the barrier. For this we multiply the wave function (3.2) with R given by equation (3.165) and the internal wave function (3.162) with the coefficient (3.167) by the factor $i\sqrt{1/v} e^{ikl/\hbar - i\delta_s(E)/2}$ and obtain

$$\psi(z; E) = \begin{cases} \frac{i}{\sqrt{v}} e^{ikl/\hbar - i\delta_s(E)/2} \tilde{C}_-(E) \chi_-(z, E), & z \leq l \\ \sqrt{\frac{4}{v}} \sin(k(z-l)/\hbar + \delta_s(E)/2), & z > l. \end{cases} \quad (3.187)$$

Expressions for $\tilde{C}_-(E)$ and $\delta_s(E)$ were derived above for $E < U$. For $E > U$ the coefficient $\tilde{C}_-(E)$ is given by the first line in equation (3.167) and the phase $\delta_s(E)$ is defined in

equation (3.166) after the replacement $\kappa \rightarrow i|\kappa|$, there and in equation (3.164). The wave functions (3.187) are normalized as

$$\int_0^\infty \psi^*(z, E) \psi(z, E') dz = 2\pi \hbar \delta(E - E'). \quad (3.188)$$

For our further study of the time evolution of a quantum system such a normalization is more convenient than that given by equation (3.42).

If we deal with a system with narrow and isolated resonances, i.e. we assume that the potential barrier is broad, $\mathfrak{p} \ll 1$, and the resonator length l_R is such that $|E_{R,i+1} - E_{R,i}| \gg \Gamma_i + \Gamma_{i+1}$, the internal wave function acquires for $E < U$ a sizable magnitude only if the energy E is close to the resonance one. In the vicinity of the i th resonance $E \sim E_{R,i}$, we may put $\sin(k_i l_R / \hbar) = k_i / \sqrt{\kappa_i^2 + k_i^2}$ in equation (3.167) and it takes the form

$$\begin{aligned} \tilde{C}_-(E) &\approx 2i \frac{4\kappa_i^2 \varepsilon_i e^{-\kappa(l-l_R)/\hbar}}{(k_i^2 + \kappa_i^2)(l_R \kappa_i / \hbar + 1)} \frac{e^{-ik_i l / \hbar + i\beta_\kappa(E)}}{E - E_{R,i} + \frac{1}{2}\Gamma_i} \\ &\approx -i \sqrt{\frac{2v}{l_R}} e^{-ikl/\hbar + i\beta_\kappa(E) + i\delta_i(E)} \sqrt{\frac{\hbar\Gamma_i}{(E - E_{R,i})^2 + \Gamma_i^2/4}}. \end{aligned} \quad (3.189)$$

Taking this into account the internal part of the wave function can be written for $E < U$ as follows

$$\psi(z \leq l; E < U) \approx \sum_{i=1}^n \sqrt{\frac{\hbar\Gamma_i}{(E - E_{R,i})^2 + \Gamma_i^2/4}} \sqrt{\frac{2}{l_R}} \chi_-(z, E), \quad z \leq l, \quad (3.190)$$

where each element of the sum contributes only for $|E - E_{R,i}| \ll |E_{R,i+1} - E_{R,i}|$. This expression shows that only particles with energies within the interval $E_{R,i} - \Gamma/2 < E < E_{R,i} + \Gamma/2$ penetrate inwards through the barrier and form the internal wave function.

The wave function in equation (3.190) allows for an important generalization. The coordinate part of the internal wave function can be replaced by the stationary wave function of the closed quantum system, which is obtained from those shown in figure 12 by extending the barrier to infinity, $l \rightarrow \infty$. Herewith the n resonance states at energies $E_{R,i}$ (with the widths Γ_i) turn into n bound states with energies ε_i with the wave functions

$$\psi_i^{(\text{bound})}(z) = C_i \chi_-(z, \varepsilon_i). \quad (3.191)$$

Since the barrier was initially broad, Γ_i being small, and the difference between the energy of the bound state and the energy of the resonance is small, $|\varepsilon_i - E_{R,i}| = O(\mathfrak{p}(E_{R,i}))$. Similarly the normalization coefficients C_i differ from $\sqrt{2/l_R}$ by a small factor $O(\mathfrak{p}(E_{R,i}))$. Then $\psi(z; E < U)$ in (3.190) is factorized as

$$\psi(z; E < U) \approx \sum_{i=1}^n \sqrt{A_i(E)} \psi_i^{(\text{bound})}(z).$$

Such a factorization of the internal wave function of a scattering problem into a wave function of the corresponding bound state problem and an enhancement factor $\sqrt{A_i(E)}$ is argued in [80, 106–108] to be possible for any finite-range potential and with some modifications also for the Coulomb potential. These results have found applications in the studies of nucleon-halo nuclei [109] and di-proton radioactivity [106, 110].

With the help of the wave functions (3.190) we can give a new interpretation for the dwell time $t_d^{s.w.}(0, l, E)$. It can be presented as the ratio of the density of states in the region of the potential to the density of the free states in the same region (i.e. the relative probability for the

particle to be inside the region of the potential compared to the scattering in the absence of the potential) multiplied by the time of the free motion inside the potential region l/v :

$$t_d^{\text{s.w.}}(0, l, E) = \hbar \frac{l}{v} \frac{\int_0^l |\psi(z; E)|^2 dz}{\int_0^l |\psi^{(\text{free})}(z; E)|^2 dz}, \quad \psi^{(\text{free})}(z; E) = \sqrt{\frac{4}{v}} \sin(kz/\hbar). \quad (3.192)$$

This is in accord with the ergodicity principle, see below, section 4.4.1.

Now consider the problem of the decay of quasi-stationary states. The problem can be formulated as follows. Assume that one sends a stationary particle flux of the energy E_1 on the potential shown in figure 12, and we ask the question how long particles from the beam will be delayed inside the region of the potential ($0 < z < l_R$) in dependence of the value E_1 of beam energy after the beam is suddenly switched off. Particles from the beams having real energies E_1 within bands, $E_{R,i} \pm \alpha\Gamma_i$, $\alpha \sim 1$, form wave packets, corresponding to initial (after the switching off of the beam) quasi-stationary states, which remain inside the potential well for a long time (if the barrier is broad), until the particles, described by these states, penetrate through the barrier to infinity. The particles with initial beam energies far from energies $E_{R,i} \pm \alpha\Gamma_i$ enter the region of the potential well only with a tiny probability. So, we may ask the question how long a particle corresponding to the initial real energy E_1 from the band $E_{R,i} \pm \alpha\Gamma_i$ (or better, particles corresponding to an energy distribution within the band provided the beam had a finite energy dispersion) stays in the resonance quasi-stationary state till its decay? (The question of how long it takes for the particle to pass the barrier has been considered above.) One can prepare, of course, a more complicated quasi-stationary state by populating not one but several resonant states using the incident wave packet with a broader energy distribution.

A similar initial state can be prepared differently. The initial localized state can be created right inside the potential well (for $0 < z < l_R$), e.g. by reactions. If the barrier is broad, at times much shorter than the decay times of the resulting quasi-stationary states the produced particles with $E < \max U$ are redistributed over the energy levels corresponding to the stationary levels related to the same problem but without a penetrable barrier. On a longer time-scale each of these levels is actually a quasi-stationary level and our problem is to find the decay time.

Considering a general case, we assume that at the time $t = 0$ our system is described by an arbitrary wave function $\Psi(z, 0)$ localized inside the potential region, i.e. we assume $\Psi(z, 0) = 0$ for $z > l_R$. The evolution of this state is determined by the unitary operator $\exp(-i\hat{H}t)$, so that at any later time $t > 0$ the wave function of the system is equal to $\Psi(z, t) = \exp(-i\hat{H}t)\Psi(z, 0)$. Expanding the initial wave function in terms of the eigenfunctions of the Hamiltonian \hat{H} , $\psi(z; E)$ for $E > 0$, normalized as in equation (3.188) we can write

$$\Psi(z, t) = \int_0^\infty \frac{dE}{2\pi\hbar} \Phi(E) \psi(z; E) e^{-iEt/\hbar}, \quad (3.193)$$

where

$$\Phi(E) = \int_0^\infty dz \psi^*(z; E) \Psi(z, 0) = \int_0^l dz \psi^*(z; E) \Psi(z, 0). \quad (3.194)$$

The unitary evolution conserves the normalization of the wave function and since the initial wave function is normalized to unity, then

$$\int_0^\infty dz |\Psi(z, t)|^2 = \int_0^l dz |\Psi(z, 0)|^2 = \int_0^\infty \frac{dE}{2\pi\hbar} |\Phi(E)|^2 = 1 \quad (3.195)$$

for any moment of time t . Note the difference in normalization of the function $\Phi(E)$ in comparison with equation (3.43).

The overlap between the wave function at time t and the initial wave function gives the amplitude of the survival probability (also called integrity)

$$\mathcal{G}(t) = \int_0^\infty \Psi^*(z, 0)\Psi(z, t) dz = \int_0^\infty \frac{dE}{2\pi\hbar} |\Phi(E)|^2 e^{-iEt/\hbar}, \quad (3.196)$$

so that $\mathcal{P}_{\text{surv}}(t) = |\mathcal{G}(t)|^2$ is the probability that the system remains in the same state after a passage of time t . Obviously at $t = 0$ probability $\mathcal{P}_{\text{surv}}$ is equal to unity, $\mathcal{G}(0) = 1$ in view of equation (3.195). At any later time it becomes smaller than unity, as follows from the Cauchy–Schwarz–Bunyakovsky inequality:

$$|\mathcal{G}(t)| = \left| \int_0^\infty \Psi^*(z, 0)\Psi(z, t) dz \right| \leq \left| \int_0^\infty |\Psi(z, 0)|^2 dz \right|^{1/2} \left| \int_0^\infty |\Psi(z, t)|^2 dz \right|^{1/2} = 1. \quad (3.197)$$

Since the function $|\Phi(E)|^2$ is integrable on the ray $[0, +\infty)$, see equation (3.195), one can prove [111] that $\lim_{t \rightarrow \infty} \mathcal{G}(t) = 0$. This means that an initial state will always decay at large times. Under the assumption of a purely exponential decay one identifies the life-time of the system in the initial state, or its decay time, as $t_{\text{dec}} = -\mathcal{P}_{\text{surv}}(t)/\dot{\mathcal{P}}_{\text{surv}}(t)$, which in this case would be a time-independent quantity. However Khalfin in [112] pointed out that $\mathcal{P}_{\text{surv}}(t)$ cannot be purely exponential. It deviates from the exponent both for very large times and for very short times. This conclusion is obtained without any assumptions about the quantum state and the system dynamics. For a more extensive discussion of this issue we address the reader to the review [66]. Possible manifestations of a non-exponential decay in nuclear systems are discussed, e.g., in [113]. Peculiarities of a many-body quantum decay are studied in [114], where the important role of the effects of the quantum statistics is demonstrated.

Since, as argued above, the purely exponential decay is not possible for all times, it would be desirable to find such a definition of the decay time, which does not depend on the assumption of a particular form of the survival probability amplitude. Following Fleming [115] let us define the decay time of the unstable state as

$$t_{\text{dec}} = \int_0^\infty dt |\mathcal{G}(t)|^2 = \frac{1}{2} \int_0^\infty \frac{dE}{2\pi\hbar} |\Phi(E)|^4, \quad (3.198)$$

where we have used equation (3.196). The integral exists, if $|\mathcal{G}(t)|^2 \lesssim 1/t^{1+\delta}$ for large t and $\delta > 0$. The sojourn time

$$t_{\text{soj}}(0, l) = \int_0^\infty dt \int_0^l dz |\Psi(z, t)|^2 \quad (3.199)$$

is a characteristic of how long the particle stays within interval $[0, l]$ starting from initial moment $t = 0$, see equation (3.92). By analogy to equation (3.93) we can express the sojourn time through the dwell time (3.173) averaged with $|\Phi(E)|^2$ over the energy

$$t_{\text{soj}}(0, l) = \frac{1}{2} \int_0^\infty \frac{dE}{2\pi\hbar} |\Phi(E)|^2 \int_0^l dz |\psi(z; E)|^2 = \frac{1}{2} \int_0^\infty \frac{dE}{2\pi\hbar} |\Phi(E)|^2 t_{\text{d}}(0, l, E). \quad (3.200)$$

Here in the last equation we take into account the different normalization of the wave function ψ_U used in equation (3.173) and the wave function ψ , equation (3.190) used in the expansion (3.193), which produces the factor $1/v$ needed in equation (3.173).

Let us now illustrate how the above formulae work for the case of very narrow isolated resonances. The preparation of the initial wave function $\Psi(z, 0)$ for such a quasi-stationary state can be done by putting an infinite wall somewhere inside the barrier or one can use the simple method of [80]: in the potential (3.161) we extend the barrier to infinity by putting

$l \rightarrow \infty$. In the latter case we can expand the initial localized wave function in terms of the wave functions (3.191) as

$$\Psi(z, 0) = \sum_i^n c_i \psi_i^{(\text{bound})}(z) + \int_U^\infty \frac{dE}{2\pi\hbar} \tilde{c}(E) \psi(z, E), \quad \sum_{i=1}^n |c_i|^2 + \int_U^\infty \frac{dE}{2\pi\hbar} |\tilde{c}(E)|^2 = 1. \quad (3.201)$$

The wave function under the integral is given by equation (3.187) for $E > U$. If we now suddenly recover the initial form of the potential (in the time $\ll \hbar / \min(|\varepsilon_i - \varepsilon_{i+1}|)$ for $i < n$) then the wave function does not change and we can substitute it in equation (3.194), and using the wave functions (3.187) and (3.190) obtain

$$\Phi(E) \approx \sum_i^n c_i \sqrt{\hbar A_i(E)} + \bar{\Phi}(E) \theta(E - U), \quad (3.202)$$

where the part $\bar{\Phi}(E)$ corresponds to the modes over the barrier which do not contribute to the resonant scattering and can be thereby dropped.

For simplicity let us now assume that the initial wave function corresponds to only one j th bound state with $1 < j < n$. We have $c_i = \delta_{ij}$ and $\tilde{c}(E > U) = 0$, and $|\Phi(E)|^2 \approx \hbar A_j(E)$. Since close to the resonance energy the dwell time is $t_d(0, l, E) \approx \hbar A_j(E)$, we find

$$\begin{aligned} t_{\text{dec}} \approx t_{\text{soj}}(0, l) &\approx \frac{1}{2} \int_0^\infty \frac{dE}{2\pi} \frac{\hbar \Gamma_j^2}{((E - E_{R,j})^2 + \Gamma_j^2/4)^2} \\ &\approx \frac{1}{2} \int_{-\infty}^\infty \frac{dE}{2\pi} \frac{\hbar \Gamma_j^2}{((E - E_{R,j})^2 + \Gamma_j^2/4)^2} = \frac{\hbar}{\Gamma_j}. \end{aligned} \quad (3.203)$$

Here we have used that for $E_{R,j} \gg \Gamma_j$ the lower limit of the integration can be extended to $-\infty$. Hence, the particles that occupied at $t = 0$ a narrow quasi-stationary state with the width Γ , will appear with the probability of the order of one to the right of the barrier after the passing of time \hbar/Γ . Compare it with equation (2.27) introduced in classical mechanics in section 2.

The explicit form of the survival probability amplitude follows from equation (3.196):

$$\mathcal{G}(t) = \int_0^\infty A_j(E) e^{-iEt/\hbar} \frac{dE}{2\pi\hbar} = e^{-iE_{R,j}t/\hbar - \Gamma_j t/2\hbar} + \frac{(1-i)}{\sqrt{2}} \int_0^\infty \frac{\Gamma_j e^{-Et/\hbar} \sqrt{E_{R,j}/E}}{(iE + E_{R,j})^2 + \Gamma_j^2/4} \frac{dE}{2\pi}. \quad (3.204)$$

To get this expression we assumed the energy dependence of the width $\Gamma(E) \simeq \Gamma \sqrt{E_{R,j}/E}$, as it follows from analysis of the available phase-space of the 1D problem at small energies, and rotated the contour of integration to coincide with the imaginary axis. For $t \gg \hbar/E_{R,j}$ we find

$$\mathcal{G}(t) \simeq e^{-iE_{R,j}t/\hbar - \Gamma_j t/2\hbar} + \frac{(1-i)}{\sqrt{8\pi}} \frac{\Gamma_j}{E_{R,j}} \left(\frac{\hbar}{E_{R,j}t} \right)^{1/2}. \quad (3.205)$$

For times of $t \ll t_{\text{dec}} \log(8\pi E_{R,j}^3/\Gamma_j^3)$, i.e. almost in the whole time interval of interest, the second term can be neglected. If we extend integration to $-\infty$ using that $A_j(E)$ is the sharp function of E near $E_{R,j} > 0$, we get

$$\mathcal{G}(t) \simeq \int_{-\infty}^\infty A_j(E) e^{-iEt/\hbar} \frac{dE}{2\pi\hbar} \simeq e^{-iE_{R,j}t/\hbar - \Gamma_j t/2\hbar}. \quad (3.206)$$

Thus, the correction term in (3.204) is fully compensated by the contribution of negative energies.

We see that in the case of a decaying system we deal with a packet propagating outwards from the resonator with an effective energy distribution given by $A_j(E)$. As we argued in section 3.8, the emergence of the packet on the outer side of the barrier cannot last shorter than $\delta t_{\text{var}} \sim \hbar/\gamma = t_{\text{dec}}^\gamma$, see the Mandelstam–Tamm inequality (3.140), where γ is the dispersion of the energy distribution. However, for the Lorentz distribution $A_j(E)$ (i.e. for $\Gamma_j = \text{const}$) the dispersion would be infinite. Here we have to remember that the resonance wave functions (3.190) can be used only for energies not far from the resonance one, i.e. for $E \in [E_{R,j} - \alpha\Gamma_j, E_{R,j} + \alpha\Gamma_j]$, for $\alpha\Gamma_j \ll |E_{R,j+1} - E_{R,j}|$. Taking these energy limits into account we can estimate

$$\gamma^2 \simeq \int_{-\alpha\Gamma_j}^{+\alpha\Gamma_j} \frac{dE}{2\pi\hbar} E^2 A_j(E + E_{R,j}) \bigg/ \int_{-\alpha\Gamma_j}^{+\alpha\Gamma_j} \frac{dE}{2\pi\hbar} A_j(E + E_{R,j}) = \Gamma_j^2 \frac{(2\alpha - \arctan 2\alpha)}{4 \arctan 2\alpha}. \quad (3.207)$$

For $\alpha \simeq 3.58$ we get $\gamma \simeq \Gamma_j$. The condition $\gamma \simeq \Gamma$ looks rather natural for the description of the wave packet in a quasi-stationary state.

Thus, the probability to find a particle outside the barrier becomes essentially non-zero before the maximum of the wave packet (according to the latter's position one defines the scattering group time) has reached the point $z = l$ with advancement $\sim t_{\text{dec}}^\gamma \sim \hbar/\Gamma$ (if we put $\gamma \simeq \Gamma$), and the real forward delay time is given by

$$\delta t_f = t_s - t_{\text{dec}}^\gamma, \quad (3.208)$$

cf. equation (3.141) above. This quantity demonstrates an advance of the formation and decay of the intermediate states forming in the scattering on the potential (3.161) at energies $|E - E_R| > \Gamma/2$ and a delay at energies in the vicinity of the resonance, for $|E - E_R| < \Gamma/2$.

Considering a scattering of a packet with an energy distribution $\Phi(E)$ on the potential well (3.161), we may introduce the quantity

$$\bar{t}_s(\bar{E}) = \int \frac{dE}{2\pi\hbar} |\Phi(E)|^2 t_s(E) \approx \int \frac{dE}{2\pi\hbar} |\Phi(E)|^2 \frac{\hbar}{2} A_i(E). \quad (3.209)$$

Here $|\Phi(E)|^2$ is normalized as in equation (3.195). For the Gaussian wave packet $|\Phi(E)|^2 = \sqrt{2\pi\hbar^2/\gamma^2} \exp(-(E - \bar{E})^2/2\gamma^2)$ in the limit of a narrow energy distribution $\gamma \ll \Gamma$ we derive $\bar{t}_s(\bar{E}) = t_s(\bar{E})$ and in the opposite limit case of a very broad distribution $\gamma \gg \Gamma$ we get $\bar{t}_s(\bar{E}) = 1/\gamma$. Thus $\delta t_f(\bar{E}) = \bar{t}_s(\bar{E}) - 1/\gamma$ for $\gamma \ll \Gamma$ and $\delta t_f(\bar{E}) = 0$ at $\gamma \gg \Gamma$, and only for a very specific choice of the energy distribution in the packet (e.g. for a Lorentzian distribution with $\gamma \simeq \Gamma$) we arrive at $\delta t_f = \bar{t}_s(\bar{E}) - 1/\Gamma$, as we obtained above for the case of an initially localized state.

It is instructive to rewrite the survival probability amplitude (3.196) in the following form

$$\mathcal{G}(t) = i \int_0^\infty dz \int_0^\infty dz' \Psi^*(z, 0) G^R(t, z, z') \Psi(z', 0), \quad (3.210)$$

where we introduce the retarded Green's function $G^R(t, z, z')$, which describes the evolution of the wave function, $\Psi(z, t) = \int_0^\infty dz' G^R(t, z, z') \Psi(z', 0)$ forward in time, i.e. $G^R(t, z, z') \equiv 0$ for $t < 0$, cf. the same quantity in classical mechanics (2.24), (2.30) and (2.31). The Green's function is expressed through the eigenfunctions (3.190) and (3.187)

$$G^R(t, z, z') = \int_{-\infty}^\infty \frac{dE}{2\pi} G_R(E, z, z') e^{-iEt/\hbar}, \quad G^R(E, z', z) = \int_0^\infty \frac{dE'}{2\pi\hbar} \frac{\psi(z; E') \psi^*(z'; E')}{E - E' + i0}. \quad (3.211)$$

The small shift of the pole in the last integral in the lower complex semi-plane assures that the Green's function vanishes for $t < 0$, since

$$\theta(t) e^{-iEt/\hbar} = i \int_{-\infty}^{+\infty} \frac{dE'}{2\pi} \frac{e^{-iE't/\hbar}}{E' - E + i0}. \quad (3.212)$$

For energies $E < U$ and for the case of narrow resonances we can use the wave function of the resonance states (3.190) with the replacement of their coordinate parts by the wave functions of the corresponding bound states (3.191). Then the coordinate and energy dependence of the Green's function separate as follows

$$G^R(E, z', z) \approx \sum_{i=1}^n G_i^R(E) [\psi_i^{(\text{bound})}(z')]^* \psi_i^{(\text{bound})}(z),$$

$$G_i^R(E) = \int_0^\infty \frac{dE'}{2\pi} \frac{A_i(E)}{E - E' + i0} = \frac{1}{E - E_{R,i} + \frac{i}{2}\Gamma_i}. \quad (3.213)$$

If the initial wave function (3.201) contains only one state j , the expression (3.206) reduces to the following one

$$\mathcal{G}(t) = i \int_{-\infty}^{+\infty} dz G^R(t, z, z) = i G_j^R(t) \approx - \int_{-\infty}^{+\infty} \frac{dE}{2\pi i} \frac{e^{-iEt/\hbar}}{E - E_{R,j} + \frac{i}{2}\Gamma_j} = \theta(t) e^{-iE_{R,j}t/\hbar - \Gamma_j t/2\hbar}. \quad (3.214)$$

The function $A(E)$ plays the role of the spectral density and can be defined as

$$A(E) = -2 \int_{-\infty}^{+\infty} dz \text{Im} G^R(E, z, z). \quad (3.215)$$

If we assume that initially we deal not with a pure quantum mechanical state (3.201) but with a mixed state such that

$$\Psi(z', 0)\Psi^*(z, 0) \approx \left(\sum_{i=1}^n n_T(\varepsilon_i) \right)^{-1} \sum_{i=1}^n n_T(\varepsilon_i) \psi^{\text{bound}}(z') [\psi^{\text{bound}}(z)]^*,$$

which contains a number of quasi-stationary states characterized by the thermal Fermi/Bose occupations n_T , we find that the decay of such a system is described by

$$\mathcal{G}_T(t) \simeq \int_0^\infty \frac{dE}{2\pi} A(E) n_T(E) e^{-iEt} / \int_0^\infty \frac{dE}{2\pi} A(E) n_T(E). \quad (3.216)$$

This expression is to be compared with equation (5.40) written below with the help of the Wigner densities.

3.10. Causality restriction

From (3.179), (3.180) we arrive at the inequality

$$\delta t_s \geq -\frac{l}{v} - \frac{\hbar}{2kv}. \quad (3.217)$$

This restriction (cf. [116]) differs from the corresponding condition, which we have derived (for $R = l$) in classical mechanics (see equation (2.81)) by the presence of the second term in the right-hand side of (3.217). The latter term is of purely quantum origin. It shows the time which the particle needs in order to pass a half of the de Broglie wavelength, $\lambda = \hbar/k$. Following the uncertainty principle free quantum particles cannot distinguish distance $\xi < \hbar/2k$.

4. Time shifts in non-relativistic quantum mechanics: 3D-scattering

4.1. Scattering of the wave packet on the potential

In the 3D scattering problem there appears new specifics. At large distances from the interaction zone the wave packet is presented as

$$\Psi(\vec{r}, t) = \int \frac{d^3k}{(2\pi\hbar)^3} \mathcal{F}(\vec{k} - \vec{p}) \psi_{\vec{k}} e^{-iE_k t/\hbar}, \quad (4.1)$$

where $\mathcal{F}(\vec{k} - \vec{p})$ is the wave packet amplitude peaked at $\vec{k} = \vec{p}$ and the stationary wave function

$$\psi_{\vec{k}} \simeq e^{ikz/\hbar} + \frac{e^{ikr/\hbar}}{r} f(E, \theta_k) \quad (4.2)$$

is the sum of the incident and the scattered ($\propto f$) waves [52], normalized to unit amplitude in the incident wave. The cross-section is determined through f as

$$d\sigma = |f|^2 d\Omega, \quad f(\theta) = \sum_{l=0}^{\infty} (2l+1) f_l P_l(\cos\theta_k), \quad (4.3)$$

cf. equation (2.90), (2.91). The scattering amplitude is expressed through the phase shift:

$$f_l = \frac{\hbar}{k} \sin \delta^l(k) e^{i\delta^l(k)}. \quad (4.4)$$

As follows from this expression, the amplitude f_l is related to the elements of the S and T -matrices [52] as: $S_l - 1 = T_l = 2ikf_l/\hbar$, $S_l = e^{2i\delta^l}$. We would like to bring to reader's attention that the partial phase δ_l vanishes identically if the scattering potential is put to zero. Thus the corresponding quantity in classical mechanics is $\delta^{\text{cl}} - \delta^{\text{cl}}(U=0)$ in equation (2.20).

Presenting $E = E_p + \delta E$ and $k = p + \delta E/v_p + \dots$ in equation (4.1), we recognize in the scattered wave the factor $\exp[i\frac{\delta E}{\hbar}(r/v_p - t + \hbar\frac{\partial \ln f_l(E_p)}{\partial E_p})]$, $v_p = p/2E_p$. Thus, using equation (4.4) we find the time delay/advance of the scattered wave

$$\delta t_s^l = \hbar \text{Im} \frac{\partial \ln f_l(E_p)}{\partial E_p} = \hbar \frac{\partial \delta^l(E_p)}{\partial E_p}. \quad (4.5)$$

On the other hand, expanding the plane wave part of the wave function (4.2), $e^{ikz/\hbar}$, in the Legendre polynomials one gets a series of converging and diverging waves:

$$\psi_{\vec{k}} \simeq \frac{\hbar}{2ikr} \sum_{l=0}^{\infty} (2l+1) P_l(\cos\theta_k) [(-1)^{l+1} e^{-ikr/\hbar} + e^{2i\delta^l(k)} e^{ikr/\hbar}]. \quad (4.6)$$

The first term in the squared brackets, the converging wave, arises as a part of the incident wave. The second term is the result of the superposition of scattered waves ($\propto f$),

$$\psi_s \simeq \frac{\hbar}{kr} \sum_l (2l+1) P_l(\cos\theta_k) \sin \delta^l(k) e^{i\delta^l(k) + ikr/\hbar}, \quad (4.7)$$

and the incident wave $e^{ikz/\hbar}$. Note that the optical theorem ($\text{Im} f(0) = \frac{k}{4\pi\hbar} \int |f|^2 d\Omega$) arises as a consequence of subtle interference that takes place in the forward direction.

From the second term in the squared brackets (4.6) one finds the average exit time delay/advance of the diverging waves with the angular momentum l (the l th partial wave) [1],

$$\delta t_W^l = 2\hbar \frac{\partial \delta^l}{\partial E_p}. \quad (4.8)$$

This result includes the interference with the incident wave and is twice as large than the time delay of the purely scattered wave (4.5). The converging wave $\propto e^{i\delta E(r/v_p - t)/\hbar}$ propagates

without any delay. Reference [67] (see also [2]) introduced the collision life-time for elastic collisions, as a difference between the time of the particle flight in presence of the potential and the free-flight time and found the relation

$$Q_l = \lim_{R \rightarrow \infty} \int^R \left(\tilde{\psi}_l^* \tilde{\psi}_l - \frac{2}{4\pi v r^2} \right) d^3 r = -i\hbar \frac{dS_l}{dE} S_l^* = \delta t_W^l, \quad (4.9)$$

with $\tilde{\psi}_l$ normalized here to unit incident flux. Note that equation (4.9) coincides with the definition of the dwell time, cf. equation (3.23), but now for the diverging waves only and with other normalization. As we will see in section 6, the meaning of the collision time is different. We also stress that δt_W^l has the meaning of the group delay/advance of the diverging wave occurring only at large distances, cf. discussion of the wave zone in section 2.2.1. The same wave at short distances near the scattering center is disturbed and is delayed/advanced differently.

Besides time delays/advancements δt_s^l and δt_W^l , the corresponding wave packets undergo a smearing since velocities of the particles depend on the energy. To be specific consider the diverging wave packet for given l (cf. second term in (4.6)):

$$\psi_l \simeq \frac{\hbar}{2ikr} (2l+1) P_l(\cos \theta_k) e^{2i\delta^l(k) + ikr/\hbar}. \quad (4.10)$$

Let

$$\mathcal{F}(\vec{k} - \vec{p}) = C \delta(\cos \theta_k - \cos \theta_p) e^{-(k-p)^2/(4\gamma_p^2)}, \quad C = \text{const}. \quad (4.11)$$

By expanding the functions of k in $k - p$ up to second order near the point $k = p$, replacing these expressions in equation (4.1) and taking the integral we find the diverging wave packet, Ψ_l , cf. [2],

$$\Psi_l = \hbar (2l+1) P_l(\cos \theta_p) \frac{2\pi^{3/2} C p \tilde{\gamma}_p}{ir(2\pi\hbar)^3} \exp \left[-\frac{\tilde{\gamma}_p^2}{\hbar^2} \left(v_p t - r - 2v_p \hbar \frac{\partial \delta^l}{\partial E_p} + \frac{i\hbar}{p} \right)^2 \right] \chi_{\vec{p}},$$

$$\frac{1}{\tilde{\gamma}^2} = \frac{1}{\gamma^2} + \frac{1}{2p^2} + \frac{i}{2m\hbar} \left[t - \hbar \frac{\partial \delta^l}{\partial E_p} - \hbar \frac{E_p}{2} \frac{\partial^2 \delta^l}{\partial E_p^2} \right], \quad \chi_{\vec{p}} = e^{ipr/\hbar - iE_p t/\hbar + 2i\delta_p^l}. \quad (4.12)$$

To get the law of the time propagation of the maximum of the packet one needs to keep only linear terms in the expansion. The smearing of the wave packet with passage of time appears due to the second-order terms kept in the expansion. Because of the presence of the term $\frac{\partial^2 \delta^l}{\partial p^2} = \frac{1}{m} \frac{\partial \delta^l}{\partial E_p} + v_p^2 \frac{\partial^2 \delta^l}{\partial E_p^2}$ the smearing of the wave packet is advanced or delayed in dependence of the sign of the term $\frac{\partial^2 \delta^l}{\partial p^2}$.

Similarly, we could consider the converging, the scattered and the incident wave packets. We also could use the expansion (3.41) instead of equation (4.1) with a $\Phi(E, \theta_k)$ distribution, multiplied by $\delta(\cos \theta_k - \cos \theta_p)$, instead of equation (4.11). Thus these results are similar to those derived above in section 3.8 in a 1D case.

[3, 19, 20] defined average time spent by the wave packet within a chamber as

$$t_{\text{vol}}^N = \frac{1}{N} \int dt \int d\Omega r^2 (\vec{n} \cdot \vec{j}(r, \Omega, t)), \quad \vec{n} = \vec{r}/r. \quad (4.13)$$

Here

$$N = \int dt \int d\Omega r^2 |\vec{j} \cdot \vec{n}| \quad (4.14)$$

is the modulus of the integrated incident unit flux through the chamber surface, cf. the expression for the classical sojourn time equation (3.95). The flow density associated with the wave function Ψ is given by equation (3.3). The value $\vec{j} \cdot \vec{n}$ is positive, when the particle exits

the volume, and negative, when it enters the volume. The incident current is the sum of the scattering current and the interference term, $\vec{j} = \vec{j}_s + \vec{j}_i$. Thereby we introduce time delays: $t_{\text{vol}}^N = t_s^N - \delta t_i^N$, all quantities being normalized by N .

Further, for simplicity, we consider only one l -partial wave. The scattering time normalized by the scattered flux N_s is as follows

$$t_s = \left(\frac{dN_s}{d\Omega} \right)^{-1} \int dt t r^2 (\vec{j}_s \vec{n}) = t_{\text{free}} + \delta t_s, \\ N_s/N = 4 \sin^2 \delta^l, \quad (4.15)$$

cf. equations (4.7), (4.10), resulting in equation (4.5) for the scattering time delay/advancement. Here $t_{\text{free}} = r/v$ is the time of the free flight in one direction (at finite angles there is no interference).

The interference delay/advancement time for a one partial wave normalized by the scattered flux is (cf. [20])

$$-\delta t_i = \left(\frac{dN_s}{d\Omega} \right)^{-1} \int dt t r^2 (\vec{j}_i \vec{n}) = \frac{\hbar^2}{4 p^2 |f_l|^2} \frac{\partial}{\partial E_p} (p (f_l + f_l^*)) = \frac{\cos(2\delta^l)}{2 \sin^2 \delta^l} \hbar \frac{\partial \delta^l}{\partial E_p}. \quad (4.16)$$

The total delay/advancement in the diverging wave is

$$\delta t_{\text{vol}}^N = \delta t_W = (\delta t_s - \delta t_i) 4 \sin^2 \delta^l = 2 \hbar \frac{\partial \delta^l}{\partial E_p}. \quad (4.17)$$

The factor $4 \sin^2 \delta^l$ arose due to different normalizations in equations (4.15)–(4.17). From here

$$\delta t_{\text{vol}} = \frac{2 \hbar}{4 \sin^2 \delta^l} \frac{\partial \delta^l}{\partial E_p} \quad (4.18)$$

is the average time spent by the wave packet within the chamber normalized by the scattered flux N_s .

4.2. Resonance scattering

For one Breit–Wigner resonance

$$\tan \delta = -\frac{\Gamma}{2M}, \quad M = E - E_R, \quad N_s = N \Gamma A, \quad (4.19)$$

the forward delay/advance time

$$\delta t_f \equiv \delta t_i = \delta t_s - t_{\text{dec}} = -\frac{\hbar(M^2 - \Gamma^2/4)}{\Gamma(M^2 + \Gamma^2/4)}, \quad (4.20)$$

being negative for $|M| > \Gamma/2$. Here the value

$$\delta t_{\text{vol}} = \delta t_{\text{vol}}^N / (4 \sin^2 \delta) = t_{\text{dec}} = \hbar/\Gamma \quad (4.21)$$

has the meaning of the decay time of the quasi-stationary state with complex energy $E_R - i\Gamma/2$ (cf. equations (2.27), (3.203)).

The probability for a particle to enter the region of the resonance interaction is $P_\Gamma = \sin^2 \delta = \frac{\Gamma^2/4}{M^2 + \Gamma^2/4}$. Thereby the cross-section of the resonance scattering can be presented as $\sigma \simeq 4\pi \lambda^2 P_\Gamma$, where $\lambda = \hbar/k$ is the de Broglie wavelength. For $M = 0$ (pure resonance) the cross-section reaches its maximum $\sigma_{\text{max}} = 4\pi \lambda^2$.

The probability for a particle not to enter the region of the resonance interaction is $P_M = \cos^2 \delta = \frac{M^2}{M^2 + \Gamma^2/4}$, $P_\Gamma + P_M = 1$. The scattering time delay is

$$\delta t_s = \hbar \frac{\partial \delta}{\partial E} = \frac{\hbar}{2} A = 2 t_{\text{dec}} P_\Gamma, \quad (4.22)$$

$2t_{\text{dec}} = \delta t_s(E = E_R) = t_{\text{dec}}^{(\text{cl})}$. The forward delay time,

$$\delta t_f = \hbar A/2 - t_{\text{dec}} = t_{\text{dec}}(P_\Gamma - P_M), \quad (4.23)$$

is the time delay of the decay due to the difference in the probability for the particle to enter the region of the resonance interaction and not to enter this region.

In section 6 we shall see that for a many-particle system the value δt_{dec} is the average time between collisions. The forward delay/advance time, δt_f , is then an average delay/advance in the scattering counted from the collision time δt_{col} . Thus, this delay/advancement time characterizes delays and advancements of collisions in quantum kinetic processes.

4.3. Scattering on hard cores

For the gas of hard core scatters [117] the scattering amplitude and its momentum derivative are

$$\tan \delta^l = -\frac{j_l(kR/\hbar)}{n_l(kR/\hbar)}, \quad \frac{\partial \delta^l}{\partial k} = -\frac{\hbar}{k^2 R [j_l^2(kR/\hbar) + n_l^2(kR/\hbar)]}. \quad (4.24)$$

E.g., for $l = 0$ from (4.24) we find $\delta t_s^0 = \hbar \frac{\partial \delta^0}{\partial E_k} = -R/v$ that agrees with equation (2.82) for $b = 0, \theta = \pi$. The same advancement, $\delta t_s^l = -R/v$, arises for rapid particles $kR/\hbar \gg l^2$ at $l \neq 0$. For slow particles, $kR/\hbar \ll l^{1/2}$, $\delta t_s^l \propto (kR/\hbar)^{2l} R/v$, since the wavelength $\lambda = \hbar/k \gg R$ in this case and the propagating wave almost does not feel the presence of the sphere. For $l \gg 1$ the cross-section becomes negligibly small.

4.4. Semiclassical scattering

The transition from the semiclassical expression for the phase shift [44]

$$\delta t_{\text{W}}^{\text{scl}} = \frac{2\hbar \partial \delta^l}{\partial E} = \frac{1}{E} \int_0^\infty (2U(r) + rU'(r)) \frac{2R_l^2(r)}{v_\infty} dr, \quad (4.25)$$

where $R_l(r) \sim \sin(kr/\hbar - l\pi/2 + \delta^l)$ is the radial wave function, to the classical equation (2.17) occurs provided one exploits the semiclassical expression for the wave function $R_M = \sqrt{v_\infty/v_r} \sin(\int_{r_0}^r v_r dr/\hbar + \pi/4)$. Substituting in equation (4.25) R_M instead of R_l and using that $R_M^2 \simeq v_\infty/(2v_r)$ we arrive at the result for the classical Wigner time delay (2.21).

The probability of the decay of a long-lived state is determined by the imaginary part of the action: $W \simeq e^{2\text{Im}S/\hbar}$. In the case of quasi-stationary level, the time-scale

$$t_{\text{dec}}^{\text{scl}} = \hbar/(2|\text{Im}E|), \quad (4.26)$$

characterizes the decay of the state, where $\text{Im}E$ is the imaginary part of the energy.

The scattering delay counted from the decay time in the given case is

$$\delta t_f^{\text{scl}} = \delta t_{\text{W}}^{\text{scl}}/2 - t_{\text{dec}}^{\text{scl}}, \quad (4.27)$$

cf. equation (4.20).

4.4.1. Ergodicity, time shifts and level density. For the scattering on the potential, as well as for binary collisions, in the virial limit the energy level density (i.e. the density of states) simply relates to the Wigner time delay as (see [20, 118])

$$\frac{dN^{\text{level}}}{dE_p} - \frac{dN^{\text{free}}}{dE_p} = \frac{1}{2\pi\hbar} \sum_l (2l+1) \delta t_{\text{W}}^l, \quad (4.28)$$

where $\frac{dN^{\text{free}}}{dE_p} = \frac{4\pi V p^2}{(2\pi\hbar)^3(dE_p/dp)}$ and V is the system volume, for binary collisions, dE_p/dp is the relative velocity of interacting particles and δt_W^l is given by equation (4.8) for given l . Since all thermodynamic quantities such as entropy and pressure can be calculated, if one knows the density of states, this condition allows to express thermodynamical variables at low densities in terms of the phase shifts and the time delays. It looks like an ergodic constraint: deviation of the density of states from that for the ideal gas is limited in time by the Wigner time delay, i.e. the delay of out-going waves.

For the scattering on the Breit–Wigner resonance the free term on the left-hand side (4.28) should be dropped, since one should take into account that the phase additionally changes by π when the energy passes the resonance region, see equation (4.19). Thus one has

$$\delta t_W = 2\hbar \frac{\partial \delta}{\partial E_p} = 2\pi\hbar \frac{dN^{\text{level}}}{dE_p}. \quad (4.29)$$

Thereby δt_W can be interpreted as a time delay in an elementary phase-space cell.

5. Time shifts in quantum field theory

5.1. Time contour formulation

From now on we use units $\hbar = c = 1$. To be specific, we consider a multi-component system with different constituents ‘ a ’ of non-relativistic particles and relativistic scalar bosonic field operators, $\hat{\phi} = \{\hat{\phi}_a(x)\}$, where from now on x is a 4-coordinate. The free Lagrangian densities of these fields are

$$\widehat{\mathcal{L}}_a^0 = \begin{cases} \frac{1}{2} \left(i\hat{\phi}_a^\dagger \partial_t \hat{\phi}_a - i\partial_t \hat{\phi}_a^\dagger \cdot \hat{\phi}_a - \frac{1}{m_a} \nabla \hat{\phi}_a^\dagger \nabla \hat{\phi}_a \right) & \text{non-rel. particles,} \\ \frac{1}{2} (\partial_\mu \hat{\phi}_a \cdot \partial^\mu \hat{\phi}_a - m_a^2 \hat{\phi}_a^2) & \text{neutral rel. bosons,} \\ \partial_\mu \hat{\phi}_a^\dagger \partial^\mu \hat{\phi}_a - m_a^2 \hat{\phi}_a^\dagger \hat{\phi}_a & \text{charged rel. bosons.} \end{cases} \quad (5.1)$$

We assume that these fields interact either via non-derivative coupling or via linear derivative coupling. In the latter case the interaction Lagrangian depends not only on the fields but also on their derivatives $\widehat{\mathcal{L}}^{\text{int}} = \widehat{\mathcal{L}}^{\text{int}}\{\hat{\phi}_a, \hat{\phi}_a^\dagger, \partial^\mu \hat{\phi}_a, \partial^\mu \hat{\phi}_a^\dagger\}$. The variational principle of stationary action determines Euler–Lagrange equations of motion for the field operators $\hat{\phi}_a$

$$\partial_\mu \frac{\partial \widehat{\mathcal{L}}^0}{\partial(\partial_\mu \hat{\phi}_a^\dagger)} - \frac{\partial \widehat{\mathcal{L}}^0}{\partial(\hat{\phi}_a^\dagger)} = \frac{\partial \widehat{\mathcal{L}}^{\text{int}}}{\partial(\hat{\phi}_a^\dagger)} - \partial_\mu \frac{\partial \widehat{\mathcal{L}}^{\text{int}}}{\partial(\partial_\mu \hat{\phi}_a^\dagger)} \equiv \frac{\delta \widehat{\mathcal{L}}^{\text{int}}}{\delta \hat{\phi}_a^\dagger(x)}, \quad (5.2)$$

and the corresponding adjoint equations; cf. [37]. The ‘variational’ δ -derivative

$$\frac{\delta}{\delta f(x)} \dots \equiv \frac{\partial}{\partial f(x)} \dots - \partial_\mu \left(\frac{\partial}{\partial(\partial_\mu f(x))} \dots \right) \quad (5.3)$$

of $\widehat{\mathcal{L}}^{\text{int}}$ permits to include derivative couplings into the interaction Lagrangian $\widehat{\mathcal{L}}^{\text{int}}$. In fact, the ‘variational’ δ -derivative means the *full* derivative over $f(x)$, implying that all derivatives acting on $f(x)$ in the action should be redirected to other terms by means of partial integration before taking derivative in $f(x)$.

Further we suppress particle index ‘ a ’. The principle of stationary action leads to the Euler–Lagrange equations of motion for the field operators [34]

$$-\widehat{G}_0^{-1} \hat{\phi}(x) = \widehat{J}(x) = \frac{\delta \widehat{\mathcal{L}}^{\text{int}}}{\delta \hat{\phi}^\dagger}; \quad (5.4)$$

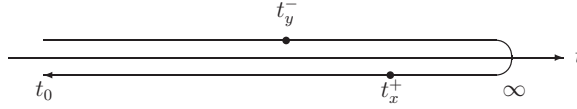


Figure 14. Schwinger–Keldysh time contour.

$$\widehat{G}_0^{-1} = \begin{cases} -\partial_\mu \partial^\mu - m^2 & \text{for relativistic bosons,} \\ i\partial_t - \frac{1}{2m} \partial_r^2 & \text{for non-rel. particles,} \end{cases} \quad (5.5)$$

cf. equation (2.23) of classical mechanics, which we introduced in section 2.1.1. The $\widehat{J}(x)$ operator is a local source current of the field $\widehat{\phi}$, while \widehat{G}_0^{-1} is the differential operator of the free evolution with the free propagator $G^0(y, x)$ as resolvent, x, y are 4-time–space points.

In the non-equilibrium case, one assumes that the system has been prepared at some initial time t_0 described in terms of a given density operator $\widehat{\rho}_0 = \sum_a P_a |a\rangle \langle a|$, where the $|a\rangle$ form a complete set of eigenstates of $\widehat{\rho}_0$. All observables can be expressed through n -point Wightman functions of Heisenberg operators $\widehat{A}(t_1), \dots, \widehat{O}(t_n)$ at some later times

$$\langle \widehat{O}(t_n) \dots \widehat{B}(t_2) \widehat{A}(t_1) \rangle = \sum_a P_a \langle a | \widehat{O}(t_n) \dots \widehat{B}(t_2) \widehat{A}(t_1) | a \rangle. \quad (5.6)$$

The non-equilibrium theory is formulated on a closed real-time contour (see figure 14) with the time argument running from t_0 to ∞ along the time-ordered branch and back to t_0 along the anti-time-ordered branch. Contour-ordered multi-point functions are defined as expectation values of contour-ordered products of operators

$$\langle \mathcal{T}_C \widehat{A}(x_1) \widehat{B}(x_2) \dots \rangle = \langle \mathcal{T}_C \widehat{A}_I(x_1) \widehat{B}_I(x_2) \dots e^{i \int_C \widehat{\mathcal{L}}_I^m dx} \rangle, \quad (5.7)$$

where \mathcal{T}_C orders the operators according to a time parameter running along the time contour ‘C’. The left-hand side is written in the Heisenberg representation, whereas the right-hand side, in the interaction (I) representation.

The contour ordering obtains its particular sense through the placement of external points on the contour. One then has to distinguish between the physical space–time coordinates x, \dots and the corresponding contour coordinates x^C , which for a given x take two values $x^- = (x_\mu^-)$ and $x^+ = (x_\mu^+)$, $\mu \in \{0, 1, 2, 3\}$, on the time-ordered and anti-time-ordered branches, respectively (see figure 14). Closed real-time contour integrations are decomposed as

$$\int_C dx \dots = \int_{t_0}^\infty dx^- \dots + \int_\infty^{t_0} dx^+ \dots = \int_{t_0}^\infty dx^- \dots - \int_{t_0}^\infty dx^+ \dots, \quad (5.8)$$

where $dx^\pm = dx_0^\pm dx^1 dx^2 dx^3$ and only the time limits are explicitly given. Thus, the anti-time-ordered branch acquires an extra minus sign, if integrated over physical times. For any two-point function \mathcal{F} , the contour values on the different branches define a 2×2 -matrix function

$$\mathcal{F}^{ij}(x, y) = \mathcal{F}(x^i, y^j), \quad i, j \in \{-, +\}, \quad (5.9)$$

depending on the physical coordinates (x, y) . The contour δ -function is determined as

$$\delta_C^{ij}(x, y) = \delta_C(x^i, y^j) = \sigma^{ij} \delta^4(x - y), \quad \sigma^{ij} = \begin{pmatrix} 1 & 0 \\ 0 & -1 \end{pmatrix}, \quad (5.10)$$

where the matrix σ^{ik} accounts for the integration sense on the two branches. For any multi-point function, the external point x_{\max} , which has the largest physical time, can be placed

on either branch of the contour without changing the value, since the contour-time evolution from x_{\max}^- to x_{\max}^+ provides unity. Therefore, one-point functions have the same value on both sides of the contour. Due to the change of operator ordering, genuine multi-point functions are discontinuous in general, when two contour coordinates become identical.

Boson fields may take non-vanishing expectation values of the field operators $\phi(x) = \langle \widehat{\phi}(x) \rangle$. The corresponding equations of motion for these classical fields are provided by the ensemble average of the operator equations of motion (5.4)

$$-\widehat{G}_0^{-1}\phi(x) = J(x), \quad \phi = \phi^0(x) - \int_C dy G^0(x, y) J(y), \quad (5.11)$$

now in full analogy to equation (2.23), which we used in classical mechanics. Here $J(x) = \langle \widehat{J}(x) \rangle$, while $\phi^0(x) = \langle \widehat{\phi}_I(x) \rangle$ is the freely evolving classical field, which starts from $\phi^0(t_0, \vec{x})$ at time t_0 . Thereby, $G^0(x, y)$ is the free contour Green's function

$$iG^0(x, y) = \langle \mathcal{T}_C \widehat{\phi}_I(x) \widehat{\phi}_I^\dagger(y) \rangle - \phi^0(x) (\phi^0(y))^*, \quad (5.12)$$

which resolves the equation

$$\widehat{G}_0^{-1}G^0(x, y) = \delta_C(x, y) \quad (5.13)$$

on the contour. Graphically equation (5.11) can be depicted as

$$\text{---}\star = \text{---}\times + \text{---}\bigcirc(iJ) \quad (5.14)$$

with the one-point function $iJ(x)$ as the driving term.

Performing replacements in equation (5.11):

$$\phi \rightarrow mz, \quad \widehat{G}_0^{-1} \rightarrow -\partial_t^2 - \Gamma\partial_t - E_R^2, \quad J \rightarrow -m\Lambda z^2 + F \quad (5.15)$$

we arrive at the results for an anharmonic oscillator in an external field, see equations (2.22)–(2.25) of section 2. Classical Maxwell equations follow with the help of the replacements

$$\phi \rightarrow A^\mu, \quad \widehat{G}_0^{-1} \rightarrow -\partial_\nu\partial^\nu, \quad J \rightarrow \frac{4\pi}{c}j^\mu. \quad (5.16)$$

Subtracting the classical fields via $\widehat{\phi}(x) = \phi(x) + \widehat{\Psi}(x)$, we define the full propagator in terms of quantum-fluctuating parts $\widehat{\phi}(x)$ of the fields

$$iG(x, y) = \langle \mathcal{T}_C \widehat{\Psi}(x) \widehat{\Psi}^\dagger(y) \rangle = \langle \mathcal{T}_C \widehat{\phi}(x) \widehat{\phi}^\dagger(y) \rangle - \phi(x)\phi^*(y). \quad (5.17)$$

Averaging the operator equations of motion (5.4) multiplied by $\widehat{\phi}^\dagger(y)$ and subtracting classical field parts one obtains the equation of motion for the propagator

$$\widehat{G}_0^{-1}(x)G(x, y) = \delta_C(x, y) + i\langle \mathcal{T}_C \widehat{J}(x) \widehat{\Psi}^\dagger(y) \rangle_c, \quad (5.18)$$

which is still exact and accounts for the full set of initial correlations contained in $\widehat{\rho}_0$. The sub-label 'c' indicates that uncorrelated parts are subtracted. The Feynman diagrammatic representation of the processes is not yet possible at this level. This description level should be still time reversible.

5.2. Weakening of short-range correlations and the Dyson equation

In order to proceed further one suggests that the typical interaction time t_{int} for the change of the correlation functions is significantly shorter than the typical time which determines the system evolution. Then, describing the system at times $t - t_0 \gg t_{\text{int}}$, one can neglect the

short-range correlations, which are supposed to die out beyond t_{int} in line with the principle of the weakening of initial and all short-range $\sim t_{\text{int}}$ correlations [119]. After dropping higher order correlations for the driving terms on the right-hand side of the equation of motion (5.18) one can apply the standard Wick decomposition. With the help of (5.7) the driving term can be expressed as functional of one-particle propagators rather than of higher order correlations

$$\begin{aligned} i\langle \mathcal{T}_C \widehat{J}(x) \widehat{\Psi}^\dagger(y) \rangle_c &= i \int_C dz \left\langle \mathcal{T}_C \frac{\partial}{\partial \widehat{\Psi}_1(z)} \left[e^{i \int_C dz' \widehat{\mathcal{L}}_1^{\text{int}}} \widehat{J}_1(x) \right] \right\rangle_{c1} \langle \mathcal{T}_C \widehat{\Psi}(z) \widehat{\Psi}^\dagger(y) \rangle \\ &= \int_C dz \Sigma(x, z) G(z, y). \end{aligned} \quad (5.19)$$


Thus one recovers the Dyson equation in the differential form

$$\widehat{G}_0^{-1}(x)G(x, y) = \delta_C(x, y) + \int_C dz \Sigma(x, z) G(z, y). \quad (5.20)$$

Since we have separated the full propagator in equation (5.19), the self-energy of the particle,

$$-i\Sigma(x, y) = -\langle \mathcal{T}_C \widehat{J}(x) \widehat{J}^\dagger(y) \rangle_{c1}, \quad (5.21)$$

here given in the Heisenberg picture, is one-particle irreducible (label c1), i.e. the corresponding diagram cannot be split into two pieces, which separate x from y by cutting a single propagator line. In diagrams free and full propagators are usually given by thin and thick lines, respectively. Therefore the Dyson equation (5.20) in a graphical form is depicted as



$$\text{---} = \text{---} + \text{---} \circ (-i\Sigma) \text{---} \quad (5.22)$$

with two-point function $-i\Sigma(x, y)$ as the driving term.

We would like to point out that in the derivation of the Dyson equation (5.20) with the application of Wick decomposition we have already lost the time reversibility. Any loss of information results in a growth of the entropy. Therefore, a dropping of short-range correlations on each time step would lead to a growth of the entropy, associated with the thus obtained Dyson equation, with time.

Actually, only two quantities among four G^{ij} are independent [34]. As these two quantities it is convenient to use the quantity

$$F(t_1, \vec{r}_1; t_2, \vec{r}_2) = (\mp) i G^{-+}(x_1, x_2) = \langle \Psi^\dagger(x_2) \Psi(x_1) \rangle, \quad (5.23)$$

which after the Wigner transform becomes the Wigner phase-space density and the retarded Green's function

$$i G^R(x_1, x_2) = \begin{cases} \langle \Psi(x_1) \Psi^\dagger(x_2) \pm \Psi^\dagger(x_2) \Psi(x_1) \rangle & \text{for } t_1 > t_2 \\ 0 & \text{for } t_1 < t_2 \end{cases}, \quad (5.24)$$

where the upper sign is for fermions and the lower one is for bosons. The equation for the retarded Green's function decouples:

$$G^R(x_1, x_2) = G_0^R(x_1, x_2) + \int_C dx_3 \int_C dx_4 G_0^R(x_1, x_3) \Sigma^R(x_3, x_4) G^R(x_4, x_2). \quad (5.25)$$

The retarded self-energy Σ^R fulfils the same relations (E.3) as the retarded Green's function.

The quantity

$$A(x_1, x_2) = -2 \text{Im } G^R(x_1, x_2) \quad (5.26)$$

is the response function. Its Fourier transform is the spectral function, cf. equations (3.183), (3.206). The Fourier transform of the quantity

$$\Gamma(x_1, x_2) \equiv -2 \text{Im } \Sigma^R(x_1, x_2) \quad (5.27)$$

has the meaning of the particle width after proper normalization. In the energy–momentum representation for the stationary spatially homogeneous systems these quantities reduce to $A(p_0, \vec{p})$ and $\Gamma(p_0, \vec{p})$. For quasiparticles (when one puts $\Gamma(p_0, \vec{p}) \rightarrow 0$ in the Green’s function), the spectral function becomes the δ -function and determines the spectrum of quasiparticles.

5.3. Φ -derivable approximation scheme

For any practical calculation one has to apply some approximation scheme. In the weak-coupling limit, the perturbative expansion may be restricted to a certain order. Then no particular problems are encountered as far as conservation laws are concerned, since they are fulfilled order by order in perturbation theory. On the other hand, such perturbative expansion may not be adequate, as, for example, in the strong coupling limit, where re-summation concepts have to be applied. Such schemes sum up certain sub-series of diagrams to any order. Furthermore, with the aim to solve dynamical equations of motion, such as transport equations, one automatically re-sums all terms in the equations of motion to any order.

A Φ -derivable approximation, first introduced by Baym [33] within the imaginary-time formulation, is constructed by confining the infinite set of diagrams for Φ to either only a few of them or some sub-series of them. Note that Φ itself is constructed in terms of ‘full’ Green’s functions, where ‘full’ now takes the sense of solving self-consistently the Dyson’s equation with the driving terms derived from this Φ through the relation $-i\Sigma = \mp\delta\Phi/\delta G$. It means that even restricting to a single diagram in Φ , in fact, we deal with a whole sub-series of diagrams in terms of free Green’s functions, and ‘full’ takes the sense of the sum of this whole sub-series. Thus, a Φ -derivable approximation offers a natural way of introducing closed, i.e. consistent approximation schemes based on summation of diagrammatic sub-series. In order to preserve the original symmetry of the exact Φ , we postulate that the set of diagrams defining the Φ -derivable approximation complies with all such symmetries. As a consequence, approximate forms of $\Phi^{(\text{appr.})}$ define effective theories, where $\Phi^{(\text{appr.})}$ serves as a generating functional for approximate self-energies $\Sigma^{(\text{appr.})}(x, y) = \mp\delta\Phi^{(\text{appr.})}/\delta G$, which then enter as driving terms in the Dyson equations (5.20). The propagators, solving this set of Dyson equations, are still called ‘full’ in the sense of the Φ -derivable scheme. For such re-summation schemes, the conservation laws are preserved [34–37].

5.4. The space–time structure of self-energy diagrams

Usually, one considers processes occurring in vacuum or in homogeneous matter in equilibrium in the Fourier representation. It is also informative to study these processes in the space–time representation, see [80, 120]. As a representative example we consider the correction to the single particle Green’s function in the scalar ϕ^3 -theory

$$\begin{aligned}
 i\delta G(x_2, x_1) &= x_1 \text{---} \text{---} \text{---} \text{---} \text{---} x_2 \\
 &= \alpha \int_C dy iG(x_2 - y) (iV_y) \int_C dx [iG(y - x)]^2 (iV_x) iG(x - x_1).
 \end{aligned}
 \tag{5.28}$$

Here iV_x and iV_y are the local vertices of the processes $1 \leftrightarrow 2$ and α is the symmetry factor. The contour integrations over internal points $x = (t_x, \vec{x})$ and $y = (t_y, \vec{y})$ cover the whole

space–time region, as dictated by the Lorentz invariance. It can be visualized by switching to the time-ordered diagrams (Schrödinger representation)

$$i\delta G(x_2, x_1) = \text{Diagram 1} + \text{Diagram 2} \quad (5.29)$$

Here in the first diagram, the integration region $t_x < t_y$ ($t_1 < t_x < t_y < t_2$) describes the time-process of the decay of the particle, being in the state 1, at $t = t_x$ into two intermediate particles in states 1' and 2', which then annihilate at the moment $t = t_y$ producing the particle in the state 2. In the second diagram in equation (5.29) the integration region $t_y < t_x$ ($t_1 < t_y < t_x < t_2$) corresponds to the process when three particles in states 1', 2' and 2 are created at $t = t_y$, two of which (1', 2') then annihilate at $t = t_x$ with the particle propagating in the state 1. Also, the Lorentz invariance requires to use the same vertices for the scattering and creation and annihilation processes (crossing symmetry). Generalization to more particles of different species is straightforward. For instance the particle 1,2 can be the zero sound and 1' and 2', a fermion and a fermion hole in case of the Fermi liquid.

For relativistic particles propagating in vacuum, the typical time interval between points x and y in diagrams in equation (5.29) is the Compton time $1/m$ since the free particle causal Green's function in coordinate representation [80] is $\propto e^{-m\tilde{x}}$ for $\tilde{x} \gg 1/m$, where $\tilde{x} = \sqrt{(\vec{x} - \vec{y})^2 - c^2(t_x - t_y)^2}$. With inclusion of the higher order processes or other types of interactions one deals with the dressed particle (describing by the dressed Green's function). The new typical time-scale characterizing the decay, $|t_x - t_y| \sim m/\Gamma$ (for relativistic bosons), can be seen from the formal replacement $m^2 \rightarrow m^2 - i\Gamma/2$. For the non-relativistic particle propagating in matter (the causal Green's function $\propto e^{-i(E_p + \Gamma)|t_x - t_y|}$) the typical time of the process is determined by its width computed through $\Gamma = -2 \text{Im} \Sigma^R(p_0, \vec{p})$, where $\Sigma^R(p_0, \vec{p})$ is the retarded self-energy in the Fourier representation. Thereby, in the latter case in the space–time picture the processes in equation (5.29) occur with the maximum probability in the time interval $|t_x - t_y| \sim 1/\Gamma$. Thus, advances of the virtual processes on a time-scale $\sim m/\Gamma$ (for relativistic boson excitations) and $\sim 1/\Gamma$ (for non-relativistic excitations) dictated by the Lorentz/Galilei invariance are in agreement with the time-energy uncertainty principle and do not contradict the quantum causality.

For the weakly non-ideal Bose gas of non-relativistic particles with mass m the spectrum of excitations (phonons) at very low temperatures is given by [121]

$$\omega(\vec{p}) = \sqrt{u^2 \vec{p}^2 + (\vec{p}^2/2m)^2}, \quad u = \sqrt{4\pi a n/m^2}, \quad (5.30)$$

where a is the scattering length, $n = N/V$ is the particle density. Inclusion of the loop-diagram to the excitation self-energy induces the excitation width $\Gamma = -2 \text{Im} \omega = dW/dt$ which corresponds to the decay of the excitation with the dispersion law (5.30) in two excitations with the same spectrum. The differential probability of the decay dW/dt can be determined with the help of the Fermi Golden rule,

$$\frac{dW}{dt} = 2\pi |H_{fi}|^2 \delta(E_f - E_i) \frac{V^2 d^3 q_1 d^3 q_2}{(2\pi)^6}, \quad (5.31)$$

where H_{fi} is the matrix element of the perturbation Hamiltonian and the excitation momenta are related as $\vec{p} = \vec{q}_1 + \vec{q}_2$. The calculation in [121] gives $\Gamma = \frac{3p^5}{320\pi m n}$. For the zero sound (boson excitation, here in relativistic kinematics) propagating in the cold Fermi liquid

the intermediate states in the loop diagram correspond to the fermion–fermion-hole and $\Gamma(p_0, \vec{p}) = (m^{*2} + \frac{1}{4}p^2) p_0/\pi|\vec{p}|$ describes the Landau damping of excitations in the space-like region, for $p_0 < |\vec{p}|v_F$, where v_F is the Fermi velocity, m^* is the effective fermion mass and the vertex in the loop-diagram is put to unity, see [122].

As the next example, consider the two-step process of the energetic proton scattering on a nucleus A with the creation of the positive pion, which propagating in vacuum decays then into the anti-muon, μ^+ and the muon neutrino: $p + A \rightarrow n + A + \pi^+$, $\pi^+ \rightarrow \mu^+ + \nu_\mu$. The characteristics of the process can be found, e.g., by computing the proton self-energy ‘+−’ diagram presented as

$$-i\Sigma_p^{+-}(y_2, y_1) = \text{Diagram} \quad (5.32)$$

where the stars indicate that the proton-to-neutron conversion takes place in the nucleus. In vacuum the Fourier transform of this self-energy, $\Sigma^{+-}(p)$, gives the probability of that the proton with momentum p being absorbed by the nucleus with radiation of the virtual pion flying far away from the nucleus in vacuum, before it decays to μ^+ and ν_μ . Here, the ‘++’ and ‘−−’ pion lines in (5.32) should include the $\mu^+\nu_\mu$ loop, otherwise the self-energy (5.32) would diverge. Thus, although appropriately normalized the vacuum pion width $\Gamma_{\pi\nu}$ of the reaction $\pi^+ \rightarrow \mu^+ + \nu_\mu$ is a tiny quantity, it should be consistently incorporated. Note that, if the process occurred in a nuclear medium, the full virtual pion ‘++’ and ‘−−’ Green’s functions would include also other processes. Nevertheless, the resulting cross-section remains $\propto \Gamma_{\pi\nu}$, mainly determined by the $\Sigma_{\mu\nu}^{+-}(x_2, x_1)$ loop-insertion. This is in line with our mechanical example considered above in section 2.2.1, where the radiation cross-section enters the factor $\Gamma_{\text{tot}}^2 B_{\text{rad}}^2 = \Gamma_{\text{rad}}^2$, see equation (2.89).

To consider the variety of the processes self-consistently one can use the Φ -derivable method, in which the reactions considered above are represented by diagrams

$$-i\Phi = \text{Diagram} + \dots, \quad (5.33)$$

where ellipses stand for the other seven diagrams with all possible combinations of ‘+ / −’ signs in the vertices. All Green’s functions here are full in the Φ -derivable sense, i.e. with the Φ constructed here up to two vertices. If we cut these diagrams through the proton ‘−+’ line

we get the proton self-energy (5.32). Cutting through the neutrino ‘+−’ line we obtain the neutrino self-energy

$$-i\Sigma_{\nu}^{-+}(x_1, x_2) = \text{Diagram} + \dots, \quad (5.34)$$

which in the momentum representation yields the neutrino production rate. For the sake of brevity we again show only one diagram out of four, which differ by the ‘+−’ signs in the y_1 and y_2 vertices. Note that only the shown diagram gives a non-vanishing contribution for the neutrino production on mass-shell in the two-step process under consideration.

The self-energy diagrams in terms of the non-equilibrium diagram technique are very convenient for calculations of reaction rates. It allows to keep explicitly self-consistent Kramers–Kronig relations between the real and imaginary parts of the retarded self-energy. This is in line with calculations of cross-sections in quantum mechanics, see section 4, with the help of the imaginary part of the forward scattering amplitude, i.e. by making use of the optical theorem. The closed diagram formalism formulated in terms of non-equilibrium Green’s functions can be found in [123]. The same reactions can be also considered within an ordinary Feynman diagram technique, via calculation of the squared matrix elements, provided one deals with the asymptotic states for the in-coming and out-going particles. The latter method is similar to the calculation of the cross-sections by angular integration of the squared scattering amplitude $|f(\theta)|^2$ in quantum mechanics, cf. the Born approximation.

Finally, we stress that existence of time delays and advances of the processes described by the diagrams in coordinate representation is purely the consequence of the Lorentz/Galilei invariance of the theory and does not depend on the specific technique used (equilibrium, non-equilibrium, closed diagram technique, calculation of probabilities of reactions via squared matrix elements, etc).

5.5. Typical time delays and advances

Equation (5.11) for classical fields is similar to that which we have considered in classical mechanics. Therefore at least in some specific cases the field dynamics is characterized by the same typical time-scales as we considered above in section 2. Moreover, within the obtained quantum field description there appear new typical time-scales for delays and advances.

- (i) Since we neglected short-range correlations one can no longer distinguish time effects on time-scale $t \lesssim t_{\text{int}}$ and spatial effects on space scale $x \lesssim x_{\text{int}} \sim ct_{\text{int}}$. Thus, we further consider a system at sufficiently large space–time scales only. Thereby, we assume that the typical time-scale of the processes under consideration obeys inequality

$$t \gg t_{\text{int}}. \quad (5.35)$$

Only then can the system be described in terms of the Feynman diagrams. The interaction time is of the order Λ_{int}/c , where Λ_{int} is the shortest distance at which we can use our interaction model and the chosen degrees of freedom.

- (ii) Some time-scales can be extracted right from expressions for the full single particle Green’s functions (G^{ij} for $i, j \in \{+, -\}$, if one uses the non-equilibrium diagram technique). Through the Dyson equations these Green’s functions are expressed in terms

of the self-energies Σ^{ij} . As we have mentioned, the equation for the retarded Green's function decouples from others and thus G^R is expressed via Σ^R .

Thus a relevant time-scale is the decay time $t_{\text{dec}} = 1/\Gamma$, provided non-relativistic kinematics is used, where Γ is the Fourier transform of $-2 \text{Im}\Sigma^R$, cf. equations (2.27), (3.203) and (4.21).

With the quantity A , where A is the Fourier transform of $-2 \text{Im}G^R$, is associated the scattering time delay $\delta t_s = A/2$ (for non-relativistic particles), as it has been introduced above, cf. equation (3.192), which in the virial limit is $\delta t_s = \frac{\partial \delta}{\partial E_p} = 2\pi \frac{dN^{\text{level}}}{dE_p}$, cf. equations (2.65), (2.66), (2.94), (4.22) and (4.29).

To demonstrate the existence of other relevant time-scales consider, as an example, a spatially uniform equilibrium high temperature gas of non-relativistic Wigner resonances (i.e., when $\Gamma_{\text{eq}} = -2 \text{Im}\Sigma_{\text{eq}}^R$ and $\text{Re}\Sigma_{\text{eq}}^R$, being Fourier transformed to the energy–momentum space, do not depend on p_0 on relevant energy–momentum scales). In the mixed time–momentum representation

$$G(t_1 - t_2, \vec{p}) = \int \frac{d p_0}{2\pi} G(p_0, \vec{p}) e^{-i p_0(t_1 - t_2)} \quad (5.36)$$

and the retarded Green's function is explicitly given by

$$G_{\text{eq}}^R(t_1 - t_2, \vec{p}) = -i e^{-i E_p(t_1 - t_2) - \frac{1}{2} \Gamma_{\text{eq}}(t_1 - t_2)} \quad \text{for } t_1 > t_2; \quad (5.37)$$

$G^R = 0$ for $t_1 < t_2$, $E_p = E_p^0 + \text{Re}\Sigma_{\text{eq}}^R$, $E_p^0 = \frac{p^2}{2m}$, cf. equation (3.214). Using the Kubo–Schwinger–Martin relation [24] for the Fourier transformed equilibrium Green's functions, $F_{\text{eq}}(p_0, \vec{p}) = A_{\text{eq}}(p_0, \vec{p}) f_{\text{eq}}(p_0, \vec{p})$ in the mixed representation we find

$$\begin{aligned} F_{\text{eq}}(t_1 - t_2, \vec{p}) &= \int \frac{d p_0}{2\pi} A_{\text{eq}}(p_0, \vec{p}) f_{\text{eq}}^{\text{Bol}}(p_0, \vec{p}) e^{-i p_0(t_1 - t_2)} \\ &= e^{\frac{\mu}{T} - i E_p(t_1 - t_2 - \delta t_s^T) - \frac{1}{2} \Gamma_{\text{eq}}(t_1 - t_2 - \delta t_{\text{col}}^T)}. \end{aligned} \quad (5.38)$$

Here A_{eq} is the spectral function for equilibrium system, $f_{\text{eq}}^{\text{Bol}} = e^{(\mu - p_0)/T}$ is the equilibrium Boltzmann distribution function, μ is the chemical potential determined by the total number of particles N . The new time-scales are

$$\delta t_s^T = \frac{\Gamma_{\text{eq}}}{2 E_p T}, \quad \delta t_{\text{col}}^T = -\frac{2 E_p}{\Gamma_{\text{eq}} T}. \quad (5.39)$$

The value δt_s^T shows a scattering delay time and δt_{col}^T is the collision advancement time for equilibrium processes. For typical energies $E_p \sim T$, $\delta t_{\text{col}}^T \sim -1/\Gamma_{\text{eq}}$. Thus the latter quantity demonstrates an advance of particles of thermal energies compared to particles being at rest. Note that in subsection 5.4 we demonstrated a principle possibility of time advances $\sim 1/\Gamma$ (being there of the order $1/\Gamma_{\pi\nu}$). Here, such an advance is shown to arise for averaged values of the particle energies.

- (iii) Since integration over z in equation (5.20) in intermediate reaction states includes all times $-\infty < t_z < \infty$, for $t_y < t_z < t_x$ the process that occurs at t_z is delayed compared to that which occurs at t_y , and for $t_z < t_y < t_x$ the process which occurs at t_z is advanced compared to that which occurs at t_y . Both time processes should be incorporated as dictated by the Lorentz invariance, cf. the discussion in the previous subsection. In figure 15 we demonstrate an example of a time delay (a) and an advancement (b) in the specific two-step processes $p \rightarrow n + X + \pi_{\text{virt}}^+$, $\pi_{\text{virt}}^+ \rightarrow \nu_\mu + \mu^+$, considered in the previous subsection in terms of a closed self-energy diagram. Such processes play an important role in the recent neutrino OPERA experiment [41]. Let the life-time of the off-mass-shell pion produced in the process $p \rightarrow n + X + \pi_{\text{virt}}^+$ be $t_{N\pi}^{\text{dec}} = 1/\Gamma_{N\pi}$ and in the process $\pi_{\text{virt}}^+ \rightarrow \nu_\mu + \mu^+$, $t_{\pi\nu}^{\text{dec}} = 1/\Gamma_{\pi\nu}$. The time $t_{\nu}^{\text{dec}} = t_{N\pi}^{\text{dec}} + t_{\pi\nu}^{\text{dec}}$ characterizes the duration of the full two-step

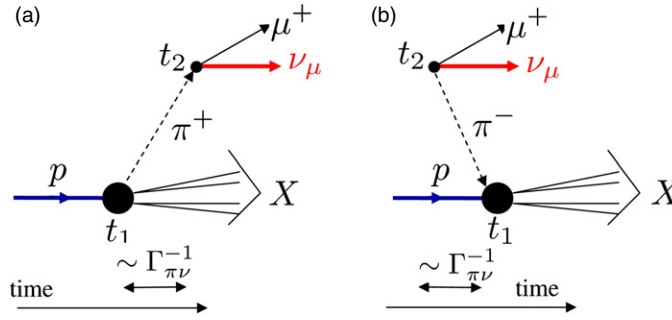


Figure 15. A graphical representation of the two-step processes $p \rightarrow n + X + \pi_{\text{virt}}^+, \pi_{\text{virt}}^+ \rightarrow \nu + \mu^+$, as they occur in the neutrino experiment of the OPERA group [41].

process. This means that virtual pions, being produced in the process $p \rightarrow n + X + \pi_{\text{virt}}^+$, undergo in the subsequent process $\pi_{\text{virt}}^+ \rightarrow \nu_{\mu} + \mu^+$ time delays and advances on a time-scale $-t_{\pi\nu}^{\text{dec}} \lesssim t_2 - t_1 \lesssim t_{\pi\nu}^{\text{dec}}$, where t_2 characterizes the act of the production of ν_{μ} and t_1 , of the absorption of p . Note that $t_{N\pi}^{\text{dec}} \ll t_{\pi\nu}^{\text{dec}}$.

The uncertainty in the production time reflects also the fact that a system undergoing some transition to a new state (e.g., a decay process) does not have the certain energy and is described in quantum mechanics by a wave packet of a finite width. The corresponding time-scale is obviously of the order of $1/\Gamma$, where Γ is the width; cf. equation (3.140). (Here we once more stress that for relativistic bosons the value $\Gamma = -2 \text{Im}\Sigma^R$ has dimensionality of m^2 and should be still appropriately normalized to get the meaning of the particle width.)

- (iv) One may yet introduce another time-scale, similarly to that which we have introduced in classical and quantum mechanical descriptions. For example, for a (1 + 1)-dimensional problem the quantity

$$t_{\text{soj}}^{(\text{1D})}(a, b; \tau) = \int_0^\tau dt \int_a^b dz F^{(\text{1D})}(t, z; t, z) / \int dz F^{(\text{1D})}(t, z; t, z) \quad (5.40)$$

is similar to that given by equation (2.3) and (3.92), and for 3 + 1 theory,

$$t_{\text{soj}}(\tau) = \int_0^\tau dt \int d^3r F(t, \vec{r}; t, \vec{r}) / \int d^3r F(t, \vec{r}; t, \vec{r}) \quad (5.41)$$

is similar to that given by equations (2.15) and (4.13).

6. Time shifts in quantum kinetics

6.1. Wigner transformation and gradient expansion

Consider slightly inhomogeneous and slowly evolving systems. Then in the spirit of the semiclassical approximation degrees of freedom can be subdivided into rapid and short-ranged, and slow and long-ranged. For any two-point function $\mathcal{F}(x, y)$, one may introduce the variable $\xi = (t_1 - t_2, \vec{r}_1 - \vec{r}_2)$, which relates to rapid and short-ranged microscopic processes, and the variable $X = \frac{1}{2}(t_1 + t_2, \vec{r}_1 + \vec{r}_2)$, which refers to slow and long-ranged collective motions. The Wigner transformation [124], i.e., the Fourier transformation in $\xi = x - y$ to 4-momentum p , leads to $\mathcal{F}(X, p)$ functions. Since the Wigner transformation is defined for physical time-space coordinates rather than for contour coordinates one has to decompose the contour integrations into the time-ordered $\{-\}$ and the anti-time-ordered $\{+\}$ branches.

Two-point functions then become matrices of the contour decomposed $\{-+\}$ components with physical space–time arguments. Thus

$$\mathcal{F}^{ij}(X, p) = \int d\xi e^{ip\xi} \mathcal{F}^{ij}\left(X + \frac{\xi}{2}, X - \frac{\xi}{2}\right), \quad i, j \in \{-+\} \quad (6.1)$$

leads to a 4-phase-space representation of two-point functions.

The Wigner transformation of the Dyson equation (5.20) is straightforward. Taking the difference and half-sum of the Dyson equation (5.20) and the corresponding adjoint equation after the Wigner transformation we arrive at equations

$$iv_\mu \partial_X^\mu G^{ij}(X, p) = \int d\xi e^{ip\xi} \int_C dz (\Sigma(x^i, z)G(z, y^j) - G(x^i, z)\Sigma(z, y^j)), \quad (6.2)$$

$$\widehat{Q}_X G^{ij}(X, p) = \sigma^{ij} + \frac{1}{2} \int d\xi e^{ip\xi} \int_C dz (\Sigma(x^i, z)G(z, y^j) + G(x^i, z)\Sigma(z, y^j)), \quad (6.3)$$

where σ^{ij} accounts for the integration sense on the two contour branches, cf. equation (5.9). For non-relativistic kinematics $v^\mu = (1, \vec{p}/m)$ and $\widehat{Q}_X = p_0 - \vec{p}^2/2m - \partial_X^2/8m$. In this matrix notation, two of equations (6.2) and (6.3), involving G^{-+} and G^{+-} on the left-hand side, are known as Kadanoff–Baym (KB) equations in the Wigner representation [24]. Particular combinations of these equations lead to the retarded and advanced equations, which completely decouple and involve only integrations over physical times rather than contour times.

We will solely deal with the gradient approximation for slow collective motions by performing the gradient expansion of equations (6.2) and (6.3). This step preserves all the invariances of the Φ functional in a Φ -derivable approximation [35]. Within the gradient expansion the Wigner transformation of a convolution of two two-point functions entering the Dyson equations (6.3), (6.2) is given by

$$\int d\xi e^{ip\xi} \left(\int dz f(x, z)\varphi(z, y) \right) \approx f(X, p)\varphi(X, p) + \frac{i\hbar}{2} \{f(X, p), \varphi(X, p)\}, \quad (6.4)$$

where

$$\{f(X, p), \varphi(X, p)\} = \frac{\partial f}{\partial p^\mu} \frac{\partial \varphi}{\partial X_\mu} - \frac{\partial f}{\partial X^\mu} \frac{\partial \varphi}{\partial p_\mu} \quad (6.5)$$

is the Poisson bracket in covariant notation. Note that the smallness of the $\hbar \partial_X \cdot \partial_p$ comes solely from the smallness of space–time gradients ∂_X , while momentum derivatives ∂_p are not assumed to be small. Such a description is meaningful only if the typical time and space scales are large compared to microscopic ones $|t_i - t_j| \sim t_{\text{mic}} \sim (1/E_F, 1/E_T)$, $|\vec{r}_i - \vec{r}_j| \sim r_{\text{mic}} \sim (1/p_F, 1/p_T)$ (for the low energy excitations in the Fermi system and for the Boltzmann gas, respectively, where index F labels the Fermi quantity and T, the thermal one).

6.2. Three forms of the quantum kinetic equation

Only two real functions of all $G^{ij}(X, p)$ are required for a complete description of the system’s evolution [35]. For these real functions it is convenient to use the Wigner density $F(X, p) = (\mp) iG^{-+}(X, p)$ and the spectral function $A(X, p)$. The kinetic equation for off-shell particles is ordinarily presented in two different forms: in the KB form, i.e. as it follows right after the first-order gradient expansion in the Dyson equation for the Wigner density [24],

$$\widehat{D}F(X, p) - \{\Gamma_{\text{in}}(X, p), \text{Re} G^R(X, p)\} = C(X, p), \quad (6.6)$$

and in the Botermans–Malfliet (BM) form [32]; see the discussion of these aspects in [35]. Similarly the kinetic equation can be written for $\tilde{F}(X, p) \equiv iG^{+-}(X, p)$. The collision term

$$C(X, p) = \Gamma^{\text{in}}(X, p) \tilde{F}(X, p) - \Gamma^{\text{out}}(X, p) F(X, p) \quad (6.7)$$

is the difference of the gain and loss terms, $\Gamma^{\text{in}}(X, p) = \mp i\Sigma^{-+}(X, p)$ (in the co-variant notations of [35]) is the reduced production (gain) source term, $\Gamma^{\text{out}}(X, p) = i\Sigma^{+-}(X, p)$ is the reduced absorption (loss) term. The differential drift operator is defined as

$$\widehat{D}(\dots) = \{\text{Re}[G^{-1}(X, p)], \dots\} = Z_{\mu}^{-1}(X, p) \frac{\partial}{\partial X_{\mu}} + \frac{\partial \text{Re}\Sigma^R(X, p)}{\partial X^{\mu}} \frac{\partial}{\partial p_{\mu}}, \quad (6.8)$$

with

$$Z_{\mu}^{-1}(X, p) = \frac{\partial}{\partial p^{\mu}} \text{Re}[G^{-1}(X, p)] = v_{\mu} - \frac{\partial \text{Re}\Sigma^R(X, p)}{\partial p^{\mu}}, \quad v^{\mu} = \frac{\partial}{\partial p_{\mu}} G_0^{-1}(p). \quad (6.9)$$

Here $G_0^{-1}(p)$ is the Fourier transform of the inverse free Green’s function (5.5):

$$G_0^{-1} = \begin{cases} p^2 - m^2 & \text{for relativistic bosons,} \\ p_0 - \vec{p}^2/(2m) & \text{for non-rel. particles,} \end{cases} \quad (6.10)$$

m is the mass of the free particle. The BM form is obtained from the KB equation, if one puts $\Gamma^{\text{in}}(X, p) = \Gamma(X, p)F(X, p)/A(X, p)$ in the Poisson-bracket term. This replacement is legitimate, if one assumes only small (the first gradient order) deviations from the local or global equilibrium (in the local and global equilibrium the collision term $C(X, p) = 0$). Then the BM form differs from the KB form only in the second order of the gradient expansion (more precisely in the first-order gradient times the first-order deviation from equilibrium), see [35] for details. At first glance these equations are equivalent in their common region of validity. However the KB equation has still one important advantage. It fulfils the conservation laws of the Noether 4-current and of the Noether energy–momentum exactly [36, 37] provided self-consistent, i.e., Φ derivable approximations are used, whereas the BM form fulfils the conservation laws only approximately (up to zero gradients). Moreover the KB equation can be applied not only to the description of the relaxation of the system toward the local equilibrium but in many other problems in which the BM form is not applicable.

The third, non-local, form of the kinetic equation was introduced in [40]:

$$\begin{aligned} \widehat{D}F(X, p) - \left\{ \Gamma(X, p) \frac{F(X, p)}{A(X, p)}, \text{Re} G^R(X, p) \right\} &= C^{\text{NL}}(X, p) \\ &= \left(1 + \left\{ \frac{1}{A(X, p)}, \text{Re} G^R(X, p) \right\} \right) C^{\text{shift}}(X, p), \\ C^{\text{shift}}(X, p) &= C(X^{\mu} - \delta X^{\mu}, p^{\mu} - \delta p^{\mu}), \\ \delta X^{\mu} &= \frac{1}{A(X, p)} \frac{\partial \text{Re} G^R(X, p)}{\partial p_{\mu}}, \quad \delta p^{\mu} = -\frac{1}{A(X, p)} \frac{\partial \text{Re} G^R(X, p)}{\partial X_{\mu}}. \end{aligned} \quad (6.11)$$

If we replace $C^{\text{NL}}(X, p) \rightarrow C(X, p)$ we obtain the BM form. If we expand $C^{\text{NL}}(X, p)$ up to first gradient terms we arrive at the KB equation. Thus equation (6.11) coincides with the BM form up to the first-order gradients and with the KB equation up to second-order gradients.

The retarded Green’s function is

$$G^R(X, p) = \frac{1}{M(X, p) + i\Gamma(X, p)/2} + O(\partial_X^2) \quad (6.12)$$

and

$$A(X, p) \equiv -2 \text{Im} G^R(X, p) \simeq \frac{\Gamma(X, p)}{M^2(X, p) + \frac{1}{4}\Gamma^2(X, p)} \quad (6.13)$$

is the spectral function with the ‘mass’ function and the width given by

$$M(X, p) = G_0^{-1}(p) - \text{Re}\Sigma^R(X, p), \quad \Gamma(X, p) \equiv -2 \text{Im}\Sigma^R(X, p) = \Gamma^{\text{out}}(X, p) \pm \Gamma^{\text{in}}(X, p), \quad (6.14)$$

cf. the introduced above definitions (5.27) and (5.26). We see that expression (6.13) has the same resonance form, as equations (2.65), (2.66) in the mechanical example considered in section 2, as equation (2.94) in the classic-electrodynamical example and as equation (3.206) in the quantum mechanical example considered in section 3. Although the solution (6.12), (6.13) is simply algebraic, it is valid up to first-order gradients.

To simplify the further consideration we imply that in the relativistic case separation of particle and antiparticle degrees of freedom is performed. Therefore, below we deal with particle species. Antiparticle quantities can be introduced similarly.

In equation (6.11) the Wigner densities can be presented as

$$F(X, p) = A(X, p)f(X, p), \quad \tilde{F}(X, p) = A(X, p)(1 \mp f(X, p)), \quad (6.15)$$

where $f(X, p)$ is a new generalized distribution function. In a local equilibrium this function takes the form

$$f_{\text{1.eq}}(X, p) = \frac{1}{e^{[p_\mu u^\mu(X) - \mu(X)]/T(X)} \pm 1}, \quad (6.16)$$

where $u^\mu(X) = (1, \vec{u}(X))/\sqrt{1 - \vec{u}^2(X)}$ and $\vec{u}(X)$ is the local velocity of a tiny element of the system. This distribution turns the collision term to zero.

Using equation (6.15) we are able to derive another form of the non-local kinetic equation (6.11):

$$\frac{1}{2}A^2(X, p)\Gamma(X, p)\left(\widehat{D}f(X, p) - \frac{M(X, p)}{\Gamma(X, p)}\{\Gamma(X, p), f(X, p)\}\right) = A(X, p)C^{\text{shift}}(X, p),$$

$$C^{\text{shift}}(X, p) = \frac{C^{\text{shift}}(X, p)}{A^{\text{shift}}(X, p)}, \quad A^{\text{shift}}(X, p) = A(X^\mu - \delta X^\mu, p^\mu - \delta p^\mu). \quad (6.17)$$

Equation (6.17) up to the second-order gradients coincides with the KB equation and up to the first-order gradients coincides with the BM form, cf. the kinetic equation in the BM form, equation (3.28) in [35]. Note that besides the non-locality introduced by the shift of variables, C^{shift} and C may still include memory effects, if the generating 2PI Φ functional contains diagrams with more than two vertices.

The key point which we want further to focus on is the variable shift in the collision term

$$\delta X^\mu(X, p) \equiv (\delta t_f^{\text{kin}}, \delta \vec{r}_f) = \frac{1}{A(X, p)} \frac{\partial \text{Re} G^R(X, p)}{\partial p_\mu} = \frac{1}{2}B^\mu(X, p) - \frac{Z^{-1, \mu}(X, p)}{\Gamma(X, p)},$$

$$\delta p^\mu(X, p) = -\frac{1}{A(X, p)} \frac{\partial \text{Re} G^R(X, p)}{\partial X_\mu}, \quad (6.18)$$

where

$$B^\mu(X, p) = (B_0(X, p), B_0(X, p)\vec{v}_{\text{gr}}(X, p)) = -2 \text{Im} \left[\left(v^\mu - \frac{\partial \text{Re}\Sigma^R(X, p)}{\partial p_\mu} \right) G^R(X, p) \right]$$

$$= A(X, p) \left[v^\mu - \frac{\partial \text{Re}\Sigma^R(X, p)}{\partial p_\mu} - \frac{M(X, p)}{\Gamma(X, p)} \frac{\partial \Gamma(X, p)}{\partial p_\mu} \right] \quad (6.19)$$

is a flow spectral function and

$$\vec{v}_{\text{gr}}(X, p) = \frac{\vec{v} + \frac{\partial \text{Re}\Sigma^R(X, p)}{\partial \vec{p}} + \frac{M(X, p)}{\Gamma(X, p)} \frac{\partial \Gamma(X, p)}{\partial \vec{p}}}{v^0 - \frac{\partial \text{Re}\Sigma^R(X, p)}{\partial p_0} - \frac{M(X, p)}{\Gamma(X, p)} \frac{\partial \Gamma(X, p)}{\partial p_0}} \quad (6.20)$$

has the meaning of a generalized group velocity of off-mass-shell particles, see [125]. The latter quantity generalizes the expression for the energy p_0 -integrated transport velocity introduced in [126] and applied for localization phenomena and resonance scattering.

The non-local kinetic equation (6.17) can be rewritten in a more convenient form

$$A_S^\mu(X, p) \frac{\partial f(X, p)}{\partial X^\mu} + A(X, p) \left[\frac{\partial \text{Re}\Sigma^R(X, p)}{\partial X_\mu} - \frac{\Gamma(X, p)}{A(X, p)} \frac{\partial \text{Re}G^R(X, p)}{\partial X_\mu} \right] \frac{\partial f(X, p)}{\partial p^\mu} = A(X, p) \mathcal{C}^{\text{shift}}(X, p). \quad (6.21)$$

This will be the key equation for our further study. Here

$$A_S^\mu(X, p) = \frac{1}{2} A(X, p) \Gamma(X, p) B^\mu(X, p). \quad (6.22)$$

The first term on the left-hand side of equation (6.21) is the entropy drift term, the second term relates to the spatial changes of a mean field. Dropping in equation (6.21) 4-phase-space delays/advances in the collision term, i.e. replacing $\mathcal{C}^{\text{shift}}(X, p) \rightarrow \mathcal{C}(X, p) = C(X, p)/A(X, p)$, we arrive at the BM form of the kinetic equation. In the latter case $A_S^\mu(X, p)$ is the BM Markovian (BMM) entropy flow spectral function (memory effects are ignored) relating to the entropy flow associated with the BM form of the kinetic equation [35]:

$$S_{\text{BMM}}^\mu(X) = \text{Tr} \int \frac{d^4 p}{(2\pi)^4} A_S^\mu(X, p) \sigma(X, p), \quad (6.23)$$

where

$$\sigma(X, p) = \mp(1 \mp f(X, p)) \ln(1 \mp f(X, p)) - f(X, p) \ln f(X, p), \quad (6.24)$$

satisfying the equation of motion

$$\frac{\partial}{\partial X^\mu} S_{\text{BMM}}^\mu(X) = -H(X) = \text{Tr} \int \frac{d^4 p}{(2\pi)^4} \ln \frac{1 \mp f(X, p)}{f(X, p)} C(X, p). \quad (6.25)$$

The symbol Tr implies summation over internal degrees of freedom like spin, etc.

It is easy to demonstrate that the kinetic equation in the BM form conserves the BM effective current exactly [37, 39]

$$j_S^\mu(X) = e \text{Tr} \int \frac{d^4 p}{(2\pi)^4} A_S^\mu(X, p) f(X, p), \quad (6.26)$$

provided we work within the Φ -derivable approximation scheme, whereas the Noether current

$$j_{\text{Noether}}^\mu(X) = e \text{Tr} \int \frac{d^4 p}{(2\pi)^4} v^\mu A(X, p) f(X, p) \quad (6.27)$$

and the effective B -current

$$j_B^\mu(X) = e \text{Tr} \int \frac{d^4 p}{(2\pi)^4} B^\mu(X, p) f(X, p) \quad (6.28)$$

are conserved approximately (up to zero gradient order). Here e is the (electric, baryon or other) charge of the species and summation over the species, if necessary, is implied.

The maxima in the flow $A_S^\mu(X, p)$, the flow $B^\mu(X, p)$ and $v^\mu A(X, p)$ are shifted relatively to each other in the energy–momentum space. The difference of (6.26) and (6.28) to the Noether current (6.27) is that the former two quantities contain contributions of the drag and back flows. The drag flow is associated with the term $-\frac{\partial \text{Re}\Sigma^R}{\partial p_\mu} A$ and the back flow, with $-\frac{M}{\Gamma} \frac{\partial \Gamma}{\partial p_\mu} A$ in the B^μ spectral function (6.19). The presence of these terms causes some additional delays and advances in the propagation of dressed off-shell particles.

The expressions for currents (6.26)–(6.28) are derived from the simple form of the 2PI-generating Φ functional. As soon as the Φ functional includes diagrams with more than two

vertices, there appears an additional term in the currents—a so-called memory current j_{mem}^μ , see equation (6.42) below, and, if the interaction contains derivative couplings, there is yet another ‘derivative’ current term j_{der}^μ . The same relates also to the entropy flow.

If we expand C^{shift} in (6.17) up to the first gradients as

$$A(X, p) C^{\text{shift}}(X, p) = A(X, p) (\Gamma_{\text{shift}}^{\text{in}}(X, p) - \Gamma_{\text{shift}}(X, p) f^{\text{shift}}(X, p)) \\ \simeq C(X, p) + \{\Gamma^{\text{in}}(X, p) - \Gamma(X, p) f(X, p), \text{Re } G^R(X, p)\}, \quad (6.29)$$

we arrive at the generalized kinetic equation in the KB form for the distribution function $f(X, p)$:

$$A(X, p) \widehat{D}f(X, p) + f(X, p) \{\Gamma(X, p), \text{Re } G(X, p)\} - \{\Gamma^{\text{in}}(X, p), \text{Re } G(X, p)\} = C(X, p), \quad (6.30)$$

where the collision term

$$C(X, p) = A(X, p) \Gamma^{\text{in}}(X, p) - A(X, p) \Gamma(X, p) f(X, p), \\ A(X, p) \widehat{D} = \widetilde{B}^\mu(X, p) \frac{\partial}{\partial X_\mu} + A(X, p) \frac{\partial \text{Re } \Sigma^R(X, p)}{\partial X^\mu} \frac{\partial}{\partial p_\mu}, \quad (6.31)$$

$$\widetilde{B}^\mu(X, p) = (A(X, p) Z_0^{-1}(X, p), A(X, p) Z_0^{-1}(X, p) \vec{v}_{\text{gr}}(X, p)), \quad (6.32)$$

and the generalized group velocity

$$\vec{v}_{\text{gr}}^i(X, p) = \frac{Z^{-1,i}(X, p)}{Z_0^{-1}(X, p)} = \frac{v^i + \frac{\partial \text{Re } \Sigma^R(X, p)}{\partial p^i}}{v^0 - \frac{\partial \text{Re } \Sigma^R(X, p)}{\partial p_0}}, \quad i = 1, 2, 3, \quad (6.33)$$

differ from the quantities introduced with the help of equations (6.19), (6.20). Recall that $v_0 = 1$ for non-relativistic particles and $2p_0$ for relativistic bosons. The BM form is obtained after replacement $\Gamma^{\text{in}}(X, p) = \Gamma(X, p) f(X, p) + O(\partial_x)$ in the second Poisson bracket in (6.30). The KB equation (6.30) exactly conserves the Noether current (6.27), provided approximations are Φ -derivable [36, 37] and it approximately (up to zero-gradient order) conserves the effective current (6.26) and the effective current (6.28).

Note that, since for off-mass-shell particles p_0 and \vec{p} can vary independently, the value $\vec{v}_{\text{gr}}(X, p)$ is not necessarily limited from the above by the velocity of light, it might be even not positively definite. Also, the factor $Z_0^{-1}(X, p)$ is not, in general, positively definite which leads to a non-trivial procedure of the particle–antiparticle separation for virtual particles. As known [127], in the quasiparticle limit $Z_0^{\text{qp}}(X, p_0(\vec{p}), \vec{p}) > 0$ determines the quasiparticle spectrum branches and the branches with $Z_0^{\text{qp}} < 0$ are related to the anti-quasiparticles after the replacement $p_0 \rightarrow -p_0$ and $\vec{p} \rightarrow -\vec{p}$. To be specific, we will further assume $Z_0^{-1} > 0$, considering only the particle and not the anti-particles.

The spectral functions A, B_0, A_S^0 fulfil sum-rules⁹

$$\int B_0(X, p) \frac{dp_0}{2\pi} = \int v^0 A(X, p) \frac{dp_0}{2\pi} = \int A_S^0(X, p) \frac{dp_0}{2\pi} = 1; \quad (6.34)$$

cf. the sum-rules (2.32), (2.67) and (3.185), (3.195), which we obtained in classical and quantum mechanics. Note that the sum-rule for $A(x, p)$ follows directly from the canonical equal-time (anti-)commutator relations for (fermionic) bosonic field operators.

Having at hand the kinetic equation for $F(X, p)$ (either in KB or in BM form) and the algebraic equation for A is sufficient to recover all kinetic quantities. However there exists still

⁹ Generally speaking, the sum-rules presented in such a form hold for non-relativistic particles and for relativistic neutral bosons. In the former case the integration goes from $-\infty$ to ∞ , in the latter case from 0 to ∞ . Otherwise, antiparticle terms are not decoupled.

one more equation, the so-called mass-shell equation [35], which, as well as the KB equation (6.30), follows from the full Dyson equations expanded up to the first gradient order:

$$M(X, p) A(X, p) f(X, p) - \text{Re } G^R(X, p) \Gamma^{\text{in}}(X, p) = \frac{1}{4} \{ \Gamma(X, p), f(X, p) A(X, p) \} - \frac{1}{4} \{ \Gamma^{\text{in}}(X, p), A(X, p) \}. \quad (6.35)$$

Presenting $\Gamma^{\text{in}}(X, p) = f(X, p) \Gamma(X, p) + \delta \Gamma^{\text{in}}(X, p)$, $\Gamma^{\text{out}}(X, p) = (1 \mp f(X, p)) \Gamma(X, p) + \delta \Gamma^{\text{out}}(X, p)$, such that in equilibrium $\delta \Gamma_{\text{eq}}^{\text{in}}(X, p) = \delta \Gamma_{\text{eq}}^{\text{out}}(X, p) = 0$, and using equation (6.14), from (6.35) we find

$$\delta \Gamma^{\text{in}}(X, p) = \frac{1}{4 \text{Re } G^R(X, p)} \{ f(X, p), A(X, p) \Gamma(X, p) \} + O(\partial_x^2) = \mp \delta \Gamma^{\text{out}}(X, p). \quad (6.36)$$

Generally speaking the mass-shell equation should be considered on equal footing with the kinetic equation. [35] proved equivalence of this equation to the kinetic equation in the BM form up to first gradients. However in the general case equivalence of (6.35) and the KB equation (6.30) is not proven.

6.3. Memory effects

A general treatment of the memory effects is a cumbersome task. Following [35], as an example, consider a system of non-relativistic fermions interacting via contact two-body potential V_0 . The self-energy up to three-vertex diagram becomes

$$-i\Sigma = -i \left(\Sigma^{(1)} + \Sigma^{(2)} + \Sigma^{(3)} \right) = \text{diagram 1} + \text{diagram 2} + \text{diagram 3}. \quad (6.37)$$

The local part of the collision term is presented in the form

$$C^{(2)} + C_{\text{loc}}^{(3)} = d^2 \int \frac{d^4 p_1}{(2\pi)^4} \frac{d^4 p_2}{(2\pi)^4} \frac{d^4 p_3}{(2\pi)^4} \left(\left| \text{diagram 1} + \text{diagram 2} \right|^2 - \left| \text{diagram 3} \right|^2 \right) \times (2\pi)^4 \delta^4(p + p_1 - p_2 - p_3) \left(F_2 F_3 \tilde{F} \tilde{F}_1 - \tilde{F}_2 \tilde{F}_3 F F_1 \right), \quad (6.38)$$

where all the vertices in the off-shell scattering amplitudes are of the same sign, say ‘-’ for definiteness, i.e. there are no ‘+-’ and ‘-+’ Green’s functions left, d accounts for summation over internal degrees of freedom, e.g. spin. Now the collision term contains a *non-local* part due to the last diagram (6.37).

The current and the entropy flows are expressed in terms of the loop functions

$$L^{jk}(x, y) = \text{diagram}$$

which in the Wigner representation take the form

$$L^{jk}(X, p) = \int \frac{d^4 p'}{(2\pi)^4} \tilde{L}^{jk}(X, p' + p, p'), \quad (6.39)$$

where

$$\tilde{L}^{jk}(X, p' + p, p') = \text{div}_0 iG^{jk}(X, p' + p) iG^{kj}(X, p'). \quad (6.40)$$

The first-order-gradient memory correction to the collision term induced by the third graph (6.37) is

$$\begin{aligned} C_{\text{mem}}^{(3)}(X, p) &= [\Sigma_{+-, \text{mem}}^{(3)}(X, p) G^{-+}(X, p) - G^{+-}(X, p) \Sigma_{-+}^{(3), \text{mem}}(X, p)] \\ &= \frac{i}{2} \int \frac{d^4 p'}{(2\pi)^4} \frac{1}{d} [\tilde{L}^{+-}(X, p' + p, p) - \tilde{L}^{-+}(X, p' + p, p)] \\ &\quad \times \{L^{+-}(X, p'), L^{-+}(X, p')\}_{p', X}. \end{aligned} \quad (6.41)$$

The memory current follows from integration of (6.41):

$$j_{\text{mem}}^\mu(X) = e \int \frac{d^4 p}{(2\pi)^4} \frac{i}{2} L^{+-}(X, p) L^{-+}(X, p) \frac{\partial}{\partial p_\mu} (L^{+-}(X, p) + L^{-+}(X, p)). \quad (6.42)$$

The expression for the entropy flow is more cumbersome but it simplifies in the case of the local equilibrium:

$$[S_{\text{mem}}^\mu(X)]_{\text{l.eq}} = \int \frac{d^4 p}{(2\pi)^4} \frac{i}{2} L^{-+}(X, p) L^{+-}(X, p) \left[\ln \frac{L^{+-}(X, p)}{L^{-+}(X, p)} - 1 \right] \frac{\partial L^{-+}(X, p)}{\partial p_\mu}. \quad (6.43)$$

6.4. Positive definiteness of kinetic quantities

In contrast with a purely quantum case considered above in section 3, in the semiclassical approximation the Wigner distributions $F(X, p)$ and $\tilde{F}(X, p)$ prove to be positively semi-definite [35]. To show this we first integrate over a large space–time volume. Using the operator definition for the Green's functions (5.17) we arrive at

$$\int dX F(X, p) = \left\langle \left(\int dy e^{ipy} \hat{\phi}^\dagger(y) \right) \left(\int dx e^{-ipx} \hat{\phi}(x) \right) \right\rangle \geq 0, \quad (6.44)$$

and likewise for self-energies Σ expressed through the current–current correlator. Thus, we get constraints

$$\int dX \tilde{F}(X, p) \geq 0, \quad \int dX F(X, p) \geq 0, \quad \int dX \Gamma^{\text{out}}(X, p) \geq 0, \quad \int dX \Gamma^{\text{in}}(X, p) \geq 0. \quad (6.45)$$

Similar relations are obtained for the integration over 4-momentum space rather than space and time. As a result, in stationary and spatially homogeneous systems, in particular in equilibrium systems, the quantities F , \tilde{F} , Γ^{out} and Γ^{in} are real and non-negative, i.e.

$$F(p) \geq 0, \quad \tilde{F}(p) \geq 0; \quad \Gamma^{\text{out}}(p) \geq 0, \quad \Gamma^{\text{in}}(p) \geq 0. \quad (6.46)$$

In deriving constraints (6.45) and (6.46) one uses the operator picture rather than the Dyson equation for the Green's functions. Any approximation, in particular if formulated in the space of Green's functions, may spoil such rigorous statements like (6.44). Still both the Φ -derivable scheme and the gradient approximation preserve the retarded relations among the different contour components and the retarded and advanced functions of any contour function, with definite values for the imaginary parts of the corresponding retarded Wigner functions

$$A(X, p) \geq 0, \quad \Gamma(X, p) \geq 0, \quad (6.47)$$

which even hold locally. In particular, solution (6.12) for the retarded Green's function shows that all retarded relations hold locally, treating the momentum part as in the homogeneous

case and considering the space–time coordinate X as a parameter. Close to equilibrium, i.e. for $|C| \ll \Gamma^{\text{in}}A$ and $|C| \ll \Gamma^{\text{out}}A$, one finds that

$$\Gamma^{\text{out}}(X, p) \approx f\Gamma(X, p) > 0 \quad \Gamma^{\text{in}}(X, p) \approx (1 \mp f)\Gamma(X, p) > 0, \quad (6.48)$$

as long as the Wigner densities F and \tilde{F} are non-negative. As the gradient approximation is a quasi-homogeneous approximation, one may therefore expect the positivity of Γ^{in} and Γ^{out} even to be preserved in the here-discussed self-consistent treatment. Also diagrammatic rules may corroborate this, since the diagrams for Γ^{in} and Γ^{out} are calculated, as in the homogeneous case.

6.5. Time advances and delays

It is rather natural to expect that the time and the position characterizing collisions of propagating particles undergo some shifts, if one incorporates the fact that collisions are not instant. In accordance with the uncertainty principle and the ergodicity the energy and the momentum are shifted as well. This is taken into account in the non-local form of the kinetic equations (6.11), (6.17); see also equation (6.18). These effects are absent in the kinetic equation written the BM form. In [35] the corresponding Poisson-bracket terms in the KB kinetic equation (see equation (6.30)) responsible for this phenomenon were associated with quantum fluctuations.

From (6.18) we find for the time delay/advance of collisions:

$$\delta t_s^{\text{kin}} = \delta t_s^B - t_{\text{col}}, \quad \delta t_s^B = B_0/2, \quad t_{\text{col}} = Z_0^{-1}/\Gamma. \quad (6.49)$$

Here and further on in this subsection we will not write out the arguments (X, p) of the quantities, unless it is explicitly needed. The value δt_s^B can be formally expressed through the quantity having the meaning of an in-medium scattering phase shift [40]

$$\delta t_s^B = \frac{B_0}{2} \equiv \frac{\partial \delta(n)}{\partial p_0}, \quad \tan \delta(n) \equiv -\frac{\Gamma}{2M}, \quad (6.50)$$

where $n = j_{\text{Noether}}^0$ indicates the dependence of δ on the particle density. Note that the quantity (6.50) describes the delay/advancement of the dressed particles (or the corresponding group of waves) at arbitrary distances in contrast with a similar quantity δt_s (4.22), which we exploited in the description of the resonance quantum mechanical scattering, showing delay/advance of the scattered waves, as measured at large distances. The second relation (6.50) demonstrates the measure of proximity of the virtual particle to the mass-shell. In the virial limit, $\frac{B_0}{2} \rightarrow \frac{\partial \delta}{\partial p_0}$, where δ has already the meaning of the real scattering phase shift. E.g. for the $\pi N\Delta$ system, the B_0^Δ spectral function of the $\Delta(1232)$ isobar relates to the energy variation of the scattering phase shift $\delta_{33}^{\pi N}$ of the P_{33} partial wave coupled to the Δ resonance. For the pion, B_0^π in the virial limit relates to the phase shift of the nucleon hole– Δ -scattering. For the nucleon, B_0^N relates to $\delta_{\pi\Delta}$. Since following equation (6.19) B_0 is expressed through A , the scattering time δt_s^B can be presented as the sum of the Noether scattering delay and the drag and the back delay/advance terms:

$$\begin{aligned} \delta t_s^B &= \delta t_s^A + \delta t_s^{\text{drag}} + \delta t_s^{\text{back}}, \\ \delta t_s^A &= \frac{v_0 A}{2} > 0, \quad \delta t_s^{\text{drag}} = -\frac{A}{2} \frac{\partial \text{Re}\Sigma^R}{\partial p_0}, \quad \delta t_s^{\text{back}} = -\frac{AM}{2\Gamma} \frac{\partial \Gamma}{\partial p_0}. \end{aligned} \quad (6.51)$$

The collision time t_{col} in equation (6.49) has the meaning of the average time between collisions. The value t_{col} does not contain a factor two compared to the classical decay time $t_{\text{dec}}^{\text{cl}}$ given by equation (2.27) of section 2, although in both cases Γ enters the poles of the retarded Green's function similarly. This is because t_{col} describes the dynamics of the Green's function (quadratic

form) rather than dynamics of the classical field (the z -variable in classical mechanics). Also, compared to the quantities $t_{\text{dec}}^{\text{cl}}$ (see equation (2.27) section 2), t_{dec} , $t_{\text{dec}}^{\text{scl}}$ (see equations (4.21), (4.26) section 3), the value t_{col} contains an additional renormalization factor; cf. also equation (5.39) section 5. Thereby the collision time can be presented as the sum of the decay time and the drag delay/advance terms:

$$t_{\text{col}} = t_{\text{dec}} + \delta t_{\text{col}}^{\text{drag}},$$

$$t_{\text{dec}} = \frac{v_0}{\Gamma} > 0, \quad \delta t_{\text{col}}^{\text{drag}} = -\frac{\partial \text{Re}\Sigma^R}{\partial p_0} \frac{1}{\Gamma}. \quad (6.52)$$

The value $\delta t_{\text{f}}^{\text{kin}}$ given by equation (6.49) can be as positive as negative. The sum-rules (6.34) for A , B_0 and A_S^0 can now be presented as

$$\int \frac{dp_0}{2\pi} \delta t_{\text{s}}^A = \int \frac{dp_0}{2\pi} \delta t_{\text{s}}^B = \int \frac{dp_0}{2\pi} \delta t_{\text{s}}^{A_S} = \frac{\hbar}{2}, \quad \delta t_{\text{s}}^{A_S} = \frac{A_S}{2}, \quad (6.53)$$

$$\int \frac{dp_0}{2\pi} (t_{\text{col}} + \delta t_{\text{f}}^{\text{kin}}) = \frac{\hbar}{2}. \quad (6.54)$$

Thus, in accord with the energy-time uncertainty principle (cf. [58, 128]), δt_{s}^B , δt_{s}^A , $\delta t_{\text{s}}^{A_S}$ are minimal resolution times of the corresponding wave packets. The collision time $t_{\text{col}} \sim t_{\text{dec}}$ is the time needed for the decay of an unstable system. The value $\delta t_{\text{f}}^{\text{kin}}$ is the minimal resolution time counted from the collision time, i.e. an average time interval between two successive collisions. The corrected causality condition for collisions should now read as

$$t - r/v_{\text{gr}} - \delta t_{\text{f}}^{\text{kin}} \geq 0. \quad (6.55)$$

In section 3 we present the relation between the level density and the particle scattering phase shift. The density of states is often determined as [129]:

$$\frac{dN_A^{\text{level}}}{dp_0/(2\pi)} = \int \frac{d^3X d^3p}{(2\pi)^3} v^0 A(X, p_0, \vec{p}). \quad (6.56)$$

Thereby in accord with equation (6.27) the level density (6.56) is related to the Noether particle density,

$$\frac{dN^{\text{Noether}}}{d^3X dp_0/(2\pi)} = \frac{dN_A^{\text{level}}}{d^3X dp_0/(2\pi)} f(X, p_0, \vec{p}). \quad (6.57)$$

Note that even in the limit of a small width the spectral density A should include both the quasiparticle term and regular terms, see equation (6.74) below, so that in the case of the conserved number of particles (e.g. baryons) N^{Noether} would coincide with the full number of particles: with the only quasiparticle Green's function equation (6.56) becomes incorrect.

We could introduce the level density of interacting particles differently relating it to the interacting particle density (6.26) (cf. [130]),

$$\frac{dN_{A_S}^{\text{level}}}{dp_0/(2\pi)} = \int \frac{d^3X d^3p}{(2\pi)^3} A_S^0(X, p_0, \vec{p}), \quad (6.58)$$

or relating it to (6.28) with B^0 spectral function [131]

$$\frac{dN_B^{\text{level}}}{dp_0/(2\pi)} = \int \frac{d^3X d^3p}{(2\pi)^3} B^0(X, p_0, \vec{p}). \quad (6.59)$$

Since following equation (4.29) in the virial limit the level density is related to the Wigner delay time, from equations (6.56), (6.58) and (6.59) we find relations

$$\delta t_{\text{W}}^A = v_0 A, \quad \delta t_{\text{W}}^{A_S} = A_S, \quad \delta t_{\text{W}}^B = B_0. \quad (6.60)$$

For the non-relativistic particle scattering on a potential $B_0 = A$ and with δt_W^B , as well as with δt_W^A , we recover results (4.8), (4.22) derived in section 4. For multi-component systems the total Noether current can be presented as $j_\mu^{\text{tot}} = \sum j_\nu^{\text{Noether}}$; see [34]. On the other hand, the interaction between different species can be redistributed in many ways. For example, the interaction from some species can be redistributed to other ones; cf. [132]. In the latter case the currents of some properly dressed species are described by equation (6.58) or by equation (6.59), whereas some other species undergo free motion. For example, for the case of a resonance like the Δ or ρ -meson resonances in hadron physics, the B_0 -function relates to the energy variations of scattering phase shift of the scattering channel coupling to the resonance in the virial limit [131, 133]. Similarly, in a quantum mechanical scattering divergent and scattered waves are relevant quantities only at large distances, being strongly distorted at short distances near the scatterer.

From equation (6.42) using equations (4.29), (6.59) and (6.60) we may also recover the memory Wigner delay/advance time

$$\delta t_W^{\text{mem}} = \frac{1}{2} \frac{\partial(L^{+-} + L^{-+})}{\partial p_0} L^{+-} L^{-+}, \quad (6.61)$$

provided self-energies include diagrams with more than two vertices. The value $\delta t_W^{\text{mem}} \propto V_0^3$ and therefore δt_W^{mem} disappears in the virial limit.

Finally, note that the quantities $t_{\text{soj}}^{(\text{ID})}(a, b; \tau)$ given by equation (5.40) and $t_{\text{soj}}(\tau)$ given by (5.41), where F is the exact non-equilibrium Green's function, have the same form, being expressed through the Wigner density F in the Wigner representation.

6.5.1. Time advances and delays for Wigner resonances. For the Wigner resonances $\text{Re}\Sigma^R$ and Γ are assumed to be independent of p_0 and equation (6.49) is simplified as

$$\delta t_f^{\text{kin}} = \delta t_s^B - t_{\text{col}} = -\frac{v_0}{\Gamma} \frac{M^2 - \Gamma^2/4}{(M^2 + \Gamma^2/4)} = \delta t_f = \delta t_s^A - t_{\text{dec}}. \quad (6.62)$$

The energy-weighted time shift $\int \frac{dp_0}{2\pi} \Gamma A \delta t_f^{\text{kin}} = 0$.

The value $\delta t_s^A = v_0 \frac{\Gamma/2}{M^2 + \Gamma^2/4} > 0$ coincides with the scattering time delay, $\delta t_s = \frac{\partial \delta}{\partial p_0}$, introduced in quantum mechanics, see equation (4.5). The collision time coincides with the quantum mechanical time, $\delta t_{\text{vol}} = \frac{1}{2 \sin^2 \delta} \frac{\partial \delta}{\partial p_0}$, when all the delays are put into scattering, see equation (4.13), (4.21). Thus, the value $-t_{\text{col}} = -t_{\text{dec}} = -v_0/\Gamma < 0$ has the meaning of the collision time advance. The value δt_f^{kin} given by (6.62) coincides with the quantity $\delta t_f = -\delta t_i = -\frac{\cos(2\delta)}{2 \sin^2 \delta} \frac{\partial \delta}{\partial p_0}$ (see equation (4.20)), being a forward delay/advance time. A propagating wave packet gets a delay/advance δt_i due to interference of the incident and reflected waves. The collision term gets a corresponding advance/delay $\delta t_f = -\delta t_i$, being the scattering time counted from the collision time, since actual collision for the particles with the width may occur a time $\sim t_{\text{col}}$ earlier than it happens in the case of the zero width. In the limit $|M| \ll \Gamma$ there is a time delay $\delta t_f = v_0/\Gamma$, for $|M| \gg \Gamma$ there arises a time advance $\delta t_f = -v_0/\Gamma$ and for $|M| = \Gamma/2$, $\delta t_f = 0$.

6.6. Test-particle method

The conserving feature is especially important for devising numerical simulation codes based on the kinetic equation. If a test-particle method is used, one should be sure that the number of test particles is conserved exactly rather than approximately. In the test-particle method the distribution function F (not f) satisfying equation (6.11) is represented by an ensemble of test

particles [40]

$$F(X, p) \sim \sum_i \delta^{(3)}(\vec{x} - \vec{x}_i(t)) \delta^{(4)}(p - p_i(t)), \quad (6.63)$$

where the i -sum runs over test particles, $p = (p^0, \vec{p})$. Then the drift term in the KB equation for F (derived from (6.11) if one expands the collision term in gradients including the first gradient terms) just corresponds to the classical motion of these test particles subjected to forces inferred from $\text{Re}\Sigma^R(X, p)$, while the collision term gives a stochastic change of test-particle's momenta, when their trajectories 'cross'. For a direct application of this method, however, there is a particular problem with the kinetic equation in the KB form. An additional Poisson-bracket term $\{\Gamma^{\text{in}}, \text{Re} G^R\}$ appears that spoils this simplistic picture, since derivatives acting on the distribution function F arise here only indirectly and thus cannot be included in the collision-less propagation of test particles. This problem, of course, does not prevent a direct solution of the KB kinetic equation applying lattice methods, which are, however, much more complicated and time-consuming as compared to the test-particle approach.

The effective BM-current was used in [134] as a basis for the construction of a test-particle ansatz for numerical solution of the non-relativistic BM kinetic equation. To fulfil the effective current conservation one introduces the test-particle ansatz for

$$\frac{1}{2}\Gamma B_0 F(X, p) \sim \sum_i \delta^{(3)}(\vec{x} - \vec{x}_i(t)) \delta^{(4)}(p - p_i(t)), \quad (6.64)$$

rather than for the distribution function itself. Note that the energy $p_i^0(t) \equiv E_i(t)$ of the test particle is an independent coordinate, not restricted by a mass-shell condition. [135] used this test-particle ansatz in the relativistic case.

The BM kinetic equation together with ansatz (6.64) for the distribution function result in the set of equations for the evolution of parameters of the test particles between collisions

$$\frac{d\vec{x}_i}{dt} = \frac{1}{v_0 - \partial_{E_i} \text{Re}\Sigma^R - (M/\Gamma)\partial_{E_i}\Gamma} (\vec{v}_i + \nabla_{p_i} \text{Re}\Sigma^R + (M/\Gamma)\nabla_{p_i}\Gamma), \quad (6.65)$$

$$\frac{d\vec{p}_i}{dt} = \frac{1}{v_0 - \partial_{E_i} \text{Re}\Sigma^R - (M/\Gamma)\partial_{E_i}\Gamma} (\nabla_{x_i} \text{Re}\Sigma^R + (M/\Gamma)\nabla_{x_i}\Gamma), \quad (6.66)$$

$$\dot{E}_i = \frac{1}{v_0 - \partial_{E_i} \text{Re}\Sigma^R - (M/\Gamma)\partial_{E_i}\Gamma} (\partial_t \text{Re}\Sigma^R + (M/\Gamma)\partial_t\Gamma). \quad (6.67)$$

All functions on the right-hand side are evaluated in the point $(t, \vec{x}_i(t), E_i(t), \vec{p}_i(t))$. These equations of motion, in particular, yield the time evolution of the mass term M , of a test particle [134, 135]

$$\frac{dM_i}{dt} = \frac{M_i}{\Gamma_i} \frac{d\Gamma_i}{dt}, \quad (6.68)$$

the origin of which can be traced back to the additional term $\{\Gamma F/A, \text{Re} G^R\}$ in the BM equation. Here $M_i(t) = M[t, \vec{x}_i(t); E_i(t), \vec{p}_i(t)]$ measures an 'off-shellness' of the test particle and $\Gamma_i(t) = \Gamma[t, \vec{x}_i(t); E_i(t), \vec{p}_i(t)]$. Equation of motion (6.68) yields $|\dot{M}_i| = \alpha_i \Gamma_i$, where $\alpha_i > 0$ do not depend on time and implies that once the width drops in time the particles are driven toward the mass on-shell, i.e. to $M = 0$. This clarifies the meaning of the additional term $\{\Gamma F/A, \text{Re} G^R\}$ in the off-shell BM kinetic equation (which follows from (6.11), if one suppresses variable shifts in the collision term): it provides the time evolution of the off-shellness.

For the non-local form of the kinetic equation [40] the set of equations for the evolution of parameters of the test particles between collisions is the same as in the BM case. The only

difference with the BM case is that collisions of test particles occur with certain time (and space) delay (or advance) as compared with the instant of their closest approach to each other.

Following equation (6.18) the shift of the space variables is

$$\delta\vec{x} = \frac{1}{A} \frac{\partial \text{Re } G^R}{\partial \vec{p}} = \delta\vec{x}_{\text{drift}} + \delta\vec{x}_{\text{col}} = \frac{1}{2} \vec{B} + \vec{v}_{\text{gr}} t_{\text{col}}. \quad (6.69)$$

We can further express the spatial shift in terms of the time delays and velocity $\frac{d\vec{x}}{dt}$ of a test particle on its trajectory (cf. equation (6.65)),

$$\delta\vec{x}_i = \frac{d\vec{x}_i}{dt} \delta t_{i,s}^B + \vec{v}_{i,\text{gr}} t_{i,\text{col}}. \quad (6.70)$$

Equation (6.70) demonstrates that before a delayed/advanced collision the test particle moves along its trajectory. Therefore, the scattering time delay $\delta t_{i,s}^B$ unambiguously results in a definite space shift. The collision itself is associated with an additional time delay $t_{i,\text{col}}$, which implies that the collision is not instant, as it is treated in the BM kinetic equation, but requires a certain time for complete decoupling from intermediate states (e.g., the pion spends some time in the intermediate Δ -nucleon-hole state, a soft photon requires a certain time to be formed in multiple collisions of the proton with neutrons). Therefore, this additional delay gives rise to an additional shift of the particle with respect to its ‘collision-less’ trajectory (6.65).

6.7. The quasiparticle limit

The quasiparticle limit is understood as the limit when Green’s functions are computed at $\text{Im}\Sigma^R \rightarrow 0$. The quasiparticle width $\Gamma_{\text{qp}}(X, \vec{p}) = -2 \text{Im}\Sigma^R(X, \vec{p}, A \rightarrow A_{\text{qp}})$ is then calculated with the quasiparticle Green’s functions and the associated quasiparticle spectral functions A_{qp} . The latter ones reduce in this limit ($|M| = \alpha\Gamma$, $|\alpha| \gg 1$) to,

$$\begin{aligned} A_{\text{qp}}(X, p) &= 2\pi Z_0^{\text{qp}}(X, \vec{p}) \delta(p_0 - E_p(X, \vec{p})), \\ Z_0^{\text{qp}}(X, \vec{p}) &= \left(v^0 - \frac{\partial \text{Re}\Sigma^R(X, p)}{\partial p_0} \right)_{p_0=E_p(X, \vec{p})}^{-1}, \end{aligned} \quad (6.71)$$

where $E_p(X, \vec{p})$ stands for the energy of a quasiparticle, being the root of the dispersion relation

$$M(X, p_0 = E_p(X, \vec{p}), \vec{p}) = 0, \quad (6.72)$$

$Z_0^{\text{qp}}(X, \vec{p}) > 0$ on the quasiparticle branch $p_0 = E_p(X, \vec{p})$.¹⁰

The quasiparticle spectral function does not fulfil the exact sum-rule (6.34) but fulfils the corresponding quasiparticle sum-rule

$$\int Z_0^{\text{qp}}(X, \vec{p}) A_{\text{qp}}(X, p) \frac{dp_0}{2\pi} = 1. \quad (6.73)$$

Formally, within the quasiparticle picture this problem is avoided by a renormalization, after which one may already deal only with the quasiparticle degrees of freedom, being well-separated from the degrees of freedom in the continuum. The reason for the difference between the exact and quasiparticle sum-rules is that the quasiparticle current $j_{\text{qp}}^\mu = (j_B^{\text{qp}})^\mu = (j_S^{\text{qp}})^\mu$ includes the quasiparticle drag flow and, thereby, differs from the Noether current. This difference is compensated due to the conservation of the Noether current by the presence of the back flow, as a back reaction of the whole energy sea to the particle drag flow. Thus, the

¹⁰ Here, for simplicity we assume that there is only one quasiparticle branch. Generalization is obvious.

exact sum-rule (6.34) for A is recovered, provided one includes the width term. It is easily demonstrated in the case of a weak interaction [136]. Then

$$A(X, p) \simeq 2\pi Z_0^{\text{qp}}(X, \vec{p})\delta(M(X, p)) + \mathcal{P} \frac{\Gamma(X, p)}{M^2(X, p)} \simeq 2\pi \delta(p_0 - E_p(X, \vec{p})), \quad (6.74)$$

where \mathcal{P} indicates the principal value. The required sum-rule is recovered after using the Kramers–Kronig relation between Γ and $\text{Re}\Sigma$.

The integration of all three forms of the kinetic equation, the BM form, the KB equation (6.30) and the non-local equation (6.21) over $dp_0/(2\pi)$ yields one and the same kinetic equation describing the quasiparticle propagation in matter:

$$\frac{\partial f_{\text{qp}}(X, \vec{p})}{\partial t} + \vec{v}_{\text{gr}}^{\text{qp}}(X, \vec{p}) \nabla f_{\text{qp}}(X, \vec{p}) - \nabla E_p(X, \vec{p}) \frac{\partial f_{\text{qp}}(X, \vec{p})}{\partial \vec{p}} = C_{\text{qp}}(X, \vec{p}), \quad (6.75)$$

here E_p obeys mass-shell condition (6.72),

$$C_{\text{qp}}^{\text{shift}}(X, \vec{p}) = \int \frac{dp_0}{2\pi} A_{\text{qp}}(X, p) C^{\text{shift}}(X, p; A \rightarrow A_{\text{qp}}) \rightarrow C_{\text{qp}}(X, \vec{p})$$

and the quasiparticle group velocity is

$$\vec{v}_{\text{gr}}^{\text{qp}}(X, \vec{p}) = \frac{\partial E_p(X, \vec{p})}{\partial \vec{p}} = \frac{\left(\vec{v} + \frac{\partial \text{Re}\Sigma^R(X, p)}{\partial \vec{p}} \right)_{p_0=E_p(X, \vec{p})}}{\left(v^0 - \frac{\partial \text{Re}\Sigma_{\text{qp}}^R(X, p)}{\partial p_0} \right)_{p_0=E_p(X, \vec{p})}}. \quad (6.76)$$

The authors of [137] constructed a non-local kinetic equation in an extended quasiparticle approximation, which included a non-local collision term. Note that their finding of cancellation of off-shell terms and remaining non-local shifts is in agreement with a similar cancellation demonstrated then in [36, 37] within the Φ -derivable approach to the kinetic KB and BM equations. Conservation laws are also fulfilled for their non-local extended quasiparticle kinetic equation, that turns out to make the link between non-local quantum shifts to classical ones, see [138].

In the quasiparticle limit the BMM entropy, equation (6.23), reads

$$S_{\text{qp}}^\mu = \int \frac{d^3p}{(2\pi)^3} \sqrt{1 - [\vec{v}_{\text{gr}}^{\text{qp}}(X, \vec{p})]^2} [u_{\text{gr}}^{\text{qp}}(X, \vec{p})]^\mu \sigma_{\text{qp}}(X, \vec{p}), \quad (6.77)$$

where we introduced notation

$$[u_{\text{gr}}^{\text{qp}}(X, \vec{p})]^\mu = \left(\frac{1}{\sqrt{1 - [\vec{v}_{\text{gr}}^{\text{qp}}(X, \vec{p})]^2}}, \frac{\vec{v}_{\text{gr}}^{\text{qp}}(X, \vec{p})}{\sqrt{1 - [\vec{v}_{\text{gr}}^{\text{qp}}(X, \vec{p})]^2}} \right). \quad (6.78)$$

The quasiparticle group velocity can significantly differ from the phase velocity. In atomic Bose–Einstein condensates [139] the light can be slowed down to the speed 17 m/s (a so-called slow light). The light also becomes ultra-slow in the hot atomic vapor of rubidium [140]. On the other hand, the quasiparticle group velocity can easily exceed the velocity of light in medium $c(n)$, $c(n) < c$. It manifests as the Cherenkov radiation. An instability of quasiparticle modes also arises in a moving medium [122, 141, 142] (even if the modes are stable in the static medium), provided $|\vec{u}||\vec{p}| > E_p(p)$, where \vec{u} is the speed of the medium and $E_p(p)$ is the quasiparticle spectrum branch. As the result, a spatially inhomogeneous condensate of Bose excitations may be formed. This phenomenon is similar to the Cherenkov effect and shock wave generation.

Obviously, the values of time delays are unlimited. The question of a possible limitation on the time advance and the possibility to have $v_{\text{qp}}^{\text{gr}} > c$ are subtle issues. As argued in [103, 104], such a possibility does not contradict causality. However the velocity of the wavefront v_{fr}

should always be limited by c ; see [18] and references therein. An apparent superluminal propagation manifested in some laser experiments can be understood as the consequence of a reshaping of the pulse envelope by interaction within the medium, see the discussion in [14–16, 18]. Although formally v_{gr} exceeds c , the forward wavefront moves with velocity $\leq c$, as it should be. There are also arguments that the advance of the pulse of light in materials is generally limited only by few pulse widths (so-called fast light). Thereby, the interpretation of a negative group delay as a superluminal propagation is, according to [16], a semantic question, since the speed of the information transport never exceeds c ; see [17].

Reference [126] used the p_0 -averaged BM equation and averaged distributions,

$$f^B(X, \vec{p}) = \int \frac{dp_0}{2\pi} B_0(X, p) f(X, p). \quad (6.79)$$

Averaged values

$$\begin{aligned} \vec{v}_{\text{gr}}^B(X, \vec{p}) &= \int \frac{dp_0}{2\pi} B_0(X, p) \vec{v}_{\text{gr}}(X, p), & \tilde{\vec{v}}_{\text{gr}}^B(X, \vec{p}) &= \int \frac{dp_0}{2\pi} \tilde{B}_0(X, p) \tilde{\vec{v}}_{\text{gr}}(X, p), \\ \vec{v}_{\text{gr}}^S(X, \vec{p}) &= \int \frac{dp_0}{2\pi} A_S(X, p) \vec{v}_{\text{gr}}(X, p), \end{aligned} \quad (6.80)$$

yield one and the same value $\vec{v}_{\text{qp}}^{\text{gr}}$ in the quasiparticle limit. It is worthwhile to mention that the quantity $\vec{v}_{\text{gr}} B_0$ enters (through \tilde{B}) the expression for the entropy flow (6.23) associated with the information transport. Therefore one may hope that the quantities (6.80) behave reasonably in the whole (p_0, \vec{p}) plane.

Finally, to avoid possible confusion recall that there are no limitations on the values of the phase velocity and the group velocity $\tilde{v}_{\text{gr}}(p_0, \vec{p})$ for off-mass-shell particles given by equation (6.33). However, the condition $v_{\text{gr}}(p_0, \vec{p}) < c$ might be satisfied. For example, in the case of a Fermi liquid the width of particle–hole excitations $\Gamma(p_0, \vec{p}) \propto p_0$ for $p_0 \rightarrow 0$, cf. [122], and the restriction $v_{\text{gr}}(p_0, \vec{p}) < c$ is then recovered, as it follows from equation (6.20). Taking into account the dependence $\Gamma(p_0, \vec{p}) \propto p_0$ is also important in some other problems, e.g. in the description of the growth of a static classical pion condensation field in dense isospin symmetric nuclear matter [133]. Also we arrived at such a dependence in the description of damped oscillations in section 2. However, in general, it is not formally excluded that $v_{\text{gr}}(p_0, \vec{p}) > c$ for p_0 in some space-like region.

For moving media, an instability of off-mass-shell modes with $p_0 < |\vec{u}| |\vec{p}|$ may result in some measurable effects, like a heating of the medium; cf. [122, 143].

6.8. Kinetic entropy and time delays

Any loss of information results in an increase of the entropy [144]. Thus, it is important to find and compare values of the entropy related to the BM, KB and non-local forms of the kinetic equations.

First, let us for simplicity disregard memory effects. Above, see equation (6.23), we introduced the expression for the BMM kinetic entropy flow. It also can be rewritten as follows [35]

$$\begin{aligned} S_{\text{BMM}}^\mu(X) &= \text{Tr} \int \frac{d^4 p}{(2\pi)^4} \left[\left(v^\mu - \frac{\partial \text{Re} \Sigma^R(X, p)}{\partial p_\mu} \right) A(X, p) \sigma(X, p) \right. \\ &\quad - \text{Re} G^R(X, p) \left(\mp \ln(1 \mp f(X, p)) \frac{\partial}{\partial p_\mu} [\Gamma(X, p) (1 \mp f(X, p))] \right. \\ &\quad \left. \left. - \ln f(X, p) \frac{\partial}{\partial p_\mu} [\Gamma(X, p) f(X, p)] \right) \right]. \end{aligned} \quad (6.81)$$

This contribution is of the zero-gradient order. Similarly, one derives [37] an expression for the KB Markovian part of the entropy flow (KBM) relating to equation (6.30),

$$S_{\text{KBM}}^\mu(X) = \text{Tr} \int \frac{d^4p}{(2\pi)^4} \left(v^\mu - \frac{\partial \text{Re} \Sigma^R(X, p)}{\partial p_\mu} \right) \times \left[A(X, p) \sigma(X, p) - \text{Re} G^R(X, p) \left(\mp \ln(1 \mp f(X, p)) \frac{\partial \Gamma^{\text{out}}(X, p)}{\partial p_\mu} - \ln f(X, p) \frac{\partial \Gamma^{\text{in}}(X, p)}{\partial p_\mu} \right) \right]. \quad (6.82)$$

For a discussion of the H theorem it is necessary to get the entropy flow including first-order gradient terms. The KB entropy flow contains an extra first-order gradient term compared to the KBM result [37],

$$\partial_\mu S_{\text{KB}}^\mu(X) = \partial_\mu S_{\text{KBM}}^\mu(X) + \partial_\mu \delta S_{\text{KB}}^\mu(X) + \delta_{\text{cor}}^\mu(X), \quad (6.83)$$

where

$$\delta S_{\text{KB}}^\mu(X) = -\text{Tr} \int \frac{d^4p}{(2\pi)^4} \frac{M(X, p)}{\Gamma(X, p)} C(X, p) \frac{\partial}{\partial p_\mu} \ln \frac{1 \mp f(X, p)}{f(X, p)}. \quad (6.84)$$

In general, $C \propto O(\delta f, \partial_X)$, where $\delta f(X, p) = f(X, p) - f_{\text{1.eq.}}(X, p)$ with $f_{\text{1.eq.}}$ given in equation (6.16), and the gradient expansion and the expansion in δf near a local equilibrium are different, see the discussion in the next subsection and in [37]. For near-local equilibrium configurations

$$\delta_{\text{cor}}^\mu(X) = \text{Tr} \int \frac{d^4p}{(2\pi)^4} \frac{C(X, p)}{A(X, p)} \left\{ \ln \frac{1 \mp f(X, p)}{f(X, p)}, \text{Re} G^R(X, p) \right\} = O(\delta f \partial_X \delta f).$$

Thus one may neglect the $\delta_{\text{cor}}^\mu(X)$ term, provided the system is very close to the local equilibrium and gradients are small. Replacing in equation (6.84) the local equilibrium distributions everywhere except C we obtain

$$\delta S_{\text{KB}}^0(X) = -\text{Tr} \int \frac{d^4p}{(2\pi)^4} \frac{M_{\text{1.eq.}}(X, p)}{\Gamma_{\text{1.eq.}}(X, p)} \frac{C(X, p)}{\bar{T}_{\text{1.eq.}}(X)}. \quad (6.85)$$

This (the first order in δf) correction is zero in the local equilibrium, where $C_{\text{1.eq.}} = 0$, and is sign-indefinite beyond the local equilibrium.

Counting the KB entropy flow from the BMM one, from equations (6.81), (6.82), (6.84) and (6.36) we find

$$S_{\text{KBM}}^\mu(X) = S_{\text{BMM}}^\mu(X) - \text{Tr} \int \frac{d^4p}{(2\pi)^4} \text{Re} G^R(X, p) \ln \frac{1 \mp f(X, p)}{f(X, p)} \frac{\partial}{\partial p_\mu} \left[\frac{C(X, p)}{A(X, p)} \right], \quad (6.86)$$

and finally

$$S_{\text{KB}}^\mu(X) = S_{\text{BMM}}^\mu(X) + \text{Tr} \int \frac{d^4p}{(2\pi)^4} \frac{C(X, p)}{A(X, p)} \frac{\partial \text{Re} G^R(X, p)}{\partial p_\mu} \ln \frac{1 \mp f(X, p)}{f(X, p)}. \quad (6.87)$$

Thus we obtain

$$S_{\text{KB}}^\mu(X) = S_{\text{BMM}}^\mu(X) + \delta S_{\text{KB}}^\mu(X),$$

$$\delta S_{\text{KB}}^\mu(X) = \int \frac{d^4p}{(2\pi)^4} C(X, p) \delta X^\mu(X, p) \ln \frac{1 \mp f(X, p)}{f(X, p)}, \quad (6.88)$$

with $\delta X^\mu(X, p)$ from (6.18). As we see, an additional purely non-equilibrium contribution $\delta S_{\text{KB}}^\mu(X)$ is proportional to a weighted average space-time delay/advance. Expression (6.88) up to first gradients also holds for the non-local form of the kinetic equation.

Using (6.18) we obtain

$$\delta S_{\text{KB}}^0(X) = \int \frac{d^4 p}{(2\pi)^4} C(X, p) \delta t_f^{\text{kin}}(X, p) \ln \frac{1 \mp f(X, p)}{f(X, p)} \quad (6.89)$$

that for configurations close to the local equilibrium produces an additional contribution to the specific heat

$$\delta c_{\text{KB}}(X) = - \int \frac{d^4 p}{(2\pi)^4} \frac{p_0}{T_{\text{1.eq}}(X)} C(X, p) (\delta t_f^{\text{kin}})_{\text{1.eq}} + \int \frac{d^4 p}{(2\pi)^4} p_0 C(X, p) \frac{\partial (\delta t_f^{\text{kin}})_{\text{1.eq}}}{\partial T}. \quad (6.90)$$

The presence or absence of an additional non-equilibrium correction $\propto C$ to the specific heat can be experimentally checked.

We can also find the entropy flow directly for the non-local form of the kinetic equation. For that we multiply the non-local kinetic equation by $\mp \ln[(1 \mp f^{\text{shift}})/f^{\text{shift}}]$ and perform 4-momentum integration. From the left-hand side of the thus-obtained equation we find, instead of equation (6.81),

$$\begin{aligned} S_{\text{NL}}^\mu(X) = & \text{Tr} \int \frac{d^4 p}{(2\pi)^4} \left[\left(v^\mu - \frac{\partial \text{Re} \Sigma^R(X, p)}{\partial p_\mu} \right) A(X, p) \sigma^{\text{shift}}(X, p) \right. \\ & - \text{Re} G^R(X, p) \left(\mp \ln(1 \mp f^{\text{shift}}(X, p)) \frac{\partial}{\partial p_\mu} [\Gamma(X, p)(1 \mp f(X, p))] \right. \\ & \left. \left. - \ln f^{\text{shift}}(X, p) \frac{\partial}{\partial p_\mu} [\Gamma(X, p) f(X, p)] \right) \right] \\ & + O(\partial_x^2) = S_{\text{KB}}^\mu(X) + O(\partial_x^2), \end{aligned} \quad (6.91)$$

with

$$\sigma^{\text{shift}}(X, p) = \mp (1 \mp f(X, p)) \ln(1 \mp f^{\text{shift}}(X, p)) - f(X, p) \ln f^{\text{shift}}(X, p). \quad (6.92)$$

Although formally equation (6.91) looks similar to the BMM term (6.81), the former incorporates 4-space-time delays/advancements.

To get the full result one should still add to S^μ the first-gradient-order memory correction S_{mem}^μ , which is non-zero, if the generating Φ functional contains diagrams with more than two vertices, see equation (6.43). For example, in [35] it was shown that only with inclusion of the memory term the value $S_{\text{BM}}^0 = S_{\text{BMM}}^0 + S_{\text{mem}}^0$ yields an appropriate thermodynamic expression for the equilibrium entropy. Since in the local equilibrium $\delta S^\mu = 0$, the same relation holds in the local equilibrium for S_{KB}^0 , i.e.

$$(S_{\text{KB}}^0)_{\text{1.eq}} = (S_{\text{BM}}^0)_{\text{1.eq}} = (S_{\text{BMM}}^0)_{\text{1.eq}} + (S_{\text{mem}}^0)_{\text{1.eq}}. \quad (6.93)$$

H theorem and the minimum of the entropy production are discussed in appendix F.

6.9. Examples of the solutions of kinetic equations

Consider a small portion of light resonances placed either in the uniform equilibrium medium consisting of heavy particles or in vacuum. To reduce the complexity of the problem we will exploit the following ansatz: assume that only the distribution f depends on the Wigner variables $X = (t, \vec{r})$, whereas the dependence of $\Sigma^R(t, \vec{r})$ on X is weaker and can be neglected.

Then the kinetic equation in the non-local form (6.11) simplifies as

$$A_S^\mu(p) \frac{\partial}{\partial X^\mu} f(X, p) = A(p) C \left(x_\mu - \frac{1}{2} B_\mu(p) + Z_\mu^{-1}(p)/\Gamma(p), p_\mu \right). \quad (6.94)$$

The BM form of the kinetic equation (when $\mathcal{C}^{\text{shift}}$ is replaced by \mathcal{C}) renders

$$A_S^\mu(p) \frac{\partial}{\partial X^\mu} f(X, p) = A(p) \Gamma^{\text{in}}(p) - A(p) \Gamma(p) f(X, p). \quad (6.95)$$

The KB equation (when $\mathcal{C}^{\text{shift}}$ is expanded up to the first-gradient-order terms) reads

$$\begin{aligned} \tilde{B}^\mu(p) \frac{\partial}{\partial X^\mu} f(X, p) + f(p) \{ \Gamma(p), \text{Re } G^R(p) \} - \{ \Gamma^{\text{in}}(p), \text{Re } G^R(p) \} = A(p) \Gamma^{\text{in}}(p) \\ - A(p) \Gamma(p) f(X, p). \end{aligned} \quad (6.96)$$

For uniformly distributed light resonances equation (6.94) still simplifies as

$$A_S^0(p) \frac{\partial}{\partial t} f(t, p) = A(p) \mathcal{C} \left(t - \frac{1}{2} B_0(p) + Z_0^{-1}(p) / \Gamma(p), p \right). \quad (6.97)$$

Equations (6.95) and (6.96) are simplified accordingly.

6.9.1. Uniformly distributed light resonances in equilibrium medium of heavy particles. Consider the behavior of a dilute admixture of uniformly distributed light resonances in equilibrium medium consisting of heavy-particles. Thereby, we assume that Σ^R is determined by the distribution of heavy particles, thus introducing ansatz $\Sigma^R \simeq \Sigma_{\text{eq}}^R$. To further proceed we need to make an additional assumption.

- (i) Let us also *assume* that the gain term $\Gamma^{\text{in}}(p) \simeq \Gamma_{\text{eq}}^{\text{in}}(p) = f_{\text{eq}}(p) \Gamma_{\text{eq}}(p)$; this means it is a function of only equilibrium quantities. Then only the distribution of light resonances f changes in time. According to equation (6.31):

$$C(p) \simeq -A(p) \Gamma(p) \delta f(t, p), \quad \delta f(t, p) = f(t, p) - f_{\text{eq}}(p).$$

Such an approximation (more accurately, an ansatz) is called a relaxation time approximation and it is often used in Boltzmann kinetics without additional justification. Replacing in the non-local kinetic equation (6.97)

$$\delta f_{\text{NL}}(t, p) = \delta f(t=0, p) e^{-\alpha(p)t / \delta t_s^B(p)}, \quad (6.98)$$

(cf. equation (6.50)) for parameter α we find the equation

$$\alpha(p) = e^{\alpha(p) - \alpha(p)t_{\text{col}}(p) / \delta t_s^B(p)}, \quad (6.99)$$

that yields $\alpha \simeq 1$ for $\delta t_s^B \simeq t_{\text{col}}$ (then all three forms of kinetic equation coincide); $\alpha \simeq \frac{\delta t_s^B}{t_{\text{col}}} \ln \frac{t_{\text{col}}}{\delta t_s^B} \ll 1$ for $\delta t_s^B / t_{\text{col}} \ll 1$. In the case $\delta t_s^B / t_{\text{col}} \gg 1$ equation (6.99) has no solutions. However, this case is not realized as it follows from explicit expressions for δt_s^B and t_{col} .

From the KB equation (6.96) we find solution

$$\delta f_{\text{KB}}(t, p) = \delta f(t=0, p) e^{-t/t_{\text{col}}(p)}. \quad (6.100)$$

In contrast, solving the BM equation (6.95) we get a different solution:

$$\delta f_{\text{BM}}(t, p) = \delta f(t=0, p) e^{-t/\delta t_s^B(p)}. \quad (6.101)$$

These three solutions (6.98), (6.100) and (6.101) coincide only for $|\delta t_s^B(p) - t_{\text{col}}(p)| \ll |\delta t_s^B(p)|$. However this condition may hold only in very specific situations. For example, for Wigner resonances it holds only for $|M - \Gamma/2| \ll \Gamma$.

The mass-shell equation (6.35) produces another solution:

$$\delta f_{\text{MS}}(t, p) = \delta f(t=0, p) e^{-t/\delta t_{\text{MS}}(p)}, \quad \delta t_{\text{MS}}(p) = \frac{1}{4M(p)} \frac{\partial \Gamma(p)}{\partial p_0}. \quad (6.102)$$

Concluding, within the relaxation time approximation we arrive at somewhat contradictory results.

- (ii) Using the BM replacement $\Gamma^{\text{in}} = \Gamma f$ in the commutator term in the KB equation and in the mass-shell equation one proves that the latter two equations coincide with the BM equation. However, as we see from the non-local kinetic equation the parameter δt_{f} is not small compared to $\delta t_{\text{s}}^{\text{B}}$ except for the case $|M - \Gamma/2| \ll \Gamma$ (for Wigner resonances) that again puts in question the correctness of the gradient expansion for $t \sim \delta t_{\text{s}}^{\text{B}}$.

6.9.2. Uniformly distributed resonances in vacuum. Now consider a spatially uniform dilute gas of non-interacting resonances produced at $t < 0$ and placed in the vacuum at $t = 0$. Then $\Sigma^R = \Sigma^R(p)$ and following [39] we put $\Gamma^{\text{in}}(t > 0) = 0$ (the production of new resonances ceases). Using the latter ansatz we find

$$C_{\text{vac.r.}} = -A(p) \Gamma(p) f(t, p). \quad (6.103)$$

From the BM equation we arrive at the distribution

$$f_{\text{BM}}(t, p) = f(t = 0, p) e^{-t/\delta t_{\text{s}}^{\text{B}}(p)}. \quad (6.104)$$

However, the BM form of the kinetic equation does not hold for $\Gamma^{\text{in}} = 0$, since its derivation is based on the equation $\Gamma^{\text{in}} = \Gamma f$.

To the contrary, from the KB equation we find another solution:

$$f_{\text{KB}}(t, p) = f(t = 0, p) e^{-t/t_{\text{col}}(p)}. \quad (6.105)$$

Similarly, the solution of the kinetic equation in the non-local form is the same as in equation (6.98) with the replacement $\delta f \rightarrow f$. From the mass-shell equation (6.35) we find solution (6.102), now for f instead of δf . Thus we meet here with the same problems as in the previous example.

6.9.3. Collision-less dynamics of propagating resonances. Let us find a class of spatially inhomogeneous distributions of propagating virtual particles. We continue to assume that Σ^R does not depend on X . As an ansatz, let us use the BM replacement $\Gamma^{\text{in}} = \Gamma f$ both in the commutator and in the collision terms in the KB equation. Since in the shifted variables also $\Gamma_{\text{shift}}^{\text{in}} = \Gamma^{\text{shift}} f^{\text{shift}}$, we obtain $C^{\text{shift}} = 0$. Thus in all three cases we now deal with equation (6.94) with zero on the right-hand side (the so-called Vlasov case). The solution of this equation is

$$f(X, p) = f_0(t - \vec{r} \vec{v}_{\text{gr}}/v_{\text{gr}}^2, p), \quad (6.106)$$

for an arbitrary function $f_0(\xi, p)$ and \vec{v}_{gr} being a function of p . Following equation (6.36), $\delta \Gamma^{\text{in}} = 0$ and the mass-shell equation (6.35) is also fulfilled. Thus, in the given collision-less case solution (6.106) fulfils the KB, BM, non-local form and the mass-shell equations.

In the specific case of the 1D propagation of a Gaussian distribution of off-shell particles, one gets

$$f(t, z, p) = f_0(p) \exp[-(z - v_{\text{gr}}t)^2 (\Gamma_z/v_{\text{gr}})^2], \quad (6.107)$$

where f_0 is an arbitrary function of p . The wave packet is propagating with the velocity v_{gr} . Particles are distributed in z near the maximum with the width $\delta z \sim v_{\text{gr}}/\Gamma_z$, Γ_z is the energy width of the initial distribution.

6.9.4. Collisional dynamics of propagating resonances. Let us continue to work with the assumption that Σ^R does not depend on X . The propagation of a resonance distribution in vacuum is described by the KB equation (6.96) with $C \neq 0$. The solution of the equation is

$$f(X, p) = f_0(t - \vec{r}\vec{v}_{\text{gr}}/\tilde{v}_{\text{gr}}^2, p) e^{-t/t_{\text{col}}(p)}, \quad (6.108)$$

where \tilde{v}_{gr} is a function of p and f_0 is an arbitrary function $f_0(\xi, p)$. The solution can be also presented as

$$f(X, p) = \tilde{f}_0(t - \vec{r}\vec{v}_{\text{gr}}/\tilde{v}_{\text{gr}}^2, p) \exp\left[-\frac{t - \vec{r}\vec{v}_{\text{gr}}/c^2}{t_{\text{col}}(p)(1 - \tilde{v}_{\text{gr}}^2/c^2)}\right], \quad (6.109)$$

with another arbitrary function $\tilde{f}_0(\xi, p)$. The solution of the kinetic equation in the BM form is obtained from (6.108), (6.109) with the help of the replacement $t_{\text{col}} \rightarrow \delta t_s^B$, $\tilde{v}_{\text{gr}} \rightarrow v_{\text{gr}}$. Note that the same solutions, for δf instead of f , exist also in the case of the propagation of light resonances in a medium consisting of heavy particles, provided we exploit the ansatz that has been used above for the given case.

As follows from the solution (6.109), if $\tilde{v}_{\text{gr}}(p) > c$ and $v_{\text{gr}}(p) > c$ in some (p_0, \vec{p}) region, there might occur an instability with respect to the growth of superluminal modes that may result in some measurable effects, like a heating of the medium; cf. [122].

6.10. Validity of the gradient expansion

Many works, e.g., the recent review [21], use the BM form of the kinetic equation in practical simulations of the dynamics of resonances in heavy-ion collisions, since it allows to apply a simplifying test-particle method. Thereby, they assume that the appropriate time for a relaxation of resonances is δt_s^B rather than t_{col} . As we have demonstrated in examples, since $|\delta t_f| \sim v_0/\Gamma \gtrsim \delta t_s^B$, the gradient expansion may not hold on a typical time-scale $t_{\text{ch}} \lesssim v_0/\Gamma$ in the above-considered problems at $C \neq 0$. Only if the typical time-scale of the problem $t_{\text{ch}} \gg v_0/\Gamma$, the solutions of all three (BM, KB and non-local) forms of the kinetic equation and the mass-shell equation coincide.

Note that although the examples considered above show that the kinetic consideration might be not applicable for a description of the system relaxation toward equilibrium at $t \lesssim \delta t_s^B, t_{\text{col}}$, provided one considers propagation of off-mass-shell particle distributions, the quasiparticle limit proves to be the same for all three equations. More generally, the kinetic approach holds at $t \gtrsim \delta t_s^B, t_{\text{col}}$ at least for the wave packets with the energy integrated over a region near the maximum of the distribution; see [126].

Another remark is in order. In spite of the formulated caution it might be practical to use one of the above kinetic equations for actual calculations even beyond its validity region, since all these kinetic equations reveal approximate or even exact (as for the KB form of the kinetic equation) conservation laws of the 4-current and the energy–momentum [36, 37], thus, reasonably approximating the system evolution.

6.11. Hydrodynamical and thermodynamical limits

The hydrodynamical limit [125] is realized for $t \gg t_{\text{col}}$, when the distribution $f(X, p)$ obtains the form of the local equilibrium distribution (6.16). The hydrodynamical equations are derived from the conservation laws associated with the kinetic equation. The kinetic coefficients entering hydrodynamical equations are derived from the BM equation (valid in this limit), see [125]. They are expressed through the scattering delay time δt_s^{As} .

In the thermodynamical limit (global equilibrium, $\vec{u} = 0, T, \mu = \text{const}$) all thermodynamical quantities can be expressed solely in terms of the spectral functions of

the species [132] and, thereby, they can be related to the above-introduced Wigner time δt_W^A . The memory term yields a contribution to thermodynamical entropy and specific heat and might be associated with the memory time.

In general all species are described with the help of the dressed Green's functions. However, since there are relations between interaction and potential energies of the species, the interaction part can be transported from some species to other ones. This procedure is nevertheless ambiguous [132]. In order to demonstrate how the interaction can be transported to one of the species consider the isospin-symmetric pion–nucleon– Δ isobar gas in the limit of very low density at finite temperature [131]. It was assumed that pion and nucleon interact only via excitation of the intermediate Δ resonances. In the virial limit the memory term disappears. The thermodynamical potential becomes

$$\begin{aligned} \Omega(T, \mu_{\text{bar}}) = & 3TV \int \frac{d^3q}{(2\pi)^3} \ln [1 - e^{-\omega_\pi^{\text{free}}(\vec{q})/T}] \\ & - 4TV \int \frac{d^3p}{(2\pi)^3} \ln [1 - e^{-(E_N^{\text{free}}(\vec{p}) - \mu_{\text{bar}})/T}] \\ & - 16TV \int \frac{d^4p}{(2\pi)^4} B_0^\Delta(p_0, \vec{p}) \ln [1 - e^{-(p_0 - \mu_{\text{bar}})/T}], \end{aligned} \quad (6.110)$$

where the first two terms correspond to ideal gases of pions and nucleons and the third interaction term is expressed via the B_0^Δ function of the Δ resonance, $\omega_\pi^{\text{free}} = \sqrt{m_\pi^2 + \vec{q}^2}$, $E_N^{\text{free}} \simeq m_N + \vec{p}^2/(2m_N)$. The baryon density is split in the free nucleon and dressed Δ contributions

$$\begin{aligned} n_{\text{bar}} = n_N + n_\Delta = & -\frac{1}{V} \left(\frac{\partial \Omega}{\partial \mu_{\text{bar}}} \right)_{T,V}, \\ n_N = n_N^{\text{free}} = & 4 \int \frac{d^3p}{(2\pi)^3} \frac{1}{e^{(E_N^{\text{free}} - \mu_{\text{bar}})/T} + 1}, \\ n_\Delta = & 16 \int \frac{d^4p}{(2\pi)^4} \frac{B_0^\Delta}{e^{(p_0 - \mu_{\text{bar}})/T} + 1}. \end{aligned} \quad (6.111)$$

By decomposing B_0^Δ we may see that the first part of $n_\Delta = n_\Delta^{\text{Noether}}$ is the proper contribution of the Δ to the baryon density, and the second part proportional to $\frac{\partial \Sigma_\Delta}{\partial p_0}$ is the contribution of πN intermediate states to the dressed Δ . Thus, the flow spectral function B_0^Δ is related to the density of the Δ states according to equations (6.59), (6.60). This result is in line with the result (6.49) for the time shift of the Δ . Moreover in the example of a model with a finite number of levels, [145] has demonstrated that expression (6.59) describes the level density in the given interacting system.

In the limit $n_B \rightarrow 0$ one has $B_0 \rightarrow B_0^{\text{free}} = v_0 A^{\text{free}}$. In this limit the spectral function becomes the delta-function for stable particles but it remains a broad Lorentzian for 'free' resonances. The thermodynamics of free resonances was considered in [132]. Then all thermodynamic quantities are obtained from the corresponding ideal gas expressions after replacement of the element of the 3-phase-space $\frac{d^3p}{(2\pi)^3} \rightarrow \frac{d^3p}{(2\pi)^3} \int \frac{dp_0}{2\pi} v_0 A^{\text{free}}(p_0, \vec{p})$ and thereby they are expressed in terms of the Wigner time delay $\delta t_W^{\text{free}} = v_0 A^{\text{free}}$.

7. Space–time delays and measurements

7.1. The speed of the propagating wave packet

Consider the propagation of an initial distribution of off-mass-shell particles in a uniform medium or in vacuum. For a particle off mass shell there is, in general, no upper limit to its

speed. The distance of the order of the mean free path Δz in the z direction is passed by the maximum of the distribution at (E_m, k_m) with the velocity

$$v_m^{\text{shift}} = \frac{\Delta z}{\Delta t} = \frac{\Delta z' + \delta z_f}{\Delta t' + \delta t_f^{\text{kin}}}, \quad (7.1)$$

where $\Delta z'$ and $\Delta t'$ would characterize two acts of the collision/measurement (on average) without the variable shifts δz_f and δt_f^{kin} in the collision integral, equations (6.18), (6.49). Thus, the arrival of the peak of the wave packet at point $\Delta z' + \delta z_f$ (not $\Delta z'$) is delayed or advanced by δt_f . Under the assumption (done here for simplicity) that the variable shifts are small, the change of the speed of the propagating peak is

$$\delta v_m \simeq v_m^{\text{shift}} - v_{\text{ph}} = -\frac{B_0}{2\Delta t'}(v_{\text{ph}} - v_{\text{gr}}) + \frac{Z_0^{-1}}{\Gamma\Delta t'}(v_{\text{ph}} - \tilde{v}_{\text{gr}}), \quad (7.2)$$

where $v_{\text{ph}} = \Delta z'/\Delta t'$. Although for $\Delta t' \rightarrow \infty$ the change of the velocity (7.2) becomes negligibly small, it might be important for not-too-large values of the time intervals $\Delta t'$. For the Wigner resonances $v_{\text{gr}} = \tilde{v}_{\text{gr}} = v_{\text{ph}}$ and $\delta v_m = 0$. Nevertheless, even in this case the particles from the forward and backward tail of the distribution (for $E_m \pm \Delta E$, $k_m \pm \Delta k$) move between collisions with velocities slightly different from that of the peak, $\delta v_{\text{tail}} \sim \pm \frac{\partial v_{\text{gr}}}{\partial E} \Delta E \pm \frac{\partial v_{\text{gr}}}{\partial k} \Delta k \pm v_{\text{gr}}/(\Gamma_z \Delta t')$, where $1/\Gamma_z$ is the width of the wave packet, see equation (6.107). This causes a smearing of the wave packet.

If the distance of the free flight L is fixed by conditions of the measurement, then δz_f should be put to zero in equation (7.1), $v_m^{\text{shift}} = \frac{L}{\Delta t'}$, and

$$\delta v_m = -\delta t_f^{\text{kin}} \frac{v_{\text{ph}}}{\Delta t'} = \left(-\frac{B_0}{2\Delta t'} + \frac{Z_0^{-1}}{\Gamma\Delta t'} \right) v_{\text{ph}}, \quad (7.3)$$

$\delta v_m > 0$ for $\delta t_f^{\text{kin}} < 0$.

7.2. Measurements and resulting time delays and advances

There are several sources of time delays and advances.

- (i) Quantum mechanics, as well as quantum kinetics, says nothing about the motion of a single identifiable particle. The distribution of quantum particles, which occurs in the process of the smearing of wave packets during propagation, a scattering on a potential, particle collisions etc, is not the same entity as the incident distribution. To be sure that the particle beam propagating from $z = 0$ to $z = L$ is described by a certain distribution, e.g. by equation (6.107), one should measure a small fraction of it (not disturbing a bulk) at $(t = 0, z = 0)$ and then at $(t = t_L, z = L)$. After the measurement at $(t = 0, z = 0)$, particles disturbed by the measurement are effectively taken out of the distribution. Thus, at $(t = t_L, z = L)$ we deal with other particles from the initial distribution which were not tagged at $(t = 0, z = 0)$. It could then happen that the first particles registered at $t = t_L, z = L$ may additionally advance those particles, which are almost identical to the particles registered at $t = 0, z = 0$, typically by a time step

$$\delta t_{\text{tail}} \sim \pm 1/\Gamma_z.$$

So, the typical time advance of the signal arriving at $z = L$ is δt_{tail} . Certainly this time advance can be diminished by performing precision measurements of the peaks of the distribution at $z = 0$ and $z = L$ but this procedure needs special care.

- (ii) Another time delay/advance, $\sim \delta t_f^{\text{kin}}$, arises as it is seen from the collision term in the non-local form, that also manifests in the appearance of the Poisson-bracket fluctuation

contributions in the KB equation (provided the kinetics is described by the KB equation or by its non-local form). The result is given by equation (6.49). This time shift characterizes (on average) the time delay/advance between two successive collisions.

- (iii) Other time delay/advance is associated with the memory effects (yielding δt_{mem}) appearing in the processes of multiple interactions described by diagrams with more than two vertices. However, the value δt_{mem} diminishes in the case of a very dilute beam, since diagrams with three and more vertices bring additional powers of density.

Summing up these three delay/advance times for the total time shift we finally obtain

$$\delta t_{\text{tot}} \sim \delta t_{\text{tail}} + \delta t_{\text{f}}^{\text{kin}} + \delta t_{\text{mem}}. \quad (7.4)$$

7.3. Apparent superluminality in neutrino experiments as a time advance effect

In September 2011 the OPERA experiment [41] (see version 1 of the e-print) claimed measurement of muon neutrinos propagating with superluminal velocity, $(v - c)/c = [2.37 \pm 0.32(\text{stat}) \pm 0.34(\text{sys})] \times 10^{-5}$, at average energies $\langle E \rangle = 17$ GeV. This data agreed with the data obtained earlier by the MINOS collaboration [42]: $(v - c)/c = (5.1 \pm 2.9) \times 10^{-5}$, E -peaking is at ~ 3 GeV with a tail extending to 100 GeV, $d = 734$ km. An initial proton beam in the OPERA experiment produces a bunch of pions. Neutrinos produced in the reactions $\pi \rightarrow \nu \bar{\mu}$ pass through the ground the distance L and reach a detector. As initially announced by the OPERA collaboration, for the distance of $L = 730 \text{ km} \pm 20 \text{ cm}$ between the neutrino source in CERN and the detector in Gran Sasso the neutrino beam has acquired a time advance of $t_{\text{adv}} = 57.8 \pm 7.8(\text{stat}) + 8.3 - 5.9(\text{sys})$ ns compared to that of neutrinos moving with the speed of light. In February 2012 the OPERA collaboration has informed [146]¹¹ that it has identified two possible effects that could have an influence on its neutrino timing measurement. The first possible effect concerns an oscillator used to provide the time stamps for a GPS synchronization. The second concerns an optical fiber connector that brings the external GPS signal to the OPERA master clock. At the 25th International Conference on Neutrino Physics and Astrophysics in Kyoto (8 June 2012), a final update on the OPERA time-of-flight measurement was reported $t_{\text{adv}} = 1.6 \pm 1.1(\text{stat}) + 6.1 - 3.7(\text{sys})$ ns.

Not entering into details of the given experiment and its deficiencies, we consider a principle possibility to obtain a time advance of the order of $\sim 10 - 10^2$ ns in the neutrino experiments. Although many different possibilities were discussed in the literature, the effects, which we will consider, were not mentioned. Simplifying, we assume that the initial $z = 0, t = 0$ point is well-fixed with the help of heavy protons. The final point $z = L, t = t_L$ is fixed by reactions of the neutrinos on the forward front of the propagating packet with nuclei in the detector. We will argue that apparent superluminality can be associated with the effects of the time advances considered in the given paper.

The maxima of the wave packets of protons and neutrinos produced in the two-step process $p \rightarrow \pi^+ + n_{\text{nucl}} \rightarrow n_{\text{nucl}} + \mu^+ + \nu_{\mu}$ at CERN (n_{nucl} is a neutron from a nucleus-target) are separated by the time interval $\sim 1/\Gamma_{N\pi} + 1/\Gamma_{\pi\nu}$, $N = p$ here. Thereby a time advance of the neutrinos arises owing to the advance of pions compared to protons and neutrinos, $\delta t_{\text{adv}}^{\nu} = \delta t_{\text{adv}}^{N\pi} + \delta t_{\text{adv}}^{\pi\nu}$, where $\delta t_{\text{adv}}^{N\pi} = -1/\Gamma_{N\pi}$ and $\delta t_{\text{adv}}^{\pi\nu} = -1/\Gamma_{\pi\nu}$. The value $\delta t_{\text{adv}}^{\pi\nu} = -1/\Gamma_{\pi\nu} = -26$ ns is due to the width $\Gamma_{\pi\nu}$ of the production of the neutrino in the process $\pi \rightarrow \nu \bar{\mu}$. The value $\delta t_{\text{adv}}^{N\pi} \sim -10^{-23}$ s is much shorter and can be neglected. The origin of the resulting time advance $\delta t_{\text{adv}}^{\nu}$ arising in this process was illustrated by figure 15. So we believe that the width $\Gamma_z \sim \Gamma_{\pi\nu}$ in the initial neutrino wave packet may yield $\delta t_{\text{tail}} \sim \delta t_{\text{adv}}^{\pi\nu}$ (-26 ns) of advance, see point (i) of section 7.2.

¹¹ From the CERN director Rolf Heuer, rolf.heuer@cern.ch, 23 February 2012.

Another contribution to the time advance $\delta t_f^{\text{kin},\nu} \sim -1/\Gamma_{\pi\nu}$ (-26 ns) arises if the virtual pion propagation is described by the KB kinetic equation or by its non-local form for $|M_\pi| \gg \Gamma_{\pi\nu}/2$, as it follows from equation (6.49), see point (ii) of section 7.2.

Summing up two possible time advances, for the ‘most rapid’ particles we find $\delta t^\nu = \delta t_{\text{adv}}^\nu + \delta t_f^\nu \sim -2/\Gamma_{\pi\nu} = -52$ ns. This agrees well with the primary announced result of the OPERA experiment.

Note that, provided neutrino flux in the ground corresponds to off-shell neutrinos, see equation (7.3), an additional time advance could occur. But this effect resulting in $\delta v_{\text{gr}} \propto G_W^2$, where G_W is the coupling constant of the weak interaction, is very small, since $c/\Gamma_{\pi\nu} \gtrsim L$. Thus, most likely neutrinos produced at CERN undergo almost free flight to the detector in Gran Sasso. Likely, the smearing effect of the wave packet is also tiny for the conditions under consideration.

Summarizing, one may expect few of $\delta t_{\text{adv}}^{\pi\nu}$, as typical time advances in the neutrino experiments like those performed by the OPERA and MINOS. If our interpretation is correct, a time advance, which could possibly be measured in neutrino experiments, like the OPERA experiment, should not significantly depend on the distance L between the source and the detector; however, its value is very sensitive to the conditions by which the initial and final time moments are fixed in the measurements. From the description of the mentioned OPERA experiment it is not sufficiently clear how this fixation was performed.

8. Conclusion

The aim of the present review is to give a coherent overview of how various measures used to quantify the durations of processes in classical and quantum physics appear and to explicate their interlinking.

8.1. Classical mechanics

For time measurements in classical mechanics, besides ordinary time characteristics, such as the oscillation period P , the phase time shift $\delta t_{\text{ph}} = \hbar\delta/E$ (here E denotes the particle energy and $\hbar\delta = S_{\text{sh}}$ stands for the mechanical shortened action) and the decay time t_{dec} , we introduced other quantities such as the dwell time t_{d} , the sojourn time t_{soj} and the group delay $t_{\text{gr}}^{\text{1D}} = \partial\hbar\delta/\partial E$. We discussed the relations between these times. For example, we demonstrated that the classical sojourn time delay is negative in the case of attractive 1D potentials and positive for repulsive 1D potentials. In the 3D case the situation is more involved. For the spherically symmetric potential there is no direct correspondence between the sign of the potential and the sign of the classical sojourn time delay. Also for the radial motion there appears an extra factor of two in the classical group time delay compared to the 1D case, because the coordinate integration is restricted by $r > 0$ in the former case, and goes from $-\infty$ to ∞ in the latter case, $t_{\text{gr}}^{\text{3D}} = \delta t_{\text{W}} = 2\partial\hbar\delta/\partial E$. Namely, the latter quantity was originally introduced by Wigner and Eisenbud for quantum scattering [1].

Then we studied examples demonstrating time advances and delays of a damped oscillator $z(t)$ under the action of different external forces $F(t)$. We applied the Green’s function formalism exploiting extensively quantum field theory and quantum kinetics. To establish a closer link to the formalism of the quantum field theory, we introduced the dynamical variable—a ‘field’— $\phi(t) = mz(t)$. The source term in the Lagrange equation depends nonlinearly on ϕ and linearly on the external force. The formalism allows a natural diagrammatic interpretation of the solution of the Lagrange equation.

First, we considered the response of the damped harmonic oscillator with the resonance frequency E_R and of the damping width Γ to a sudden change of an external constant force. The response is purely causal in this case. The larger is the damping width Γ of the oscillator, respectively the shorter is the damping time $t_{\text{dec}} = 1/\Gamma$ and the longer is the phase time δt_{ph} , showing the time shift of the oscillations. For $\Gamma \rightarrow 2E_R$ the oscillation frequency vanishes, $P \rightarrow \infty$, and the phase shift δt_{ph} becomes infinite, but the ratio $\delta t_{\text{ph}}/P$ remains finite, $\delta t_{\text{ph}}/P \rightarrow 1/4$.

Then we demonstrated that in the case of an external force acting over a finite time interval, the damped harmonic oscillator can exhibit an apparently acausal reaction: the maximum of the oscillator response may occur before the maximum of the external force. Thus, if for the identification of a signal we used a detector with the threshold close to the pulse peak, such a detector would register a peak of the response of the system before the input's peak.

Next we considered a possibility of an advanced response also on the example of a periodic driving force with a constant frequency acting on a damped nonlinear oscillator. In the linear approximation with respect to the anharmonicity parameter, there appears an overtone peaked at frequency $E_R/2$. Thus, there arises an extra phase time-scale characterizing the dynamics of the overtone. When the frequency of the force is $E_p \sim \frac{1}{2}E_R$, the overtone can produce an additional maximum in $z(t)$, which would appear, as occurring before the actual action of the force. The system would seem to 'react' in advance.

In the case when the external force acting on a damped anharmonic oscillator with the resonance frequency E_R is a packet of modes grouped near frequency E_p with the width $\sim \gamma$, the typical time for which the envelope function fades away is $t_{\text{dec}}^{\gamma,(\text{cl})} = 1/\gamma$ for $\gamma \ll \Gamma$. In a linear approximation in anharmonicity parameter there appear two resonance group time delays, $t_{\text{gr}}^{(1)} = A_1/2 = \frac{\Gamma/2}{(E_p - E_R)^2 + \Gamma^2/4}$ and $t_{\text{gr}}^{(2)} = A_2/2 = \frac{\Gamma/4}{(E_p - E_R/2)^2 + (\Gamma/2)^2/4}$ one peaked at E_R , and another one, at $E_R/2$. These group time delays appear because the system responds slightly differently to various frequency modes contained in the force envelope. Oscillations of the carrier wave are delayed by the phase times, whereas the amplitude modulation is delayed by the group times. We introduced a new quantity—the forward time delay/advance, $\delta t_f^\gamma = t_{\text{gr}} - t_{\text{dec}}^{\gamma,(\text{cl})}$ —which takes into account that the delays of the wave groups are starting to accumulate before the external force reaches its maximum with an advance determined by the width of the force packet. When the external force frequency E_p is near the oscillator resonance frequency E_R the forward time is positive, which corresponds to a delayed response, but in the off-resonance region the forward time changes its sign, that corresponds to an advanced response. In the limit $\gamma \rightarrow 0$ we arrive at the case of a purely periodic force. An interesting effect is that the frequency of the carrier wave is changed and becomes time dependent. When E_p approaches E_R not only the amplitude of the system response grows but also the response lasts much longer than the force acts. Thereby we demonstrate the effect of a smearing of the wave packet in classical mechanics.

Further on, time shifts appearing in the 3D classical scattering problem were considered in the example of the particle scattering on hard spheres of radius R . We derived the limits on the values of time advances: the sojourn time advance, being equal to the Wigner time advance, is limited by $\delta t_W = 2 \frac{\partial \hbar \delta}{\partial E} > -2R/v$, where v is the particle velocity. We introduced another relevant quantity, the scattering time delay: the difference in time when the particle touches the sphere surface and the time when the particle freely reaches the center of the sphere. This time characterizing delay of scattered waves is half the size of the Wigner time delay.

Next, we discussed time delays appearing in classical electrodynamics. More specifically, we studied the problem of the radiation of a damped charged oscillator induced by an external electromagnetic plane wave. We introduced the scattering amplitude, the cross-section and

related them to the phase shift. As the cross-section, the scattering group time delay has a resonance shape. The damping is determined by the sum of the oscillator and radiation damping widths. The scattering group time delay (the scattering delay time) is half the size as the Wigner delay time.

For the scattering of light on a hard sphere of radius R , we show that the appearance of a temporal advance in the signal propagation does not contradict causality.

8.2. Quantum mechanics

We studied time shifts arising in different quantum mechanical problems. More specifically we considered 1D tunneling and 3D quantum scattering of non-relativistic particles.

8.2.1. One-dimensional quantum mechanical motion. To be specific we assumed that the potential $U > 0$ acts within a finite segment $-L/2 \leq z \leq L/2$. For the particle motion above the barrier ($E > U$) both the dwell time and the traversal time t_{trav} are relevant quantities depending on the distance passed by the particle. High above the barrier they are reduced to the free flight time L/v . However at energies below the barrier the traversal time becomes imaginary. For the rectangular barrier the dwell time is always smaller than the classical traversal time for energies of the scattered particle $E < U$ for a broad barrier and for $E < \frac{3}{4}U$ for a thin barrier. For the case of the tunneling through a very broad barrier of an arbitrary form the dwell time in the region under the barrier is determined by the evanescent wave and describes, thereby, neither particle transmission nor the dwell of transmitted waves. In this particular case the dwell time is determined by the quantum time-scale, which is shorter than the classical traversal time of the same region would be.

Then we considered propagation of wave packets. For a free moving packet we recover the well-known result that the width of packet increases with time. For a typical time of smearing of the packet we get $t_{\text{sm}} \sim \hbar m / \gamma_p^2$, where γ_p is the width of the packet momentum distribution. Then we consider scattering of wave packets with negligibly small momentum uncertainty. According to the method of the stationary phase, the position of the maximum of an oscillatory integral is determined by the stationarity of the complex phase of the integrand. Eisenbud and Wigner used this method to introduce two measures of time that could characterize the wave propagation within the potential region: the difference of time when the maximum of the incident packet is at the coordinate $z = -L/2$ and the time when the maximum of the transmitted packet is at $z = +L/2$, and the difference of the time when the maximum of the incident packet and the maximum of the reflected packet are at the same spatial point $z = -L/2$. We call these time intervals the transmission and reflection group time delays, t_T and t_R . Moreover one introduces the bidirectional scattering group time t_{bs} composed of the transmitted and reflected group times weighted with probabilities of the transmission and the reflection. We argue that in the case of tunneling the group times show time delays on the edges of the barrier on the scale of quantum length near the turning points. In case of the broad barrier the bidirectional group time delay is mainly determined by the reflection group time delay. The difference between the bidirectional scattering time delay and the dwell time is now a time delay/advance due to the interference of waves δt_i . This interference time term is absent in the case of classical motion. The interference time proves to be negative (advance) for under-the-barrier motion. Within the semiclassical approach for the tunneling the bidirectional scattering time equals zero. The difference with the exact result is due to the fact that in the region near the turning points, where the group time delays are accumulated, the semiclassical approximation is not applicable. For the scattering of an arbitrary wave packet the sojourn time appears as the dwell time averaged over the momentum distribution in the packet. Therefore,

from the definition of the sojourn time one extracts basically the same information as from the definition of the dwell time. For the particle motion well above the barrier the dwell and the group times are reduced to the appropriate traversal time proportional to the length of the distance passed by the particle, and the interference time vanishes.

The phenomenon that for a very broad barrier the dwell and the group times are reduced to the quantum time not proportional to the barrier length is known as the Hartmann effect. We clarified the reasons for the appearance of the Hartmann effect and formulated arguments why the group times and the dwell time are not appropriate quantities to measure the tunneling time.

Operating with the group times, and then related to them dwell time, one assumes that the position of a particle can be identified with the position of the maximum of the wave packet. However, it is not so easy to experimentally distinguish the peak position of a spatially broad packet. Then, to specify the position of the particle we studied the motion of the centroids (centers of mass) of the incident, transmitted and reflected wave packets. We showed that the barrier acts as a filter letting with higher probability penetration for the modes with higher energies. As the result, all three packets move with different velocities at large distances from the potential region. Also the widths of transmitted and reflected packets differ from the width of the incident packet. We demonstrated that in the case of $\gamma_p L \ll \hbar$ the centroid transmission and the reflection time delays are mainly determined by the wave packet formation times $t_{\text{form,T}}$, $t_{\text{form,R}}$. These quantities show averaged passage times by particles of the typical spatial packet length \hbar/γ_p . The term $\propto L\gamma_p$ entering the expression for $t_{\text{form,T}}$ but not entering $t_{\text{form,R}} \simeq t_{\text{form,I}}$ corresponds to an advance, since the transmitted wave packet moves with a higher velocity compared to the reflected and incident wave packets. Dependence on L may indicate that the passage time of the barrier might be proportional to its length.

More complete information about the temporal behavior of the packets can be extracted from the explicit forms of the spatial distributions. To elucidate these aspects further, we have considered explicitly a Gaussian wave packet tunneling through a barrier. We found that because of the smearing effect the longer is the barrier, the broader is the transmitted wave packet being formed for $z \geq L/2$ with a delay depending on the length scale. In further study, considering the propagation of waves on time-scales shorter than t_{sm} we neglected the effects of smearing. The probability (on the right wing of the packet) to meet the particle at $z = L/2$ becomes the same, as it were in the case of the monochromatic wave with $E = E_p$ (the stationary problem), at the time moment when the maximum of the incident wave packet did not yet reach the barrier and the maximum of the transmitted wave packet did not yet emerge at $z = L/2$. For a very broad rectangular barrier of the height U placed at $-L/2 \leq z \leq L/2$, the peak of the transmitted wave packet is formed at the right border of the barrier, after a quantum time delay (not dependent on the barrier depth) from the moment when the peak of the incident wave packet reaches the left border of the barrier (the Hartmann effect). The probability to meet the particle at $z = L/2$ again (now on the left wing of the packet) becomes the same, as it were in the case of the monochromatic wave with the energy E_p , when the maximum of the transmitted wave packet achieves the point $z \simeq L/2 + Lvm/\kappa + \hbar p(p^{-2} - \kappa_p^{-2})$, where $\kappa_p = \sqrt{2mU - p^2}/\hbar$, the traversal time $t_{\text{trav}}^{\text{un}} = Lm/\kappa$ is much larger than the (third) quantum time term. Thus, we are able to associate the time $t_{\text{trav}}^{\text{un}}$ with the passage time of the barrier for waves with $E \simeq E_p$. Thereby, we believe that this observation can be interpreted, as a resolution of the Hartmann paradox.

Since the packet has a width, the probability to find the particle at a given point becomes essentially non-zero already before the center of the packet with the energy dispersion γ has reached it, with an advance $t_{\text{dec}}^\gamma = \hbar/\gamma$. In accord with the Mandelstam–Tamm uncertainty relation it has the meaning of the time during which the wave packet passes a given

space point. Thus, the real (forward) delay/advance time at $z = L/2$ is not t_{bs} but $\delta t_{\text{f}}^{\text{un}} = t_{\text{bs}} - t_{\text{dec}}^{\text{r}}$.

Next, we studied resonance states and their time evolution. We considered a scattering on the potential well of the length l_{R} (a resonator) with an infinite wall at the origin separated from the region $z > l$ by the rectangular barrier of the height U and thickness $l - l_{\text{R}}$. The scattering amplitude is shown to possess simple poles for complex energies $E = E_{\text{R},i} - i\Gamma_i/2$, $i = 1, \dots, n$. The calculated dwell and reflected group time exhibit strong resonance enhancement for energies $E \sim E_{\text{R},i}$. Hence, the incident packet spends in the interaction region much longer time than the typical passage time of this region by a particle with the mean velocity of the packet. For energies tuned from $E_{\text{R},i}$ by more than the resonance width the internal part of the potential becomes inaccessible to the incident wave. In view of the symmetry of the problem it is possible to introduce the single-way dwell time and the scattering time, which can be related to the number of resonance states per unit energy and are equal $t_{\text{d}}^{\text{s.w.}}(0, l) \simeq t_{\text{s}} = \hbar A/2 = \frac{\hbar\Gamma/2}{(E-E_{\text{R}})^2+\Gamma^2/4}$. The sum-rule for the scattering time delay is preserved. We constructed the set of the eigenfunctions for the given scattering problem and used them in the analysis of the evolution of some initially localized state. The properties of the survival probability for this state are discussed. The relations between the survival probability and the retarded Green's function are obtained. It is shown that the decay time $t_{\text{dec}} = \hbar/\Gamma$ of the resonance state can be calculated as the sojourn time of the wave function within the interval $(0, l)$. The forward scattering time $\delta t_{\text{f}} = t_{\text{s}} - t_{\text{dec}}$ is shown to correspond to some delay in the scattering of particles with energies nearby the energy of the quasi-stationary level and to an advance for $|E - E_{\text{R}}| > \Gamma/2$. The causality restriction becomes $\delta t_{\text{s}} = \frac{\partial \hbar \delta}{\partial E} > -l/v - \hbar/2kv$. The term $\hbar/2kv$ is of purely quantum origin. It shows the time, which the particle needs in order to pass half of the de Broglie wavelength of the particle, $\lambda = \hbar/k$. Following the uncertainty principle free quantum particles cannot distinguish distance $\xi < \hbar/2k$.

8.2.2. The three-dimensional scattering problem. We considered the 3D scattering problem on a central potential and discussed the difference compared with 1D-scattering. We introduced the sojourn time $\delta t_{\text{vol}}^N = \delta t_{\text{s}}^N - \delta t_{\text{i}}^N$ and the corresponding scattering and interference times, all normalized by the incident flux. The Wigner group time delay $\delta t_{\text{W}}^N = \delta t_{\text{vol}}^N = 2 \frac{\partial \hbar \delta^l}{\partial E_p}$ appears as the group time delay of the divergent wave taking into account interference with the incident plane wave, δ^l is the phase shift of the radial wave function. The scattering group time $t_{\text{s}} = t_{\text{free}} + \delta t_{\text{s}}$ is normalized by the scattered flux. The scattering group time delay $\delta t_{\text{s}} = \delta t_{\text{W}}/2$ appears as the delay of the purely scattered wave. The decay time appears as $t_{\text{dec}} = \delta t_{\text{vol}}^N/4 \sin^2 \delta^l$.

Then we studied scattering on a Wigner resonance with a constant width Γ . The probability for a particle to enter the region of the resonance interaction can be written as $P_{\Gamma} = \sin^2 \delta = \frac{\Gamma^2/4}{M^2 + \Gamma^2/4} = A\Gamma/4$, where $M = E - E_{\text{R}}$. The cross-section of the resonance scattering can be presented as $\sigma \simeq 4\pi\lambda^2 P_{\Gamma}$ with $\lambda = \hbar/k$ standing for the de Broglie wavelength. For $M = 0$ (i.e. exactly at the resonance) the cross-section reaches its maximum $\sigma_{\text{max}} = 4\pi\lambda^2$. The scattering time delay coincides with the single-way dwell time $\delta t_{\text{s}} = \hbar \frac{\partial \delta}{\partial E} = t_{\text{d}}^{\text{s.w.}} = \hbar A/2$. The forward time delay coincides with the interference time. The forward time delay $\delta t_{\text{f}} = \delta t_{\text{i}} = \hbar A/2 - t_{\text{dec}} = t_{\text{dec}} (\sin^2 \delta - \cos^2 \delta)$ is the time delay of the decay because of the difference in the probability for the particle to enter the region of the resonance interaction ($\sin^2 \delta$) and not to enter this region ($\cos^2 \delta$). The forward delay/advance time, δt_{f} , is then an average delay/advance in the scattering counted from the decay time t_{dec} . Explicitly, for the Wigner resonances we derive expression $\delta t_{\text{f}} = -\hbar \frac{M^2 - \Gamma^2/4}{\Gamma(M^2 + \Gamma^2/4)}$. Thus δt_{f} corresponds to a delay for $|M| < \Gamma/2$ and to an advance for $|M| > \Gamma/2$.

We discussed quantum mechanical scattering on hard spheres of radius R . For $l = 0$ we find $\delta t_s^0 = \hbar \frac{\partial \delta^0}{\partial E_k} = -R/v$. The same advance, $\delta t_s^l = -R/v$, arises for rapid particles $kR/\hbar \gg l^2$ at angular momenta $l \neq 0$. For slow particles, $kR/\hbar \ll l^{1/2}$, $\delta t_s^l \propto (kR/\hbar)^2 R/v$. When the de Broglie wavelength $\lambda = \hbar/k \gg R$ the propagating wave almost does not feel the presence of the sphere. Thus, for $l \gg 1$ the cross-section becomes negligibly small.

Then, using a semiclassical expression for the phase shift we considered the similarity and difference between semiclassical and classical expressions for the time delays. Also, we discussed ergodicity and related the scattering time shifts to the level density. The Wigner delay can be interpreted as a time delay in an elementary phase-space cell: $\delta t_W = 2\delta t_s = 2\pi \hbar dN^{\text{level}}/dE_p$. Examples of the resonance scattering and scattering on hard spheres were considered.

8.3. Quantum field theory

We considered time shifts as they appear in quantum field theory. Knowing the Lagrangian one constructs the generating functional on the Schwinger–Keldysh contour [34]. Varying this functional one reproduces the equation of motion for the mean field and four Dyson equations for the non-equilibrium Green's functions G^{ij} , $i, j = \{+, -\}$. These Green's functions can be expressed in terms of Feynman diagrams only, if the typical times in the problem are longer than the typical time-scale of the interaction t_{int} (the principle of weakening of initial correlations) and the typical spatial scale is longer than the interaction scale l_{int} . Further we assume that these conditions are fulfilled. Dropping short-range correlations at each time step causes a growth of the entropy with time, which is associated with the thus obtained Dyson equations. The scattering time delay is expressed in terms of the Wigner-transformed imaginary part of the retarded Green's function $A = -2 \text{Im} G^R(X, p)$ and the decay time, in terms of the Wigner-transformed imaginary part of the retarded self-energy, $\Gamma = -2 \text{Im} \Sigma^R(X, p)$. The self-energy is defined here as $\Sigma^R = G_0^{-1} - [G^R]^{-1}$, where G_0 is the free Green's function. The equilibrium particle occupations (in the Boltzmann limit) relate to a delay of the scattering time and an advance of the collision time.

We discussed typical duration times for the reactions, which occur via intermediate states. We showed that the reaction times may cause an advance for some processes. Integration over 4-coordinates in intermediate reaction states of Feynman diagrams, runs over all times, $-\infty < t_z < \infty$ for any point z corresponding to an intermediate reaction state. For $t_y < t_z < t_x$, where x and y are external space–time points and $t_x < t_y$, the process which occurs at t_z is delayed compared to that which occurs at t_y , and for $t_z < t_y < t_x$ the process which occurs at t_z is advanced compared to that which occurs at t_y . Both time processes must be incorporated, as dictated by the Lorentz invariance. A typical time-scale of the integration over t_z is $v_0 \hbar/\Gamma$, where Γ is the typical width of the process under consideration and $v_0 = \partial G_0^{-1}/\partial p_0$. In other words, $v_0 \hbar/\Gamma$ is the typical time required for the formation of the wave packets of the resulting particles. For instance, if there occurs a two-step process, e.g. $p \rightarrow n + X + \pi_{\text{virt}}^+ \rightarrow n + X + \nu_\mu + \mu^+$, its duration is characterized by the time $t_v^{\text{dec}} = t_{N\pi}^{\text{dec}} + t_{\pi\nu}^{\text{dec}}$. Here $t_{N\pi}^{\text{dec}} = \hbar/\Gamma_{N\pi}$ is the life-time of the virtual pion produced in the process $p \rightarrow n + X + \pi_{\text{virt}}^+$ and $t_{\pi\nu}^{\text{dec}} = \hbar/\Gamma_{\pi\nu}$ is the life-time of the virtual pion produced in the process $\pi_{\text{virt}}^+ \rightarrow \nu_\mu + \mu^+$. This means that virtual pions, being produced in the process $p \rightarrow n + X + \pi_{\text{virt}}^+$, in the subsequent process $\pi_{\text{virt}}^+ \rightarrow \nu_\mu + \mu^+$ undergo time delays and advances on a time-scale $-t_{\pi\nu}^{\text{dec}} \lesssim t_2 - t_1 \lesssim t_{\pi\nu}^{\text{dec}}$, where t_2 characterizes the act of the production of ν and t_1 , of the absorption of p .

Also, we showed how the sojourn time can be expressed in terms of the non-equilibrium Green's function.

8.4. Quantum kinetics

Assuming that time–space scales characterizing the dynamics of collective modes are larger than microscopic time–space scales one exploits the Wigner transformation for the Green’s functions (the Fourier transformation in $\xi = (t_1 - t_2, \vec{r}_1 - \vec{r}_2)$). Within the first-order space–time gradient approximation over $\frac{1}{2}(t_1 + t_2, \vec{r}_1 + \vec{r}_2)$ one derives dynamical equations for the four Green’s functions. It is important to notice that although we derived four Dyson equations for four complex Green’s functions, only two real quantities are independent. As independent real variables it is convenient to use the spectral function $A(X, p) = -2 \text{Im} G^R(X, p)$ and the $iG^{-+}(X, p)$ Green’s function (the Wigner density). It proves to be that the retarded Green’s function satisfies the algebraic equation (up to second-order space–time gradients) and iG^{-+} Green’s function fulfils the first-order gradient generalized kinetic equation. The other (mass-shell) equation, describing propagation of the off-mass-shell particles on equal footing with the generalized kinetic equation, should coincide with the generalized kinetic equation provided all approximations are done consistently.

We demonstrated that the generalized kinetic equation can be presented in three forms, the proper Kadanoff–Baym (KB) form, the Botermans–Malfliet (BM) form and the non-local form. The BM form follows from the KB form provided space–time gradients are small and moreover the system is close to the local equilibrium. The non-local form differs from the KB one only in the second-order gradient terms in the expansion of the collision term and it coincides with the BM form, if one retains only zero-gradient terms in the gradient expansion of the collision term. In the collision term of the non-local kinetic equation there arise 4-coordinate-momentum shifts in space–time variables. They appeared due to the Poisson-bracket term that differs the KB form of the kinetic equation from the BM one. We discussed the meaning of the BM effective current, the Noether and the effective B -current and the memory current. Then we analyzed delays and advances, as they appear in the non-local form of the kinetic equation for off-mass-shell particles. There appear several time delays: the Wigner, scattering, collision, forward, memory, Noether, drag-flow and back-flow delays. Thus, the physical meaning of the Poisson-bracket term in the KB equation is fully clarified. The forward time delay appears as the time shift in the collision term: $\delta t_f^{\text{kin}} = \delta t_s^B - t_{\text{col}}$, where the kinetic scattering time delay is $\delta t_s^B = \hbar B_0/2$ and the collision delay is $t_{\text{col}} = \hbar Z_0^{-1}/\Gamma$, $B_0 = A(Z_0^{-1} - M\Gamma^{-1} \frac{\partial \Gamma}{\partial E})$, and for non-relativistic particles $M = E - p^2/2m + \text{Re}\Sigma^R$, $Z_0^{-1} = 1 - \frac{\partial \text{Re}\Sigma^R}{\partial E}$. In the absence of the energy retardations in the response of the medium (Wigner resonances) the kinetic times δt_s^B , t_{col} and δt_f^{kin} appropriately transform into the similar quantities introduced in quantum mechanical scattering on potentials and in the case of resonance scattering.

Moreover we related time delays to the density of energy states with and without interaction terms. In the low density limit the time-shift which appears in the non-local collision term is just the forward time delay/advance discussed above for classical and quantum mechanical motions. Then we discussed application of the test-particle method to solve the BM and non-local kinetic equations. The analysis of the test-particle trajectories also sheds light on the meaning of the space–time shifts. We showed then how the appropriate quasiparticle limit can be recovered. A superluminality problem is briefly discussed. Apparent superluminal propagation has been indeed manifested in some laser experiments. This phenomenon can be understood as the consequence of a reshaping of the pulse envelope by interaction within the medium. Although formally the group velocity may in some cases exceed c , the forward wavefront moves with velocity $\leq c$.

Next, we calculated entropy flow for the non-local form of the kinetic equation and compared it with the flows for the BM and the KB forms of the kinetic equation. We related the forward time delay to the difference in the expressions for the KB and the BM kinetic

entropies. Note that, in principle, the presence or absence of an additional non-equilibrium correction to the specific heat proportional to the collision term can be experimentally verified.

Then choosing some reduction ansatz for the initial non-equilibrium configurations we found specific solutions of the kinetic equations in the BM, KB and non-local forms and solutions of the mass-shell equation, which, in general, differ from each other and coincide only, if the typical time-scale characterizing the system dynamics is larger than the forward time delay/advance. The latter is typically of the order of the collision time. Thus, we uncover some problems with simulations of heavy-ion collisions using the test-particle method, if one deals with the kinetic equation in the BM form for typical time of the order of the mentioned time-scales. In specific energy–momentum regions (e.g. for small Γ and larger $|M|$) the typical scattering time, which characterizes the evolution of the BM equation, $\delta t_s^B \sim \hbar v_0 A/2$, can be much shorter than $t_{\text{col}} \sim \hbar v_0/\Gamma$ characterizing evolution of the KB equation. In spite of the mentioned problems it might be practical to use one of the above kinetic equations for actual calculations even beyond its validity region, since all these kinetic equations reveal approximate or even exact (as the KB form of the kinetic equation) conservation laws of the 4-current and the energy–momentum tensor, thus approximating reasonably the system evolution. The hydrodynamical limit is realized for $t \gg t_{\text{col}}$, when particle distributions acquire the form of the local-equilibrium distribution. For such a distribution the collision term turns to zero. The hydrodynamical equations are derived from the conservation laws associated with the kinetic equation. The kinetic coefficients entering hydrodynamical equations are derived from the BM equation (valid in this limit). They can be expressed through the scattering time delay δt_s^B . We also demonstrated the possibility of the appearance of an instability for superluminal off-mass-shell particles.

Finally we presented a possible interpretation of the apparent superluminality, which may manifest in experiments, like the OPERA and MINOS neutrino experiments, and in similar experiments expected to be settled in nearest future. The maxima of the wave packets of protons and neutrinos produced in the two-step process $p \rightarrow \pi^+ + n_{\text{nuc}} \rightarrow n_{\text{nuc}} + \mu^+ + \nu_\mu$ at CERN (here n_{nuc} is a neutron from a target nucleus) are separated by the time interval $\sim \hbar/\Gamma_{p\pi} + \hbar/\Gamma_{\pi\nu}$. Thereby a time advance of the neutrinos may arise owing to an advance of pions compared to protons and neutrinos, $\delta t_{\text{adv}}^\nu = \delta t_{\text{adv}}^{N\pi} + \delta t_{\text{adv}}^{\pi\nu}$, where $\delta t_{\text{adv}}^{N\pi} = -\hbar/\Gamma_{N\pi}$ and $\delta t_{\text{adv}}^{\pi\nu} = -\hbar/\Gamma_{\pi\nu}$. The value $\delta t_{\text{adv}}^{\pi\nu} \sim -\hbar/\Gamma_{\pi\nu} = -26$ ns is due to the width $\Gamma_{\pi\nu}$ of the production of the neutrino in the process $\pi^+ \rightarrow \nu_\mu + \mu^+$. Thus, one may expect a few $\delta t_{\text{adv}}^{\pi\nu}$, as a typical time advance in the neutrino experiments like those performed by the OPERA and MINOS.

Some details of calculations and helpful relations are deferred to appendices A–E. In appendix F we discuss H theorem for three forms of the generalized kinetic equation and argue for the minimum of the entropy production related to the generalized kinetic equation.

Concluding, we discussed the similarities between the description of time delays and advances for various systems, like classical oscillating systems, 1D quantum mechanical tunneling, the decay of quasi-stationary states, 3D scattering, reactions and quantum kinetical processes.

Acknowledgements

We thank Yu B Ivanov, B M Karnakov and V D Mur for fruitful discussions. The work was partially supported by ESF Research Networking Programme POLATOM and by grants VEGA 1/0457/12 and APVV-0050-11 (Slovakia).

Appendix A. Virial theorem for infinite classical motion in a central potential

Here we give a short recount of the derivation of the virial theorem (2.17) by Demkov in [44]. The derivation is based on the suggestion of Fock [147] to combine the variational principle of mechanics and the scale transformation of coordinates.

Consider a particle of mass m moving in a central field $U(r)$ diminishing sufficiently rapidly for $r \rightarrow \infty$. The equation of motion of the particle between times t_1 and t_2 follows from the requirement of the vanishing of the action variation around the true trajectory

$$\delta S = \int_{t_1}^{t_2} \delta L(\vec{r}, \vec{v}) dt \quad (\text{A.1})$$

with the Lagrange function $L = \frac{1}{2}m v^2 - U(r)$.

Consider now a particular variation around the trajectory, $\delta \vec{r} = \epsilon \vec{r}(t)$, with an infinitesimally small parameter ϵ . The variation of the action is now not zero, since the variation $\delta \vec{r}$ does not vanish at the ends of the time interval and is given by $\delta S = \epsilon \left(\frac{\partial L(t_2)}{\partial \vec{v}} \vec{r}(t_2) - \frac{\partial L(t_1)}{\partial \vec{v}} \vec{r}(t_1) \right)$. On the other hand we can calculate δS by expanding the Lagrange function in (A.1) directly. Equating terms linear in ϵ in both expressions, we obtain

$$\delta S = \epsilon \int_{t_1}^{t_2} \left(\frac{\partial L}{\partial \vec{r}} \vec{r} + \frac{\partial L}{\partial \vec{v}} \vec{v} \right) dt = \epsilon \left(\frac{\partial L(t_2)}{\partial \vec{v}} \vec{r}(t_2) - \frac{\partial L(t_1)}{\partial \vec{v}} \vec{r}(t_1) \right), \quad (\text{A.2})$$

and, substituting the Lagrange function, arrive at

$$\int_{t_1}^{t_2} \left(m v^2(t) - r(t) \frac{dU(r(t))}{dr} \right) dt = m(\vec{v}(t_2) \vec{r}(t_2) - \vec{v}(t_1) \vec{r}(t_1)). \quad (\text{A.3})$$

For $t_1 \rightarrow \pm\infty$ the particle speed is v_∞ . Let us assign the time $t = 0$ to the position of the closest approach of the particle to the center $r = r_0$. Then for large times (either positive or negative) the distance from the origin is given by $r = s + v_\infty |t|$, where s is the difference of the distance that the particle, moving in the potential, passed from the moment $t = 0$ to t and the distance it would pass during the same time interval if it moved freely (for $U = 0$) with the velocity v_∞ . The scattering time delay/advance of the particle in the potential can be defined as

$$\delta t_s^{\text{cl}} = -s/v_\infty. \quad (\text{A.4})$$

Since both sides of equation (A.3) diverge in the limit $t_1 \rightarrow \pm\infty$, we regularize them by subtracting $v_\infty^2 (t_2 - t_1)$. Then on the left-hand side we can use the energy conservation $m(v^2 - v_\infty^2) = -2U$ and on the right-hand side we get $2m v_\infty \lim_{t \rightarrow \infty} (r - v_\infty t) = 2m v_\infty s$. We take here into account that at large distances from the center $\vec{v} \uparrow \downarrow \vec{r}$ before collision ($t_1 \rightarrow -\infty$) and $\vec{v} \uparrow \uparrow \vec{r}$ after collision ($t_2 \rightarrow +\infty$). Thus we rewrite equation (A.3) as

$$\int_{-\infty}^{+\infty} \left(2U(r(t)) + r(t) \frac{dU(r(t))}{dr} \right) dt = -2m v_\infty s = 2m v_\infty^2 \delta t_s^{\text{cl}} \quad (\text{A.5})$$

and introducing the Wigner time delay $\delta t_W^{\text{cl}} = 2\delta t_s^{\text{cl}}$ we recover equation (2.17).

Another derivation of this relation from the point of view of hypervirial theorems, introduced by Hirschfelder for classical and quantum systems in [148], can be found in [149].

Appendix B. Relations for wave functions obeying the Schrödinger equation

Consider two solutions of the Schrödinger equation with a potential $U(x)$ and slightly different energies E and E' :

$$\begin{aligned} -\frac{\hbar^2}{2m} \frac{\partial^2}{\partial z^2} \psi(z, E) + U(z) \psi(z, E) &= E \psi(z, E), \\ -\frac{\hbar^2}{2m} \frac{\partial^2}{\partial z^2} \psi^*(z, E') + U(z) \psi^*(z, E') &= E'^* \psi^*(z, E'). \end{aligned} \quad (\text{B.1})$$

For the sake of generality we assume that the energy might be complex. Let us multiply the first equation by $\psi^*(z, E')$ and the second one by $\psi(z, E)$, subtract one from another and integrate from a to b . Then we put $E' \rightarrow E$. In this limit $\text{Re}(E'^* - E) = \delta E \rightarrow 0$ and $\text{Im}(E'^* - E) \rightarrow -2 \text{Im} E$. Keeping only the leading terms in δE and $\text{Im} E$ on the right-hand side we obtain

$$\int_a^b dz [E'^* \psi(z, E) \psi^*(z, E') - E \psi^*(z, E') \psi(z, E)] \approx (\delta E - 2i \text{Im} E) \int_a^b dz |\psi(z, E)|^2. \quad (\text{B.2})$$

On the left-hand side

$$\begin{aligned} \frac{\hbar^2}{2m} \int_a^b dz \left[\psi^*(z, E') \frac{\partial^2}{\partial z^2} \psi(z, E) - \psi(z, E) \frac{\partial^2}{\partial z^2} \psi^*(z, E') \right] &\approx i \hbar (j(b; E) - j(a; E)) \\ + \delta E \frac{\hbar^2}{2m} \left[\left(\frac{\partial}{\partial E} \psi^*(z, E) \right) \frac{\partial}{\partial z} \psi(z, E) - \psi(z, E) \frac{\partial}{\partial z} \left(\frac{\partial}{\partial E} \psi^*(z, E) \right) \right] &\Bigg|_a^b, \end{aligned} \quad (\text{B.3})$$

where the currents at coordinates a and b are determined according to equation (3.3), $j(z; E) = \mathcal{J}[\psi(z; E)]$. Equating real and imaginary parts of equations (B.2) and (B.3) we arrive at the relations

$$\int_a^b dz |\psi(z, E)|^2 = \frac{\hbar^2}{2m} \left[\left(\frac{\partial}{\partial E} \psi^*(z, E) \right) \frac{\partial}{\partial z} \psi(z, E) - \psi(z, E) \frac{\partial}{\partial z} \left(\frac{\partial}{\partial E} \psi^*(z, E) \right) \right] \Bigg|_a^b, \quad (\text{B.4})$$

and

$$-2 \text{Im} E = \hbar (j(b; E) - j(a; E)) / \int_a^b dz |\psi(z, E)|^2. \quad (\text{B.5})$$

The first relation is used to get equation (3.13). The last relation demonstrates the equivalence between the current conservation and the vanishing of the imaginary part of the energy. If the current is not conserved, $j(a; E) \neq j(b; E)$, we are dealing with an exponentially increasing ($\text{Im} E > 0$) or decreasing ($\text{Im} E < 0$) wave function in the interval $[a, b]$. For a bound state the wave function can always be chosen real and therefore both $j(a; E)$ and $j(b; E)$ vanish and $\text{Im} E = 0$. In the scattering problem (e.g., as given by equations (3.1) and (3.1)) the currents are independent of the coordinate and $j(a; E) = j(b; E)$ thus yielding $\text{Im} E = 0$. Only the wave functions satisfying the boundary conditions

$$\begin{aligned} (a) \psi(z; E) &\rightarrow e^{+i|z|\sqrt{2mE}}, & z &\rightarrow \pm\infty, \\ (b) \psi(z; E) &\rightarrow e^{-i|z|\sqrt{2mE}}, & z &\rightarrow \pm\infty, \\ (c) \psi(z; E) &\rightarrow e^{\pm iz\sqrt{2mE}}, & z &\rightarrow \infty; \psi(z; E) = 0, & z < a, \\ (d) \psi(z; E) &\rightarrow e^{\mp iz\sqrt{2mE}}, & z &\rightarrow -\infty; \psi(z; E) = 0, & z > b \end{aligned} \quad (\text{B.6})$$

describe states with complex energies. The imaginary part of the energy is negative (decaying state) for cases (a) and (c), (d) with upper signs, and is positive (process of a state formation) for cases (b) and (c), (d) with lower signs.

It is instructive to express equations (B.4) and (B.5) through the logarithmic derivatives

$$d(z; E) = \frac{z}{\psi(z; E)} \frac{\partial}{\partial z} \psi(z; E). \quad (\text{B.7})$$

After simple algebra we get from equation (B.4)

$$\int_a^b dz |\psi(z, E)|^2 = \frac{\hbar^2}{2m} \left[\frac{1}{z} (d(z; E) - d^*(z; E)) \psi(z; E) \frac{\partial}{\partial E} \psi^*(z; E) - \frac{1}{z} |\psi(z; E)|^2 \frac{\partial}{\partial E} d^*(z; E) \right] \Big|_a^b. \quad (\text{B.8})$$

Since the integral on the left-hand side is real we can add to the right-hand side its complex conjugated value and halve it. Then we obtain

$$\begin{aligned} \int_a^b dz |\psi(z, E)|^2 &= \left[l_q[\psi(z; E)] \text{Im} d(z; E) - \frac{\hbar^2}{2mz} |\psi(z; E)|^2 \frac{\partial}{\partial E} \text{Re} d(z; E) \right] \Big|_a^b \\ &= l_q[\psi(b; E)] \text{Im} d(b; E) - l_q[\psi(a; E)] \text{Im} d(a; E) \\ &\quad + \frac{\hbar^2}{2m} \left[|\psi(a; E)|^2 \frac{1}{a} \frac{\partial}{\partial E} \text{Re} d(a; E) - |\psi(b; E)|^2 \frac{1}{b} \frac{\partial}{\partial E} \text{Re} d(b; E) \right], \end{aligned} \quad (\text{B.9})$$

where we introduced the characteristic quantum length characterizing a stationary wave function $\psi(z; E)$:

$$l_q[\psi(z; E)] = \frac{i\hbar^2}{2mz} \left(\psi(z; E) \frac{\partial}{\partial E} \psi^*(z; E) - \psi^*(z; E) \frac{\partial}{\partial E} \psi(z; E) \right). \quad (\text{B.10})$$

For example, for the plane wave this quantity is the de Broglie wavelength $l_q[\exp(ikz/\hbar)] = \hbar/k$. For the wave function (3.1) and $z > L/2$ we find $l_q[T(E) \exp(ikz/\hbar)] = (\hbar/k) |T(E)|^2 \left(1 + \frac{k}{zm} \hbar \frac{d}{dE} \phi_T(E) \right)$.

From equation (B.5) straightforwardly follows

$$-2 \text{Im} E \int_a^b dz |\psi(z, E)|^2 = \frac{\hbar^2}{mb} |\psi(b; E)|^2 \text{Im} d(b; E) - \frac{\hbar^2}{ma} |\psi(a; E)|^2 \text{Im} d(a; E). \quad (\text{B.11})$$

Appendix C. Asymptotic centroids of the wave packets

Let us perform the derivation of equation (3.53). Substituting equation (3.49) in the standard definition of the average coordinate we have

$$\begin{aligned} \bar{z}_1^{(\text{as})}(t) &= \int_{-\infty}^{+\infty} dz z |\Psi_1(z, t)|^2 \\ &= \int_0^{+\infty} \frac{dk}{2\pi\hbar} \int_0^{+\infty} \frac{dk'}{2\pi\hbar} \varphi(k) \varphi^*(k') e^{i(E'-E)t/\hbar} \int_{-\infty}^{+\infty} dz z e^{i(k-k')z/\hbar}, \end{aligned} \quad (\text{C.1})$$

where $E = k^2/2m$ and $E' = k'^2/2m$. Changing variables to $Q = (k + k')/2$ and $q = k - k'$ with $dkdk' = dQdq$ we write

$$\bar{z}_1^{(\text{as})}(t) = \int_0^{+\infty} \frac{dQ}{2\pi\hbar} \int_{-\infty}^{+\infty} \frac{dq}{2\pi\hbar} \varphi(Q + q/2) \varphi^*(Q - q/2) e^{-i\frac{Qq}{m} \frac{t}{\hbar}} \int_{-\infty}^{+\infty} dz z e^{+iqz/\hbar}. \quad (\text{C.2})$$

Using

$$\int_{-\infty}^{+\infty} dz z^n e^{+iqz/\hbar} = (-i\hbar)^n (2\pi\hbar) \frac{d^n}{dq^n} \delta(q) \quad (C.3)$$

after integration by parts we obtain

$$\bar{z}_1^{(as)}(t) = i \int_0^{+\infty} \frac{dQ}{2\pi} \left\{ \frac{1}{2} \varphi'(Q) \varphi^*(Q) - \frac{1}{2} \varphi(Q) \varphi'^*(Q) - i \frac{Q}{m} \frac{t}{\hbar} |\varphi(Q)|^2 \right\}. \quad (C.4)$$

Introducing the phase of the momentum profile function $\xi(k)$ as $\varphi(k) = |\varphi(k)| e^{i\xi(k)}$ after the replacement $Q \rightarrow k$ we cast the integral in the form

$$\bar{z}_1^{(as)}(t) = \int_0^{+\infty} \frac{dk}{2\pi\hbar} \left(-\hbar \xi'(k) + \frac{k}{m} t \right) |\varphi(k)|^2 \quad (C.5)$$

and recover equation (3.53).

Similarly to the above we derive

$$\begin{aligned} \overline{[z_1^{(as)}(t)]^2} &= \int_{-\infty}^{+\infty} dz z^2 |\Psi_I(z, t)|^2 \\ &= -\hbar^2 \int_0^{+\infty} \frac{dQ}{2\pi\hbar} \int_{-\infty}^{+\infty} dq \varphi(Q + q/2) \varphi^*(Q - q/2) e^{-i\frac{Qq}{m} \frac{t}{\hbar}} \frac{d^2}{dq^2} \delta(q). \end{aligned} \quad (C.6)$$

The integration by parts over q after the replacement $Q \rightarrow k$ yields

$$\begin{aligned} \overline{[z_1^{(as)}(t)]^2} &= -\hbar^2 \int_0^{+\infty} \frac{dk}{2\pi\hbar} \left\{ \frac{1}{4} \varphi''(k) \varphi^*(k) + \frac{1}{4} \varphi(k) \varphi''^*(k) - \frac{1}{2} \varphi'(k) \varphi'^*(k) \right. \\ &\quad \left. - i \frac{k}{m} \frac{t}{\hbar} (\varphi'(k) \varphi^*(k) - \varphi(k) \varphi'^*(k)) - \frac{k^2}{m^2} \frac{t^2}{\hbar^2} |\varphi(k)|^2 \right\} \\ &= \frac{\hbar}{4\pi} |\varphi(0)|' |\varphi(0)| + \int_0^{+\infty} \frac{dk}{2\pi\hbar} \left\{ \hbar^2 (|\varphi(k)|')^2 + \left(\hbar \xi'(k) - \frac{k}{m} t \right)^2 |\varphi(k)|^2 \right\} \end{aligned} \quad (C.7)$$

and thereby equation (3.54) is recovered.

The results (C.3) and (C.6) can be generalized as follows

$$\int_{-\infty}^{+\infty} dz z^n |\Psi_I(z, t)|^2 = (-i\hbar)^n \int_0^{+\infty} \frac{dQ}{2\pi\hbar} \int_{-\infty}^{+\infty} dq \varphi(Q + q/2) \varphi^*(Q - q/2) e^{-i\frac{Qq}{m} \frac{t}{\hbar}} \frac{d^n}{dq^n} \delta(q). \quad (C.8)$$

Now we turn to the derivation of the asymptotic centroid evolution for the transmitted packets (equation (3.105)). To evaluate the integrals of the type $\int_{-\infty}^{+\infty} dz z^n |\Psi_T(z, t)|^2$ we can use equation (C.8) with the only replacement $\varphi \rightarrow \varphi T$. Then for the normalization integral we immediately obtain

$$\int_{-\infty}^{+\infty} dz |\Psi_T(z, t)|^2 = \int_0^{+\infty} \frac{dk}{2\pi\hbar} |\varphi(k)|^2 |T(k)|^2 = \langle T(E) \rangle_k. \quad (C.9)$$

Now we adopt equation (C.4) and write

$$\begin{aligned} \int_{-\infty}^{+\infty} dz z |\Psi_T(z, t)|^2 &= i\hbar \int_0^{+\infty} \frac{dk}{2\pi\hbar} \left\{ \frac{1}{2} \varphi^*(k) T^*(k) \frac{d}{dk} (\varphi(k) T(k)) \right. \\ &\quad \left. - \frac{1}{2} \varphi(k) T(k) \frac{d}{dk} (\varphi^*(k) T^*(k)) - i \frac{k}{m} \frac{t}{\hbar} |\varphi(k)|^2 |T(k)|^2 \right\}. \end{aligned} \quad (C.10)$$

Substituting $\varphi(k) T(k) = |\varphi(k)| |T(k)| e^{i\xi(k) + i\phi_T(k)}$ we find

$$\int_{-\infty}^{+\infty} dz z |\Psi_T(z, t)|^2 = \int_0^{+\infty} \frac{dk}{2\pi\hbar} \left\{ -\hbar \xi'(k) - \hbar \phi_T'(k) + \frac{k}{m} t \right\} |\varphi(k)|^2 |T(k)|^2. \quad (C.11)$$

Dividing equation (C.11) by equation (C.9) we recover the first equation in (3.105).

To get similar expressions for the reflected packet we have to replace $\varphi \rightarrow \varphi R$ in equation (C.8) and also change $q \rightarrow -q$. The corresponding result in (3.105) follows in full analogy to equation (C.9), and (C.11) with the change of the overall sign in the latter.

To calculate the width of the transmitted packet that appeared in equation (3.103) we need to calculate $[z_T^{(as)}(t)]^2$. Making the replacement $\varphi \rightarrow \varphi T$ in equation (C.7) and taking into account that $T(0) = 0$ we can write

$$\begin{aligned} \overline{[z_T^{(as)}(t)]^2} &= \frac{1}{\langle |T(k)|^2 \rangle_k} \left\langle \hbar^2 (|T(k)|' + |T(k)||\varphi(k)|/|\varphi(k)|')^2 \right. \\ &\quad \left. + \left(\hbar \xi'(k) + \hbar \phi_T'(k) - \frac{k}{m} t \right)^2 |T(k)|^2 \right\rangle_k \\ &= \left\langle \hbar^2 \left[\frac{d}{dk} \log(|\varphi(k)||T(k)|) \right]^2 \right\rangle_{k,T} + \left\langle \left(\hbar \xi'(k) + \hbar \phi_T'(k) - \frac{k}{m} t \right)^2 \right\rangle_{k,T}. \end{aligned} \quad (C.12)$$

Here in the last equality we use the definition of the average (3.106). For the reflected packet we can write by analogy

$$\overline{[z_R^{(as)}(t)]^2} = \left\langle \hbar^2 \left[\frac{d}{dk} \log(|\varphi(k)||R(k)|) \right]^2 \right\rangle_{k,R} + \left\langle \left(\hbar \xi'(k) + \hbar \phi_R'(k) - \frac{k}{m} t \right)^2 \right\rangle_{k,R}. \quad (C.13)$$

Appendix D. Relations for the sojourn time

Let us perform derivation of the relation between the sojourn time and the dwell time (3.93). Using equation (3.48) and performing the integration over time we find

$$\begin{aligned} t_{\text{soj}}(a, b) &= \int_{-\infty}^{+\infty} dt \int_a^b dz |\Psi(z, t)|^2 \\ &= \int_0^{+\infty} \frac{dk}{2\pi \hbar} \int_0^{+\infty} \frac{dk'}{2\pi \hbar} \varphi(k) \varphi^*(k') \int_a^b dz \psi(z, E) \psi^*(z, E') (2\pi \hbar) \delta(E - E'), \end{aligned}$$

where we used that $E = k^2/2m$ and $E' = k'^2/2m$. Taking the integral over momentum k' we obtain

$$t_{\text{soj}}(a, b) = \int_0^{+\infty} \frac{dk}{2\pi \hbar} |\varphi(k)|^2 \frac{m}{k} \int_a^b dx |\psi(x, E)|^2, \quad (D.1)$$

thus equation (3.93) is recovered.

Now let us derive equation (3.96). Using the definitions of the wave function on the left and right sides of the barrier (Equations (3.49), (3.76) and (3.77)) we can write the current as follows

$$\begin{aligned} j(z \geq L/2, t) &= \frac{i\hbar}{2m} \left(\Psi_T(z, t) \nabla_z \Psi_T^*(z, t) - \Psi_T^*(z, t) \nabla_z \Psi_T(z, t) \right) \\ &= \frac{1}{2m} \int_0^\infty \frac{dk}{2\pi \hbar} \int_0^\infty \frac{dk'}{2\pi \hbar} \varphi(k) \varphi^*(k') T(E) T^*(E') e^{i(E'-E)t/\hbar} e^{+i(k-k')z/\hbar} (k' + k), \\ j(z \leq -L/2, t) &= \frac{i\hbar}{2m} ([\Psi_I(z, t) + \Psi_R(z, t)] \nabla [\Psi_I^*(z, t) + \Psi_R^*(z, t)] \\ &\quad - [\Psi_I^*(z, t) + \Psi_R^*(z, t)] \nabla [\Psi_I(z, t) + \Psi_R(z, t)]) \\ &= \frac{1}{2m} \int_0^\infty \frac{dk}{2\pi \hbar} \int_0^\infty \frac{dk'}{2\pi \hbar} \varphi(k) \varphi^*(k') e^{i(E'-E)t/\hbar} \\ &\quad \times \{ (k' + k) [e^{i(k-k')x/\hbar} - R^*(E') R(E) e^{-i(k-k')k/\hbar}] \\ &\quad + (k - k') [R^*(E') e^{+i(k'+k)z/\hbar} - R(E) e^{-i(k+k')z/\hbar}] \}. \end{aligned} \quad (D.2)$$

Performing the replacement of momenta $k = Q + \frac{1}{2}q$, $k' = Q - \frac{1}{2}q$, $dk dk' = dQ dq$ and using that $E' - E = \frac{1}{2m}[(Q - \frac{1}{2}q)^2 - (Q + \frac{1}{2}q)^2] = Qq/m$, we find

$$\begin{aligned}
 j(z \geq L/2, t) &= \frac{1}{2m} \int_0^\infty \frac{dQ}{2\pi\hbar} \int_{-\infty}^\infty \frac{dq}{2\pi\hbar} \varphi\left(Q + \frac{1}{2}q\right) \varphi^*\left(Q - \frac{1}{2}q\right) \\
 &\quad \times T(E_{Q+q/2}) T^*(E_{Q-q/2}) e^{-iQqt/m\hbar} e^{+iqz/\hbar} 2Q, \\
 j(z \leq -L/2, t) &= \frac{1}{2m} \int_0^\infty \frac{dQ}{2\pi\hbar} \int_{-\infty}^\infty \frac{dq}{2\pi\hbar} \varphi\left(Q + \frac{1}{2}q\right) \varphi^*\left(Q - \frac{1}{2}q\right) e^{iQqt/m\hbar} \\
 &\quad \times \{2Q[e^{iqx/\hbar} - R^*(E_{Q-q/2}) R(E_{Q+q/2}) e^{-iqz/\hbar}] \\
 &\quad + q[R^*(E_{Q-q/2}) e^{+i2Qx/\hbar} - R(E_{Q+q/2}) e^{-i2Qx/\hbar}]\}. \tag{D.3}
 \end{aligned}$$

Integrating over the time in equation (3.95) with the help of expression

$$\int_{-\infty}^{+\infty} dt \int_{-\infty}^t dt' e^{iQqt'/m\hbar} = 2\pi \frac{im^2\hbar^2}{Q^2 q} \delta(q) \tag{D.4}$$

we derive

$$\begin{aligned}
 &\int_{-\infty}^{+\infty} dt \int_{-\infty}^t dt' (j(L/2, t') - j(-L/2, t')) \\
 &= \int_0^\infty \frac{dQ}{2\pi\hbar} \int_{-\infty}^\infty dq \varphi\left(Q + \frac{1}{2}q\right) \varphi^*\left(Q - \frac{1}{2}q\right) \frac{im\hbar}{Q} \delta(q) \\
 &\quad \times \left[\frac{1}{q} (T(E_{Q+q/2}) T^*(E_{Q-q/2}) + R(E_{Q+q/2}) R^*(E_{Q-q/2}) - e^{-iqL/\hbar}) e^{+i\frac{qL}{2\hbar}} \right. \\
 &\quad \left. - \frac{1}{2Q} (R^*(E_{Q-q/2}) e^{-i2QL/2\hbar} - R(E_{Q+q/2}) e^{+i2QL/2\hbar}) \right].
 \end{aligned}$$

Taking into account that the expression in the squared bracket at the term with $1/q$ vanishes for $q \rightarrow 0$, so that only the first derivative of this expression contributes, we obtain

$$\begin{aligned}
 &\int_{-\infty}^{+\infty} dt \int_{-\infty}^t dt' (j(L/2, t') - j(-L/2, t')) \\
 &= - \int_0^\infty \frac{dQ}{2\pi} |\varphi(Q)|^2 \left[|T(E_Q)|^2 \hbar \frac{\partial \phi_T(E_Q)}{\partial E} + |R(E_Q)|^2 \hbar \frac{\partial \phi_R(E_Q)}{\partial E} \right. \\
 &\quad \left. + \frac{mL}{Q} + \frac{\hbar m}{Q^2} \text{Im}(R(E_Q) e^{iQL/\hbar}) \right].
 \end{aligned}$$

Substituting here definitions of the phases $\phi_{R,T}$ from equation (3.9), we recover equation (3.96).

Appendix E. Matrix notation

For any two-point function (5.9) (e.g., for the Green's function or the self-energy), the contour values [35] are defined as,

$$\begin{aligned}
 \mathcal{F}_i^j(x, y) &= \sigma_{ik} \mathcal{F}^{kj}(x, y), \quad \mathcal{F}_j^i(x, y) = \mathcal{F}^{ik}(x, y) \sigma_{ki}, \\
 \mathcal{F}_{ij}(x, y) &= \sigma_{ik} \sigma_{jl} \mathcal{F}^{kl}(x, y), \quad \sigma_i^k = \delta_{ik}
 \end{aligned} \tag{E.1}$$

on the different branches of the contour, i, k mean $+$ or $-$. Summation over repeated indices is implied. The contour folding of contour two-point functions, e.g. in Dyson equations, are

$$H(x^i, y^k) = H^{ik}(x, y) = \int_C dz^C \mathcal{F}(x^i, z^C) G(z^C, y^k) = \int dz \mathcal{F}_j^i(x, z) G^{jk}(z, y) \tag{E.2}$$

in the matrix notation.

Due to the change of operator ordering, genuine multi-point functions are, in general, discontinuous when two contour coordinates become identical. In particular, two-point functions like $i\mathcal{F}(x, y) = \langle \mathcal{T}_C \widehat{A}(x) \widehat{B}(y) \rangle$ become

$$i\mathcal{F}(x, y) = \begin{pmatrix} i\mathcal{F}^{--}(x, y) & i\mathcal{F}^{-+}(x, y) \\ i\mathcal{F}^{+-}(x, y) & i\mathcal{F}^{++}(x, y) \end{pmatrix} = \begin{pmatrix} \langle \mathcal{T} \widehat{A}(x) \widehat{B}(y) \rangle & \mp \langle \widehat{B}(y) \widehat{A}(x) \rangle \\ \langle \widehat{A}(x) \widehat{B}(y) \rangle & \langle \mathcal{T}^{-1} \widehat{A}(x) \widehat{B}(y) \rangle \end{pmatrix}, \quad (\text{E.3})$$

where \mathcal{T} and \mathcal{T}^{-1} are the usual time and anti-time ordering operators. Equation (E.3) implies the following relations among non-equilibrium and usual retarded and advanced functions

$$\begin{aligned} \mathcal{F}^R(x, y) &= \mathcal{F}^{--}(x, y) - \mathcal{F}^{-+}(x, y) = \mathcal{F}^{+-}(x, y) - \mathcal{F}^{++}(x, y) \\ &:= \Theta(x_0 - y_0) (\mathcal{F}^{+-}(x, y) - \mathcal{F}^{-+}(x, y)), \\ \mathcal{F}^A(x, y) &= \mathcal{F}^{--}(x, y) - \mathcal{F}^{+-}(x, y) = \mathcal{F}^{-+}(x, y) - \mathcal{F}^{++}(x, y) \\ &:= -\Theta(y_0 - x_0) (\mathcal{F}^{+-}(x, y) - \mathcal{F}^{-+}(x, y)), \end{aligned} \quad (\text{E.4})$$

where $\Theta(x_0 - y_0)$ is the step function of the time difference. The rules for the co-contour functions \mathcal{F}_{--} etc follow from equation (5.9). Complex conjugation implies

$$\begin{aligned} (i\mathcal{F}^{-+}(x, y))^* &= i\mathcal{F}^{-+}(y, x) \Rightarrow i\mathcal{F}^{-+}(X, p) = \text{real}, \\ (i\mathcal{F}^{+-}(x, y))^* &= i\mathcal{F}^{+-}(y, x) \Rightarrow i\mathcal{F}^{+-}(X, p) = \text{real}, \\ (i\mathcal{F}^{--}(x, y))^* &= i\mathcal{F}^{++}(y, x) \Rightarrow (i\mathcal{F}^{--}(X, p))^* = i\mathcal{F}^{++}(X, p), \\ (\mathcal{F}^R(x, y))^* &= \mathcal{F}^A(y, x) \Rightarrow (\mathcal{F}^R(X, p))^* = \mathcal{F}^A(X, p), \end{aligned} \quad (\text{E.5})$$

where the right parts specify the corresponding properties in the Wigner representation; see section 6.1.

In thermal equilibrium all the Green's functions are expressed through the retarded and advanced Green's functions

$$G^{ik}(p) = \begin{pmatrix} G^R(p) \pm inA(p) & \pm inA(p) \\ -i[1 \mp n]A(p) & -G^A(p) \mp inA(p) \end{pmatrix}, \quad i, k = \{+, -\}, \quad (\text{E.6})$$

and the self-energies take a similar form

$$\Sigma_{ik}(p) = \begin{pmatrix} \Sigma^R(p) \pm in\Gamma(p) & \mp in\Gamma(p) \\ i[1 \mp n]\Gamma(p) & -\Sigma^A(p) \pm in\Gamma(p) \end{pmatrix}, \quad (\text{E.7})$$

where

$$n(\varepsilon) = [\exp(\varepsilon/T) \pm 1]^{-1} \quad (\text{E.8})$$

are thermal Fermi/Bose–Einstein occupations.

Appendix F. H theorem and the minimum of entropy production

Reference [35] presented arguments for H theorem and could prove it for some specific examples, e.g. for the Φ -derivable theories for Φ diagrams with two vertices. the equation for the entropy flow for all three forms of the kinetic equation, the BM, KB and non-local form, is as follows:

$$\partial_\mu S^\mu = -H, \quad (\text{F.1})$$

where now in the left-hand side S^μ is either S_{BMM}^μ , or S_{KB}^μ , or S_{NL}^μ , the latter quantity is up to first gradients the same as for the KB choice. The memory contribution can be also incorporated as an additional term $\partial_\mu S_{\text{mem}}^\mu$ in the left-hand side.

For the BM and the KB forms of the kinetic equation we multiply the kinetic equation by $\ln \frac{1 \mp f}{f}$. Using the multi-particle process decomposition [35] we arrive at the relation

$$\begin{aligned}
 H = -\text{Tr} \int \frac{d^4 p}{(2\pi)^4} \ln \frac{1 \mp f}{f} C = -\text{Tr} \sum_{m, \bar{m}} \frac{1}{2} \int \frac{d^4 p_1}{(2\pi)^4} \cdots \frac{d^4 p_m}{(2\pi)^4} \frac{d^4 \tilde{p}_1}{(2\pi)^4} \cdots \frac{d^4 \tilde{p}_{\bar{m}}}{(2\pi)^4} \\
 \times [A_1 f_1 \cdots A_m f_m A'_1 (1 \mp f'_1) \cdots A'_{\bar{m}} (1 \mp f'_{\bar{m}}) \\
 - A_1 (1 \mp f_1) \cdots A_m (1 \mp f_m) A'_1 f'_1 \cdots A'_{\bar{m}} f'_{\bar{m}}] \\
 \times \ln \frac{f_1 \cdots f_m (1 \mp f'_1) \cdots (1 \mp f'_{\bar{m}})}{(1 \mp f_1) \cdots (1 \mp f_m) f'_1 \cdots f'_{\bar{m}}} R_{m, \bar{m}} \delta^4 \left(\sum_{i=1}^m p_i - \sum_{i=1}^{\bar{m}} \tilde{p}_i \right). \quad (\text{F.2})
 \end{aligned}$$

Here we assume different flavors and intrinsic quantum numbers to be absorbed in the momenta p_i and \tilde{p}_i .

In the case when all rates $R_{m, \bar{m}}$ are non-negative, i.e. $R_{m, \bar{m}} \geq 0$, this expression is non-negative, since $(x - y) \ln(x/y) \geq 0$ for any positive x and y . In particular, $R_{m, \bar{m}} \geq 0$ takes place for all Φ -functionals up to two vertices. Then the divergence of s^μ is non-negative which proves the H theorem in this case.

For the non-local form of the kinetic equation we multiply the latter by $\ln \frac{1 \mp f^{\text{shift}}}{f^{\text{shift}}}$ and get

$$H^{\text{shift}} = -\text{Tr} \int \frac{d^4 p}{(2\pi)^4} \ln \frac{1 \mp f^{\text{shift}}}{f^{\text{shift}}} \frac{AC^{\text{shift}}}{A^{\text{shift}}} \simeq -\text{Tr} \int \frac{d^4 p}{(2\pi)^4} \ln \frac{1 \mp f^{\text{shift}}}{f^{\text{shift}}} C^{\text{shift}}$$

instead of H . Thus equation (F.2) continues to hold but now in shifted variables.

Assume that the system is closed, i.e. there is no entropy flow through the volume boundary. Then

$$\left[\frac{d \int S^0 d^3 X}{dt} \right]_{\text{l.eq}} = 0, \quad \left[\frac{d^2 \int S^0 d^3 X}{dt^2} \right]_{\text{l.eq}} = 0, \quad (\text{F.3})$$

since both the curved-bracket term and the \ln -term in (F.2) are zero in the local equilibrium that results in zero of the function and its derivative.

Assuming the validity of the H theorem (the entropy should be maximum in the local equilibrium) we have

$$\left(\frac{d^3 \int S^0 d^3 X}{dt^3} \right)_{\text{l.eq}} \leq 0. \quad (\text{F.4})$$

Thus we argue for the principle of the minimum of the entropy production (previously postulated by Prigogine; see [150])¹² now related to the generalized kinetic equation, provided the H theorem is satisfied.

References

- [1] Eisenbud L and Wigner E P 1947 Higher angular momenta and long range interaction in resonance reactions *Phys. Rev.* **72** 29
- Wigner E P 1955 Lower limit for the energy derivative of the scattering phase shift *Phys. Rev.* **98** 145
- [2] Wu T-Y and Ohmura T 1962 *Quantum Theory of Scattering* (Englewood Cliffs, NJ: Prentice-Hall)
- [3] Goldberger M L and Watson K M 1964 *Collision Theory* (New York: Wiley) p 485
- [4] Nussenzveig H M 1972 *Causality and Dispersion Relations* (New York: Academic)
- [5] Bosanas S D 1988 *Long-lived States in Collisions* (Boca Raton, FL: CRC Press)
- [6] de Carvalho C A A and Nussenzveig H M 2002 Time delay *Phys. Rep.* **364** 83
- [7] Razavi M 2003 *Quantum Theory of Tunneling* (Singapore: Word Scientific)

¹² Please do not mix this principle with the principle of the maximum of the entropy production, being at work in open systems with a large deviation from the thermodynamic equilibrium; see [151].

- [8] Winful H G 2006 Tunneling time, the Hartmann effect, and superluminality: a proposed resolution of an old paradox *Phys. Rep.* **436** 1
- [9] Shvartsburg A B 2007 Tunneling of electromagnetic waves: paradoxes and prospects *Usp. Fiz. Nauk* **177** 43 (*Phys.—Usp.* **50** 37)
- [10] Muga J G, Mayato R S and Egusquiza L L (ed) 2002 *Time in Quantum Mechanics (Lecture Notes in Physics vol 72)* vol 1 (Berlin: Springer)
- [11] Muga J G, Ruschhaupt A and del Campo A (ed) 2009 *Time in Quantum Mechanics (Lecture Notes in Physics vol 789)* vol 2 (Berlin: Springer)
- [12] del Campo A, García-Calderón G and Muga J G 2009 Quantum transients *Phys. Rep.* **476** 1
- [13] Hartman T F 1962 Tunneling of a wave packet *J. Appl. Phys.* **33** 3427
- [14] Garrett C G B and McCumber D E 1970 Propagation of a Gaussian light pulse through an anomalous dispersion medium *Phys. Rev. A* **1** 305
- [15] Faxfog F R, Chow C N Y, Bieber T and Carruthers J A 1970 Measured pulse velocity greater than c in a Ne absorption cell *Appl. Phys. Lett.* **17** 192
- [16] Garrison J C, Mitchell M W, Chiao R Y and Bolda E L 1998 Superluminal signals: causal loop paradoxes revisited *Phys. Lett. A* **245** 19
- [17] Stenner M D, Gauthier D J and Neifeld M A 2003 The speed of information in ‘a fast light’ optical medium *Nature* **425** 695
Stenner M D, Gauthier D J and Neifeld M A 2005 Fast causal information transmission in a medium with a slow group velocity *Phys. Rev. Lett.* **94** 053902
- [18] Boyd R W and Narum P 2007 Slow- and fast-light: fundamental limitations *J. Mod. Opt.* **54** 2403
- [19] Nussenzevig H M 1972 Time delay in quantum scattering *Phys. Rev. D* **6** 1534
- [20] Danielewicz P and Pratt S 1996 Delays associated with elementary processes in nuclear reaction simulations *Phys. Rev. C* **53** 249
- [21] Buss O, Gaitanos T, Gallmeister K, van Hees H, Kaskulov M, Lalakulich O, Larionov A B, Leitner T, Weil J and Mosel U 2012 Transport-theoretical description of nuclear reactions *Phys. Rep.* **512** 1
- [22] Schwinger J 1961 Brownian motion of a quantum oscillator *J. Math. Phys.* **2** 407
- [23] Baym G and Kadanoff L P 1961 Conservation laws and correlation functions *Phys. Rev.* **124** 287
- [24] Kadanoff L P and Baym G 1962 *Quantum Statistical Mechanics* (New York: Benjamin)
- [25] Keldysh L P 1964 Diagram technique for nonequilibrium processes *Zh. Eksp. Teor. Fiz.* **47** 1515 (*Sov. Phys.—JETP* **20** 1018)
- [26] Danielewicz P 1984 Quantum theory of nonequilibrium processes: I *Ann. Phys.* **152** 239
Danielewicz P 1984 Quantum theory of nonequilibrium processes: II. Application to nuclear collisions *Ann. Phys.* **152** 305
- [27] Bezzerides B and DuBois D F 1972 Quantum electrodynamics of nonthermal relativistic plasmas: kinetic theory *Ann. Phys.* **70** 10
- [28] Serene J W and Rainer D 1983 The quasiclassical approach to superfluid ^3He *Phys. Rep.* **101** 221
- [29] Chou K, Su Z, Hao B and Yu L 1985 Equilibrium and nonequilibrium formalisms made unified *Phys. Rep.* **118** 1
- [30] Rammer J and Smith H 1986 Quantum field-theoretical methods in transport theory of metals *Rev. Mod. Phys.* **58** 323
- [31] Berges J 2005 Introduction to nonequilibrium quantum field theory *AIP Conf. Proc.* **739** 3 (arXiv: hep-ph/0409233)
- [32] Botermans W and Malfliet R 1990 Quantum transport theory of nuclear matter *Phys. Rep.* **198** 115
- [33] Baym G 1962 Self-consistent approximations in many-body systems *Phys. Rev.* **127** 1391
- [34] Ivanov Yu B, Knoll J and Voskresensky D N 1999 Self-consistent approximations to non-equilibrium many-body theory *Nucl. Phys. A* **657** 413
- [35] Ivanov Yu B, Knoll J and Voskresensky D N 2000 Resonance transport and kinetic entropy *Nucl. Phys. A* **672** 313
- [36] Knoll J, Ivanov Yu B and Voskresensky D N 2001 Exact conservation laws of the gradient expanded Kadanoff–Baym equations *Ann. Phys.* **293** 126
- [37] Ivanov Yu B, Knoll J and Voskresensky D N 2003 Self-consistent approach to off-shell transport *Yad. Fiz.* **66** 1950 (*Phys. At. Nucl.* **66** 1902)
- [38] Cassing W and Juchem S 2000 Semiclassical transport of particles with dynamical spectral functions *Nucl. Phys. A* **665** 377
- [39] Leupold S 2001 Life time of resonances in transport simulations *Nucl. Phys. A* **695** 377
- [40] Ivanov Yu B and Voskresensky D N 2009 Nonlocal form of quantum off-shell kinetic equation *Yad. Fiz.* **72** 1168 (*Phys. At. Nucl.* **72** 1168)
- [41] Adam T *et al* 2012 Measurement of the neutrino velocity with the OPERA detector in the CNGS beam *J. High Energy Phys.* **JHEP10(2012)093** (arXiv:1109.4897)

- [42] Adamson P *et al* 2007 Measurement of neutrino velocity with the MINOS detectors and NuMI neutrino beam *Phys. Rev. D* **76** 072005
- [43] Landau L D and Lifshitz E M 1976 *Mechanics* 3rd edn (Oxford: Butterworth-Heinemann)
- [44] Demkov Yu N 1953 Variational principles and the virial theorem for continuum-spectrum problems in quantum mechanics *Dokl. Akad. Nauk SSSR* **89** 249
Demkov Yu N 1961 Virial theorem and its generalization in scattering theory *Dokl. Akad. Nauk SSSR* **138** 86 (*Sov. Phys.—Dokl.* **6** 393)
- [45] Bateman H 1931 On dissipative systems and related variational principles *Phys. Rev.* **38** 815
- [46] Um C-I, Yeon K-H and George T F 2002 The quantum damped harmonic oscillator *Phys. Rep.* **362** 63
- [47] Majima H and Suzuki A 2011 Quantization and instability of the damped harmonic oscillator subject to a time-dependent force *Ann. Phys.* **326** 3000
- [48] Caldeira A O and Leggett A J 1983 Quantum tunnelling in a dissipative system *Ann. Phys.* **149** 374
- [49] Martin P C 1968 *Measurements and Correlation Functions* (New York: Gordon and Breach)
- [50] Mitchell M W and Chiao R Y 1997 Negative group delay and ‘fronts’ in a causal system: an experiment with very low frequency bandpass amplifiers *Phys. Lett. A* **230** 133
- [51] Landau L D and Lifshitz E M 1975 *The Classical Theory of Fields* 4th edn (Oxford: Butterworth-Heinemann)
- [52] Landau L D and Lifshitz E M 1977 *Quantum Mechanics: Non-Relativistic Theory* 3rd edn (Oxford: Pergamon)
- [53] Particle Data Group 2010 Review of particle physics *J. Phys. G: Nucl. Part. Phys.* **37** 075021
- [54] Pauli W 1958 *Die allgemeinen Prinzipien der Wellenmechanik (Handbuch der Physik vol 5)* ed S Flügge (Berlin: Springer)
Pauli W 1980 *General Principles of Quantum Mechanics* (Berlin: Springer)
- [55] Delgado V and Muga J G 1997 Arrival time in quantum mechanics *Phys. Rev. A* **56** 3425
Olkhovsky V S 2009 Time as a quantum observable, canonically conjugated to energy, and foundations of self-consistent time analysis of quantum processes *Adv. Math. Phys.* **2009** 859710
Olkhovsky V S 2011 On time as a quantum observable canonically conjugate to energy *Usp. Fiz. Nauk* **181** 860 (*Phys.—Usp.* **54** 829)
Mielnik B and Torres-Vega G 2011 ‘Time operator’: the challenge persists arXiv:1112.4198 [quant-ph]
- [56] Hegerfeldt G C 2009 The quantum jump approach and some of its applications *Time in Quantum Mechanics (Lecture Notes in Physics vol 789)* vol 2 (Berlin: Springer) p 127
- [57] Schulman L G 1997 Observational line broadening and the duration of a quantum jump *J. Phys. A: Math. Gen.* **30** L293
Schulman L S 2002 Jump time and passage time: the duration of a quantum transition *Time in Quantum Mechanics (Lecture Notes in Physics vol 72)* vol 1 (Berlin: Springer) p 99
- [58] Mandelstam L and Tamm I E 1945 The energy–time uncertainty relation in non-relativistic quantum mechanics *Izv. Akad. Nauk SSSR* **9** 122
Mandelstam L and Tamm I E 1945 *J. Phys. USSR* **9** 249
- [59] Aharonov Y and Vaidman L 1990 Properties of a quantum system during the time interval between two measurements *Phys. Rev. A* **41** 11
- [60] Allcock G R 1969 The time of arrival in quantum mechanics: I. Formal considerations *Ann. Phys.* **53** 253
Allcock G R 1969 The time of arrival in quantum mechanics: II. The individual measurement *Ann. Phys.* **53** 286
Allcock G R 1969 The time of arrival in quantum mechanics: III. The measurement ensemble *Ann. Phys.* **53** 311
- [61] MacColl L A 1932 Note on transmission and reflection of wave packets by potential barriers *Phys. Rev.* **40** 621
- [62] Hauge E H and Støvneng J A 1989 Tunneling times: a critical review *Rev. Mod. Phys.* **61** 917
- [63] Landauer R and Martin Th 1994 Barrier interaction time in tunneling *Rev. Mod. Phys.* **66** 217
- [64] Collins S, Lowe D and Barker J R 1987 The quantum mechanical tunneling time problem *J. Phys. C: Solid State Phys.* **20** 6213
- [65] Baz A I 1967 Lifetime of intermediate states *Yad. Fiz.* **4** 252 (*Sov. J. Nucl. Phys.* **4** 182)
Baz A I 1967 *Sov. J. Nucl. Phys.* **5** 161
- [66] Fonda L, Ghirardi G C and Rimini A 1978 Decay theory of unstable systems *Rep. Prog. Phys.* **41** 587
- [67] Smith F T 1960 Lifetime matrix in collision theory *Phys. Rev.* **118** 349
Smith F T 1960 Erratum: Lifetime matrix in collision theory *Phys. Rev.* **119** 2098 (erratum)
- [68] Nussenzveig H M 2000 Average dwell time and tunneling *Phys. Rev. A* **62** 042107
- [69] Faddeev L D 1964 Properties of the *S*-matrix of the one-dimensional Schrödinger equation *Trudy Mat. Inst. Steklov* **73** 314 (*Am. Math. Soc. Transl.* **2** 139)
- [70] Salecker H and Wigner E P 1958 Quantum limitations of the measurement of space-time distances *Phys. Rev.* **109** 571
- [71] Peres A 1980 Measurement of time by quantum clocks *Am. J. Phys.* **48** 552
- [72] Rybachenko V F 1967 *Yad. Fiz.* **5** 895 (*Sov. J. Nucl. Phys.* **5** 635)

- [73] Verhaar B J, Schulte A M and de Kam J 1978 On the lifetime of the intermediate system in quantum-mechanical collisions *Physica A* **91** 119
- [74] Büttiker M 1983 Larmor precession and the traversal time for tunneling *Phys. Rev. B* **27** 6178
- [75] Popov V S 2005 Imaginary-time method in quantum mechanics and field theory *Yad. Fiz.* **68** 717 (*Phys. At. Nucl.* **68** 686)
- [76] Popov V S 1971 Pair production in a varying external field (quasiclassical approximation) *Zh. Eksp. Teor. Fiz.* **61** 1334 (*Sov. Phys.—JETP* **34** 709)
- [77] Büttiker M and Landauer R 1982 Traversal time tunneling *Phys. Rev. Lett.* **49** 1739
- [78] Olkhovskiy V S, Recami E and Jakiel J 2004 Unified time analysis of photon and particle tunneling *Phys. Rep.* **398** 133
- [79] Dyakonov M I and Gornyi I V 1996 Electromagnetic radiation by a tunneling charge *Phys. Rev. Lett.* **76** 3542
- [80] Migdal A B 1977 *Qualitative Methods in Quantum Theory* (New York: Benjamin)
- [81] Hauge E H, Falck J P and Fjeldly T A 1987 Transmission and reflection times for scattering of wave packets off tunneling barriers *Phys. Rev. B* **36** 4203
- [82] Bracken A J and Melloy G F 1994 Probability backflow and a new dimensionless quantum number *J. Phys. A: Math. Gen.* **27** 2197
- [83] Muga J G and Leavens C R 2000 Arrival time in quantum mechanics *Phys. Rep.* **338** 353
- [84] Eveson S P, Fewster C J and Verch R 2005 Quantum inequalities in quantum mechanics *Ann. Inst. Henri Poincaré* **6** 1
- Penz M, Gröbl G, Kreidl S and Wagner P 2006 A new approach to quantum backflow *J. Phys. A: Math. Gen.* **39** 423
- [85] Palmero M, Torrontegui E, Modugno M and Muga J G 2013 Detecting quantum backflow by the density of a Bose–Einstein condensate *Phys. Rev. A* **87** 053618
- [86] Brouard S and Muga J G 1996 Transient and asymptotic effects in tunneling *Phys. Rev. A* **54** 3055
- [87] Moshinsky M 1952 Diffraction in time *Phys. Rev.* **88** 625
- [88] García-Calderón G and Rubio A 1997 Transient effects and delay time in the dynamics of resonant tunneling *Phys. Rev. A* **55** 3361
- [89] García-Calderón G and Villavicencio J 2001 Time dependence of the probability density in the transient regime for tunneling *Phys. Rev. A* **64** 012107
- García-Calderón G and Villavicencio J 2002 Delay time and tunneling transient phenomena *Phys. Rev. A* **66** 032104
- [90] Bohm D 1952 *Quantum Theory* (New York: Prentice-Hall)
- [91] Eisenbud L 1948 Formal properties of nuclear collisions *Doctoral Dissertation* Princeton University
- [92] García-Calderón G and Rubio A 1989 Properties of the dwell time and the transmission and reflection times for resonant tunneling *Solid State Commun.* **71** 237
- [93] Winful H G 2003 Delay time and the Hartman effect in quantum tunneling *Phys. Rev. Lett.* **91** 260401
- [94] Ricco B and Azbel M Ya 1981 Physics of resonant tunneling: the one-dimensional double-barrier case *Phys. Rev. B* **29** 1970
- [95] Moura M A and de Albuquerque D F 1990 Remarks on the traversal time in a tunneling process *Solid State Commun.* **74** 353
- [96] Splitter T P, Clark T D, Prance R J and Prance H 1990 Barrier traversal time in a quantum potential picture *Europhys. Lett.* **12** 1
- [97] Bracher Ch, Kleber M and Riza M 1999 Variational approach to the tunneling-time problem *Phys. Rev. A* **60** 1864
- [98] Campi M and Cohen M M 1970 An interpretation of tunneling time *IEEE Trans. Electron Devices* **17** 157
- [99] Baskin L M and Sokolovskii D G 1987 Tunneling time of electrons through a potential barrier *Izv. VUZ Fiz.* **3** 26 (*Sov. Phys. J.* **30** 204)
- Jaworski W and Wardlaw D M 1988 Time delay in tunneling: transmission and reflection time delays *Phys. Rev. A* **37** 2843
- [100] Leavens C R and Aers G C 1989 Dwell time and phase times for transmission and reflection *Phys. Rev. B* **39** 1202
- [101] Winful H G, Ngom M and Litchinitzer N M 2004 Relation between quantum tunneling times for relativistic particles *Phys. Rev. A* **70** 052112
- Bernardini A E 2008 Relation between phase and dwell times for quantum tunneling of a relativistically propagating particle *Europhys. Lett.* **82** 60005
- [102] Enders A and Nimtz G 1992 On superluminal barrier traversal *J. Physique I* **2** 1693
- Steinberg A M, Kwiat P G and Chiao R Y 1993 Measurement of single-photon tunneling time *Phys. Rev. Lett.* **71** 708
- Enders A and Nimtz G 1993 Evanescent-mode propagation and quantum tunneling *Phys. Rev. E* **48** 632

- [103] Chiao R Y, Kozhekin A E and Kurizki G 1996 Tachyonlike excitations in inverted two-level media *Phys. Rev. Lett.* **77** 1254
- [104] Aharonov Y, Reznik B and Stern A 1998 Quantum limitations on superluminal propagation *Phys. Rev. Lett.* **81** 2190
Segev B, Milloni P W, Babb J F and Chiao R Y 2000 Quantum noise and superluminal propagation *Phys. Rev. A* **62** 022114
- [105] Bonifacio R (ed) 1999 *Mysteries, Puzzles and Paradoxes in Quantum Mechanics* (Woodbury, NY: American Institute of Physics)
- [106] Galitsky V M and Chel'tsov V F 1964 Two-proton radioactivity theory *Nucl. Phys.* **56** 86
- [107] Migdal A B, Perelomov A M and Popov V S 1971 Analytical properties of wave functions at low energy *Yad. Fiz.* **14** 874 (*Sov. J. Nucl. Phys.* **14** 488)
Migdal A B, Perelomov A M and Popov V S 1973 Remarks on the analytic properties of wave functions at low energies *Yad. Fiz.* **16** 222 (*Sov. J. Nucl. Phys.* **16** 120)
- [108] Perelomov A M and Popov V S 1972 Perturbation of a continuum spectrum by a close-lying level *Zh. Eksp. Theor. Fiz.* **61** 1743 (*Sov. Phys.—JETP* **34** 928)
- [109] Migdal A B 1972 Two interacting particles in a potential well *Yad. Fiz.* **16** 427 (*Sov. J. Nucl. Phys.* **16** 238)
- [110] Pfützner M, Karny M, Grigorenko L V and Riisager K 2012 Radioactive decays at limits of nuclear stability *Rev. Mod. Phys.* **84** 567
- [111] Krylov N S and Fock F A 1947 On the two main interpretations of the energy–time uncertainty relationship *Zh. Eksp. Theor. Fiz.* **17** 93
- [112] Khal'fin L A 1957 Contribution to the decay theory of a quasi-stationary state *Zh. Eksp. Theor. Fiz.* **33** 1371 (*Sov. Phys.—JETP* **6** 1053)
- [113] Kelkar N G, Nowakowski M and Khemchandani K P 2004 Hidden evidence of nonexponential nuclear decay *Phys. Rev. C* **70** 024601
Kelkar N G and Nowakowski M 2010 No classical limit of quantum decay for broad states *J. Phys. A: Math. Theor.* **43** 385308
- [114] del Campo A 2011 Long-time behavior of many-particle quantum decay *Phys. Rev. A* **84** 012113
Pons M, Sokolovski D and del Campo A 2012 Fidelity of fermionic atom-number states subjected to tunneling decay *Phys. Rev. A* **85** 022107
- [115] Fleming G N 1973 A unitary bound on the evolution of nonstationary states *Nuovo Cimento A* **16** 232
- [116] Muga J G, Egusquiza I L, Damborenea J A and Delgado F 2002 Bounds and enhancements for negative scattering time delays *Phys. Rev. A* **66** 042115
- [117] Mekjian A Z 1978 Explosive nucleosynthesis, equilibrium thermodynamics, and relativistic heavy-ion collisions *Phys. Rev.* **17** 1051
- [118] Landau L D and Lifshitz E M 1980 *Statistical Physics: Part 1* 3rd edn (Oxford: Butterworth-Heinemann)
- [119] Bogoliubov N N 1946 *J. Phys. USSR* **10** 256
Klimontovich Yu L 1982 *Statistical Physics* (Moscow: Nauka)
- [120] Gribov V N and Nyiri J 2001 *Quantum Electrodynamics: Gribov Lectures on Theoretical Physics* (Cambridge: Cambridge University Press)
- [121] Lifshitz E M and Pitaevskii L P 1980 *Statistical Physics: Part 2* (Oxford: Pergamon)
- [122] Voskresensky D N 1995 Exponential growth and possible condensation of the particle-hole excitations in moving hot Fermi liquids *Phys. Lett. B* **358** 1
- [123] Voskresensky D N and Senatorov A V 1987 Description of nuclear interaction in Keldysh's diagram technique and neutrino luminosity of neutron stars *Yad. Fiz.* **45** 657 (*Sov. J. Nucl. Phys.* **45** 411)
Knoll J and Voskresensky D N 1996 Classical and quantum many body description of bremsstrahlung in dense matter (Landau–Pomeranchuk–Migdal effect) *Ann. Phys.* **249** 532
Kolomeitsev E E and Voskresensky D N 1999 Strangeness modes in nuclei tested by anti-neutrinos *Phys. Rev. C* **60** 034610
Voskresensky D N 2001 Neutrino cooling of neutron stars: medium effects *Physics of Neutron Star Interiors (Lecture Notes in Physics vol 578)* (Berlin: Springer) p 467
Kolomeitsev E E and Voskresensky D N 2011 Superfluid nucleon matter in and out of equilibrium and weak interactions *Yad. Fiz.* **74** 1343 (*Phys. At. Nucl.* **74** 1316)
- [124] Wigner E P 1932 On the quantum correction for thermodynamic equilibrium *Phys. Rev.* **40** 749
- [125] Voskresensky D N 2011 Hydrodynamics of resonances *Nucl. Phys. A* **849** 120
- [126] Malfliet R 1998 Quantum transport velocity in strongly scattering media *Phys. Rev. B* **57** R11027
- [127] Migdal A B 1978 Pion field in nuclear matter *Rev. Mod. Phys.* **50** 107
Migdal A B, Saperstein E E, Troitsky M A and Voskresensky D N 1990 Pion degrees of freedom in nuclear matter *Phys. Rep.* **192** 179

- [128] Perel'man M E 2005 Uncertainty restrictions describing short-term violations of Lorentz invariance: superluminal phenomena, particle transformations arXiv:[quant-ph/0510123](https://arxiv.org/abs/quant-ph/0510123)
- [129] Abrikosov A A, Gorkov L P and Dzyaloshinski I E 1975 *Methods of Quantum Field Theory in Statistical Physics* (New York: Dover)
- [130] Delano M D 1969 Some properties of unstable particle gases *Phys. Rev. A* **1** 1175
- [131] Weinhold W, Friman B and Nörenberg W 1998 Thermodynamics of Δ resonances *Phys. Lett. B* **433** 236
- [132] Voskresensky D N 2008 Thermodynamics of resonances and blurred particles *Nucl. Phys. A* **812** 158
- [133] Ivanov Yu B, Knoll J, van Hees H and Voskresensky D N 2001 Soft modes, resonances, and quantum transport *Yad. Fiz.* **64** 711 (*Phys. At. Nucl.* **64** 652)
- [134] Leupold S 2000 Towards a test particle description of transport processes for states with continuous mass spectra *Nucl. Phys. A* **672** 475
- [135] Cassing W and Juchem S 2000 Semiclassical transport of hadrons with dynamical spectral functions in A + A collisions at SIS/AGS energies *Nucl. Phys. A* **672** 417
- [136] Schmidt M, Röpke G and Schulz H 1990 Generalized Beth–Uhlenbeck approach for hot nuclear matter *Ann. Phys.* **202** 57
- [137] Špička V, Lipavský P and Morawetz K 1997 Quasiparticle transport equation with collisional delay: I. Phenomenological approach *Phys. Rev. B* **55** 5084
Špička V, Lipavský P and Morawetz K 1997 Quasiparticle transport equation with collisional delay: II. Quantum statistical approach *Phys. Rev. B* **55** 5095
Morawetz K, Lipavský P and Špička V 1999 Nonlocal kinetic equation and simulations of heavy ion reactions *Prog. Part. Nucl. Phys.* **42** 147
Morawetz K, Lipavský P and Špička V 2001 Retarded versus time-nonlocal quantum kinetic equations *Ann. Phys.* **294** 135
- [138] Lipavský P, Špička V and Morawetz K 2001 Kinetic equation for strongly interacting dense Fermi systems *Ann. Phys. Fr.* **26** 1
- [139] Hau L V, Harris S E, Dutton Z and Behroozi C H 1999 Light speed reduction to 17 meters per second in an ultracold atomic gas *Nature* **397** 594
- [140] Kash M M *et al* 1999 Ultraslow group velocity and enhanced nonlinear optical effects in a coherently driven hot atomic gas *Phys. Rev. Lett.* **82** 5229
- [141] Pitaevsky L P 1984 Layered structure of superfluid ^4He with supercritical motion *Pis'ma Zh. Eksp. Teor. Fiz.* **39** 423 (*JETP Lett.* **39** 511)
Voskresensky D N 1993 Condensate with a finite momentum in a moving medium *Zh. Eksp. Teor. Fiz.* **104** 3982 (*J. Exp. Theor. Phys.* **77** 917)
- [142] Baym G and Pethick C J 2012 Landau critical velocity in weakly interacting Bose gases *Phys. Rev. A* **86** 023602
- [143] Weldon H A 1995 Exponential growth of space-like gluon distribution functions *Nucl. Phys. A* **590** 503c
- [144] Wehrl A 1978 General properties of entropy *Rev. Mod. Phys.* **50** 221
- [145] Weinhold W 1995 Zur Thermodynamik des Pion-Nukleon-Systems *Diploma Thesis* GSI (http://theory.gsi.de/the/phd/weinhold_dipl.ps.gz)
- [146] Adam T *et al* 2012 Measurement of the neutrino velocity with the OPERA detector in the CNGS beam using the 2012 dedicated data arXiv:[1212.1276](https://arxiv.org/abs/1212.1276) [hep-ex]
- [147] Fock V I 1930 Bemerkun zum Virialsatz *Z. Phys.* **63** 855
- [148] Hirschfelder J O 1960 Classical and quantum mechanical hypervirial theorems *J. Chem. Phys.* **33** 1462
- [149] Robinson P D and Hirschfelder J O 1963 Virial theorem and its generalization in scattering theory *Phys. Rev.* **129** 1391
- [150] Prigogine L 1967 *Introduction to Thermodynamics of Irreversible Processes* (New York: Wiley)
- [151] Kleidon A and Lorenz R D (ed) 2005 *Non-Equilibrium Thermodynamics and the Production of the Entropy* (Berlin: Springer)